Trinity College Dublin
Coláiste na Tríonóide, Baile Átha Cliath
The University of Dublin

Network Analysis in Amyotrophic Lateral Sclerosis during Voluntary Motor Task: Neurophysiological Biomarkers of Disrupted Cortical Connections

A Thesis Submitted to School of Medicine, Trinity College Dublin,

the University of Dublin, in partial fulfilment of the requirements for the degree of Doctor of Philosophy, 2024

By

Saroj Bista

BEng, MSc

Supervised by:

Assistant Prof. Bahman Nasseroleslami

Prof. Orla Hardiman

April 2024

Declaration and Statement of Plagiarism

I declare that this thesis has not been submitted as an exercise for a degree at this or any other university and it is entirely my own work. I have read and I understand the plagiarism provisions in the General Regulations of the University Calendar for the current year, found at: http://www.tcd.ie/calendar.

I have also completed the Online Tutorial on avoiding plagiarism 'Ready, Steady, Write', located at http://tcd-ie.libguides.com/plagiarism/ready-steady-write.

I understand that plagiarism could result in the failure.

Signed,

Saroj Bista

To my parents

Who taught me the importance of kindness and patience in life.

Acknowledgements

I would like to express my sincere gratitude to my PI **Prof. Orla Hardiman** and my supervisor **Assistant Prof. Bahman Nasseroleslami** for providing me all the necessary resources, motivation, and guidance to carry out this research work. I am grateful to my team members **Dr. Amina Coffey**, **Mr. Matthew Mitchell**, and **Ms. Eileen Rose Giglia** for helping me to collect data. I would like to acknowledge all the team members of the Electrophysiology strand of the Academic Unit of Neurology, especially **Dr. Lara McManus**, **Dr. Stefan Dukics**, **Dr. Roisin McMackin**, **Ms. Marjorie Metzger**, **Mr. Prabhav Mehra**, **Ms. Serena Plaitano** and **Mr. Vladyslav Sirenko** for their continuous help, support, and feedback on my work. I am also thankful **to Mr. Mark Heverin**, Research Manager, **Ms. Sara Batsukh** and Ms. **Adelais Fernell Sharp**, Administrative Officers of the Academic Unit of Neurology, for their continuous help and support.

This work couldn't have reached this stage without the participation of patients and healthy control volunteers. So, I am grateful to all the research participants and their family members for supporting our research. I would like to thank the staffs of Wellcome Trust HRB Clinical Research Facility, St. James's Hospital, especially **Ms. Derval Reidy** and **Ms. Maria Figueiredo**.

I would like to thank the Irish Research Council (IRC), the Health Research Board (HRB), and Health Research Charities Ireland (HRCI) for providing necessary funds to carry out this research work.

Finally, I would like to thank my wife, parents, and all my family members for their love and support.

Abstract

Amyotrophic lateral sclerosis (ALS) is a fatal progressive neurodegenerative disease that causes degeneration of both upper and lower motor neurons primarily affecting the motor system, but individual people with ALS show heterogenous presentations of motor and non-motor symptoms and disease progression rate. Therefore, diagnosis of ALS, which is based on the clinical examination and exclusion of mimic conditions like spinal muscular atrophy (SMA), Kennedy's disease, Myasthenia gravis, multiple sclerosis (MS), is extremely challenging. Additionally, ALS progression is measured using clinical scales that are subject to variance (i.e., cannot effectively capture heterogeneity) and are a proxy for underlying disease pathobiology. Therefore, there is an urgent need for reliable and quantitative biomarkers that can be used for early diagnosis, tracking disease progression, and importantly, deep phenotyping and stratification for clinical trials.

Neurophysiological studies in ALS have illustrated the potential of network connectivity measures to enable early detection of brain networks impairments before manifestation of clinical symptoms and before structural alterations become visible in structural imaging. ALS is a multi-network dysfunction causing deficits in motor and extra-motor brain networks. Understanding the changes in motor networks is key to unveiling disease pathology in ALS. Impairment of sensorimotor and extra-motor networks in ALS has been identified from resting-state paradigm. However, motor paradigms, that involve the pre-motor stage, motor planning, and motor execution and can directly access sensorimotor pathways, might be needed to unravel motor networks pathology in ALS for biomarker design.

In this project, high-density electroencephalogram (EEG) and bipolar surface electromyogram (EMG) were recorded from people with ALS and healthy controls when

they were performing an isometric motor task: pincer grip between thumb and index finger of the right hand at 10% of their maximal voluntary contraction. The neuroelectric signal analysis was done at both sensor and source levels to interrogate ALS-related motor network pathology. The spectral power and banded spectral coherence were obtained from EEG signals at sensor level to investigate the effect of neurodegeneration in functional motor networks during different stages of the task such as rest, pre-motor stage and motor execution. Similarly, banded corticomuscular coherence (CMC) at source level, which measures the synchrony between EEG and EMG signals, was used to investigate the dysfunctional involvement of corticospinal tracts in the cortico-peripheral networks in ALS. Furthermore, at source level, generalised partial directed coherence (gPDC) was used to investigate the effect of neurodegeneration on effective (directional or causal) cortical networks in ALS during pre-motor (motor planning) and motor execution.

This work has established that 'banded spectral coherence,' based on non-parametric methods such as 1-sample signed rank statistics and 2-D spatial median, was a simpler and improved alternative to classical 'magnitude squared coherence' to investigate functional network disruption in motor neuron disease. This study revealed more widespread point-to-point network connectivity (using banded spectral coherence), reflecting hyperactivation of cortical regions in ALS during rest and motor task. Such cortical hyperactivation is potentially due to a loss of inhibitory interneurons. Similarly, this study revealed increased beta event related spectral perturbations over non-dominant-motor and parietal regions. Furthermore, it demonstrated abnormal motor-parietal functional network at beta-band during motor execution, which was also negatively correlated with clinical motoric impairments. These findings indicate compensatory mechanism in ALS. More importantly, this study revealed that pre-motor networks that were impaired in ALS were distinct and not an extension of impairment in the primary motor cortex (M1). Furthermore, this study

found reduction of CMC in alpha, beta, and gamma frequency bands in brain regions within primary sensorimotor cortices (M1/S1), the supplementary motor area (SMA) and the superior parietal lobule implying broader network impairment in ALS beyond the sensorimotor networks, potentially reflecting dysfunction of other aspects of motor control such as motor planning, task attention, and visuomotor processes. Finally, the study identified several disruptions in directional networks within motor systems in ALS with higher order motor regions such as SMA. Specifically, the SMA-driven sensorimotor network was notably weaker in ALS, suggesting impaired motor planning. Also, the SMA potentially compensated for M1 degeneration during motor execution, as evidenced by stronger connections from ipsilateral SMA to contralateral M1 which could be attributed to interhemispheric disinhibition and heightened motor demands in ALS.

The cortico-cortical and cortico-muscular network impairments underpinned by this study have the potential to be used for clinical diagnostic, prognostic and phenotyping applications or as primary/secondary outcome measure to track network changes in the setting of disease modifying clinical trials.

Keywords: *Amyotrophic Lateral Sclerosis, Network Connectivity, Corticomuscular Coherence, Generalised Partial Directed Coherence, Biomarkers.*

Peer-reviewed publication from this thesis

1. **Bista S**, Coffey A, Fasano A, et al., Cortico-muscular coherence in primary lateral sclerosis reveals abnormal cortical engagement during motor function beyond primary motor areas, Cerebral Cortex, 2023.

Papers under review from this thesis

1. **Bista S,** Coffey A, Fasano A, et al., Abnormal EEG spectral power and coherence measures during pre-motor stage in Amyotrophic Lateral Sclerosis: Implications for developing biomarker candidates, Journal of Neural Engineering, 2024 (Under review).

Manuscripts under preparation from this thesis

1. **Bista S,** Coffey A, Mitchell M, et al., Corticomuscular Coherence Revealed Dysfunction in Multiple Aspects of Motor Control in ALS, in preparation.
2. **Bista S,** Coffey A, Mitchell M, et al., Effective Connectivity Patterns between Cortical Sources of Neuroelectric Activity during Motor Tasks Reflect Network-Level Abnormalities in ALS, in preparation.

Oral presentations regarding this thesis

1. **Bista S,** Coffey A, Mitchell M, et al., Corticomuscular coherence: A promising biomarker of neurodegeneration in ALS. Oral presentation- Surrogate Markers, 34th International Symposium for ALS/MND 2023.
2. **Bista S,** Coffey A, Mitchell M, et al., Corticomuscular coherence in ALS during performance of a motor task. Oral presentation- Applied Neurophysiology, European Network to Cure ALS (ENCALS) meeting 2023.

3. **Bista S,** Time runs faster for some people. Oral presentation- School of Medicine Heat, Trinity College Dublin Three-minute thesis (3MT) competition 2023.
4. **Bista S**, Corticomuscular coherence revealed motor cognition decline in ALS during voluntary contractions. Oral presentation- Research exchange in Brain-Computer Interface, Sheffield University Visit 2023.

Poster presentations regarding this thesis

1. **Bista S**, Coffey A, Fasano A, et al., Abnormal EEG Connectivity during Resting States, Motor Planning, and Motor Execution in Amyotrophic Lateral Sclerosis. Poster- Clinical imaging and electrophysiology, 31st International Symposium on ALS/MND, 2020.
2. **Bista S**, Coffey A, Fasano A, et al., Effective Brain Networks during Motor Task Reflects Cortical Plasticity in ALS. Poster- Clinical imaging and electrophysiology, 32nd International Symposium on ALS/MND 2021.
3. **Bista S**, Coffey A, Fasano A, et al., Impaired Corticomuscular Synchrony in ALS during Transient and Sustained Voluntary Task. Poster- Imaging, European Network to Cure ALS (ENCALS) meeting 2022.
4. **Bista S**, Coffey A, Fasano A, et al., Corticomuscular Coherence Revealed Engagement of Different Cortical Regions in Transient and Sustained Phases of an Isometric Motor Task. Poster- Neural and Rehabilitation Engineering, 44th Annual International Conference of the IEEE Engineering in Medicine and Biology Society, 2022.
5. **Bista S**, Coffey A, Fasano A, et al., Corticomuscular Coherence Revealed Engagement of Different Cortical Regions in Transient and Sustained Phases of an Isometric Motor Task. Poster-Society for Neural Control of Movement (NCM), 2022.

Table of Contents

List of Figures

List of Tables

List of Abbreviations

ACC	Anterior Cingulate Cortex
ALS	Amyotrophic Lateral Sclerosis
ALSFRS-R	Amyotrophic Lateral Sclerosis Functional Rating Scale Revised
APB	Abductor Pollicis Brevis
AUROC	Area Under the Curve of Receiver Operating Characteristics
BOLD	Blood Oxygen Level-Dependent
BP	Bereitschaftspotential
C9orf72	Chromosome 9 open reading frame 72
CDF	Cumulative Distribution Function
CMC	Corticomuscular Coherence
CNV	Contingent Negative Variations
Coh	Coherence
DCM	Dynamic Causal Modelling
DLPFC	Dorsolateral Prefrontal Cortex
DMPFC	Dorsomedial Prefrontal Cortex
DTI	Diffusion Tensor Imaging
EC	Effective Connectivity
ECAS	Edinburgh Cognitive and Behavioural Assessment Scale
EEG	Electroencephalography
EHI	Edinburgh Handedness Inventory
EMG	Electromyogram
ERD	Event Related Desynchronization
ERP	Event Related Potential

ERSP	Event Related Spectral Perturbations
ESMN	Executive Sensorimotor Network
FA	Fractional Anisotropy
FC	Functional Connectivity
FDI	First Dorsal Interosseous
FDR	False Discovery Rate
fMRI	Functional Magnetic Resonance Imaging
fNIRS	Functional Near-Infrared Spectroscopy
FPB	Flexor Pollicis Brevis
FTD	Frontotemporal Dementia
GCC	Global Clustering Coefficient
gPDC	Generalized Partial Directed Coherence
HC	Healthy Controls
LCMV	Linearly Constrained Minimum Variance
LMN	Lower Motor Neuron
LSVM	Linear Support Vector Machines
M1	Primary Motor Cortex
ME	Motor Execution
MEG	Magnetoencephalography
MEP	Motor Evoked Potential
MND	Motor Neuron Disease
MP	Motor Planning
MRI	Magnetic Resonance Imaging
MRS	Magnetic Resonance Spectroscopy

MUNE	Motor Unit Number Estimate
MUNIX	Motor Unit Number Index
MVC	Maximum Voluntary Contraction
PDC	Partial Directed Coherence
PFC	Prefrontal Cortex
PLS	Primary Lateral Sclerosis
PM	Premotor Cortex
PMA	Progressive Muscular Atrophy
PPS	Post-polio Syndrome
ROI	Region of Interest
S1	Primary Sensory Cortex
SMA	Supplementary Motor Area
SPL	Superior Parietal Lobule
UMN	Upper Motor Neuron

1. Introduction

1.1 Amyotrophic Lateral Sclerosis

Neurodegenerative diseases exert billions of euros of costs on the economy and dramatically affect the quality of life of patients and caregivers. The neurodegeneration causes failure in the brain's neural networks which is poorly understood, can differ across individuals, and is difficult to quantify in clinics. Alzheimer's disease, Parkinson's disease, Huntington's disease, and Motor Neuron Disease (MND) are such diseases. MND is an umbrella term that covers a wide range of rare neurodegenerative diseases that destroy motor neurons, the nerve cells responsible for control of voluntary movement of the body. MND includes diseases such as amyotrophic lateral sclerosis (ALS), primary lateral sclerosis (PLS), progressive muscular atrophy (PMA), spinal muscular atrophy (SMA), post-polio syndrome (PPS), and Kennedy's disease. ALS is a progressive neurodegenerative disease which primarily affects the motor neurons of the brain (upper motor neurons, UMN) and spinal cord (lower motor neurons, LMN). In early stages of the disease, the motor neurons (upper and lower), which carry neural signals from the brain to muscles via the spinal cord and vice-versa, start to degenerate. This causes muscles to weaken, fasciculate (twitch of a muscle), and waste (also called atrophy). The motor neuron degeneration progresses over time and the patient gradually loses control over the voluntary movement of muscles. Consequently, the patient suffers deterioration of strength and ability to do simple day-to-day tasks. Over time, the motor neurodegeneration causes severe dysphagia (difficulty in swallowing) and dyspnoea (shortness of breath) so that the patient is unable to breathe and generally dies from respiratory failure. This happens typically 3-5 years after symptom onset, except in some cases (about 10%), where the patient survives more than 10 years and has a slower disease progression rate.

1.1.1 ALS Epidemiology

ALS is the most common type of MND worldwide and can affect people between the ages of 40 years and 90 years. The incidence of ALS increases with age and is reported to be highest between 60 years and 79 years (Marin et al., 2018). There are no clear indicators that the incidence of ALS has changed in the past couple of decades. Some studies have reported that the incidence of ALS is stable over the past three decades (Ryan et al., 2019), whereas others have reported a possible increase in the incidence rate (Xu et al., 2020). The perceived increase in incidence could be the result of improved diagnosis, and improved quality of ALS registries around the world (Feldman et al., 2022). Similarly, the prevalence of ALS is also expected to increase because of an ageing population, improved disease management, improved and personalised healthcare, and personalised treatment plans to some extent, which increase the life expectancy by at a least few months. However, ALS is still a rare disease with an overall crude global prevalence rate of 4.42 per 100,000 population (Xu et al., 2020). The overall crude global incidence of ALS is 1.75 per 100,000 person-years and 1.68 per 100,000 person-years after standardisation (Marin et al., 2017). The incidence of ALS is heterogenous worldwide with a standardised incidence rate of 1.89 per 100,000 person-years in Northen Europe, 0.83 in East Asia and 0.73 in South Asia (Marin et al., 2017). Oceania has the highest incidence of 2.25 per 100,000 person-years (Marin et al., 2017). This variation of ALS incidence between the subcontinents could be related to genetic factors, especially populations' ancestries (Marin et al., 2017). On the other hand, homogeneous incidence rates have been reported in populations from Europe, North America, and New Zealand with a pooled ALS standardised incidence of 1.81 per 100,000 person-years (Marin et al., 2017).

Sex is another factor that affects the incidence of ALS, with male population being at higher risk than female. A noticeable male-to-female sex ratio has been consistently reported by population studies in ALS, with an overall pooled male-to-female ratio of 1.28 (Fontana et al., 2021). In Irish population, the mean male-specific annual incidence rate is 1.8 per 100,000 persons and mean female-specific annual incidence rate is 1.3 per 100,000 persons (Ryan et al., 2019). The predominance of male cases could be linked to difference of response between male vs female to ALS risk factors (McCombe and Henderson, 2010). Higher incidence of male cases could also be linked to some other factors such as an occupational bias towards exposure to risk factors. For example, some studies have put forward that, for some unknown reasons, military veterans are at higher risk (about 1.5 to 2 times) of developing ALS (McKay et al., 2021) and it is a well-known fact that the majority of military personnel is male.

Genetics also play an important role in the incidence of ALS. Studies have shown that the heritability of ALS is higher in mother-daughter pairings (Ryan et al., 2019). The C9orf72 gene, which is the most common gene associated with ALS, lowers the age of onset in the male versus female population (Murphy et al., 2017). Similarly, the low incidence of ALS in Asia compared to Europe and North America may be related to the low frequency of C9orf72 gene mutation in Asian cohorts (Shahrizaila et al., 2016, Zou et al., 2017). The C9orf72 repeat expansion accounts for more than 34% of familial ALS and about 5-20% of sporadic ALS in the Caucasian population (Williams et al., 2013, Zou et al., 2017). In contrast, the C9orf72 gene mutation accounts for less than 2% of the familial or sporadic ALS in Asia (Ogaki et al., 2012, Shahrizaila et al., 2016, Zou et al., 2017). Thus, occurrence of ALS is influenced by interrelationships between genetic factors, age, and sex, and this has significant implications for both preclinical and clinical research, as well as clinical trials.

1.1.2 Genetic Aspects of ALS

ALS is classified as either familial or sporadic based on the family history or the cause of the disease. If the disease occurs at random without any family history or any clearly linked risk factors than it is Sporadic ALS. Sporadic ALS is the most common form of ALS and affects from 85% of people with the disease. For the remaining 10 to 15% of people with ALS, the cause is genetic (Familial ALS) i.e., they inherit the disease from family members with ALS or associated syndromes such as frontotemporal dementia or other neuropsychiatric conditions (Goutman et al., 2022). Although sporadic ALS occurs without the evidence that the disease was inherited, it shares several risk genes with familial ALS. With increasing genetic studies in ALS, more and more gene mutations are being associated with ALS. More than 40 ALS genes have been identified so far (Goutman et al., 2022) and four genes, namely C9orf72 (chromosome 9 open reading frame 72), SOD1 (superoxide dismutase 1), TARDBP (transactive response DNA binding protein 43), and FUS (fused in sarcoma) account for about 48% of familial and 5% of sporadic ALS (Zou et al., 2017). However, the distributions of these major ALS-related genes are not homogeneous amongst the ALS population and there is a distinct genetic architecture between European and Asian ALS populations (Zou et al., 2017). These four major ALS-related genes (C9orf72, SOD1, TARDBP, and FUS) account for 55% of familial and 7% of sporadic ALS within the population of European origin, and for about 40% of familial and 3% of sporadic ALS within the population of Asian origin (Zou et al., 2017). In the European population, the most common gene mutation in ALS is C9orf72 repeat expansion (~34% familial and ~5% sporadic), followed by SOD1 (~15% familial and ~1% sporadic). On the other hand, in Asian populations, the most common gene mutation in ALS is SOD1 (~30% familial and ~2% sporadic), followed by FUS (~6% familial and ~1% sporadic). The Irish ALS

population shows similar familial genetic traits as the European population with C9orf72 repeat expansion accounting for about 33% of known familial cases of ALS (Ryan et al., 2018).

1.1.3 Clinical Presentation of ALS

1.1.3.1 Phenotypic Heterogeneity of ALS

Motor Phenotypes

ALS exhibits phenotypic heterogeneity due to dysfunction of either upper motor neurons (UMN) that originate from the cerebral cortex and travel down to the brain stem or spinal cord, or lower motor neurons (LMN) that begin from the spinal cord and innervate muscles, or both (Figure 1.1 A). UMN dysfunction is characterised by increased and pathological reflexes, pathological spread of reflexes, preserved reflexes in weak limb, and spasticity. LMN dysfunction is characterised by muscle weakness, atrophy, and fasciculations. These motor neuron dysfunctions lead to progressive weakening of voluntary skeletal muscles involved in the movement of limbs, swallowing, speaking, and respiratory function, with various phenotypic clinical presentations (Figure 1.1 B). Spinal onset and bulbar onset are two most common phenotypic presentations of ALS, each constituting more than 30% of the cases (Chiò et al., 2011) . Spinal onset ALS is characterised by muscle weakness starting either in the upper limbs, or lower limbs, or both. It presents both UMN and LMN signs. The bulbar onset phenotype, which presents both UMN and LMN signs, is characterised by weakness starting in the bulbar muscles that control speaking and swallowing. Other less frequent phenotypic presentations of ALS are pyramidal, flail limbs (flail arm and flail leg), primary lateral sclerosis (PLS), progressive muscular atrophy (PMA), respiratory onset, or hemiplegia. Flail arm ALS is characterised by LMN involvement with progressive, predominantly proximal weakness and wasting of the upper

limbs, whereas flail leg ALS is characterised by LMN involvement with progressive distal onset weakness and wasting of the lower limbs. Flail limb ALS is a relatively milder variants of ALS as it showed better survival than spinal or bulbar onset ALS (Wijesekera et al., 2009). PLS is characterised by pure UMN dysfunction with no sign of LMN involvement, causing weakness in limb muscles, speaking, and swallowing. Similarly, PMA is characterised by LMN dysfunction with no sign of UMN involvement at onset causing progressive weakness and muscle atrophy. However, as much as 70% of patients with PMA will eventually show the signs of UMN degeneration (Latif, 2018). There is no clear distinction, whether to consider PLS and PMA as separate clinical entities or a phenotypic presentation of ALS. However, they have been often studied as part of the clinical spectrum of ALS (Fontana et al., 2021, Mehta et al., 2022). Pyramidal variants, also referred to as predominantly upper motor neuron ALS, concern patients with ALS having a clinical manifestation dominated by pyramidal signs such as hyperreflexia, spasticity, and Babinski signs at onset and not all patients with ALS show such signs. In a cohort of 130 patients with ALS studied by Álvarez et al. (2018), only about 11% had a complete pyramidal syndrome. Respiratory onset ALS is characterised by the prevalence of respiratory impairments such as orthopnoea (shortness of breath when lying down) or dyspnoea (shortness of breath) at onset. Such patients present with mild involvement of spinal or bulbar signs in the first 6 months after onset and mild UMN involvement (Chiò et al., 2020). Hemiplegic ALS, also known as Mill's syndrome, is an extremely rare variant of ALS with asymmetric corticospinal degeneration. Case studies of hemiplegic ALS have shown UMN involvement (Chugh et al., 2013, Algahtani et al., 2021).

Cognitive Phenotypes

Phenotypic heterogeneity in ALS is not only due to motor symptoms but also due to cognitive and behavioural symptoms. Not all individuals with ALS develop cognitive and

behavioural symptoms but about 35-45% of individuals with ALS may experience some degree of cognitive or behavioural involvement with symptoms overlapping with Frontotemporal Dementia (FTD) and about 14% meet the diagnostic criteria of FTD (Pender et al., 2020). Therefore, ALS is introduced as part of the ALS-FTD spectrum (Figure 1.1 C). Cognitive impairment in ALS is commonly characterised by manifestation of executive and language dysfunction whereas behavioural impairment is characterised by apathy, loss of sympathy and empathy, disinhibition, stereotyped or compulsive behaviours and dietary changes (Pender et al., 2020, Strong et al., 2017). Based on the presentation of cognitive and/or behavioural involvement, five phenotypes of ALS have been reported namely, pure ALS (only motor symptoms, no cognitive or behavioural involvement), ALS with cognitive impairment (ALSci), ALS with behavioural impairment (ALSbi), ALS with cognitive and behavioural impairment (ALScbi), and ALS with concurrent dementia that meets diagnostic criteria for FTD (ALS-FTD).

1.1.3.2 ALS as Multi-system Disorder

Although ALS has traditionally been viewed as a disease that specifically affects the motor system, recent imaging and pathological research has shown that it is a multisystem neurodegenerative disorder (Strong, 2017, Geser et al., 2008). In addition to motor deficits, which is a primary ALS pathophysiology, cognitive deficits are consistently reported by several clinical-based and large population-based studies (Chiò et al., 2019).

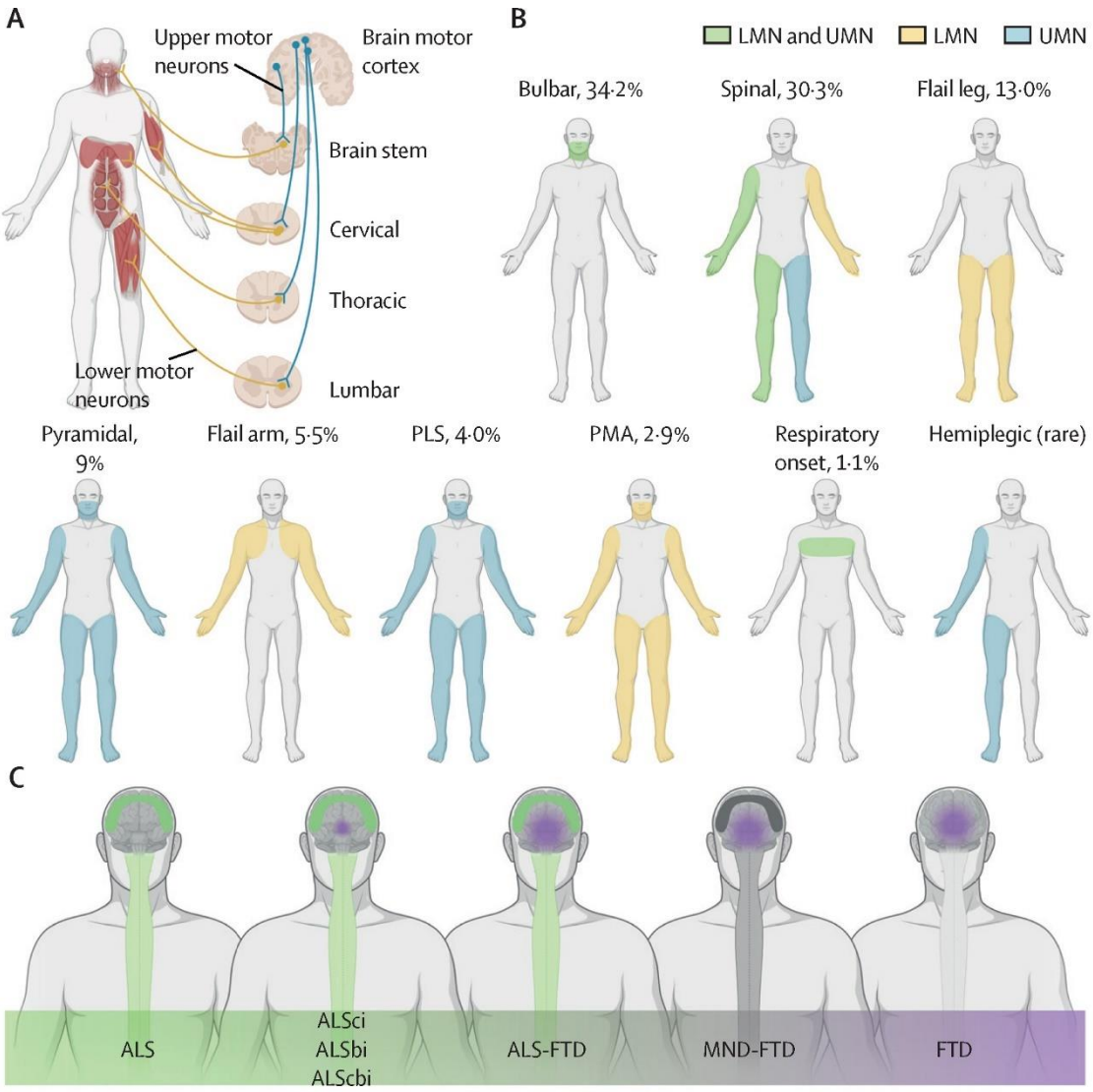

Figure 1.1 Amyotrophic lateral sclerosis (ALS) phenotypical heterogeneity and spectrum with frontotemporal dementia (FTD). *Figure taken from Feldman et al. (2022). (A) Schematics showing UMN (blue) and LMN (yellow) which relay signals from the motor cortex to muscles. LMNs from the brain stem innervate bulbar muscles, LMNs from the cervical region of spinal cord innervate muscles on upper limbs and respiratory muscles, LMNs from thoracic region of the spinal cord innervate abdominal muscles, and LMNs from the lumbar region of the spinal cord innervate lower limbs. (B) Schematics showing phenotypical presentations of people with ALS based on the signs and anatomical locations of UMN (blue), LMN (yellow), and combined UMN and LMN (green) dysfunctions. The percentages in the figure show the proportion of ALS phenotypes from the total representative ALS population reported by Chiò et al. (2011). (C) Schematics showing the ALS-FTD spectrum. ALS is one end of the spectrum and presents with pure motor signs from UMN and LMN degeneration. FTD is on the other end of the spectrum and presents with cognitive and*

behavioural impairments from frontotemporal degeneration. Abbreviations: ***ALS****, amyotrophic lateral sclerosis;* ***ALSci****, amyotrophic lateral sclerosis cognitive impairment;* ***ALSbi****, amyotrophic lateral sclerosis behavioural impairment;* ***ALScbi****, amyotrophic lateral sclerosis cognitive and behavioural impairment;* ***FTD****, frontotemporal dementia;* ***LMN****, lower motor neuron;* ***UMN****, upper motor neuron;* ***PLS****, primary lateral sclerosis;* ***PMA****, progressive muscular atrophy;* ***MND****, motor neuron disease.*

It has been reported that about 50% of patients diagnosed as possible, probable, or definite ALS have detectable cognitive or behavioural changes, and about one-third of these patients exhibits the neurological signatures of frontotemporal degeneration (FTD) (Grossman, 2019). The neurodegeneration in ALS begins in the pyramidal motor system which includes motor cortex, brainstem motor nuclei of cranial nerves, and motor neurons of spinal cord (Brettschneider et al., 2013). Over time, the neurodegeneration spreads to neighbouring cortical regions by diffusion or to distant cerebral cites mediated by axonal projections. The pathology initially spreads to brain regions such as premotor, sensory, and prefrontal cortices, and eventually to portions of the parietal and temporal lobes, corpus callosum, and deep grey structures (Fatima et al., 2015, Chiò et al., 2014). This spreading pathology causes several non-motor impairments in ALS such as in executive control (difficulty with planning, organizing and inhibitory control), changes in behaviour and personality (apathy, loss of empathy and disinhibition) and language disorders (non-fluent, agrammatic speech and comprehension)(Grossman, 2019). In addition to cognitive and behavioural impairment, recent studies have provided evidence of episodic memory impairments in ALS subjected to the thinning of medial temporal lobe grey matter (Machts et al., 2014, Machts et al., 2020). A clear understanding of multisystem nature of ALS will be vital for improved diagnosis, prognosis, and disease management.

1.1.4 Propagation of ALS pathology

ALS is increasingly recognized as a network disorder. Disruption of network connectivity, which involve multiple interconnected regions of the nervous system, could lead to the propagation of pathology throughout the nervous system. Two hypotheses have been debated to explain the pathogenesis of ALS namely 'dying forward' and 'dying backward.' The dying forward hypothesis suggests that ALS begins in the pyramidal neurons of motor and premotor cortices of the brain and then progresses to affect the lower motor neurons in the spinal cord and brainstem (Eisen, 2021). This hypothesis proposes that glutamate excitotoxicity at the motor cortex is an important factor resulting in deficit of anterior horn cell metabolism (Kiernan et al., 2011). The TMS studies reporting cortical hyperexcitability as an early feature in sporadic ALS patients (Vucic and Kiernan, 2006) and precedes the clinical onset of familial ALS (Vucic et al., 2008) support the dying forward hypothesis.

The dying backward hypothesis, on the other hand, proposes that ALS begins in the peripheral nervous system such as muscle cells or at the neuromuscular junction, affecting the lower motor neurons first, and then progresses centrally to involve the upper motor neurons in the brain (Kiernan et al., 2011). This hypothesis is supported by the studies reporting that synaptic denervation precedes motor neuron degeneration and is facilitated by the accumulation of mutant SOD1 protein in Schwann cells (Clark et al., 2016).

1.1.5 Diagnostic Criteria for ALS

ALS is a heterogeneous disease, involving motor, cognitive, or behavioural impairments, with the presentation of various clinical phenotypes which makes it difficult to diagnose. Researchers and clinicians have been working for decades to come up with a gold standard criterion that can be used for the diagnosis of ALS but with limited success. The definitive diagnosis of ALS is difficult as there are several syndromes that mimic the symptoms of

ALS, particularly in the early stages of the disease (Hardiman et al., 2011). To date, the diagnosis of ALS is based on the clinical signs and symptoms in addition to investigations to eliminate mimicking syndromes. The first widely recognised diagnostic criteria for ALS were published in 1994 and are known as the El Escorial criteria (Brooks, 1994). They were revised in 2000 as the El Escorial revisited criteria in order to increase their sensitivity (Brooks et al., 2000). The revised criteria allowed the patients to be categorised on the spectrum of probability from 'Possible' to 'Definite' ALS on clinical criteria alone based on the involvement of UMN or LMN or both, the number and specific bodily regions affected, and the presence or absence of supportive neurophysiological findings. A summary of the El Escorial revisited criteria is shown in Table 1.1.

Table 1.1 Summary of the El Escorial revisited criteria for diagnosis of ALS from Brooks et al. (2000)

The diagnosis of ALS requires:	
(A) the presence of: (A: 1) evidence of LMN degeneration by clinical, electrophysiological, or neurological examination, (A: 2) evidence of UMN degeneration by clinical examination, and (A: 3) progressive spread of symptoms or signs within a region or to other regions, as determined by history or examination,	
together with:	
(B) the absence of: (B: 1) electrophysiological or pathological evidence of other disease processes that might explain the signs of LMN and/or UMN degeneration, and (B: 2) neuroimaging evidence of other disease processes that might explain the observed clinical and electrophysiological signs.	
Categories of clinical diagnostic certainty on clinical criteria alone	
Definite ALS	Presence of UMN, as well as LMN signs, in the bulbar region and at least two spinal regions or

	Presence of UMN and LMN signs in three spinal regions
Probable ALS	Presence of UMN and LMN signs in at least two regions with some UMN signs necessarily rostral to (above) the LMN signs.
Probable ALS – Laboratory supported	Presence of UMN and LMN signs in only one region, or Presence of UMN signs alone in one region, and LMN signs defined by EMG criteria are present in at least two regions
Possible ALS	Presence of UMN and LMN signs in only one region or Presence of UMN signs in two or more regions or Presence of LMN signs rostral to UMN signs and the diagnosis of Probable ALS – Laboratory supported cannot be proven

To improve the diagnostic sensitivity of the El Escorial criteria, the revised El Escorial criteria introduced the category "Suspected ALS" that allowed the use of Electromyography (EMG) results to support the clinical findings for the diagnosis (Brooks et al., 2000) and removed the category "Laboratory-supported probable ALS". The four ALS categories of El Escorial revisited criteria (see Table 1.1) identified patients with ALS with high specificity, but concern was raised on their sensitivity because of the way EMG contributes to the diagnosis (De Carvalho et al., 1999). An Irish population-based study by Traynor et al. (2000) indicated that the El Escorial and their revision were highly restrictive and about 10% of deceased patients died without reaching trial eligibility. To solve this issue, the Awaji criteria (de Carvalho et al., 2008) were introduced which modified the El Escorial revisited criteria by further integrating electrophysiological criteria with clinical findings. The Awaji criteria considered the EMG changes showing LMN dysfunction and presence of fasciculations as LMN signs, removed "Laboratory-supported probable ALS", and retained definite, probable, and possible ALS categories.

Although, the Awaji criteria has demonstrated an improved diagnostic certainty of ALS over the El Escorial revisited criteria (Gawel et al., 2014), both criteria are complex with

high inter-rater variability and require training to use (Johnsen et al., 2019). Therefore, to simplify, improve inter-rater reliability, and potentially replace the El Escorial revisited and Awaji criteria, new diagnostic criterion for ALS called Gold Coast criteria (Shefner et al., 2020) have been proposed in 2019. The Gold Coast criteria for diagnosis of ALS are shown in Table 1.2. Multicentre population studies as well as regional population studies have shown that the Gold Coast criteria offer greater diagnostic sensitivity compared to the El Escorial revisited and Awaji criteria by considering the 'definite' or 'probable' diagnostic categories as a positive finding and recommend using the criteria in clinical practice and therapeutic trials (Hannaford et al., 2021, Pugdahl et al., 2021, Shen et al., 2021).

Table 1.2 Gold Coast criteria for diagnosis of ALS from Shefner et al. (2020)

1. Progressive motor impairment documented by history or repeated clinical assessment, preceded by normal motor function, and
2. Presence of upper[1] and lower[2] motor neuron dysfunction in at least 1 body region[3], (with upper and lower motor neuron dysfunction noted in the same body region if only one body region is involved) or lower motor neuron dysfunction in at least 2 body regions, and
3. Investigations[4] excluding other disease processes
Footnotes:
[1]Upper motor neuron dysfunction implies at least one of the following: 1. Increased deep tendon reflexes, including the presence of a reflex in a clinically weak and wasted muscle, or spread to adjacent muscles. 2. Presence of pathological reflexes, including Hoffman sign, Babinski sign, crossed adductor reflex, or snout reflex 3. Increase in velocity-dependent tone (spasticity) 4. Slowed, poorly coordinated voluntary movement, not attributable to weakness of lower motor neuron origin or Parkinsonian features
[2]Lower motor neuron dysfunctions in a given muscle requires either: 1. Clinical examination evidence of muscle weakness and muscle wasting, or

2. EMG abnormalities that must include both: Evidence of chronic neurogenic change, defined by large motor unit potentials of increased duration and/or increased amplitude, with polyphasia and motor unit instability regarded as supportive but not obligatory evidence, and Evidence of ongoing denervation, including fibrillation potentials or positive sharp waves, or fasciculation potentials
[3]Body regions are defined as bulbar, cervical, thoracic, and lumbosacral. To be classified as an involved region with respect to lower motor neuron involvement, there must be abnormalities in two limb muscles innervated by different roots and nerves, or one bulbar muscle, or one thoracic muscle either by clinical examination or by EMG.
[4]The appropriate investigations depend on the clinical presentation, and may include nerve conduction studies and needle EMG, MRI or other imaging, fluid studies of blood or CSF, or other modalities as clinically necessary.

1.1.6 Diagnostic Delay and its Impact in ALS

The diagnosis of ALS is based primarily on clinical examination using the El Escorial, El Escorial revisited or Awaji criteria, and is often slow taking about 10 to 16 months from symptoms onset (Richards et al., 2020). The newly proposed Gold Coast criteria, which are simplified and have higher sensitivity compared to the former criteria, have the potential to reduce the diagnostic delay (Falcão de Campos et al., 2023) if used in clinical practice. The revised El Escorial criteria are still the mainstay of ALS diagnosis, but the field is slowly moving towards the Gold Coast criteria (Feldman et al., 2022). Several factors contribute to the delay in diagnosis of ALS such as delays from referrals to specialists, delays from misdiagnosis, delays related to site of disease onset, age of onset-related delays, and delays related to the presence of comorbidities (Richards et al., 2020). Studies have demonstrated that ALS with spinal onset and younger age onset have longer diagnostic delays (Richards et al., 2020, Galvin et al., 2017, Falcão de Campos et al., 2023, Nzwalo et al., 2014). The

time from first symptom onset noted by the patient to their first visit to a physician or general practitioner is about 3-6 months and about 60% of patients are referred to a neurologist after their first or subsequent visit to a physician (Richards et al., 2020).

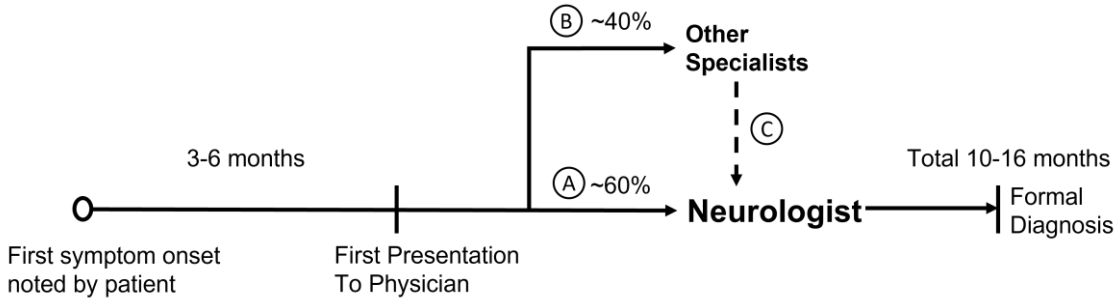

Figure 1.2 Pathway to ALS diagnosis from first symptom onset to final diagnosis. *Figure taken from Richards et al. (2020).*

There is no treatment to halt or reverse the progressive neurodegeneration in ALS till date. Early diagnosis of the disease could help individuals to receive personalized supportive care from multidisciplinary teams of health care professionals, which could help to prolong their life as well as improve their and their caregiver's quality of life. The delay in diagnosis also adds financial burden to the patient and/or state because of the significant waste of financial resources arising from misdiagnosis and delayed diagnosis (Galvin et al., 2017). More importantly, the emotional and psychological burden of misdiagnosis and delayed diagnosis is significant for patients and their family. The delayed diagnosis prevents patients and their family to adequately prepare for their future in terms of end-of-life care, finances, social relationships, and psychological well-being.

1.1.7 Prognosis of ALS

The Amyotrophic Lateral Sclerosis Functional Rating Scale Revised (ALSFRS-R) is the most widely used tool to measure functional decline and to monitor disease progression in ALS by clinicians and researchers. The ALSFRS-R is a 48 points validated questionnaire-

based clinical scale that ranges from score 0 (severe functional impairment) to 48 (no functional impairment) (Cedarbaum et al., 1999). The 48-point total score can be divided into 4 sub-scales namely bulbar (0-12), fine motor (0-16), gross motor (0-8), and respiratory (0-12). Due to the lack of suitable alternatives, the ALSFRS-R remains the gold standard of primary or secondary efficacy of clinical trial outcome (van Eijk et al., 2021) despite having issues with multidimensionality (Franchignoni et al., 2013) i.e., the ALSFRS-R is a composite scale that combines assessments of various functional domains, including bulbar function, limb strength, fine motor skills, and respiratory function. Each domain may progress at a different rate and be affected to a different extent in individual patients. Another limitation with the ALSFRS-R is that some sub-scores improve with symptoms management or with change in behaviour even though the disease is progressing (Fournier et al., 2020).

To overcome the limitations of the ALSFRS-R, Fournier et al. (2020) proposed a new clinical outcome measure to use in patients with ALS called the Rasch-Built Overall Amyotrophic Lateral Sclerosis Disability Scale (ROADS). The ROADS consists of 28 patient-reported questions about their ability to perform daily activities that can be weighted as 0 (able to perform without difficulty), 1 (able to perform, but with difficulty), and 2 (unable to perform). The ROADS is a linearly weighted scale with high test-retest reliability that captures overall disability of ALS patients (Fournier et al., 2020). The ability of the ROADS questionnaire to capture overall disability of ALS was successfully validated against the ALSFRS-R in a Chinese ALS population by modifying the questionnaire (Chinese version of ROADS) through standardised forward-backward translation and cultural adaptation (Sun et al., 2021). A longitudinal study comparing the ROADS and ALSFRS-R concluded that the performance of both measures was similar, however, the ROADS offered psychometric advantages, such as Rasch-modelling and

unidimensionality (Johnson et al., 2022). Similarly, a recent study evaluating the ROADS and ALSFRS-R has shown that the ROADS detected clinically meaningful decline in about 60% of ALS versus about 46% detected by the ALSFRS-R on same ALS cohort (Fournier et al., 2023). Therefore, the ROADS offers advantages over the ALSFRS-R and could be a valuable tool for prognosis of ALS and in clinical trials, but more clinical validation from multiple ALS centres is needed before it can be adopted globally.

A staging system, which identifies an individual's position in the disease course, is another way of measuring progression in ALS. Staging systems can be useful in clinical trials to measure the efficacy of an intervention to halt or delay advancement from less-severe to more-severe disease stages. Staging systems such as King's staging (Roche et al., 2012) and Amyotrophic Lateral Sclerosis Milano-Torino staging (ALS-MiToS) (Chiò et al., 2015) have been proposed for ALS but neither of them has a widespread use in clinical practice and trials. King's staging defines four disease stages where each stage reflects the severity of the disease and its association with survival (Figure 1.3 A). King's staging differs from El Escorial categorisation because it doesn't need information about

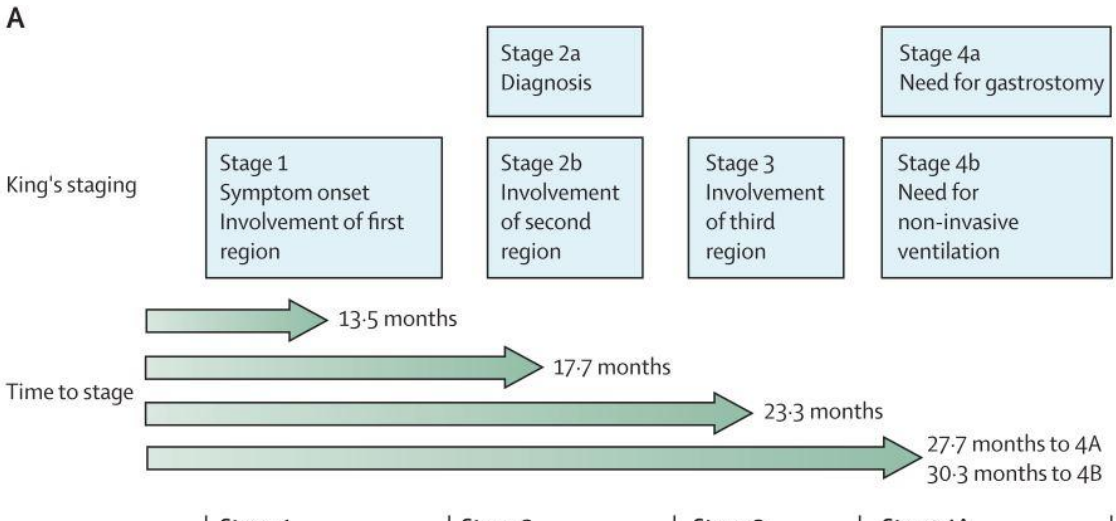

	Stage 1	Stage 2	Stage 3	Stage 4A
Median survival at each stage (bulbar or limb)	19 months for bulbar, 59 months for limb	19 months for bulbar, 28 months for limb	13 months for bulbar and limb	9 months for bulbar, 6 months for limb Stage 4B, 3 months for bulbar, 8 months for limb

B

	Stage 0	Stage 1	Stage 2	Stage 3	Stage 4	Stage 5
ALS-MiToS staging	No loss of a functional domain	Loss of 1 domain	Loss of 2 domains	Loss of 3 domains	Loss of 4 domains	Death
Probability of death at each stage	0·07	0·26	0·33	0·33	0·86	

Figure 1.3 ALS prognosis. Figure taken from Feldman et al. (2022). (A) King's staging showing time to reach each stage and survival at each stage. (B) ALS-MiToS staging showing number of functions loss at each stage and probability of death at each stage.

UMN or LMN involvement and it is easy to use because it corresponds to symptoms reported by patients and information relevant to the neurologist (Roche et al., 2012). ALS-MiToS staging defines six disease stages (Stage 0 to Stage 5) based on the number of functional domains lost and each stage is associated with probability of death (Figure 1.3 B). The functional domains of ALS-MiToS are four independent functions namely walking/self-care, swallowing, communicating, and breathing, that are included in the ALSRFS/ALSFRS-R scales. King's staging and ALS-MiToS are complimentary to each

other, with King's staging showing higher resolution in early to mid-disease course, and MiToS showing higher resolution for late disease course (Luna et al., 2021, Fang et al., 2017).

1.2 Biomarkers in ALS

1.2.1 Definition of a Biomarker

Biomarkers are measurable indicators of normal biological processes, pathogenic processes, or responses to an intervention (Group, 2001). Biomarkers play a crucial role in diagnosing, monitoring progression, predicting outcomes, and evaluating the effectiveness of treatments in ALS. One avenue of finding biomarker candidates for ALS is to study the neurophysiological processes in the disease such as motor neuron degeneration (Holasek et al., 2005), excitotoxicity (Foran and Trotti, 2009), protein misfolding and aggregation (Parakh and Atkin, 2016), mitochondrial dysfunctions (Zhao et al., 2022), axonal transport deficits (De Vos and Hafezparast, 2017), glial cell dysfunction (Philips and Rothstein, 2014) and neuroinflammation (Liu and Wang, 2017) amongst many others. By comparing the measures of these neurophysiological processes with the healthy controls or other diseased controls such as post-polio syndrome or multiple sclerosis, it is possible to identify biomarkers that can identify neuropathophysiologies that are specific to ALS. Moreover, if these neurophysiological process measures correlate with clinical impairments in ALS or change over time, it becomes possible to identify biomarkers sensitive to the progression of the disease or treatment effects. Table 1.3 shows the types of biomarkers in ALS, their definition, and the current gold standards.

Table 1.3 Types of biomarkers in ALS, their definition, and current benchmarks.

Biomarker Type	Definition	Current Gold Standards
Diagnostic	Guide the clinical diagnostic process of ALS at an early stage when signs are localized and subtle allowing for timely treatment and trial enrolment	Neurological examinations, Revised El Escorial/Awaji criteria, Electromyography
Prognostic	Identify patterns of progression and stratify ALS patients for better trial design by broadly distinguishing between ALS sub-groups	Neurological evaluation, Revised ALSFRS scores
Pharmacodynamic	Ensure that an experimental drug is having the desired effect on the pre-clinically identified therapeutic pathway and curtail ineffective therapeutic interventions at an early stage	Revised ALSFRS scores

1.2.2 Properties of an Ideal Biomarker Candidate for ALS

An ideal biomarker candidate for ALS should have the following properties (Lesko and Atkinson, 2001).

a. **Clinical Relevance:** Ability to reflect measures of, or change in, pathophysiological process by showing association with the clinically relevant measures such as disease duration, or clinically measured scores (ALSFRS-R, UMN/LMN scores).
b. **Specificity and sensitivity:** Ability to identify ALS specific impairments and discriminate it from healthy people or mimicking conditions. Detect smaller changes in disease processes to effectively track disease progression or response to therapeutic interventions.

c. **Reliability:** Ability to reflect measure of, or change in, a pathophysiological process with acceptable accuracy, precision, robustness, and reproducibility.
d. **Practicality:** Should be non-invasive or minimally invasive to avoid inconvenience and discomfort to healthy controls or ALS patients.
e. **Simplicity:** Should be cost effective, suitable for routine utilisation without extensive time requirement, and have wider acceptance.

1.2.3 Neurophysiological Biomarkers of ALS

The diagnostic utility of neurophysiological biomarkers for diagnosis of ALS has been underlined in both the El Escorial revisited criteria (Brooks et al., 2000) and the Gold Coast criteria (Shefner et al., 2020). Quantitative neurophysiological approaches such as motor unit number estimate/index (MUNE/MUNIX) (Bromberg and Brownell, 2008, Gooch et al., 2014, McComas et al., 1971, Nandedkar et al., 2004), electromyography (EMG) (Joyce and Carter, 2013, de Carvalho et al., 2008), neurophysiological index (NI) (Swash and de Carvalho, 2004), transcranial magnetic stimulation (TMS) (Huynh et al., 2019, Vucic and Kiernan, 2017), and spectral electroencephalogram (EEG) have potential as biomarkers of LMN/UMN degeneration. About 40% of clinical interventional trials in ALS using the aforementioned neurophysiological measures as primary or secondary endpoint reported a positive outcome with respect to at least one neurophysiological measure (Ahmed et al., 2022).

MUNE/MUNIX, NI, and EMG biomarkers are widely used to identify LMN dysfunction in individuals after they are clinically suspected of ALS and also for excluding mimicking neurological disorders. However, these biomarkers alone cannot diagnose ALS without clinical support (Wijesekera and Leigh, 2009). MUNE/MUNIX has shown potential to quantify motor neuronal loss in ALS and track disease progression with high sensitivity

and reproducibility (Fukada et al., 2016, Jacobsen et al., 2019). Similarly, NI has been validated as a clinical meaningful measure for ALS prognosis with high sensitivity, favourable reproducibility, and low intraindividual variability (Swash and de Carvalho, 2004, Cheah et al., 2011).

Cortical hyperexcitability, which is a pathogenic and distinguishing feature of UMN degeneration in ALS, can be detected by using threshold-tracking paired pulse TMS in terms of reduced short-interval intracortical inhibition (SICI) and increased motor evoked potentials (MEP) (Vucic et al., 2011, Menon et al., 2020) or by using resting-state spectral EEG in terms of increased functional connectivity between the frontal-parietal cortical regions and bilateral motor regions (Iyer et al., 2015, Nasseroleslami et al., 2017, Dukic et al., 2019). EEG-based biomarkers of network degeneration can identify novel patient populations (Al-Chalabi et al., 2016), with indications of what brain networks should be targeted for therapeutic treatment. There is increasing evidence that TMS based biomarkers have potential to identify UMN dysfunction in ALS, even before UMN clinical symptoms arise, and to distinguish ALS from mimic disorders (Huynh et al., 2019, Vucic and Kiernan, 2017). However, TMS biomarkers are still in the research phase and need validation from more studies before they can be used as biomarkers of UMN dysfunction in ALS in clinical settings.

1.3 Thesis Outline

This thesis is organised as a 9-chapter document. This 1st chapter introduced about ALS and its various aspects such as epidemiology, genetics, phenotypes, multi-systemic nature, diagnosis, prognosis, and existing neurophysiological biomarkers. The 2nd chapter "Aims and Objectives" lists the aims and objectives of the research. The 3rd chapter "Literature Review" details the existing literatures about brain networks in ALS and the

neurophysiological underpinnings of the materials and methods used in this study. The 4th chapter is “Materials and Methods” which explains the equipment, experimental paradigms, and mathematical/statistical methods and tools used in the study and the rationale behind it. The 5th, 6th, 7th, and 8th chapters contain the results from the four different studies highlighting a different aspect of the research methodologically including introduction, methods, results, discussion, conclusion, and limitations. The 9th chapter is the overall discussions and conclusion of the research. Chapter 9 is followed by the list of the references used in this thesis which is followed by the additional materials used in the study as appendices.

2. Aims and Objectives

2.1 Aims

The primary aim of my PhD research was to utilize high-density EEG and surface EMG, known for their non-invasive electrophysiological properties in characterizing and measuring ALS pathology, to address the urgent need for more economical, accurate, and objective ALS biomarkers. EEG Functional/Effective connectivity and Corticomuscular coherence (CMC) served as the key measures, with the primary hypothesis being that these network connectivity measures could provide insights into specific alterations in the brain's motor networks, both within and beyond the primary sensorimotor cortex in ALS. By using these methods, I aimed to enhance our understanding of both motor and non-motor network pathology in ALS and explore their potential application in the development of prognostic and diagnostic ALS biomarkers. More specifically, I aimed to determine the following—

1. To characterize and measure the dysfunction in cortical networks in ALS during planning and execution of voluntary tasks.
2. To detect reduced or enhanced cortex-muscle synchrony in ALS using CMC.
3. To define reliable neurophysiological biomarkers of the integrity of cortical and spinal networks in ALS and to validate them against clinical scores, specifically ALSFRS-R.

2.2 Objectives

The objective of this research was to provide quantitative data that could support the identification of network-specific diagnostic and prognostic biomarkers in clinical settings. To achieve this, I conducted neuro-electrophysiological recordings, specifically high-density EEG, and surface EMG, along with neural signal analysis to examine the spectral characteristics and synchrony of the neuro-electric signals. The poorly understood

mechanism of network-based propagation in ALS has encouraged me to set the following objectives for this research—

2.2.1 Develop and validate a new method for the calculation of functional connectivity (coherence) between neuro-electric signals.

The rationale for developing a new method for the calculation of functional connectivity (coherence) is to harness the robustness of the non-parametric (median based) functional connectivity measure against artefacts (Dukic et al., 2017) and represent the collective connectivity strength with a single value over the range of frequencies within each distinct neurophysiological frequency band. More importantly, the new method utilises non-parametric rank statistics for coherence (Nasseroleslami et al., 2019) which presents connectivity strengths as p-values so there is no need for separate significance testing (close form solution or non-parametric bootstrapping) as required by other existing connectivity measures. Additionally, the new method is robust against the bias introduced by the number of epochs (L) used to estimate functional connectivity (Nasseroleslami et al., 2019).

We hypothesised that the new method of estimating functional connectivity provides stronger detection of network connectivity with a singular value for a frequency band, reducing the effect of volume conduction and be useful to identify abnormal network connections in patient groups.

2.2.2 Compare pre-motor stage and motor execution functional connectivity between an ALS cohort and age-matched healthy controls.

Functional connectivity of brain networks have the potential to detect and quantify disease specific adaptive and compensatory patterns of network activity. Prior to this study, the functional connectivity differences between ALS and age-matched controls during rest has

been investigated by our group reporting abnormal sensorimotor networks in ALS (Dukic et al., 2019). However, motor paradigms, such as pre-motor (motor planning) and motor execution that can directly access sensorimotor pathways, might be needed to unravel the dynamics of motor network pathology in ALS for better biomarker design. Therefore, understanding the impairment in functional motor networks is important to understand disease pathology because the motor region is predominantly affected by the neurodegeneration in ALS.

The involvement of cortical regions such as premotor cortex (PM) and supplementary motor area (SMA), which are largely associated with pre-movement or pre-motor activity (Churchland et al., 2006, Li et al., 2015, Shibasaki and Hallett, 2006, Glover et al., 2012), during motor execution indicates an alternative strategy for optimizing motor performance in ALS (Konrad et al., 2002). However, the alternative strategy or compensatory mechanism during pre-motor stage in ALS, which is impaired as reported by event related potential (ERP) studies (Thorns et al., 2010, Westphal et al., 1998), is unclear. So, we hypothesized that understanding the EEG network topology in ALS during pre-motor stage and motor execution could offer new insights for understanding motor network dysfunction that can be useful for biomarker development.

2.2.3 Compare effective connectivity and graph-based causal network parameters during motor planning and motor execution between an ALS cohort and age-matched healthy controls.

Effective connectivity refers to the directional influence and information flow between different brain regions, while graph-based causal network parameters such as inflow and outflow provide insights into the causal interactions within the brain networks. The rationale for comparing effective connectivity and graph-based causal network parameters

during motor planning and motor execution between an ALS cohort and age-matched healthy controls is to elucidate the dynamics of information processing and integration in sensorimotor neural circuits which may help shed light on the underlying pathophysiological mechanisms of ALS.

We hypothesize that individuals with ALS will exhibit altered effective connectivity and graph-based causal network parameters during both motor planning and motor execution compared to age-matched healthy controls. Specifically, we expect to observe disruptions in the directional information flow and graph-based measures within the motor networks of ALS cohort, indicating impaired neural communication and coordination during motor tasks. These alterations in effective connectivity and graph-based network parameters are likely to contribute to the motor deficits observed in ALS and may serve as potential neurophysiological biomarkers for the disease.

2.2.4 Compare the connections that links brain to muscles using Corticomuscular coherence (CMC) between an ALS cohort and age-matched healthy controls.

Studies have shown that beta CMC can provide valuable insights into the pathophysiology of ALS, as well as potential biomarkers for diagnosis and disease progression (Issa et al., 2017, Proudfoot et al., 2018b). Despite its potential as a biomarker for neurodegenerative diseases, CMC analysis is still premature, and there is much that remains to be understood about its correlation with ALS pathophysiology. Our recent sensor-level CMC studies on patient with lower motor neuron dysfunction such as post-polio syndrome (Coffey et al., 2021) and patients with upper motor neuron dysfunction, such as PLS (Bista et al., 2023), exhibit abnormal patterns of brain activity in frontal, parietal and non-dominant primary motor cortex (M1) including and beyond the beta band during voluntary movement. ALS being the disease where both upper and lower motor neurons are affected, we, therefore,

hypothesized that, impaired CMC could be detected beyond the beta frequency band and dominant M1 in ALS and CMC could be a tool to reveal multiple aspects of motor network dysfunction (such as motor planning, sensorimotor integration, and visuomotor integration) in ALS.

3. Literature Review

3.1 Structural Connectivity

Structural connectivity pertains to the way the brain is anatomically organized through fibre tracts. Recent developments in magnetic resonance imaging (MRI) and image processing have introduced several non-invasive methods for quantifying structural connectivity. These techniques utilize short-range local measures and long-range tract tracing procedures, known as diffusion tractography (Babaeeghazvini et al., 2021). Understanding the underlying structural connectivity alterations in ALS can help unravel the disease's pathophysiology and identifying potential therapeutic targets. Structural connectivity helps to uncover the specific white matter tracts and brain regions affected by neurodegeneration, elucidating how the disease spreads and progresses over time. This section aims to provide an overview of the current knowledge regarding structural connectivity changes in ALS, highlighting the techniques used to assess these alterations, their clinical implications, and their limitations.

3.1.1 Quantitative Techniques for Assessing Structural Connectivity

The assessment of structural changes of brain networks in ALS using conventional clinical magnetic resonance imaging (MRI) is challenging (Zhang et al., 2003, Renga, 2022). Therefore, research studies rely on quantitative techniques such as diffusion tensor imaging (DTI) (Baek et al., 2020, Behler et al., 2023), cortical thickness mapping (Agosta et al., 2012, Ferrea et al., 2021, Dieckmann et al., 2022), or MRI spectroscopy (Kalra, 2019, Caldwell and Rothman, 2021) which can provide clinically relevant quantitative measures of structural network impairment in ALS. The most commonly used quantitative neuroimaging techniques and measures to access structural connectivity in ALS are explained in this section.

2.1.1.1 Diffusion Tensor Imaging (DTI)

DTI is the most popular technique for structural connectivity analysis in ALS. DTI is primarily used to assess microstructural brain changes by examining water molecule motility within tissue and relies on determining the orientation and diffusion characteristics of white matter (Acosta-Cabronero et al., 2010). Recent improvements in DTI resolution allow for the identification of pathology-specific details, such as changes in axons and myelin in brain white matter (Zeineh et al., 2012). Various DTI parameters derived from raw DTI data, such as fractional anisotropy (FA), axial diffusivity (AD), radial diffusivity (RD) and mean diffusivity (MD), capture different pathological changes in ALS (Baek et al., 2020). Among them, FA is the most used DTI parameter, offering insights into the number and size of axon fibres and the density of crossing fibres (Roberts et al., 2013). In ALS, DTI studies have shown reductions in FA in both motor and extra-motor regions (Müller et al., 2016, Andica et al., 2020), with FA proving to be a sensitive and specific metric (biomarker) for diagnosis (Baek et al., 2020, Tahedl et al., 2021) and disease progression (Kassubek et al., 2018, Menke et al., 2018).

Despite its widespread application in various clinical conditions (Tae et al., 2018, Baek et al., 2020, Oishi et al., 2011), the semiquantitative nature of DTI data analysis poses a significant limitation (Oishi et al., 2011, Tae et al., 2018) because DTI parameters are influenced by scanner acquisition parameters such as voxel size, signal-to-noise ratio, gradient strength and echo time. Additionally, DTI is sensitive to noise and artifacts, which can affect the accuracy of diffusion measurements and subsequent tractography especially when studying small or subtle changes in white matter integrity (Jones and Cercignani, 2010).

3.1.1.2 Cortical Thickness Mapping

Cortical thickness mapping is a neuroimaging technique that utilizes structural MRI scans to measure the thickness of the cerebral cortex, enabling detection of changes in cortical thickness and identification of potential diagnostic markers in neurodegenerative and psychiatric disorders (Fischl and Dale, 2000). Cortical thickness studies have reported cortical thinning of motor and extra-motor cortices in ALS compared to healthy controls (Chen et al., 2018, Verstraete et al., 2012). The thinning of primary motor cortex or precentral gyrus was dominant in ALS with clinical UMN involvement (Walhout et al., 2015) and correlated to the speed of disease progression i.e., patient with faster disease progression experienced a more severe M1 thinning (Agosta et al., 2012). A distinct trajectory of cortical thinning at right fronto-temporal insular cortex was reported by Consonni et al. (2020) in relation to King's clinical disease stages suggesting a distinct pattern of spread of neurodegeneration in ALS. Similarly, a multimodal longitudinal study of structural brain involvement in ALS, with cortical thickness and other measures, reported distinct patterns of cerebral degeneration based on phenotype and C9orf72 genotype (van der Burgh et al., 2020). The cortical thickness of precentral gyrus and temporal lobe, which showed significant cortical thinning, has been used to distinguish ALS from healthy controls and UMN/LMN ALS phenotypes resulting in an accuracy of 94% and 75%, respectively (Ferrea et al., 2021). Cortical thickness has also been used as a feature and was shown to have higher contribution within multimodal machine learning models to improve diagnostic accuracy of ALS compared to disease controls (non-ALS neurodegenerative diagnosis) and healthy controls (Bede et al., 2022, Wirth et al., 2018, Pisharady et al., 2023).

3.1.1.3 Magnetic Resonance Spectroscopy (MRS)

Magnetic Resonance Spectroscopy (MRS) is a non-invasive neuroimaging technique used to analyse the neurochemical composition of brain tissues (Radda et al., 1989). It offers insights into neurotransmitters such as glutamate/GABA and metabolites such as N-acetylaspartate (NAA), providing valuable information on neurochemical changes associated with the ALS (Caldwell and Rothman, 2021). Glutamate excitotoxicity is increasingly believed to be a key mechanism implicated in the pathogenesis of ALS (Van Den Bosch et al., 2006, King et al., 2016), however, some believe that the elevated level of extracellular glutamate is beneficial to ALS (Schiel, 2021). MRS studies in ALS have revealed decreased NAA, reflecting neuronal loss or dysfunction in motor cortex (Foerster et al., 2013, Atassi et al., 2017) and corticospinal tracts (Stagg et al., 2013), as well as a reduced level of inhibitory neurotransmitter GABA in motor cortex (Foerster et al., 2013, Foerster et al., 2012a). The levels of change in excitatory neurotransmitters such as glutamate (Glu) in the motor cortex of ALS patients have been reported rather inconsistently by MRS studies. For example, Atassi et al. (2017) reported decreased levels of Glu in the precentral gyrus of people with ALS compared to healthy controls. On the other hand, Han and Ma (2010) reported increased levels of Glu and Foerster et al. (2013) reported normal levels of Glu in the motor cortex of ALS compared to healthy controls. Although, there is some inconsistencies about the level of Glu in ALS, majority of the MRS studies has reported increased neuronal Glu level (Caldwell and Rothman, 2021) supporting the hypothesis of Glu excitotoxicity in ALS. These neurochemical changes identified by MRS hold promise as biomarkers for early diagnosis, monitoring disease progression, and assessing treatment effects in ALS (Kalra, 2019). While MRS has limitations of low temporal and spatial resolution (Serkova and Brown, 2012), it remains a

valuable tool for understanding the neurobiology of ALS and has potential as a research and diagnostic tool (Caldwell and Rothman, 2021).

3.1.2 White Matter Alterations in ALS

White matter abnormality has been widely documented in ALS. Studies using DTI have consistently reported reduced fractional anisotropy (FA) and increased mean diffusivity (MD) compared to healthy controls indicating disrupted white matter integrity in various regions, including the corticospinal tract, corpus callosum, frontal regions, brainstem and hippocampal regions (Baek et al., 2020, Müller et al., 2016, Li et al., 2012). The corticospinal tract, which is crucial for motor function, demonstrates pronounced white matter alterations, likely contributing to the motor impairments observed in ALS (Müller et al., 2016, Sarica et al., 2014, Metwalli et al., 2010). A multi-centre longitudinal study has reported decline in white matter integrity in corticospinal tract over time in ALS patients compared to healthy controls (Kalra et al., 2020). Additionally, alterations in the corpus callosum, a major white matter pathway connecting the two cerebral hemispheres, have been reported in ALS patients compared to healthy controls and may be linked to the spread of pathological changes between brain regions (Sage et al., 2009, Bede et al., 2013b). Moreover, white matter alterations have also been observed in frontotemporal pathways (Agosta et al., 2017, Bede et al., 2013b) in ALS with C9orf72 genotype compared to C9orf72-negative reflecting the overlap between ALS and frontotemporal dementia (FTD). Furthermore, the correlation between white matter changes and clinical measures of disease severity and progression reinforces the clinical relevance of these neuroimaging findings (Kalra et al., 2020). White matter alterations have been linked to motor functions (Thivard et al., 2007, Sage et al., 2009, Agosta et al., 2010a), cognitive and behavioural measures (Agosta et al., 2016) and survival rates (Schuster et al., 2017, Agosta et al., 2010a)

in ALS patients, suggesting their potential as biomarkers for the diagnostic pathway and the prognostic stratification of patients (Agosta et al., 2016).

3.1.3 Network-Level Connectivity Alterations

ALS affects multiple brain regions including motor and extra-motor regions structurally (Baek et al., 2020), therefore, studying structural connectivity alterations in ALS can provide insights into the disease's overall effects. This section focuses on network-based approaches, such as graph theory analysis, to understand the alterations in structural connectivity networks in ALS. Connectomics, a field based on graph theory, provides a valuable tool for analysing the organization of cerebral networks and understanding the relationships between brain regions (Sporns et al., 2005). Graph analysis and connectomics involve representing brain regions as nodes connected by edges representing structural connections, with cortical and subcortical brain regions represented as nodes and white matter tracts between them represented as the edges. The human connectome exhibits non-random features, including highly connected regions known as hubs (Achard et al., 2006). These hubs play a crucial role in integrative processing and adaptive behaviours and are vulnerable to neurodegeneration (van den Heuvel et al., 2013, Proudfoot et al., 2019). While many brain disorders, such as brain injury (Warren et al., 2014), Parkinson's disease (Baggio et al., 2014), FTD (Agosta et al., 2013), Alzheimer's disease (Dai et al., 2014) or schizophrenia (Shi et al., 2012, Rubinov and Bullmore, 2013) exhibit a hub-centred pattern, this finding is not evident in ALS connectivity studies (Fortanier et al., 2019, Crossley et al., 2014). In terms of global network parameters such as global efficiency and clustering coefficients, the white matter structural network studies have reported inconsistent findings. For example, Dimond et al. (2017) reported preserved global efficiency, while Buchanan et al. (2015) reported no significant difference in clustering coefficient and

global efficiency in ALS compared to healthy controls. On the other hand, Fortanier et al. (2019) reported significant decreased global efficiency and Li et al. (2021) reported significant decreased clustering coefficient in ALS compared to healthy controls. In terms of brain regions (nodes) in the structural network, studies have reported impairment in both motor (Verstraete et al., 2011, Verstraete et al., 2014, Li et al., 2021) and extra-motor regions (Buchanan et al., 2015, Dimond et al., 2017, Li et al., 2021). Until now, there have been limited longitudinal studies focusing on how ALS affects the structural brain network over time. Previously, a study by Verstraete et al. (2014) revealed an increasing loss of network structures after six months, with a key involvement of the primary motor regions. The loss of structural connectivity extended to frontal and parietal regions, indicating that the disease may spread through motor neuron networks, starting in specific regions of the brain or spinal cord and gradually affecting neighbouring neurons (Bede et al., 2013a, Brettschneider et al., 2013). Recently, a longitudinal study has reported loss of white matter integrity over time in regions connected to the motor cortex in a subgroup of ALS with short disease duration (<10 months)(Burgh et al., 2020) .

3.1.4 Clinical Implications

The study of structural connectivity changes in ALS has significantly advanced our understanding of the pathophysiology and underlying mechanisms of progressive neurodegeneration in ALS and has indicated potential biomarkers for diagnosis, disease stratification, and monitoring disease progression (Baek et al., 2020, Kalra, 2019, Agosta et al., 2016). However, the main challenge lies in integrating these biomarkers into clinical trials as study endpoints and clinical practice. So far, results have been promising but highly variable due to small sample sizes, suboptimal patient characterization, and lack of standardization in schemes and analysis procedures (Menke et al., 2017). Although, the FA

changes in corticospinal tract have consistently been reported by the DTI studies, their ability to differentiate patients from healthy controls is not promising (pooled sensitivity 65%) as reported by a meta-analysis of 30 studies (Foerster et al., 2012b). However, a diagnostic accuracy as high as 80% has been reported by studies using ALS vs healthy controls machine learning models and white matter diffusivity measures (Sarica et al., 2017, Bede et al., 2022). Additionally, a few multi-centre studies have shown that using a harmonized imaging protocol across multiple sites and pooling data together could be the way going forward for having a clinically useful biomarker for therapeutic outcome (Müller et al., 2016, Kalra et al., 2020). Therefore, using machine learning models on multimodal imaging data from multiple sites could pave the way for finding novel biomarkers for diagnosis, disease stratification, and monitoring disease progression.

3.2 Functional Connectivity

The study of functional brain connectivity is crucial in ALS, despite promising results from studies of structural connectivity. ALS is a complex neurodegenerative disease with both structural and functional brain impairments (Basaia et al., 2020). While structural connectivity studies provide insights into the anatomical connections between brain regions, functional connectivity highlights the interactions and communication between these regions during different tasks and states (Lang et al., 2012). Functional connectivity measures, such as resting-state functional magnetic resonance imaging (fMRI) or resting-state electroencephalogram (EEG), have shown promise in identifying specific patterns of brain activity that correlate with ALS progression and clinical features (Dukic et al., 2019, Bharti et al., 2022). These functional network biomarkers have the potential to serve as valuable indicators of disease at the early symptomatic phase (Govaarts et al., 2022), of disease severity (Sorrentino et al., 2018), disease progression (Castelnovo et al., 2020),

phenotyping (Dukic et al., 2021), and response to treatment (Wei et al., 2022a). Early detection of functional disruptions may enable early diagnosis and intervention, leading to improved patient outcomes, and monitoring functional changes over time can provide insights into disease progression and treatment efficacy. The following section describes the tools and techniques for accessing functional connectivity of the brain in health or in disease.

3.2.1 Techniques for Assessing Functional Connectivity

3.2.1.1 Functional Magnetic Resonance Imaging (fMRI)

Functional Magnetic Resonance Imaging (fMRI) is a non-invasive neuroimaging technique that relies on the blood oxygen level-dependent (BOLD) signal, which reflects changes in blood flow and oxygenation related to neural activity (Ogawa et al., 1990). By measuring changes in BOLD signal, fMRI can identify brain regions that are functionally connected and communicate with each other during specific tasks or at rest (Biswal et al., 1995, Fox and Raichle, 2007). Resting-state fMRI (rs-fMRI) captures the brain's spontaneous BOLD signal fluctuations while participants are at rest, revealing functionally connected brain regions without the need for specific tasks (Fox and Raichle, 2007). Task-based fMRI involves measuring BOLD signal changes during specific cognitive, motor, or sensory tasks to identify task-specific functional networks (Biswal et al., 1995). Seed-based correlation is a commonly used method in fMRI to analyse functional connectivity, where a seed region's BOLD signal is correlated with other brain regions to identify connected networks (Glover, 2011). Independent Component Analysis (ICA) (Wei et al., 2022b) and graph theory analysis (Medaglia, 2017) are also employed to study functional connectivity, providing insights into the spatial patterns of coherent BOLD activity. fMRI has significantly advanced our understanding of functional connectivity in various neurological

disorders, including ALS, facilitating investigations into disease-related alterations in functional brain networks and their implications for cognitive and motor functions (Du et al., 2018, Filippi et al., 2019).

3.2.1.2 Magnetoencephalogram (MEG)

Magnetoencephalography (MEG) is a non-invasive neuroimaging technique that measures the magnetic fields generated by electrical activity of neurons using highly sensitive sensors called magnetometers placed outside the skull (Cohen, 1972). The magnetic fields generated by electric currents in the brain is extremely small, in the range of femto-tesla to pico-tesla, which requires highly sensitive magnetic field meters such as superconducting quantum interference devices (SQUIDS) (Hämäläinen et al., 1993). Therefore, MEG is recorded in a magnetically shielded room to attenuate the external magnetic noise. The sensor level MEG signals are converted into source level signals using source localisation techniques which overcome the effect of field spread (Schoffelen and Gross, 2009). The functional connectivity between different brain regions using MEG is commonly assessed through coherence analysis, which measures the neuronal amplitude or phase synchrony between the brain regions (Gross et al., 2001). Other methods such the imaginary part of coherence (iCOH) (Brookes et al., 2011), the phase lag index (PLI) (Stam et al., 2007), and the weighted phase lag index (wPLI) (Vinck et al., 2011) are also used to evaluate functional brain networks using MEG. MEG has been used to investigate functional connectivity in healthy individuals and various neurodegenerative disorders such as Alzheimer's disease (Schoonhoven et al., 2022, Stam et al., 2008) or motor neurone disease (Proudfoot et al., 2018a, Sorrentino et al., 2018), offering insights into pathological brain networks.

3.2.1.3 Electroencephalogram (EEG)

Electroencephalography (EEG) is a low-cost non-invasive technique which is pivotal for unravelling real-time functional brain connectivity, with recent advancements in high density montage (up to 256 channels) and source reconstruction techniques enhancing its spatial resolution (Burle et al., 2015). EEG captures neuronal electrical activity at the scalp, providing insights into the functional interactions among brain regions during rest (Dukic et al., 2019), cognitive (McMackin et al., 2021), or motor tasks (Coffey et al., 2021). Source reconstruction techniques (Kaur et al., 2022) enable the estimation of the neural sources underlying the observed scalp EEG signals, significantly minimizing the effect of volume conduction, increasing spatial resolution, and revealing the specific brain regions engaged in functional networks. Functional connectivity analysis using EEG involves assessing temporal correlations or synchronization patterns between EEG or between EEG and muscle signals (EMG) at sensor or source level. Methods like coherence, phase synchronization, and mutual information can quantify connection strength, offering insights into EEG functional connectivity (Cao et al., 2022). In the study of neurodegenerative conditions like ALS, EEG-based functional connectivity analysis can reveal disease effects on brain network integrity (Dukic et al., 2019), assisting early diagnosis (Iyer et al., 2015), tracking disease progression (Nasseroleslami et al., 2017), and phenotyping based on neurophysiological signatures (Dukic et al., 2021).

3.2.1.4 Surface Electromyogram (sEMG)

Surface electromyography (sEMG) serves as a valuable non-invasive technique for investigating functional connectivity, especially in the context of voluntary motor tasks in the realm of motor control. sEMG records electrical activity during muscle contractions, offering insights into coordinated muscle actions and the neural pathways underlying motor

tasks. sEMG is recorded with surface electrodes strategically positioned on skin regions directly above the targeted muscle tissue being assessed. Through simultaneous recording of sEMG signals from multiple muscles and EEG/MEG signals from the brain during voluntary movements, techniques like coherence analysis can reveal functional connectivity between the muscle groups (Weersink et al., 2021) or between brain and muscles (Roeder et al., 2020). In the study of neurodegenerative disorders such as ALS/PLS, sEMG-based functional connectivity analysis such as intermuscular coherence (IMC) has provided insights into how UMN involvement impacts muscle synchronization (Issa et al., 2017, Fisher et al., 2012). Additionally, sEMG-EEG/MEG functional connectivity analysis such as Corticomuscular coherence (CMC) has provided insights into the involvement of extra-motor regions and dysfunctional corticospinal tract in ALS (Proudfoot et al., 2018b) and PLS (Bista et al., 2023). Despite being susceptible to noise such as cross talk, electrical and mechanical artefacts (Türker, 1993), sEMG-based analysis, when combined with other modalities such as EEG or MEG, can contribute to a comprehensive understanding of neural mechanisms of motor control in healthy people or in people with movement disorders (Liu et al., 2019).

3.2.1.5 Positron Emission Tomography (PET)

Positron Emission Tomography (PET) is a non-invasive neuroimaging technique that primarily focuses on measuring cerebral blood flow, glucose metabolism, and neurotransmitter receptor binding, providing insights into brain functions (Berger, 2003). While PET is commonly used for assessing regional brain activity based on local change in blood flow (Raichle, 1998), recent studies have explored its potential to offer insights into functional connectivity among different brain regions (Watabe and Hatazawa, 2019). PET studies employing resting-state paradigms have identified correlated regional brain

activities referred to as default mode network (DMN) (Raichle et al., 2001), which is equivalent to resting-state functional networks observed in techniques like fMRI (Greicius et al., 2003), indicating synchronized intrinsic activity during rest (Raichle and Mintun, 2006). Additionally, PET has been used to study glucose metabolic connectivity, examining how metabolic activity in one region correlates with others, revealing potential functional connections between those regions (Passow et al., 2015). Furthermore, PET has been used to study specific neurotransmitter systems such as Glutamate (DeLorenzo et al., 2015) or GABA (Stokes et al., 2014) indirectly providing information about connectivity among regions involved in those pathways. In case of neurodegenerative diseases such as ALS, PET studies have reported glucose hypometabolism in sensorimotor cortices (Hatazawa et al., 1988), bilateral frontal lobes (Jeong et al., 2005), and thalamus (Cistaro et al., 2014) and hypermetabolism in brainstem (Liao et al., 2020), and cerebellum (Liao et al., 2020) compared to healthy controls suggesting its potential for clinical utility as diagnostic biomarker (Agosta et al., 2018). For a detailed review of PET in ALS, see the review by Chew and Atassi (2019). However, it is important to consider the limitations of PET, including lower temporal resolution compared to techniques like fMRI, and constraints related to radioactive tracers and radiation exposure (Sander and Hesse, 2017).

3.2.1.6 Functional Near-Infrared Spectroscopy (fNIRS)

Functional near-infrared spectroscopy (fNIRS) is a non-invasive neuroimaging technique that measures changes in the concentration of oxygenated, deoxygenated, and total haemoglobin using pairs of light sources and detectors on the scalp, reflecting functional interaction between different brain regions during rest or task (Villringer et al., 1994). Resting-state fNIRS studies have been used to study functional brain reorganisation during recovery from stroke (Arun et al., 2020), to evaluate the degree of damage to executive

function in people with neurocognitive disorder after traumatic brain injury (Chang et al., 2022), to understand typical and atypical development of functional brain networks and topological organization from neonates to children (Hu et al., 2020), or access the involvement of non-motor areas in ALS (Borgheai et al., 2019). Similarly, fNIRS has been used in task paradigms to study neural correlates of motor control in healthy people (Koenraadt et al., 2014) and people recovering from hemiplegic stroke (Fujimoto et al., 2014), or cognitive decline in people with ALS compared to healthy controls (Kuruvilla et al., 2013). While fNIRS has the advantage of being portable, less susceptible to motion artifacts than MEG or fMRI, and well-suited for various populations, it also has limitations such as its shallow penetration depth and sensitivity to superficial cortical regions (Pinti et al., 2020). Nevertheless, fNIRS remains a valuable technique for studying functional brain connectivity, providing a non-invasive and accessible window into the complex interactions between different brain areas in health and in disease (Ferrari and Quaresima, 2012).

3.2.2 Comparison of techniques used for assessing functional connectivity

The properties of techniques used for assessment of functional brain networks are summarised in Table 2.1. Each of these techniques has its strengths and limitations and the choice of technique depends on the available resources and the balance between spatial and temporal resolution needed to address the specific scientific question related to functional connectivity. Having said that, EEG's high temporal resolution, the availability of robust source localisation methods to improve spatial resolution, its ability to measure neural activity directly in real time, its non-invasiveness, affordability, and suitability for various research settings during rest or tasks make it a valuable and frequently used technique for studying functional connectivity in neurodegenerative disease such as ALS.

Table 3.1 Comparison of imaging techniques used for assessing functional connectivity. Summarized from Sadaghiani et al. (2022).

Imaging Modality	Cost	Spatial Resolution	Temporal Resolution	SNR	Operational Complexity
fMRI	High	Good (1-2 mm)	Moderate (2-3 s)	High	Complex
MEG	High	Moderate (2-3 cm)	Excellent (ms)	High	Complex
EEG	Low	Moderate (2-3 cm)	Excellent (ms)	Low to Moderate	Low
sEMG	Low	Excellent (mm)	Excellent (ms)	High	Low
PET	High	Moderate (4-6 mm)	Poor (20-40 s)	Moderate to High	Complex
fNIRS	Low	Moderate (cm)	Good (ms)	Moderate	Low

Abbreviations: MEG, magnetoencephalography; fMRI, functional magnetic resonance imaging; EEG, electroencephalography; sEMG, surface electromyography; PET, positron emission tomography; fNIRS, functional near-infrared spectroscopy; SNR, signal-to-noise ratio

3.2.3 Methods for Accessing Functional Connectivity

3.2.3.1 Correlation Analysis

This is a simple statistical method of estimating functional connectivity between brain regions most common with fMRI data. Pairwise correlations are computed between the time series of different brain regions, or a 'seed' region is chosen as a point of interest, and the correlation between the time series of this seed region and the time series of other brain regions is calculated. A significant correlation between two time series indicates that those brain regions are functionally connected. The most common measure used is Pearson correlation coefficient, which measures the linear relationship between two time series. Other correlation measures like Spearman's rank correlation or Kendall's tau are also used, especially when the data are non-normally distributed. Studies have shown that the functional connectivity estimated by non-parametric methods such as Spearman's rank

correlation or Kendall's tau are superior to Pearson correlation for differentiating disease from health (Ahmadi et al., 2023). For EEG/MEG data, functional coupling is also estimated by correlating amplitude envelop between two narrow-band time series referred to as amplitude envelop correlation (AEC) (Bruns et al., 2000).

3.2.3.2 Magnitude Squared Coherence

Magnitude squared coherence (MSC) is one of the most popular methods of estimating functional connectivity using EEG/MEG. It measures squared correlation coefficient in frequency domain that estimates relative amplitude and phase consistency between two signals (Bendat and Piersol, 2011). In practice, EEG/MEG coherence depends mostly on the consistency of phase differences between the channels (Nunez, 1995). High magnitude squared coherence between two EEG/MEG channels indicate that brain regions associated with those channels are functionally connected with each other. Although coherence is widely used method to assess functional connectivity in the brain using EEG/MEG, a significant limitation the method possess is the interference caused by volume conduction through the tissues that separate the brain sources and electrodes. This causes superfluous coherence between the nearby electrodes and overestimation of functional connectivity. However, this limitation can be partly overcome by using surface Laplacian filtering of the EEG/MEG channels (Bradshaw and Wikswo, 2001). The surface Laplacian technique isolates the source activity under each electrode that is distinct from the surrounding tissue under adjacent electrodes. Therefore, the coherence measured between electrodes that underwent surface Laplacian filtering can be directly related to coherence between the underlying sources, facilitating the interpretation of functional connectivity in the brain. However, surface Laplacian may remove genuine source coherence associated with widely

distributed source regions and very low spatial frequencies, leading to potential loss of important neural information (Nunez and Srinivasan, 2006).

3.2.3.3 Imaginary Coherence

Imaginary coherence (iCOH) is another popular method for the estimation of functional connectivity between neural signals recorded by EEG/MEG. Its popularity is based on the fact that it is robust to the effect of volume conduction and measures true phase synchrony between the neural signals disregarding the amplitude information (Nolte et al., 2004). Unlike magnitude squared coherence, which considers both phase and amplitude, imaginary coherence exclusively captures phase relationships, making it particularly suitable for studying the temporal coordination of neural oscillations. By focusing on the phase component of the signals, imaginary coherence can attenuate spurious coherence caused by volume conduction because volume conduction tends to preserve the amplitude of neural signals but not their phase relationships (Shahbazi et al., 2010).

3.2.3.4 Phase Lag Index

Phase lag index (PLI) is a measure that evaluates the asymmetry of distribution of instantaneous phase differences between two signals, thereby reflecting the strength of functional interconnection between the underlying brain regions (Stam et al., 2007). Just like imaginary coherence, PLI is motivated by the fact that non-zero phase differences cannot be caused by volume conduction. Several studies have demonstrated the effectiveness of PLI in mitigating the effects of volume conduction and have shown that it provides more accurate estimates of functional connectivity compared to imaginary coherence, particularly in the presence of volume conduction artifacts (Ruiz-Gómez et al., 2019, Stam et al., 2007). Vinck et al. (2011) has proposed some adjustments to the PLI, yielding the weighted PLI (wPLI) make the metric more robust against volume conduction,

and noise. wPLI modifies the PLI by weighting the contribution of observed phase leads and lags by the magnitude of the imaginary component of the cross-spectrum, making it sensitive to additional, uncorrelated noise sources and increasing its capacity to detect true changes in phase-synchronization.

3.2.3.5 Independent Component Analysis

Independent component analysis (ICA) is a powerful data-driven method for estimating functional connectivity (often using fMRI data). The fundamental concept of ICA involves decomposition of a time series into a set of distinct and interrelated time sequences to identify groups of voxels or areas that exhibit simultaneous fluctuations over time or activation across experiments (rest or task). Consequently, each component represents a network of regions demonstrating functional connectivity with one another (Eickhoff and Müller, 2015).

3.2.3.6 Mutual Information

The methods such as correlations, MSC, iCOH and PLI for measuring functional connectivity estimate a linear relationship between the neuronal sources. However, the communication between the neuronal sources is not always linear. To quantify nonlinear coupling between the brain source, information theory-based methods such as mutual information (MI) can be used (Ostwald and Bagshaw, 2011). This approach helps uncover both linear and nonlinear patterns of neural communication and can reveal underlying functional networks within the brain, contributing to better understanding of brain function and connectivity in health and in disease (Ince et al., 2017).

3.2.4 Resting-state Functional Networks Impairments in ALS

Resting state functional connectivity (FC) has been used to identify abnormal brain networks in ALS compared to healthy controls (Nasseroleslami et al., 2017, Dukic et al.,

2019) and to monitor disease progression (Menke et al., 2018, Iyer et al., 2015). Reduced FC has been reported by fMRI (Trojsi et al., 2023, Avyarthana et al., 2023, Barry et al., 2021, Zhou et al., 2014) and EEG (Dukic et al., 2019) studies within resting state sensorimotor networks (networks that include somatosensory regions and motor regions, specifically M1 and S1) in ALS, when compared to healthy individuals. This reduced FC of sensorimotor networks was correlated to high disease severity as indicated by lower ALSFRS-R scores (Zhou et al., 2014, Dukic et al., 2019). On the other hand, a higher resting state FC was observed within motor and non-motor areas (brain regions that are not primarily involved in the control and execution of voluntary movements, such as prefrontal cortex, temporal cortex, parietal cortex etc.) in ALS compared to healthy controls by fMRI (Deligani et al., 2020, Basaia et al., 2020, Zhou et al., 2014), EEG (Nasseroleslami et al., 2017, Iyer et al., 2015) and MEG studies (Proudfoot et al., 2018a, Govaarts et al., 2022) and this increased cortical FC was subjected to altered intracortical inhibition resulting in cortical hyperexcitability in ALS compared to healthy controls (Proudfoot et al., 2018a, Iyer et al., 2015, Govaarts et al., 2022). Additionally, longitudinal studies using fMRI have shown decreased FC in the resting state sensorimotor network and increased FC in the left fronto-parietal network over time (Menke et al., 2018, Castelnovo et al., 2020). A fronto-parietal network FC increase over time in ALS in the gamma band was also reported by an EEG study (Nasseroleslami et al., 2017). In terms of network topology from graph analysis of FC measures of M/EEG, the nodal strength was reduced in ALS compared to healthy controls in alpha (Romano et al., 2022) and beta (Fraschini et al., 2016) frequency bands. Moreover, resting state EEG FC networks have been used in phenotyping ALS in four sub-groups based on distinct neurophysiological profiles such as impairment of sensorimotor, frontotemporal and frontoparietal networks (Dukic et al., 2021).

These findings collectively highlight altered FC patterns in ALS compared to healthy controls in terms of brain regions involved, temporal characteristics, connectivity strength and network topology, as observed through various FC methods and neuroimaging techniques (See Table 3.2). These studies were identified by searching over the databases (PubMed, Google Scholar, and Scopus) using the combinations of keywords such as 'resting state', 'functional connectivity', 'ALS', 'EEG', 'MEG', 'fMRI' and 'fNIRS' and filtered by date to exclude publications that were published before 2014.

Table 3.2 Resting state functional network impairments in ALS. FC— Functional connectivity, HC— Healthy controls, fMRI— functional magnetic resonance imaging, EEG— Electroencephalography, MEG— Magnetoencephalography, fNIRS— functional near-infrared spectroscopy.

Reference; Modality; Participants; FC Method	**Findings**
Zhou et al., 2014; fMRI; 12 HC, 12 ALS; Coherence	ALS showed reduced FC in the right sensorimotor network (postcentral/precentral/superior frontal gyrus) compared to HC, which was correlated with high disease severity (as indicated by lower ALSFRS-R scores). On the other hand, ALS showed higher FC in the left sensory network (postcentral gyrus and inferior parietal cortex) compared to HC, which was related to longer disease duration.
Iyer et al., 2015; EEG (Source level); 17 HC, 18 ALS; Cross spectral density	FC was higher in ALS compared to HC in the parietal region in the theta and alpha bands.
Fraschini et al., 2016; EEG (Sensor level); 16	Network topology parameters such as leaf fraction were significantly lower in ALS compared to HC in the beta

HC, 21 ALS; Phase lag index and graph analysis	band. ALS network topology tended to deviate from more centralized (star-like topology) to more decentralized (line-like topology).
Nasseroleslami et al., 2017; EEG (Sensor level); 34 HC, 100 ALS; Median Coherence	Widespread increases in average connectivity in ALS compared to HC with most notable increase detected over bilateral motor regions in the theta band and parietal and frontal regions in the gamma band.
Menek et al., 2018; fMRI; 13 ALS; ICA and Regression analysis	Progressive decreases in resting state FC between the sensorimotor and frontal pole, between a network comprising thalamic and an area in the visual cortex over time and in relation to ALSFRS-R decline. Progressive increases in resting state FC between the left primary motor cortex and the left fronto-parietal networks over time and in relation to ALSFRS-R decline.
Proudfoot et al., 2018; MEG (Source level); 24 HC, 24 ALS; Correlations	FC was higher throughout the cortical networks in ALS compared to HC, particularly in posterior cingulate cortex.
Dukic et al., 2019; EEG (Source level); 47 HC, 74 ALS; Imaginary Coherence	Reduced FC in the sensorimotor region in the beta band and in frontal and temporal regions in the delta band in ALS compared to HC.
Basaia et al., 2020; fMRI; 79 HC, 173 ALS; Pearson's Correlation and graph analysis	Increased local FC (pair-wise functional connectivity between the nodes within a same region) was observed in ALS in the precentral, middle, and superior frontal areas compared to HC.
Castelnovo et al., 2020; fMRI; 39 HC, 25 ALS; Regression analysis	After 6 months from baseline fMRI scan, ALS showed reduced FC of the right middle frontal gyrus (MFG) with frontoparietal regions compared to HC. After 6 months from baseline, ALS showed an increased FC of left anterior cingulate, left MFG and left superior frontal gyrus within the frontostriatal network, and left MFG,

	left supramarginal gyrus and right angular gyrus within the left fronto-parietal network.
Deligani et al., 2020; EEG/fNIRS; 9 HC, 10 ALS; Coherence for EEG FC, Pearson's correlation for fNIRS FC	Increased fronto-parietal EEG connectivity in the alpha and beta bands and increased interhemispheric and right intra-hemispheric fNIRS connectivity in the frontal and prefrontal regions observed in ALS compared to HC.
Dukic et al., 2021; EEG (Source level); 77 HC, 95 ALS; Amplitude envelope correlation and imaginary coherence	ALS were sub-grouped into four phenotypes with distinct neurophysiological profiles characterized by disruption in the somatomotor (increased alpha band FC), frontotemporal (increase beta-band power and decreased gamma-band FC) and frontoparietal (increased gamma-band FC) networks, which correlated with distinct clinical profiles and different disease trajectories.
Barry et al., 2021; fMRI; 9 HC, 12 ALS; Correlation	Reduced FC between bilateral cerebellar lobule VI and sensorimotor cortex in ALS compared to HC.
Romano et al., 2022; MEG (Source level); 39 HC, 39 ALS; Phase linearity measurement	Nodal strength in the alpha band was reduced in ALS compared to HC in the right inferior parietal lobule, right cuneus, right parahippocampal gyrus, and left amygdala in the alpha band.
Govaarts et al., 2022; MEG (Source level); 18 HC, 34 ALS; Amplitude envelope correlation	FC was higher in frontal, temporal, limbic and sub-cortical regions in delta and gamma frequency bands in ALS compared to HC.
Avyarthana et al., 2023; fMRI; 52 HC, 52 ALS; Correlation	ALS showed reduced functional connectivity between primary motor cortex and primary sensory, premotor, supplementary motor, frontal, temporal, and putamen regions compared to HC.

Trojsi et al., 2023; fMRI; 26 HC, 26 ALS; Independent component analysis (ICA)	*Sensorimotor networks*: ALS patients showed reduced FC in left medial frontal gyrus (MFG), and in the left postcentral gyrus compared to HC. *Default mode networks*: ALS patients showed reduced FC in right MFG and left precuneus and higher FC in the left middle temporal gyrus compared to HC. *Frontoparietal networks*: ALS showed reduced FC in right and left MFG and in the left inferior frontal gyrus compared to HC. *Salience networks:* ALS patients showed reduced FC in the right and left anterior insular cortices and in the anterior cingulate cortex compared to HC.

3.2.5 Motor Task Cortical Activity and Functional Networks Impairments in ALS

Impairment of sensorimotor and non-motor networks in ALS has been identified from resting state paradigms as discussed in previous subsection. However, motor paradigms, such as motor preparation, planning and execution that can directly access sensorimotor pathways, can unravel the dynamics of motor networks pathology in ALS for biomarker design.

3.2.5.1 Motor preparation and planning

Event related potentials

Before initiating voluntary movements, the brain prepares and plans the movements and represents them, with the premotor area (PM) (Cisek et al., 2003, Churchland et al., 2006) and the supplementary motor area (SMA) (Ball et al., 1999, Cunnington et al., 2005) playing a crucial role in preparation and planning preceding motor execution activity in M1. The pre-movement cortical activity has been reported in terms of event related

potentials (ERP) such as the Bereitschaftspotential (BP) or readiness potential (Deecke, 1987) and contingent negative variation (CNV) (Walter et al., 1964). Investigation of the BP reveals preparatory and planning activity up to 2 seconds before voluntary action (Deecke, 1996), associated with movement-specific preparation/planning like direction (Cui and Deecke, 1999), body part (Kitamura et al., 1993), force (Becker and Kristeva, 1980), and cognitive control (Baker et al., 2011) but its precise function is still unclear. Similarly, another ERP that precedes voluntary movement is the CNV, which occurs in response to a warning stimulus (get ready cue) that precedes the imperative stimulus (go cue) that requires a motor action (Walter et al., 1964). The CNV is the result of anticipation of an upcoming stimulus and sustained attention needed to generate a correct motor response, which shows a wide distribution over prefrontal, M1, S1, SMA, temporal and occipital regions (Hamano et al., 1997, Ikeda et al., 1996).

ALS being a motor neurone disease that primarily affects sensorimotor regions, it is expected that the pre-movement ERPs such as BP or CNV are impaired, but very few studies have investigated the pre-movement ERPs in ALS. A study by Westphal et al. (1998) reported reduced amplitude of BP along central midline electrodes in ALS with pronounced spasticity (hyperreflexia) compared to healthy controls indicating impaired pre-movement cortical activity in ALS. This finding was reinforced by Thorns et al. (2010) who reported reduced amplitude of the lateralised readiness potential over the premotor cortex highlighting impaired movement preparation in ALS compared to healthy controls. The reduction of BP amplitude has also been reported in other neurological disorders, as indication of impaired movement preparation, such as multiple sclerosis (MS) (Bardel et al., 2022). The CNV has been used to study cognitive and attentional impairment in ALS (Mannarelli et al., 2014, Hanagasi et al., 2002) with inconsistent findings. A higher mean CNV amplitude in ALS compared to healthy controls was reported by Hanagasi et al.

(2002) and related to cortical hyperexcitability in ALS. On the other hand, Mannarelli et al. (2014) reported a significant reduction in CNV amplitude in bulbar onset ALS compared to healthy controls indicating dysfunctional attention in that cohort. In other movement disorders such as Parkinson's disease, significant reduction in late CNV amplitude has also been reported (Tzvetanov et al., 2022).

Event related desynchronisation

Sensorimotor mu or beta power decreases pre-movement or during movement compared to baseline (rest), referred to as event related desynchronisation (ERD), indicating cortical activation during motor preparation, planning, and execution (Pfurtscheller and Berghold, 1989). Following the motor execution, sensorimotor mu or beta power increases or rebounds to baseline (rest), referred to as event related synchronisation (ERS), indicating cortical idling post-execution (Neuper et al., 2006). Therefore, ERD/ERS captures the cortical signature of different phases of voluntary movement (Nasseroleslami et al., 2014). The pathophysiological cortical oscillatory mechanisms during motor preparation and planning to neurodegeneration in ALS have been studied previously by using ERD (Riva et al., 2012, Proudfoot et al., 2017, Bizovicar et al., 2014). However, the results reported by these studies are inconsistent. Riva et al. (2012) reported unaltered mu or beta ERD in ALS compared to healthy controls during motor preparation. Similarly, an EEG study during self-paced finger movement reported reduced beta ERD during movement preparation (Bizovicar et al., 2014). On the contrary, a magnetoencephalography (MEG) study by Proudfoot et al. (2017) reported intensified beta ERD during preparation in ALS during a cued finger movement task.

Although, the study ERD in ALS provides abnormal engagement of sensorimotor cortices and non-motor areas during motor preparation and planning, the results are inconsistent

between studies. Furthermore, ERD do not provide a direct measure of influence of non-motor cortices or sub-cortical regions on the sensorimotor cortices (functional connectivity) which could be key to understanding neuropathophysiological mechanisms in ALS.

Corticocortical connectivity

Functional assessments of brain networks have the potential to detect and quantify disease specific network impairments or adaptive and compensatory patterns of network activity pre-movement during motor preparation and planning. Studies have shown the involvement of M1, S1, PM, SMA and parietal regions during movement preparation and planning (Churchland et al., 2006, Li et al., 2015, Shibasaki and Hallett, 2006, Ariani et al., 2022, Nasseroleslami et al., 2014, Glover et al., 2012). By managing functional communication among these cortical areas, the brain forms comprehensive motor plans and generates precise motor commands based on sensory and visual feedback (Wong et al., 2015, Requin et al., 1990). Previous studies have suggested a crucial role of parietalM1 (Koch et al., 2010, Mackenzie et al., 2016) and PM-M1 (Vesia et al., 2018, Koch et al., 2010) pathways for movement preparation. Corticocortical functional connectivity in ALS during motor preparation and planning has been seldom studied despite evidence of impaired preparation and planning from ERPs and ERDs studies (Thorns et al., 2010, Bizovicar et al., 2014).

3.2.5.2 Motor execution

Event related desynchronisation

Similar to pre-movement (motor preparation and planning), motor execution is characterised by mu/beta ERD of primary sensorimotor (M1/S1) cortices (Pfurtscheller and Lopes da Silva, 1999), and parietal regions (Nasseroleslami et al., 2014). In addition to the

cortical regions, deeper brain regions such as thalamus (Alegre et al., 2005) and basal ganglia (Klostermann et al., 2007) also show mu/beta ERD during movement execution in healthy individuals. The pathophysiological cortical oscillatory mechanisms during motor execution due to neurodegeneration in ALS have been widely studied by using ERD, but just like for motor preparation or planning, inconsistent results are reported (Riva et al., 2012, Proudfoot et al., 2017, Bizovicar et al., 2014). Riva et al. (2012) found no changes in mu or beta ERD in ALS compared to healthy controls during motor task execution. Bizovicar et al. (2014) reported reduced beta ERD in ALS compared to healthy controls using EEG. On the contrary, a MEG study by Proudfoot et al. (2017) reported intensified beta ERD in ALS compared to healthy controls during execution of a cued finger movement task. The inconsistency in the ERD/ERS results in ALS reported by these studies could be due to the heterogenous phenotypical presentations of ALS populations, differences in the selections of the range of beta band, and the tasks' demand (Peter et al., 2022).

Corticocortical connectivity

Corticocortical connectivity is fundamental to motor control, reflecting the coordination of neural signals between different regions of the primary motor (M1), primary sensory (S1), premotor (PM), and supplementary motor area (SMA) (Grefkes et al., 2008, Ohara et al., 2001). Other brain regions such as dorsolateral prefrontal cortex (DLPF), cingulate cortex, and superior parietal lobule also play an important role involuntary motor control (Alahmadi et al., 2015, Nasseroleslami et al., 2014).

Very few studies have interrogated the corticocortical functional connectivity in ALS during a motor task. A MEG study by Proudfoot et al. (2018b) has reported significant reduction in beta coupling between interhemispheric M1 during bilateral grip force

production. However, numerous studies have compared activation patterns of cortical and sub-cortical regions between healthy controls and ALS patients using fMRI during performance of voluntary motor tasks. The activation of contralateral motor regions (Stanton et al., 2007, Kollewe et al., 2011), ipsilateral sensorimotor regions and SMA (Konrad et al., 2002, Kollewe et al., 2011), bilateral premotor and cerebellum (Schoenfeld et al., 2005) and bilateral S1 and parietal regions (Poujois et al., 2013) was higher in ALS compared to controls during execution of a motor task. On the other hand, reduced activation of primary sensorimotor and premotor areas in ALS has also been previously reported using fMRI (Cosottini et al., 2012). The involvement of cortical regions such as premotor and SMA, which are largely associated with movement planning and initiation (Churchland et al., 2006, Li et al., 2015, Shibasaki and Hallett, 2006, Glover et al., 2012), during motor execution underlines the alternative strategy for optimizing motor performance in ALS (Konrad et al., 2002).

Corticomuscular connectivity

During voluntary contractions, oscillatory signals originating from the sensorimotor cortices are coherent with contralateral muscle signals. This cortex-muscle synchrony can be measured using Corticomuscular coherence (CMC) (Conway et al., 1995). CMC is typically observed as synchrony (in the beta and gamma-bands) between EEG/MEG electrodes over M1 and EMG activity (Halliday et al., 1998). It is indicative of the efferent drive to the spinal motoneurons, while also being subject to the modulating influence of peripheral afference (Witham et al., 2011). The frequency of synchrony between cortex and muscles is modulated by various factors including the type of task and level of contraction force (Kilner et al., 2000, Liu et al., 2019). For low force isometric contractions, the CMC is observed in the beta band (13-30 Hz) whereas in more forceful and dynamic contractions,

the CMC shifts to the gamma band (31-97Hz) (Omlor et al., 2007, Gwin and Ferris, 2012, Andrykiewicz et al., 2007).

Recent studies have shown that CMC can provide valuable insights into the pathophysiology of ALS, as well as potential biomarkers for diagnosis and disease progression. A study using MEG has previously reported that the beta-band CMC over the motor cortex is reduced in ALS compared to healthy controls (Proudfoot et al., 2018b). This reduction is thought to be due to the progressive loss of motor neurons, which results in a decrease in the number of signals that can be transmitted between the brain and muscles leading to a decline in motor function. Even in ALS with preserved motor functionality (ALSFRS-R scores ≥40), no significant CMC (compared to statistical threshold) was reported for either hand during tonic wrist-extension at 30-50% of maximum voluntary contraction (Yazawa et al., 2017), indicating the potential of CMC for early diagnosis of ALS. The reduction of beta CMC was also observed in other neurodegenerative diseases with a movement deficit such as Parkinson's disease (Yokoyama et al., 2020, Zokaei et al., 2021) and neurological disorders that cause motor impairment such as chronic stroke (Meng et al., 2009).

3.2.6 Clinical Implications

Functional connectivity has the capacity to enable early detection of brain networks impairments before clinical symptoms emerge and before structural alterations are visible on structural imaging such as MRI (Marzetti et al., 2019, Sadaghiani et al., 2022). Studying functional connectivity in ALS during various experimental paradigm such as rest, pre-movement (motor preparation and planning) and motor execution, encompassing event-related potentials (ERPs), event-related desynchronization (ERD), corticocortical connectivity, and corticomuscular connectivity, may have clinical implications. Analysing

resting-state functional connectivity have shown potential for the early detection of neural network changes, as markers of neurodegeneration, and phenotyping (Dukic et al., 2019, Dukic et al., 2021). Exploration of motor preparation and planning phases through ERPs and ERD offers insights into the neural processes underlying motor anticipation and planning deficits in ALS (Thorns et al., 2010, Bizovicar et al., 2014). Concurrently, changes in ERD, corticocortical connectivity, and corticomuscular connectivity during motor execution may unveil disruptions in cortical and corticospinal neural networks responsible for motor control, and could be indicators of disease progression and therapeutic responses (Proudfoot et al., 2019, Proudfoot et al., 2017, Proudfoot et al., 2018b). Similarly, reduced corticomuscular coherence post-stroke and increased coherence during motor recovery (Krauth et al., 2019) indicate its potential as an objective primary outcome for drug trials, surpassing subjective measures like ALSFRS-R scores. Moreover, combining insights from both structural and functional connectivity studies links brain anatomy changes with functional impairments, potentially enhance the understanding of ALS pathophysiology and potential therapeutic targets (Verstraete et al., 2010, Douaud et al., 2011). This comprehensive approach may reveal the neural mechanisms underlying ALS progression and the interplay between structural alterations and brain function (Schmidt et al., 2014, Nasseroleslami et al., 2018). This knowledge could potentially aid in early diagnosis, treatment efficacy assessment, and the formulation of personalized interventions for ALS.

3.3 Effective Connectivity

3.3.1 Methods for Assessing Effective Connectivity

Functional connectivity gives the correlation between neural activities in the interacting brain regions, but the direction of information flow is not defined (Friston, 2011). So, cortical networks derived from functional connectivity lack the causal information, such as

inflow or outflow, which could be crucial for explaining a neurophysiological process in health and in disease. Effective connectivity resolves the issue by providing a causal relationship between the brain regions of interest (Friston, 2011). The effective brain networks can be estimated from the EEG/MEG/fMRI/PET/fNIRS time series by a using model-based method, where the causal pathways are specified and anatomical and functional knowledge are provided, such as Dynamic causal modelling (DCM) or a model-free data driven method, where the signals are used directly for estimation, such as Granger causality, directed transfer function (DTF), partial directed coherence (PDC), or transfer entropy (TE).

Granger causality is a statistical method used for inferring causal relationships between time series data, used to estimate the effective connectivity in brain networks (Geweke, 1982). It assesses whether the past values of one time series can predict the future values of another time series using a multivariate auto-regressive model (MVAR), indicating a causal influence. This approach has been employed in neuroimaging studies to infer directional interactions between brain regions (Seth et al., 2015). Another MVAR method for estimation of effective connectivity is partial directed coherence (PDC) (Baccalá and Sameshima, 2001), which is a frequency domain version of Granger causality. PDC is a widely used method which has proven to be more reliable and faster than DTF to quantify causal interactions between multi-channel EEG signals (Huang et al., 2016). The asymptotic distribution of the PDC is not well known, therefore, bootstrap-based approaches are commonly used to test for significant connectivity. Variance stabilisation is recommended when it comes to bootstrap-based PDC connectivity approaches (Baccala et al., 2007), that can be done by using normalised PDC or generalised PDC (gPDC)(Baccalá and Sameshima, 2021). Other Granger causality-based frequency domain methods such as the direct transfer function (DTF) (Kaminski and Blinowska, 1991) can

be used to find the causal interaction between the brain regions, however, DTF is prone to be affected by alternative interactions or unpredictable factors (Baccalá and Sameshima, 2001).

Effective connectivity can also be estimated using information theory such as transfer entropy (TE) that measures the directed exchange of information between brain regions, and unlike mutual information, ignores static correlations due to common inputs (Schreiber, 2000). TE has been used previously on fMRI time series data to establish the directed information structure between brain regions during rest (Wu et al., 2021) or during a visuo-motor tracking task (Lizier et al., 2011) in healthy controls. However, despite its evident strengths, such as ability to estimate non-linear directed interactions, the accuracy of TE estimation can be affected by several elements within the estimation procedure including the embedding dimension, delays in state space reconstruction, the size of the data sample, and the specific approach employed to estimate high-dimensional conditional probabilities (Zhou et al., 2022, Hlaváčková-Schindler et al., 2007, Vicente et al., 2011). Dynamic Causal Modelling (DCM) is another popular non-linear method for estimating causal interactions between the brain sources, but it requires a prior specification of connectivity linkages (Sato et al., 2009).

3.3.2 Effective Connectivity Impairments in ALS

3.3.2.1 Resting-state effective network impairments in ALS

Studies using functional connectivity measures have reported altered sensorimotor and extra-motor networks in ALS compared to healthy individuals during rest (Agosta et al., 2011, Zhou et al., 2014, Douaud et al., 2011, Menke et al., 2018, Dukic et al., 2019). Although resting state effective connectivity measures have the potential to reveal more on ALS network neuropathophysiology compared to functional connectivity, the use of the

measure to estimate brain network abnormalities in ALS have been rather limited. Iyer et al. (2015) studied the effective network topology in ALS using partial directed coherence measures on resting state EEG and reported that degree values of the network nodes (no. of connections converging into a node) were higher in ALS compared to healthy controls in central and frontal regions in the theta band suggesting pathological alteration of neural networks. A resting state fMRI based effective connectivity study on ALS and healthy controls showed altered causal interaction between sensorimotor cortices, specifically loss of bidirectional communication between M1 and SMA and unidirectional communication from SMA to S1, reflecting damage in motor neurons (Fang et al., 2016). Since the study focused on three cortical regions only (M1, S1 and SMA), the causal interaction of cortices beyond sensorimotor regions was not known.

3.3.2.2 Motor task effective network impairments in ALS

The study of effective connectivity networks in healthy individuals during motor execution has underpinned significant bidirectional interaction between primary motor (M1), primary sensory (S1), and higher order motor regions such as premotor (PM) and supplementary motor area (SMA) (Grefkes et al., 2008, Kim et al., 2018, Brovelli et al., 2004, Gao et al., 2011, Anwar et al., 2016). Similarly, during the execution of a visuomotor task, inputs to/from dorsolateral prefrontal (DLPF) and posterior parietal cortex (PPC) into the sensorimotor regions were found (Kim et al., 2018, Rowe et al., 2004, Gao et al., 2011, Anwar et al., 2016). However, the impairment of effective connectivity networks in ALS during motor tasks such as motor preparation, planning and execution has been rarely studied. Recently, using fMRI, Abidi et al. (2020) reported that the effective connectivity of SMA to striatum was decreased, whereas, connectivity from striatum to superior parietal

lobule was increased in upper motor neuron predominant ALS during the preparation of self-initiated movement.

3.3.3 Clinical Implications

Although, the effect of neurodegeneration in effective connectivity brain networks has rarely been studied in ALS, it has potential to untangle complex network neuropathophysiology. It is believed that ALS pathology is propagated via networks, the study of effective networks could therefore shed more light on the dying forward or dying backward hypothesis in ALS.

3.4 Discussion

Functional and effective connectivity network analysis during motor tasks in ALS has potential for unravelling the neuropathophysiology of the disease and designing biomarkers for diagnosis and tracking disease progression. While structural connectivity studies offer insights into the static physical interconnections between brain regions, the functional and effective connectivity network analyses quantify dynamic interactions and information flow within neural circuits which has potential for early detection of brain networks impairments before clinical symptoms emerge and before structural alterations are visible in structural imaging such as MRI (Marzetti et al., 2019, Sadaghiani et al., 2022).

Functional and effective connectivity network measures identified from resting-state or task-based paradigms have shown promise in identifying specific patterns of brain activity that correlate with ALS progression and clinical features (Dukic et al., 2019, Bharti et al., 2022). These network biomarkers have the potential to serve as valuable indicators of disease at the early symptomatic phase (Govaarts et al., 2022), of disease severity (Sorrentino et al., 2018), disease progression (Castelnovo et al., 2020), phenotyping (Dukic et al., 2021), and response to treatment (Wei et al., 2022a).

In conclusion, functional and effective connectivity network analysis during motor tasks in ALS offers profound insights into the disease's neuropathophysiology. By deciphering alterations in network connectivity, synchronization, and causal interactions, we not only advance our understanding of ALS as a complex multi-system neurodegenerative disorder but also lay the foundation for objective biomarkers, predictive tools, and personalised interventions.

4. Materials and Methods

This chapter describes the general methodology used for the research study. Section 4.1 explains the participant recruitment along with inclusion/exclusion criteria. Section 4.2 explains the ethical approval of the study and consent procedures. Section 4.3 describes the details of experiments performed including the materials/equipment used for the experiments and the clinical data collected. The section 4.4 details the sensor level and source level data analysis pipelines and network connectivity methods. In section 4.5, the statistical analysis and tools used in this study are explained.

4.1 Participants Recruitment, Inclusion and Exclusion Criteria

The ALS cohort was recruited from the National ALS Specialty Clinic at Beaumont Hospital whereas the healthy controls were recruited from a database of volunteers maintained at the Academic Unit of Neurology, Trinity College Dublin and through the National Volunteering Database (i-VOL).

Any healthy individual (health based on the questionnaires that assess present medical conditions and past medical history) aged above 18 could be included in the study as control. Any individual aged above 18, with a diagnosis of ALS or its subtypes could be included in the study as patient. However, people with psychiatric disease, or a medical condition that affects the nervous system (e.g., diabetes) were excluded from the study. Similarly, people who previously had allergic reactions in a similar recording environment (e.g., with an allergy to electrode gels) and pregnant women were also excluded from the study.

4.2 Ethical Approval and Informed Consent

Ethical approval was obtained from the Tallaght Hospital/St. James's Hospital Joint Research Ethics Committee for St. James's Hospital, Dublin, Ireland [REC: 2019-07

Chairman's Action (22)] (See appendix). All participants provided written informed consent before the recording of EEG/EMG and force data (See appendices for consent forms). All experiments were conducted in accordance with the standards set by the Declaration of Helsinki, 2013.

4.3 Experimental Paradigm and Data Collection

4.3.1 Experimental Setup

The participants were comfortably seated on a chair in front of a screen (23" computer monitor), on which visual cues for the experiments were presented, inside a shielded room (Faraday cage) at HRB-Wellcome Clinical Research Facility (CRF), St. James's Hospital. The screen was positioned at eye level, approximately 1 metre from the participants. A semi-deflated aircushion was used to support their elbow, with the upper arm elevated at approximately 40 degrees from the shoulder and the elbow was flexed at 90 degrees.

4.3.1.1 Electroencephalography (EEG)

The EEG signal was recorded with 128 active electrodes (Biosemi ActiveTwo system, Biosemi B.V., Amsterdam, The Netherlands) with a sampling frequency of 2048 Hz. An EEG headcap was chosen and positioned based on the size of the participant's head (i.e., maximum head circumference, distance between Inion and Nasion, and distance between ear lobes) using measuring tape such that the electrode Cz was centred above the scalp. The electrode holders of the headcap were then gelled with electrolyte gel (SignaGel, Parker Laboratories, Inc.) and the active electrodes were connected to the headcap. Eight external channels were connected using flat active sintered Ag-AgCl electrodes (BioSemi B.V., Amsterdam, The Netherlands) with the help of alcohol swabs, disposable adhesive disks, electrode gel and medical tape. The positions of external electrodes were— (i) above and below the left eye, (ii) to the left of the left eye and to the right of the right eye, (iii) left and

right mastoid, and (iv) left and right earlobe. All electrode signals (128 EEG + 8 external) were visually inspected to maintain electrode offset below ± 25μV.

4.3.1.2 Surface Electromyography (EMG)

Surface EMG recordings were conducted simultaneously with EEG using the same BioSemi ActiveTwo system with flat active sintered Ag-AgCl electrodes (BioSemi B.V., Amsterdam, The Netherlands), which provided a circular recording area (d=3mm) in a 17×10mm support surface area. Surface EMG was recorded with a sampling frequency of 2048 Hz from eight muscles in the right upper arm: FDI (first dorsal interosseous); EDC2 (Extensor Digitorum Communis); FDS2 (Flexor Digitorum Superficialis); APL (Abductor Pollicis Longus) and EPB (Extensor Pollicis Brevis); FPB (Flexor Pollicis Brevis); APB (Abductor Pollicis Brevis); ADM (Abductor Digiti Minimi); FDMB (Flexor Digiti Minimi Brevis). The electrode locations were chosen based on surface anatomy guidelines and activation manoeuvres (Lee and DeLisa 2004; Pease et al. 2007; Cram and Criswell 2011; Barbero et al. 2012). Bipolar channels were used according to the provided recommendation by SENIAM (Hermens et al. 2000; Merletti and Hermens 2000). For skin preparation, the electrode areas were cleansed with alcohol swabs. The electrodes cables were fixed with a light flexible elastic mesh to minimise movement artefacts. The presence of reliable EMG signal (signal amplitude and frequency increased during muscle contraction) was verified by visual inspection of the recordings and the electrodes were re-attached as needed to assure reliable signals.

4.3.1.3 Force

The grip force was recorded using two flat resistive force sensors (FlexiForce A201 Sensor, Tekscan, Inc., Boston, MA, USA) with their circular sensing area (d=9.7mm) attached to the two bases of a hexagonal wooden prism (edge=30mm, thickness=25mm) as in Figure

4.1. The resistance was converted to analogue voltage using a small circuit board (Tekscan, Inc., Boston, MA, USA) and was recorded and digitised using a Data Acquisition Card (PCIe-6321, National Instruments, Austin, TX, USA). Simulink Desktop Real-Time (Mathworks, Inc.) was used to record the grip force from the data acquisition device at 2000 Hz in real time, send to a local User Datagram Protocol (UDP) port and subsequently visualised.

4.3.2 Experiments

Resting state (eyes open) and voluntary motor task (isometric pincer grip between thumb and index/little finger) simultaneous EEG/EMG data were recorded from an ALS cohort and age-matched healthy controls. In addition to EEG/EMG data, during the voluntary motor task, force data were also recorded. The experiments were designed by Assistant Professor Bahman Nasseroleslami, Trinity College Dublin, who is also the supervisor of this study. The participants were instructed to minimize their eye movements and stay relaxed during the experiments.

4.3.2.1 Resting States

During this experiment, resting-state EEG data were recorded with eyes open. The participants were requested to fixate their eyes on a cross on the presentation screen with mind wandering. In this experiment, three blocks of EEG data were recorded, each block 2 minutes long, with short breaks (~30 sec) between blocks. This recording allowed comparisons of the findings in subsequent experiments to the recently found ALS-related brain network changes in resting-state EEG (Dukic et al., 2019).

4.3.2.2 Voluntary Motor Tasks

Experiment 1: Participants were asked to perform an isometric pinch grip of the force sensor between thumb and index finger of the right upper limb, irrespective of the right or

the left-hand dominance, producing maximum force (Figure 4.1). The participants applied maximum force for 5 seconds when an arrow appeared at the top of the screen and relaxed when the arrow shifted to the bottom of the screen. Participants were provided with real-time feedback of the force applied, given by the height of a filled rectangular green bar visible on screen (shown in Figure 4.2). Five trials were recorded with 30 s rest between the trials. The average peak of the five trials, which were within 10% of each other, was used as the maximal voluntary contraction (MVC). This experiment was used to quantify the participants' strength to be used for other experiment.

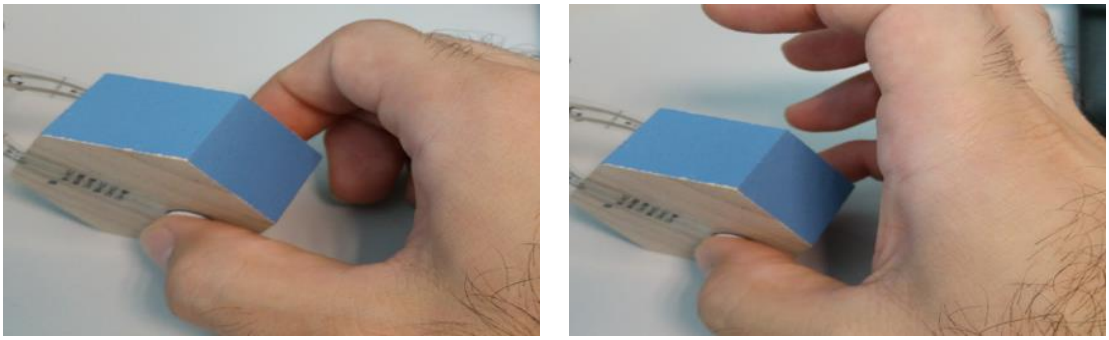

Figure 4.1 Experimental grip tasks using thumb-index (left) and thumb-little (right) fingers. *The force is applied on two flat force sensors on the wooden prism.*

Experiment 2: Participants were asked to perform 30 trials of isometric pinch grips of the force sensor between thumb and index finger of right upper limb at 10% MVC (target force), according to visual cues. Five seconds after the start of a trial, an empty rectangular box was displayed onscreen as go cue where the height of the box represented target force. Participants were provided with real-time feedback of the force applied by filling the box with a green bar. The participants then pinched the force sensors to increase the height of the green bar to reach the height of the rectangular box and then hold to keep a constant force. After 5 seconds, the box disappeared as a cue for participants to relax. Participants were told to use their preferred pace for increasing and decreasing the grip

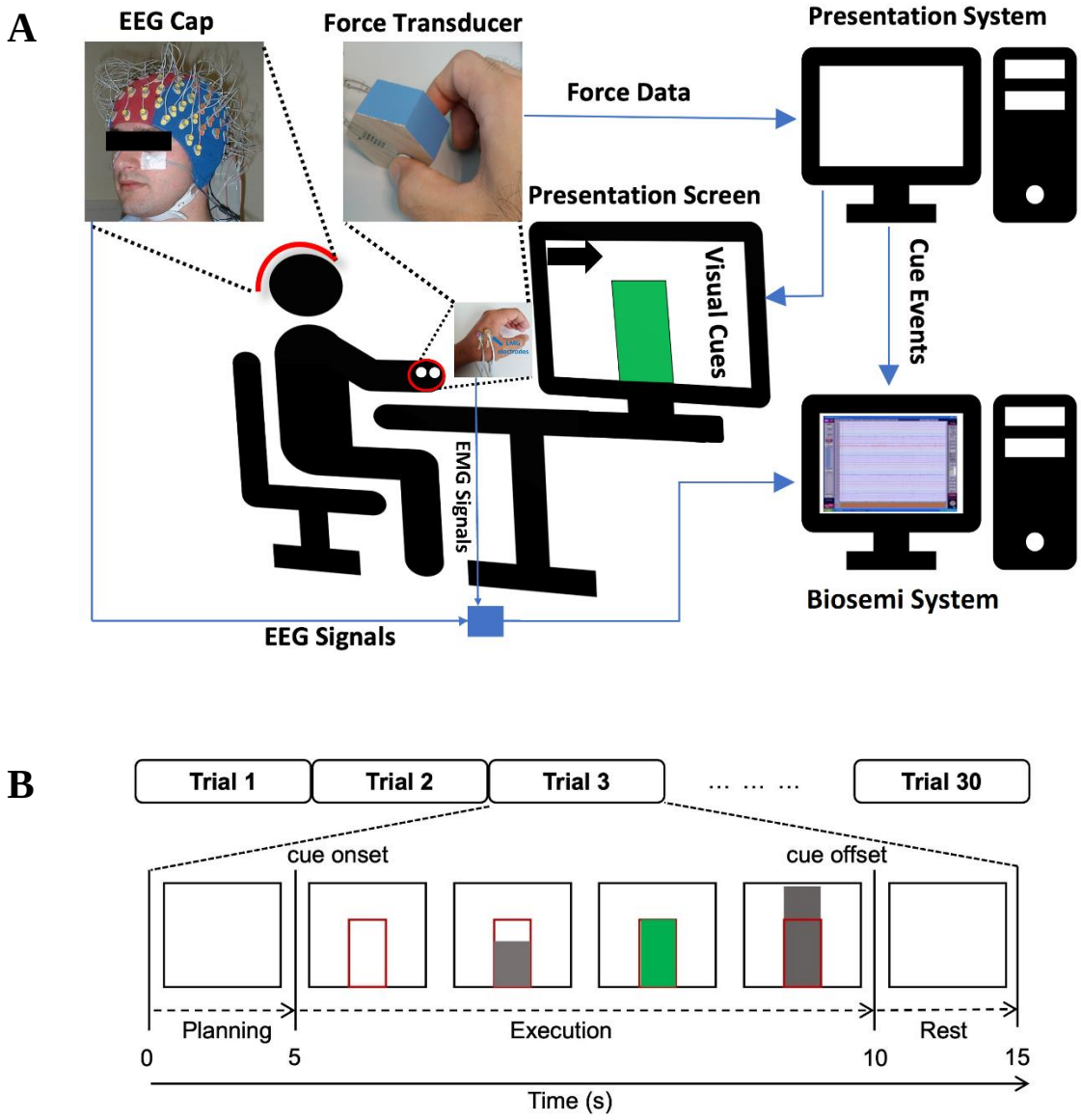

Figure 4.2 Experimental setup and EEG/EMG/Force data format for Experiment 2. *(A) A Biosemi system-based simultaneous EEG, EMG and force recording experimental setup, (B) EEG/EMG/Force data format for experiment 2 showing 30 trials, each trial consists of 3 phases. The 5 seconds before the start of the visual cue are the motor planning phase, the 5 seconds during the visual cue are the motor execution phase, and the 5 seconds after the end of the cue are the between trial rest phases.*

force but to avoid abrupt changes. Each trial lasted for 15 seconds as shown in Figure 4.2 B. The exerted force level by the participants was deemed correct, if the error was less than 10% of the range. This experiment aimed to capture brain networks, brain-muscle

coordination, and muscle-muscle coordination during low-force levels, as well as during slow force onset and offset.

Experiments 3-4 were similar to experiments 1-2, except that the requested isometric pinch grip force was the opposition between the thumb and little finger of the right upper limb (See Figure 4.1).

4.3.3 Clinical Measures

The students/staff of the Academic Unit of Neurology, Trinity College Dublin and the National ALS Clinic, Beaumont Hospital collected functional, behavioural, and cognitive scores that were obtained separately from this research project. The clinical measures were recorded at least once for most of the ALS participants who took part in this study. The scores were obtained by a neurologist or a trained member of the research team from the Academic Unit of Neurology, during the patients' visits to the Irish National ALS Clinic at Beaumont Hospital. The clinical scores recorded closest in time (ideally within a week before or after) to the EEG/EMG recording were chosen for the correlation analysis.

4.3.3.1 ALS Functional Rating Scale Revised (ALSFRS-R)

The ALS functional rating scale revised (ALSFRS-R) is 48 points validated questionnaire-based clinical scale that measures the severity of various functional impairments associated with ALS. It consists of 12 items, a revision from the 10-item original ALSFR scale, related to different aspects of daily functioning, including speech, swallowing, handwriting, cutting food, dressing, walking, and breathing. Each item is rated on a scale from 0 to 4, with higher scores indicating better functioning. The total ALSFRS-R score ranges from 0 to 48, with 48 representing normal functioning. The 48-point total score can be divided into 4 sub-scales namely bulbar (0-12), fine motor (0-16), gross motor (0-8), and respiratory (0-

12) (Cedarbaum et al., 1999). Each sub-scale can be used to assess a specific functional impairment due to neurodegeneration.

4.3.3.2 Edinburgh Cognitive and Behavioural Assessment Scale (ECAS)

The Edinburgh Cognitive and Behavioural Assessment Scale (ECAS) is a neuropsychological assessment tool designed to evaluate cognitive and behavioural functions in individuals with neurodegenerative disorders, including ALS. ECAS is a 136 points clinical scale which assesses a range of cognitive domains affected by ALS including executive functions (0-48), memory (0-24), language (0-28), visuospatial skills (0-12), and verbal fluency (0-24). A higher score means better cognitive performance. The scores can be divided into two domains namely ALS specific (0-100) and ALS non-specific (0-36). The ALS specific domain combines the scores of language, verbal fluency, and executive functions, whereas the ALS non-specific domain combines the scores of memory and visuospatial scales. In addition to cognitive assessment, the ECAS also includes a section to assess behavioural changes, such as apathy and disinhibition.

4.3.4 EEG/EMG Data Sets

Each EEG/EMG data recording session lasted for about 3 hours with two or three experimenters involved, which included time for written consenting (approximately 15 minutes), EEG/EMG set up (approximately 45 minutes), running experiments (approximately 90 minutes) and cleaning up the equipment (approximately 30 minutes). So, it was difficult to collect EEG/EMG data solely by one individual because it would take double the amount of time. Furthermore, the gel used for EEG/EMG recording would dry out and the data would be very noisy. In addition, ALS participant wouldn't be able to sit on a chair for a long time to perform the experiments. Therefore, at least two experimenters (most of the time three experimenters) were present during the EEG/EMG data recording

to avoid longer sessions. Table 4.1 shows the total EEG/EMG data collected, from different patient populations and my contribution (involvement in number of 3-hour recording session), before the submission of this thesis (September 2023).

Table 4.1 Number of EEG/EMG recording sessions (data collected) per group and my contribution in those sessions.

Groups	Total	My Contribution
Healthy Controls	30	18
ALS	40	27
PLS	16	5
PPS	25	10
SMA	11	11
Grand Total	**122**	**71**

Abbreviations: **ALS** Amyotrophic Lateral Sclerosis, **PLS** Primary Lateral Sclerosis, **PPS** Post-polio Syndrome, **SMA** Spinal Muscular Atrophy

4.4 Data Analysis

The data processing pipelines are different based on the type of analysis, so they have been discussed separately accordingly.

4.4.1 Sensor Level Study

In this study, the data collected during rest and Experiment 2 (self-paced isometric pinch grip motor task) were studied. The motor task was studied during planning and execution phases. A separate visual cue was not provided for motor planning to resemble a real-life motor planning scenario. Therefore, 5 seconds period before the execution cue was taken as the motor planning phase (See Figure 4.2 B).

4.4.1.1 Data Pre-processing

The pre-processing of resting-state EEG and motor task simultaneous EEG/EMG data was

carried out in MATLAB R2021a using the Fieldtrip toolbox (fieldtrip.org). The various steps performed during pre-processing of the data in sensor space are explained below—

Data Extraction

The segment of raw EEG/EMG data extracted for the analysis depended upon the type of connectivity analysis performed such as EEG-EEG or EEG-EMG (Corticomuscular) coherence.

1. **EEG-EEG Coherence:** For resting state, 30 seconds of data from the first block, which was 120 seconds long, were extracted for analysis. Similarly, for the pre-motor stage, 1 second of data between the 3rd and the 4th second, and for motor execution 1 second of data between the 8th and the 9th second of each trial were extracted. Therefore, the total length of data extracted for analysis for each participant was 30 seconds (1 s x 30 trials) for each task condition (rest, pre-motor, and execution). For motor tasks, data epochs where the coefficient of variation of the force produced during sustained contraction was above 0.2, or where the mean force was less than 8% or more than 20% MVC, were excluded from analysis.
2. **EEG-EMG Coherence:** Corticomuscular coherence or EEG-EMG coherence is manifested during performance of a voluntary task (Halliday et al., 1998) and quantifies the cortex-muscle synchrony for motor control. Therefore, for the EEG-EMG coherence study, the section of trials where the participant exerted force (motor execution) were extracted. Specifically, a 4 second segment between 6 to 10 seconds of a 15 second trial (1 second after presentation of visual cue until presentation of the relax cue) was extracted for the analysis. Therefore, a total of 120 seconds (4 x 30 trials) were extracted for each participant. Data epochs where the coefficient of variation of the force produced was above 0.2, or where the mean

force was less than 8% or more than 20% MVC, were excluded from analysis.

Channel Selection

Bad channels were detected by visual inspection of the 128-channels of EEG data. Bad channels were removed and reconstructed by using weighted average interpolation of the neighbouring channels (Perrin et al., 1989). Based on the type of analysis and their neurophysiological underpinnings, different sets of EEG channels were selected.

Eight EEG channels A5, B22, B31, C25, D4, D12, D19, and D28 (International 10-10 System equivalent P1, C4, FC4, F1, F3, FC3, C3, and CP3) were chosen a prior for the EEG-EEG coherence analysis (marked by blue circles in Figure 4.3 A). D19/B22 cover the left/right primary motor cortex (M1) whereas left/right premotor cortex (PM) is covered by the electrodes D12/B31. The left primary sensory cortex (S1) is covered by D28 and left superior parietal lobule (SPL) is covered by A5. Similarly, the electrodes D4 and C25 cover left dorsolateral prefrontal cortex (DLPFC) and left dorsomedial prefrontal cortex (DMPFC) respectively. The electrodes pertaining to the aforementioned cortical regions were chosen because they are known to be activated during planning (Churchland et al., 2006, Riehle, 2005, Pfurtscheller and Berghold, 1989, Glover et al., 2012, Ariani et al., 2015, Papitto et al., 2020) and execution (Hanakawa et al., 2008, Papitto et al., 2020, Lacourse et al., 2005, Alahmadi et al., 2015, Cisek et al., 2003) of motor tasks in healthy individuals.

Five EEG channels A1, A19, B22, C21 and D19 (International 10-20 System equivalent Cz, Pz, C4, Fz and C3 respectively) and 3 EMG signals (first dorsal interosseous [FDI], flexor pollicis brevis [FPB], and abductor pollicis brevis [APB]) were chosen a priori for

A

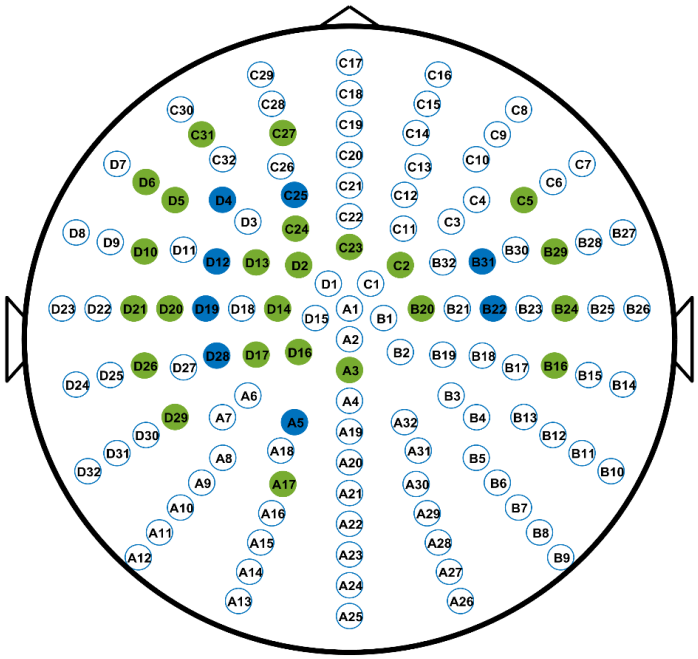

B

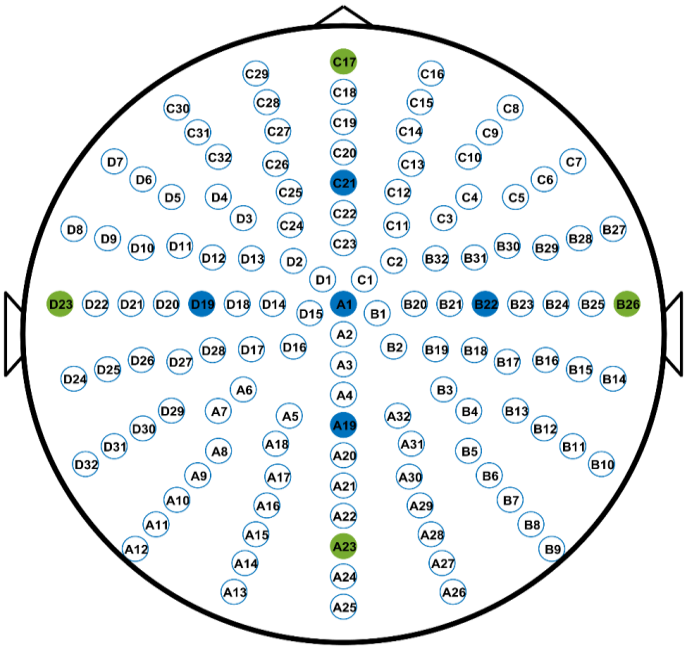

Figure 4.3 Channels selected for analysis and their surface Laplacian electrodes. *(A) EEG channels (blue) and their surface Laplacian electrodes (green) for sensor level EEG-EEG coherence analysis. (B) EEG channels (blue) and their surface Laplacian electrodes (green) for sensor level EEG-EMG or Corticomuscular coherence analysis.*

the EEG-EMG analysis (EEG channels marked by blue circles in Figure 4.3 B). The EEG electrodes were chosen due to their representative coverage of the cortical motor network.

The C3, Cz, and C4 cover the contralateral hand area, central, and ipsilateral hand sensorimotor regions for the chosen tasks. Fz pertains to the frontal areas that reflect the activity from supplementary motor regions (and, to some extent, premotor areas). Finally, Pz reflects the activity from parietal areas that play important roles in visuomotor tasks (Nasseroleslami et al., 2014). Importantly, these regions have minimal spatial overlaps and allow the activity of more distinct regions to be assessed. The target muscles were selected based on their biomechanical involvement in the pincer grip task (Danna-Dos Santos et al. 2010).

Referencing and Filtering

The selected channels were (re)referenced using a surface Laplacian spatial filter. Laplacian filtering was used because it helps to minimize the effect of volume conduction in EEG data (Bradshaw and Wikswo, 2001). For 8 electrode EEG-EEG coherence analysis, the surface Laplacian filter was designed with 3 neighbouring channels within the radius of ~20 mm separated approximately by 120 degrees, such that no Laplacian channel is a common neighbour for any of the 8 selected channels. The Laplacian electrodes chosen (marked as green circle in Figure 4.3 A) were A3, A17, D17 for A5; B16, B20, B29 for B22; B24, C2, C5 for B31; C23, C27, D13 for C25; C31, D6, C24 for D4; D2, D5, D21 for D12; D10, D14, D26 for D19; and D16, D20, D29 for D28. Similarly, for 5 electrode EEG-EMG coherence analysis four channels were chosen as Laplacian electrodes based on the Large Surface Laplacian configuration defined by McFarland et al. (1997). Specifically, the Laplacian electrodes chosen were A19, B22, C21, D19 for A1 (Cz); A1, A23, B22, D19 for A19 (Pz); A1, A19, C21, D23 for D19 (C3); A1, A19, C21, B26 for B23 (C4); and A1, B22, D19, C17 for C21 (Fz).

The Laplacian filtering was followed by dual-pass band pass filtering between 1-100 Hz using a 4th order Butterworth filter to remove very-low frequency noise (<1Hz) and high frequency noise (>100Hz) from the EEG data. Similarly, a dual-pass band pass filtering between 10-100 Hz using a 4th order Butterworth filter was used for EMG data. A dual-pass band stop Butterworth filter of a 4th order with cut-off frequencies 49-51 Hz was used to remove powerline noise from the EEG/EMG data. EMG was not rectified because our preliminary analysis showed that when EEG was filtered between 1-100 Hz, rectification of EMG did not affect the significance of EEG-EMG coherence at beta (14-30 Hz) band.

Automatic Artefact Detection and Rejection

Fieldtrip implemented threshold-based automatic artefact detection and rejection was used to detect and remove eyeblink artefacts, muscle artefacts, and jump artefacts. The same pipeline was used to detect and reject artefacts for all sensor level analysis (EEG-EEG or EEG-EMG coherence analysis). A copy of the data was filtered according to the nature of the artefact, for example a bandpass filter of 1-15 Hz was used to detect eyeblinks. For each channel, the filtered data were converted into z-scores using mean and standard deviation calculated over all trials. The z-scores were averaged over the channels to get a single time series with accumulated artefacts. The artefactual trials were detected using threshold z-values i.e., if the average z-score was greater than the threshold z-value for any timepoint in a trial, the trial was considered artefactual and removed from the original data. The threshold z-values were selected using visual inspection. Each trial was browsed using a low threshold z-value i.e., 4 for eyeblinks, 8 for muscles, and 12 for jump artefacts. The threshold z-value was adjusted (increased or decreased in steps of 1) looking into the segment of original data marked as artefactual data. The adjustment of the threshold z-value was continued until all artefactual data were marked and non-artefactual data were

unmarked. The threshold value was set such that no more than 20% of trials were rejected as artefactual trials.

4.4.2 Source Level Study

Similar to the sensor level study, this study focused on the data collected from Experiment 2 (self-paced isometric pinch grip motor task). The motor task was studied during pre-movement (referred to as motor planning) and execution phases.

4.4.2.1 Data Pre-processing

Data Extraction

Data extraction for source level studies was similar to the data extraction for sensor level studies explained in sub-section 4.4.1.1 except that for pre-movement (motor planning), 1 second data segments between the 4^{th} and 5^{th} second of the trials were taken.

Referencing and Filtering

The EEG data were common average referenced followed by 1-100 Hz dual-pass band pass filtering using a 4^{th} order Butterworth filter. Similarly, dual-pass band pass filtering between 10-100 Hz using a 4^{th} order Butterworth filter was used for EMG data. A 4^{th} order dual-pass Butterworth band stop filter with a stop band of 49-51 Hz was used to remove power line noise from EEG/EMG data. EMG was not rectified as stated in the previous section.

Automatic Artefacts Detection and Rejection

Artefacts such as electrooculogram (EOG), electromyogram (EMG), electrocardiogram (ECG), and jump artifacts were removed automatically using the Fieldtrip toolbox just like in sensor level studies using paradigm explained in *automatic artefacts detection and rejection* sub-topic in sub-section 4.4.1.1.

4.4.2.2 Source Reconstruction

A template structural MRI (https://identifiers.org/neurovault.image:29404) was used to compute the forward model (lead-field matrix). The source reconstruction was done using linearly constrained minimum variance (LCMV) beamformer (Van Veen et al., 1997) using the Fieldtrip toolbox. Twelve anatomical brain regions were chosen bilaterally, 6 on each side of the brain, using the automated anatomical labelling (AAL) atlas (Tzourio-Mazoyer et al., 2002). The chosen anatomical brain regions (regions of interest, ROI) were the Primary Motor Cortex (M1), Primary Sensory Cortex (S1), Supplementary Motor Area (SMA), Medial Prefrontal Cortex (PFC), Superior Parietal Lobule (SPL) and Anterior Cingulate Cortex (ACC) of both hemispheres. To derive a single time-series for each ROI all time-series within a ROI were weighted using a Gaussian weighting function with the half width at half maximum set to approximately 17 mm (Dukic et al., 2019, Brookes et al., 2016, Tewarie et al., 2016). This implies that signals located 17 mm away from the centre of the region of interest (ROI) will be weakened by a factor of 0.5. However, it should be noted that the orientation of each estimated dipole may not align with the orientations of other dipoles within the ROI. This can lead to interference and incorrect estimation of the effective activity of the ROI if a simple averaging of neighbouring dipoles' time-series is performed. To address this, after Gaussian weighting, we first determined the dominant direction of each ROI by conducting singular value decomposition on the dipole orientations within the ROI. Any dipoles with orientations opposite (>90 degrees) to the estimated maximal activity vector of the ROI were inverted. Following these procedures, we obtained 12 broadband time-series, each representing an individual ROI. This process was performed for each subject independently.

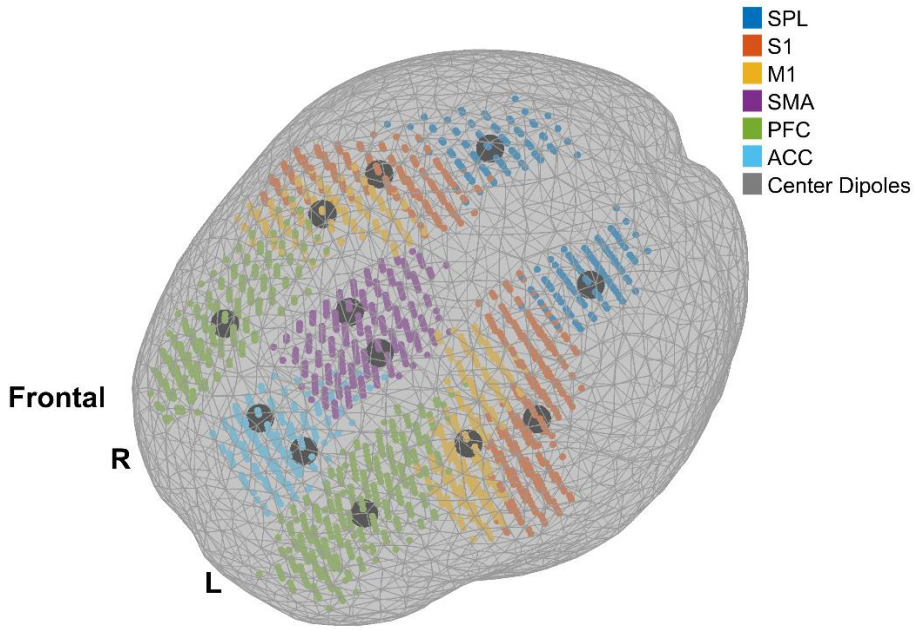

Figure 4.4 Cortical regions of interest (ROIs) and the central dipole current sources used for source reconstruction. ***SPL****: Superior parietal lobule,* ***S1****: Primary sensory cortex,* ***M1****: Primary motor cortex,* ***SMA****: Supplementary motor area,* ***PFC****: Medial prefrontal cortex,* ***ACC****: Anterior cingulate cortex,* ***L****: Left,* ***R****: Right.*

4.4.3 Time-Frequency Analysis

The pre-processed time series EEG data, $x_t(n, c)$; n: $number\ of\ trials$, c: $number\ of\ channels$, of motor experiments (planning and execution), was first averaged over trials (Equation 4.1) to get event-related potentials $erp_t(c)$. The erp_t was then subtracted from every trial of x_t to get non-phase locked time series data $npl_t(n, c)$ (Equation 4.2).

$$erp_t(c) = \frac{1}{n}\sum_{k=1}^{n} x_t(k, c) \qquad (4.1)$$

$$npl_t(n, c) = x_t(n, c) - erp_t(c) \qquad (4.2)$$

npl_t was decomposed into time-frequency components using wavelet transform with the Fieldtrip toolbox. A Morlet wavelet with 5 cycles, a frequency resolution of 1 Hz, and a time resolution of 0.025 seconds was used. The output time-frequency power obtained from wavelet decomposition of npl_t was normalised to an inter-trial rest period of 5 seconds of

motor task experiment (i.e., -3 to 2 second baseline window). The normalised time-frequency power was averaged over time components to obtain event related spectral perturbations (ERSP). Finally, the ERSP was averaged over participants of each group separately to get the group average ERSP.

4.4.4 Connectivity Analysis

4.4.4.1 Functional Connectivity (Banded Spectral Coherence)

The pre-processed EEG data were converted into the frequency domain using the Fourier Transform (Hanning taper, 1 Hz spectral smoothing, 2-100 Hz bandwidth, and 1 Hz frequency resolution).

Auto spectra ($S_{ii}(f), i = 1, 2, \dots, c;\ (number\ of\ channels);\ f = 2, 3, \dots 100\ Hz$) and cross spectra ($S_{ij}(f), j = 1, 2, \dots, c;\ i < j$) were calculated using the Fieldtrip toolbox for each trial. The 2-100 Hz spectral bandwidth was divided into 8 frequency bands as shown in Table 4.2, excluding the 48-52Hz range to avoid mains power interference. The frequency bands were defined based on the typical physiological EEG frequency bands (Sanei and Chambers, 2007) as well as their relevance both in sensorimotor control (Nasseroleslami et al., 2014) and quantifying network dysfunction in motor neuron diseases (Dukic et al., 2019, Dukic et al., 2021).

The band auto spectra [$S_{ii}^{*}(fb),\ fb = \delta, \theta, \alpha_l, \alpha_h, \beta_l, \beta_h, \gamma_l, \gamma_h$] and band cross spectra [$S_{ij}^{*}(fb)$] were calculated for each trial by taking the spatial median, which minimizes the sum of Euclidean distances, of the signal spectra over the specific band frequencies (Equation 4.3). For example, the banded spectrum for the δ band is the spatial median of the signal spectrum at 2, 3 and 4 Hz; the banded spectrum for θ band is the spatial median of the signal spectrum at 5, 6 and 7 Hz, and so on. The spatial median is a variation of the median operator for complex-valued spectra, which is more robust to outliers when

compared to the algebraic averaging (Niinimaa and Oja, 2014, Nasseroleslami et al., 2019, Dukic et al., 2017).

$$S^*(fb) = \underset{\boldsymbol{\Theta}}{arg\,min}\left(\sum_{f=fb}\|S(f) - \boldsymbol{\Theta}\|\right) \qquad (4.3)$$

Table 4.2 Division of EEG spectral bandwidth into frequency bands.

Frequency band	Notation	Frequency range (Hz)
Delta	**δ**	**2-4**
Theta	**θ**	**5-7**
Low-alpha	**α_l**	**8-10**
High-alpha	**α_h**	**11-13**
Low-beta	**β_l**	**14-20**
High-beta	**β_h**	**21-30**
Low-gamma	**γ_l**	**31-47**
High-gamma	**γ_h**	**53-97**

The optimisation of equation 4.3 was done by Weiszfeld's algorithm (Weiszfeld, 1937). The banded cross spectrum was then normalised by using banded auto spectra for a given frequency band to obtain a banded spectral coherency (C_{ij}^*) estimate for each trial (Equation 4.4) (Nasseroleslami et al., 2019).

$$C_{ij}^*(fb) = \frac{S_{ij}^*(fb)}{\sqrt{S_{ii}^*(fb) \times S_{jj}^*(fb)}} \qquad (4.4)$$

4.4.4.2 Effective Connectivity (Generalised Partial Directed Coherence)

Generalized partial directed coherence ($gPDC$) was used to evaluate the causal influences or effective connectivity between the cortical regions of interest (ROIs). $gPDC$ is a normalized form of Partial directed coherence (PDC). PDC is a frequency domain multivariate method based on Granger causality introduced by Baccalá and Sameshima (2001). "Partial directed coherence describes the direction of information flow between

multivariate time series data based on the decomposition of multivariate partial coherences computed from multivariate autoregressive models" (Baccalá and Sameshima, 2001).

A multivariate autoregressive model of EEG time series data $X(t) = [x_1(t), \dots, x_N(t)]$ with N channels and of order p can be defined by,

$$\begin{bmatrix} x_1(t) \\ \vdots \\ x_N(t) \end{bmatrix} = \sum_{r=1}^{p} A(r) \begin{bmatrix} x_1(t-r) \\ \vdots \\ x_N(t-r) \end{bmatrix} + \begin{bmatrix} w_1(t) \\ \vdots \\ w_N(t) \end{bmatrix} \qquad (4.5)$$

where, $A(r) = \begin{bmatrix} a_{11}(r) & \cdots & a_{1N}(r) \\ \vdots & \ddots & \vdots \\ a_{N1}(r) & \cdots & a_{NN}(r) \end{bmatrix}$ is the autoregressive parameter.

The coefficients $a_{ij}(r)$ represent the linear interaction effects of $x_j(t-r)$ onto $x_i(t)$. $w_i(t), i = 1,2, \dots, N$ are the estimated errors. After adequate estimation of $A(r)$, it can be converted into the frequency domain $A(f)$ as follows:

$$A(f) = \sum_{r=1}^{p} A(r)\, e^{-i2\pi fr} \qquad (4.6)$$

The transfer function for N channel EEG signals can be defined as $\bar{A}(f) = I - A(f) = [\bar{a}_1(f)\bar{a}_2(f) \cdots \bar{a}_N(f)]$. The column vector $\bar{a}_i(f)$ $(i = 1, 2, \dots N)$ is the ith column of the matrix $\bar{A}(f)$. The i, jth element of $\bar{A}(f)$ is denoted by $\bar{A}_{ij}(f)$ and given by,

$$\bar{A}_{ij}(f) = \begin{cases} 1 - \sum_{r=1}^{p} a_{ij}(r)\, e^{-i2\pi fr}, & if\ i = j \\ -\sum_{r=1}^{p} a_{ij}(r)\, e^{-i2\pi fr}, & otherwise \end{cases} \qquad (4.7)$$

The PDC from channel j to i defined by Baccalá and Sameshima (2001) as follows:

$$PDC_{ij} = \frac{\bar{A}_{ij}(f)}{\sqrt{\sum_{k=1}^{N} |\bar{A}_{kj}(f)|^2}} \qquad (4.8)$$

Finally, the PDC was normalized by its variance (σ_i^2) to get the generalized PDC (Baccala et al., 2007).

$$gPDC_{ij} = \frac{\bar{A}_{ij}(f)/\sigma_i}{\sqrt{\sum_{k=1}^{N} \frac{1}{\sigma_k^2} |\bar{A}_{kj}(f)|^2}} \qquad (4.9)$$

In this study, $gPDC$ for a bandwidth of 1-100 Hz was calculated using the Fieldtrip toolbox. The 1-100 Hz bandwidth was divided into 8 frequency bands as mentioned in Table 4.2, excluding the 48-52Hz range to avoid mains power interference. One $gPDC$ value was obtained for each frequency band by taking the spatial median of the $gPDC$ values at the frequencies covering the band, according to equation 4.3.

4.4.5 Graph Analysis

4.4.5.1 Global Clustering Coefficient (GCC)

The clustering coefficient of an undirected network captures the small-worldness of that network. Small-worldness of a network is characterised by the maximum connectedness and the short average path length between the nodes. Cortical networks are small-world networks (Masuda et al., 2018). We used the global clustering coefficient (GCC) to calculate small-worldness (or density) of functional networks using the Watts and Strogatz method (Watts and Strogatz, 1998). Based on the significant banded spectral coherence (See sub-section 4.5.1 for the details), an EEG functional network was constructed using electrodes as vertices (nodes) and significant EEG-EEG banded coherence as edges. In a functionally connected EEG network, suppose that a node v has k_v neighbouring nodes; then the maximum number of connections or edges (E_m) that exist between the node v and its neighbour is given by:

$$E_m = \frac{k_v(k_v - 1)}{2} \qquad (4.10)$$

This occurs when every neighbour of node v is connected to every other neighbour of v. Let E_v denote the number of these allowable edges that actually exist i.e., the number of significant EEG-EEG banded coherence between node v and its neighbours. Then, the local clustering coefficient C_v of node v is given by:

$$C_v = \frac{E_v}{E_m} \qquad (4.11)$$

Finally, the GCC for the functionally connected EEG network is the average of local clustering coefficients C_v over all v nodes:

$$GCC = \frac{1}{v}\sum_{i=1}^{v} C_v \qquad (4.12)$$

The value of GCC ranges from 0 (no connection) to 1 (fully connected network).

4.4.5.2 Causal Flow

The adjacency matrix for effective connectivity was created by comparing the significance (p values) of generalised partial directed coherence ($gPDC$), which was obtained by bootstrapping (described in sub-section 4.5.2), with a significance level of 0.01. For a $gPDC$ value, if $p < 0.01$, the effective connectivity was considered significant and represented by 1 in the adjacency matrix. The adjacency matrix was visualized by using directed graphs, which represented a network of causally influencing brain regions. In the directed graph representation of causal networks or effective connectivity, nodes represented ROIs and arrows represented the causal interaction between the ROIs. Furthermore, for each node/ROI in the network, causal inflow and outflow were calculated. Causal inflow (InF) of a node is the number of incoming links/arcs to the node from the rest of the nodes in the network. Similarly, causal outflow ($OutF$) is the number of outgoing links/arcs from the node to the rest of the nodes in the network. Therefore, the causal flow (CF) of a node is given by the difference between the causal outflow and causal inflow.

$$CF = OutF - InF \qquad (4.13)$$

In effective/causal networks, if $OutF \gg InF$ for a node, then the node acts as a source whereas, if $InF \gg OutF$, the node acts as a sink.

4.5 Statistical Analysis

4.5.1 Banded Spectral Coherence Statistics

Coherence was presented based on equivalent z-scores and p-values at both individual and group-level. This approach prevents bias by eliminating the dependence on the number of trials for the coherence analysis.

4.5.1.1 Participant (Individual) Level

Participant-level statistics were calculated using one-sample non-parametric rank statistics for spectral coherence (Nasseroleslami et al., 2019). This method provides individual p-values for spectral coherence in each frequency band for both patient and control groups. Stouffer's method (Stouffer et al., 1949, Westfall, 2014) was used to combine individual p-values to derive group average p-values (p_{avg}).

Let, individual p-values be $p_k, k = 1, 2, \dots, n$, where n is the number of p-values to be combined and the p_{avg} be the combined/average p-value.

The z-scores of the p-values are given by:

$$Z_k = \Phi^{-1}(1 - p_k) \qquad (4.14)$$

where, Φ is the standard normal cumulative distribution function.

The average z-score, Z_{avg}, and the average p-value, p_{avg}, are given by:

$$Z_{avg} = \frac{\sum_{k=1}^{n} Z_k}{\sqrt{n}} \qquad (4.15)$$

$$p_{avg} = 1 - \Phi\left(Z_{avg}\right) \qquad (4.16)$$

This procedure is similar, but not procedurally equivalent, to pooled coherence analysis (Amjad et al., 1997). Both methods can be used to combine information from several participants (or trials). The p-values were corrected for multiple comparisons using the

false discovery rate (FDR) at q = 0.05 (Benjamini and Hochberg, 1995) (See sub-section 4.5.4 for details of correction for multiple comparison procedures). The negative logarithm of the average p-value was used to visualise group average banded coherence (C_{avg}).

$$C_{avg} = -log_{10}(p_{avg}) \qquad (4.17)$$

A coherence value greater than 1.30 (i.e., p_{avg}< 0.05) indicated a significant functional connectivity between two regions.

4.5.1.2 Group Level

The banded coherence of the patient group was compared with the control group using 2 sample non-parametric rank statistics (Nasseroleslami et al., 2019, Oja and Randles, 2004, Nordhausen and Oja, 2011) with the resulting p-value (p_{diff}) corrected for multiple comparisons using adaptive FDR at q = 0.05 (Benjamini and Hochberg, 2000) (See sub-section 4.5.4 for details of correction for multiple comparison procedures).

4.5.2 Effective Connectivity (Generalised PDC) Statistics

4.5.2.1 Participant (Individual) Level

The asymptotic distribution of the generalised partial directed coherence ($gPDC$) is not well known therefore non-parametric bootstrap-based approaches are commonly used to test for significant connectivity. Gaussian white noise was used for non-parametric bootstrapping (Efron and Tibshirani, 1993) with 2000 repetitions to estimate the null distribution for banded $gPDC$ values. The Empirical Bayesian Inference (EBI) method (Nasseroleslami, 2019) was used to calculate p-values for $gPDC$ values. The p-values were corrected for multiple comparison using false discovery rate (FDR) at q=0.05 (Benjamini and Hochberg, 1995) (See sub-section 4.5.4 for details of correction for multiple comparison procedures).

4.5.2.2 Group Level

For group analysis, the spatial median of the individual $gPDC$ was taken as group effect whereas the individual p-values were combined or averaged using Stouffer's method (Stouffer et al., 1949) (See sub-section 4.5.1.1 for details of Stouffer's method) to get group level significance of $gPDC$. The group level difference (patients vs controls) between the effective connectivity measure ($gPDC$) was calculated by using non-parametric Wilcoxon rank sum test (Gibbons and Chakraborti, 2003). The p-values obtained from group comparisons were subjected to correction for multiple comparison using adaptive FDR at q=0.05 (See sub-section 4.5.4 for details of correction for multiple comparison procedures).

4.5.3 Effect Size

The effect size provides a standardized measure of the magnitude or strength of an observed effect or relationship and helps to better understand the practical significance of the findings. In this study, the effect size of the abnormal network measures (significantly different measure in patients compared to controls) was reported to indicate its usefulness as a network biomarker. Effect sizes are often categorized as small ($d = 0.2$), medium ($d = 0.5$), or large ($d = 0.8$) based on benchmarks proposed by Cohen (1988). However, it is important to note that these benchmarks are somewhat arbitrary and should not be interpreted in a rigid manner (Thompson, 2007, Correll et al., 2020). The following measures of effect size have been reported in this study.

4.5.3.1 Cohen's d

Suppose n_1 and n_2 are the number of participants in two groups (control and patient) and $\overline{X_1}$ and $\overline{X_2}$ are the mean of a network measure (for example, coherence) for the two groups, respectively. If SD_1 and SD_2 are the standard deviations of the network measure, then the pooled standard deviation of the measure is given by:

$$SD_{pooled} = \sqrt{\frac{(n_1-1)SD_1^2+(n_2-1)SD_2^2}{n_1+n_1-2}} \qquad (4.18)$$

Cohen's d for the measure is then given by:

$$d = \frac{\overline{X_1}-\overline{X_2}}{SD_{pooled}} \qquad (4.19)$$

4.5.3.2 Hedge's g

Cohen's d as explained above is based on the difference between the sample means and gives a biased estimate of the population effect size especially for small sample sizes ($n < 20$) (Hedges and Olkin, 1985). For this reason, Cohen's d is sometimes referred to as the uncorrected effect size (Lakens, 2013). The corrected effect size which is unbiased for smaller samples is given by Hedge's g (Hedges and Olkin, 1985).

$$g = d \times \left(1 - \frac{3}{4(n_1+n_2)-9}\right) \qquad (4.20)$$

Here d is Cohen's d (equation 4.19). Although Cohen's d and Hedge's g are similar for large sample sizes ($n > 20$), Hedge's g is more useful if the sample size is small ($n < 20$) (Kline, 2004).

4.5.4 Correction for Multiple Comparisons

Typically, during single hypothesis testing, to reject the null hypothesis and consider the observed difference or change as statistically significant, researchers aim for a significance level of α=0.05. However, when multiple hypothesis tests are conducted within an experiment (for example, the hypotheses that EEG-EMG coherence between an ALS cohort and healthy controls differs in multiple frequency bands), the likelihood of false positive findings (type I error) or incorrectly rejecting the null-hypothesis increases. Correcting for multiple comparisons is then required to reduce the likelihood of obtaining false positive results when testing multiple hypotheses.

One straightforward and commonly used method for multiple comparison correction is the Bonferroni method, where the significance level is divided by the number of comparisons made. This method is suitable for small numbers of comparisons, but it becomes more conservative, leading to limited statistical power and a higher chance of false negative findings (type II error) when the number of comparisons increases (Valerie et al., 1999).

To counteract the multiplicity problem with higher statistical power, an alternative method is to control the false discovery rate (FDR). The FDR represents the proportion of errors committed by falsely rejecting null hypotheses, providing a more flexible approach compared to familywise error rate control such as the Bonferroni method (Benjamini and Hochberg, 1995).

4.5.4.1 False Discovery Rate (FDR) Correction

We have used the Benjamini-Hochberg procedure (Benjamini and Hochberg, 1995) which is the most commonly used method for controlling the false discovery rate (FDR). The steps involved in applying the FDR correction with Benjamini-Hochberg method are as follows:

Step 1: Perform the individual statistical tests for each hypothesis of interest (say $H_1, H_2, \ldots H_n$ where n is the number of hypotheses tested).

Step 2: Obtain the p-values associated with each test (say $p_1, p_2, \ldots p_n$ be p-values associated with hypothesis $H_1, H_2, \ldots H_n$, respectively).

Step 3: Sort the p-values in ascending order, from smallest to largest (say $p_1 \leq p_2 \leq \cdots \leq p_n$).

Step 4: Estimate the critical threshold or alpha level for controlling the FDR by determining the desired FDR level, typically denoted as q. For example, if we want to control the FDR at 0.05, then $q = 0.05$.

Step 5: Calculate the critical value, k, which is the largest index where $p_k \leq \frac{kq}{n}$.

Step 6: Reject the null hypothesis for p-values less than or equal to p_k i.e., reject all H_x where $x = 1,2, \ldots, k$.

4.5.4.2 Adaptive False Discovery Rate (adaptive FDR) Correction

During multiple independent significance testing of group differences, an FRD correction could be less powerful or more conservative and may not reject the hypotheses that are in fact false (Benjamini and Hochberg, 2000). To overcome this limitation, an adaptive FDR correction method has been proposed by Benjamini and Hochberg (2000). We have used adaptive FRD correction after comparing the groups (for example, ALS cohort vs healthy controls) and to correct p-values for the correlation analysis. The steps involved in adaptive FDR correction method are as follows:

Step 1: Perform Step 1 to Step 5 of the FDR correction procedure from sub-section 4.5.4.1 above. If k doesn't exist, then do not reject any hypothesis, and stop, otherwise proceed to the next step.

Step 2: Calculate the slope $S_i = (1 - p_i)/(m = 1 - i)$, where $i = 1,2, \ldots, n$.

Step 3: Starting with $i = 2$, proceed if $S_i \geq S_{i-1}$. When for the first time $S_j < S_{j-1}$ stop and set $\widehat{n_0} = \min\left(\left[\frac{1}{S_j} + 1\right], m\right)$.

Step 4: Starting with the largest p-value p_n, compare each p_i to $iq/\widehat{n_0}$ (where q is FDR level) until reaching the first p-value that satisfies $p_k \leq kq/\widehat{n_0}$.

Step 5: Reject all k null-hypotheses having p-values smaller than p_k.

4.5.5 Correlation Analysis

The association of the ALS network measures, such as functional/effective connectivity and causal inflow/outflow, with clinical measures such as ALSFRS-R scores was tested

using non-parametric Spearman's rank correlation coefficients. Spearman's rank correlation uses the rank of the data as opposed to the data itself for the estimation of the correlation which makes it robust against outliers. If d_i is the difference of the rank between the i^{th} observations of two variables x and y within total n observations, then the Spearman's correlation coefficient ρ_{xy} between variables x and y is given by:

$$\rho_{xy} = 1 - \frac{6\sum_{i=1}^{n} d_i^2}{n(n-1)} \qquad (4.21)$$

The p-values of Spearman's rank correlation can be obtained by using test statistics such as z-statistics with the help of Fisher's transformation.

In this study, the p-values obtained from multiple correlation tests were adjusted for multiple comparisons using adaptive FDR at q = 0.05 (See sub-section 4.5.4 for details of correction for multiple comparison procedures). A line was fitted to the data in scatter plots, to visualise the relationship, using Robust linear least-square fitting method (Holland and Welsch, 1977).

5. Results: Banded Spectral Coherence as a Tool

Published Work List

The work described in this chapter has been published in the peer-reviews journal Cerebral Cortex as:

Bista S, Coffey A, Fasano A, et al., Cortico-muscular coherence in primary lateral sclerosis reveals abnormal cortical engagement during motor function beyond primary motor areas, *Cerebral Cortex*, Volume 33, Issue 13, 1 July 2023, Pages 8712–8723, https://doi.org/10.1093/cercor/bhad152

This chapter describes the new method we have developed to assess the functional connectivity (coherence) of neuro-electric signals in relation to sensor level CMC in healthy controls and PLS. It contains all figures and tables as well as the results and discussion section text from this publication. In addition, the figures and text from the supplementary materials of this publication have been included in this chapter. Introduction and methods section text from this publication have been abbreviated in this chapter to avoid repetition of the contents of chapters 1-4.

5.1 Introduction

Functional connectivity (FC) is a measure of functional coupling or synchrony between neuronal sources. The modalities and methods used for functional connectivity analysis within brain (EEG-EEG) or between brain and muscles (EEG-EMG) have already been reviewed in literature review chapter with each modality/method having their own advantages and disadvantages. The rationale for developing a new method for the calculation of functional connectivity (coherence) is to harness the robustness of the non-parametric (median based) functional connectivity measure against artefacts (Dukic et al., 2017) and to represent the collective connectivity strength with a single value over the

range of frequencies within each distinct neurophysiological frequency band. More importantly, the new method utilises non-parametric rank statistics for coherence (Nasseroleslami et al., 2019) which presents connectivity strengths as p-values so there is no need for separate significance testing (close form solution or non-parametric bootstrapping) as required by other existing connectivity measures. Additionally, the new method is robust against the bias introduced by the number of epochs (L) used to estimate the functional connectivity (Nasseroleslami et al., 2019) which is not in the case of existing coherence based methods.

We hypothesised that the new method of estimating functional connectivity provides robust detection of network connectivity with a singular value for a frequency band and will be useful to identify the abnormal network connections in patient groups.

5.2 Methods

5.2.1 Ethics

The study was approved by the Tallaght University Hospital / St. James's Hospital Joint Research Ethics Committee - Dublin [REC Reference: 2019-05 List 17 (01)] and performed in accordance with the Declaration of Helsinki (2013). All participants provided informed written consent to the procedures before undergoing assessment.

5.2.2 PLS Cohort

The PLS cohort was prospectively recruited in this cross-sectional study between June 2017-August 2019 through the national ALS clinic at Beaumont Hospital. All participants with PLS fulfilled the clinical criteria for PLS (Turner et al., 2020). Healthy controls, age-matched to the PLS cohort, were recruited from a database of healthy controls interested in taking part in the ongoing research studies in the Academic Unit of Neurology, Trinity College Dublin, the University of Dublin.

Subjects with a history of major head trauma or other neurological conditions that could affect cognition, alcohol dependence syndrome, current use of neuroleptic medications or high-dose psychoactive medication were excluded. Those with diabetes mellitus, a history of cerebrovascular disease, and those with neuropathy from other causes were also excluded. The entire PLS cohort underwent nerve conduction studies and electromyography to exclude other concurrent peripheral nerve disorders that could interfere with CMC analyses.

5.2.3 Clinical assessment

On the day of EEG recording the PLS cohort underwent an extensive clinical assessment. Disease duration from symptom onset and site of disease onset were recorded. Muscle strength was assessed using the Medical Research Council (MRC) score (Compston, 2010) in 9 bilateral (i.e., 18) upper limb muscles, including deltoid, triceps, biceps, wrist flexors and extensors, fingers flexors and extensors, and abductors of the index fingers and thumbs. The degree of clinical upper motor neuron (UMN) involvement in the upper limbs was graded by an UMN score (de Carvalho et al., 2003). An adapted UMN score based on Kent-Braun et al (Kent-Braun et al., 1998) was calculated using reflex and UMN signs assessment. Reflexes were assessed at three sites in the upper limbs (biceps, triceps and brachioradialis). The UMN-score ranges from 0 (normal) to 16 (reflecting hyperreflexia [0-6], hypertonia [0-4], clonus [0-2], Babinski [0-2] and Hoffmann sign [0-2]). The Edinburgh Cognitive ALS Screen (ECAS), which evaluates cognitive performance across language, verbal fluency, executive, memory and visuospatial domains (Abrahams et al., 2014), was performed on 14 of the 16 PLS participants (two declined). The Edinburgh handedness inventory (EHI) (Oldfield, 1971) with 10 questions was performed to assess the handedness of the PLS cohort as well as healthy controls.

HD-EEG and bipolar surface EMG were subsequently recorded in all participants for calculation of CMC during motor tasks.

5.2.4 Experimental Paradigm

Assessment was conducted in the same manner for the PLS and control groups, described as Experiment 2 in sub-section 4.3.2.2 in chapter 4 Materials and Methods. The reason behind choosing for experiment 2 for the analysis is explained in sub-section 5.3.3 below. Participants held a force transducer between the thumb and the index finger of their right hand, irrespective of the right- or left-hand dominance, to measure pincer grip force. The maximal voluntary contraction (MVC) was determined as the average peak force achieved during three short (5 s) maximal contractions, where the peak force in these attempts lay within 10% of each other. Participants were asked to produce a force at 10% MVC for 5 s while holding the force transducer in pincer grip, guided by visual force feedback on screen (pincer grip task). Participants attempted a total of 30 trials for each task.

5.2.5 Recording of (Neuro-)electrophysiological Signals

All participants were seated comfortably, EEG data were recorded in a special-purpose laboratory, using a 128-channel scalp electrode cap. Data were filtered over the range of 0–400 Hz and digitized at 2048 Hz using the BioSemi® ActiveTwo system (BioSemi B.V, Amsterdam, Netherlands). Each participant was fitted with an appropriately sized EEG cap. Surface EMG data were recorded simultaneously with EEG using a bipolar electrode configuration from eight muscles in the right upper arm, with the electrode pairs placed in accordance with the SENIAM guidelines (Hermens et al., 2000). The online hardware gain and filter settings for the EMG signals during recordings were the same as for the EEG channels. Recording was followed by further offline pre-processing. Five EEG channels (Cz, Pz, C4, Fz, C3) and three EMG signals (first dorsal interosseous, FDI; Flexor Pollicis

Brevis, FPB and Abductor Pollicis Brevis, APB) were chosen apriori for the cortico-muscular coherence analysis (CMC). The EEG electrodes were chosen due to their representative coverage of the cortical motor network. The C3, Cz, and C4 cover the contralateral, central, and ipsilateral hand sensorimotor regions for the chosen tasks. Fz pertains to the frontal areas that reflect the activity from supplementary motor regions (and to some extent premotor areas). Finally, Pz reflects the activity from parietal areas that play important roles in visuomotor tasks and spatiotemporal integration (Nasseroleslami et al., 2014). Importantly, these regions have minimal spatial overlap and allow the activity of more distinct regions to be assessed. The target muscles were selected based on their biomechanical involvement in the pincer grip task (Danna-Dos Santos et al., 2010).

5.2.6 Signal Pre-processing and Spectral Analysis

EEG/EMG data analysis (Figure 5.1) was performed as described in detail in sub-section 4.4.1 of section *4.4 Sensor Level Analysis* in this thesis and in a previous study (Coffey et al., 2021). Briefly, automated artefact rejection routines (Fieldtrip Toolbox) (Oostenveld et al., 2011) were used to discard data contaminated by noise. After visual inspection of the 128-channel recordings, EEG channels with higher levels of noise were removed and reconstructed using weighted average interpolation of neighbouring channels (Perrin et al., 1989). An average of 22±6 trials (i.e., 88±24 seconds) for the five target EEG channels were retained for the Corticomuscular coherence calculation across all participants. A time window/epoch duration of 4 s (starting 1s after the visual cue) was chosen for analysis. Data epochs where the coefficient of variation of the force produced was above 0.2, or where the mean force was less than 8% or more than 20% MVC, were excluded from further analysis. An average of 3 ± 6 trials (i.e., 12 ± 24 seconds) were removed across all participants for these reasons. The raw EEG data were (re-)referenced using a surface

Laplacian spatial filter (Bradshaw and Wikswo, 2001, McFarland et al., 1997), which served to provide signals that are more spatially specific to each EEG electrode (See topic Referencing and Filtering of sub-section 4.4.1.1 and Figure 4.3 in chapter 4 Materials and Methods for the details). The EMG data (signal amplitude) were normalized with respect to root mean square EMG amplitude at 100 % MVC. EEG and EMG data were filtered between 1-100Hz and 10-100 Hz respectively using a dual-pass 4th order Butterworth bandpass filter. The auto-spectrum of each EEG/EMG signal, and the cross-spectrum between all combinations of EEG-EMG signals (frequency resolution 1Hz, bandwidth 2-100Hz) were calculated using the Fieldtrip toolbox (Hanning taper and frequency smoothing at 1Hz, non-overlapping windows of 1s). EMG signals were not rectified.

5.2.7 Estimation of Coherence Spectrum and Banded Coherence

Coherence is presented based on equivalent z-scores and p-values at both subject and group-level. This approach prevents bias by eliminating the dependence on the number of trials for the coherence analysis. See sub-sections 4.4.4.1 and 4.5.1 in chapter 4 Materials and Methods for the detailed formulation and statistics of banded spectral coherence.

CMC was examined in 8 different frequency bands (Table 4.2) and a single coherence estimate was obtained for each band. CMC was estimated based on the spatial median using the following procedure. Coherence was estimated using the median value of the auto- and cross-spectra represented by their real and imaginary components in two-dimensional space calculated across epochs (Niinimaa and Oja, 2014, Weiszfeld, 1937) and Figure 2 in Nasseroleslami et al. (2019). This contrasts with classical coherence estimates which are based on the expected value or arithmetic mean of the spectra. The auto- and cross-spectra for each 1 s epoch were calculated for each participant. The spatial median coherence was then estimated from the spatial median of the auto- and cross-spectra with a resolution of

2 Hz, Figure 5.1 F, and across each of the 8 defined frequency bands to obtain the 'banded coherence', Figure 5.1 H. The banded spectral cortico-muscular coherence was normalized by dividing the band cross-spectrum by the respective band auto-spectra. The strength of coherence was subsequently presented using the equivalent p-value as -log(p), which we denote as "pCoh".

To represent the banded CMC as a probability, each coherence value was compared against zero using a non-parametric one-sample test for significant coherence [spatial (signed) ranks (Hannu Oja & Randles, 2004; Hannu Oja, 2010; Nordhausen & Oja, 2011)]. This procedure yielded individual p-values for each frequency band, for each individual (both PLS and control groups). Stouffer's method was used to combine individual p-values to derive average p-values within each group, i.e. in the healthy group, and in the PLS group (Stouffer et al., 1949, Westfall, 2014). This procedure is similar, but not procedurally equivalent, to the pooled coherence analysis (Amjad et al., 1997). Both methods can be used to combine information from several participants (or trials). The negative logarithm of the p-values, i.e. -log10(p), was used as a measure of CMC strength to visualize cortico-muscular coherence. The band-specific coherence values, expressed in -log10(p), were used to represent the collective coherence over the range of frequencies within each distinct frequency band (Figure 5.1 H).

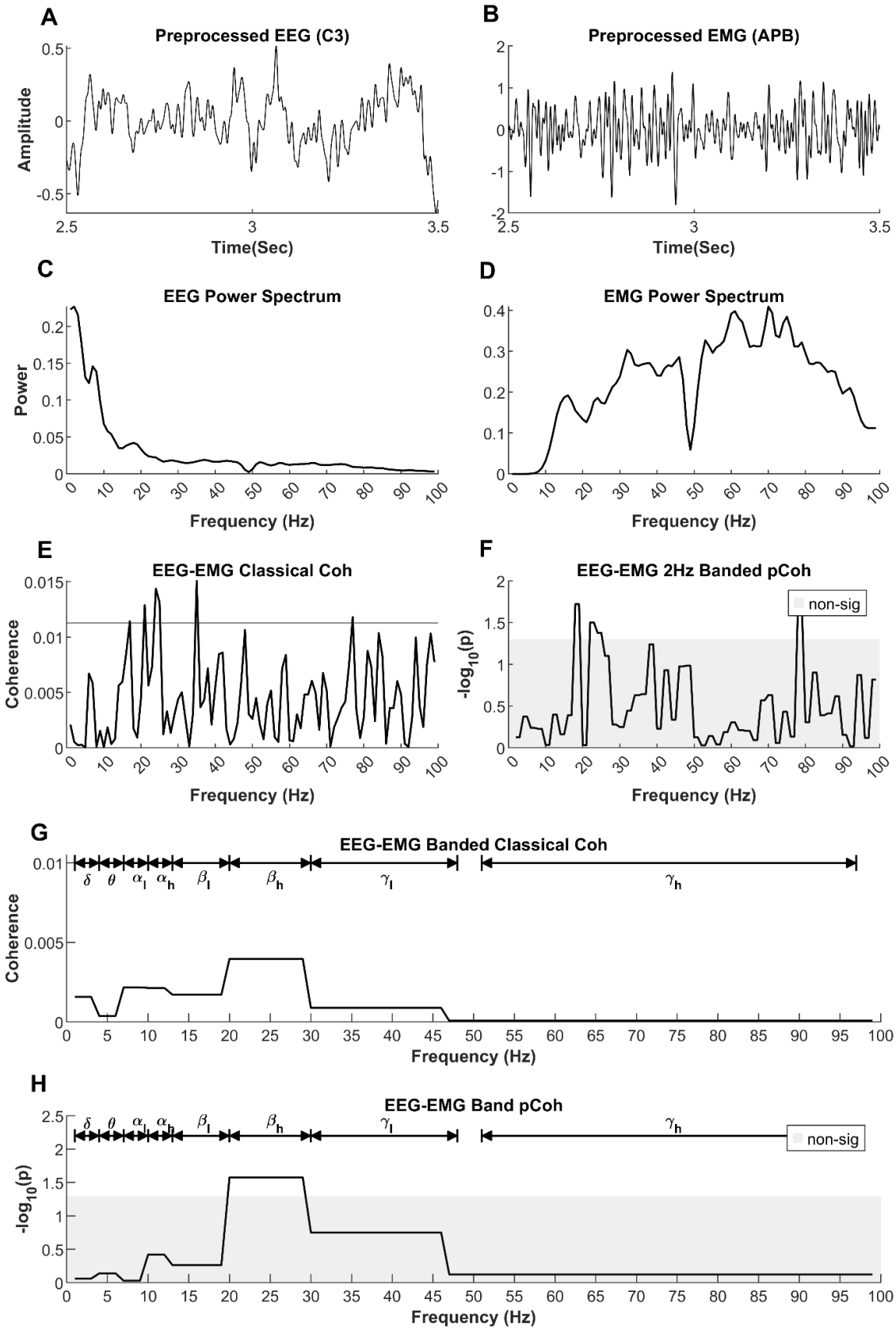

Figure 5.1 Example showing the estimation of banded cortico-muscular coherence (CMC), using data from a healthy control participant.*pre-processed EEG signal recorded from C3 electrode, (B) pre-processed*

EMG signal recorded from abductor pollicis brevis (APB) muscle during the same time interval, (C) Power spectrum of EEG signal, (D) Power spectrum of EMG signal in the frequency range of interest, (E) CMC estimated using the magnitude squared coherence with spectral smoothing ("classical coherence"), (F) CMC calculated using the spatial median to estimate the auto- and cross-spectra of the EEG and EMG data ("pCoh"). Here the spatial median was used to group the coherence spectra over bands with a 2Hz interval to facilitate the comparison of pCoh with classical coherence, (G) conversion of classical magnitude squared coherence into banded CMC values. Here the spatial median method is used to group the classical coherence spectra so that there is one coherence value for each of the pre-defined bands, (H) pCoh CMC calculated using the spatial median method to group coherence spectra over pre-defined bands. Note that F and H use the same coherence methodology, with the only difference being the bandwidth of the frequency bands used for grouping the coherence spectra. Frequency bands: delta (δ), theta (θ), low alpha (αl), high alpha (α_h), low beta (β_l), high beta (β_h), low gamma (γ_l), high gamma (γ_h). This figure has been published in Bista et al. (2023) as Figure 2, see appendix 5.1.

For comparison, the magnitude squared coherence, referred to here as "classical coherence", was also estimated in the frequency range 2-100 Hz in addition to the banded coherence. Spectral smoothing of auto- and cross-spectrum was done using a Hanning filter. The significance threshold (upper 95% confidence limit) was calculated as $1 - 0.05^{\frac{1}{(L-1)*0.375}}$, where L is the number of segments used to calculate coherence and the factor 0.375 is a correction for spectral smoothing using a Hanning filter (Halliday and Rosenberg, 1999).

5.3 Results

5.3.1 Clinical Profile

16 participants with PLS (7 females and 9 males, age: 62.7 ± 8.7 [mean ± SD]) were prospectively recruited from the national ALS Clinic based in Beaumont hospital, Dublin. All participants with PLS were diagnosed with definite PLS fulfilling the consensus criteria (Turner et al., 2020) defined as the absence of LMN degeneration 4 or more years from

symptom onset. 18 healthy controls (7 female) were recruited (age: 62.5 ± 8.97 [mean ± SD]). Table 5.1 shows the detailed profile of the recruited participants.

Table 5.1 Clinical and demographic data of the analysed PLS and control groups. This table has been published as Table 1 in Bista et al. (2023), see appendix 5.1.

	PLS	**Controls**
Biological Sex (Female/Male)	7/9	7/11
Average age at recording (years)	62.7±8.7	62.5±8.9
EHI (Right/Left)	14/2	16/2
Disease duration (years)	7.6± 6.01	-
UMN score (max 16)	12.8 ± 2.3	
Spasticity score (upper limb) (max 4)	3.5±1.09	
MRC (upper limb) (max 100)	71.6±4.08	
ECAS Total abnormal score n (%)	4 (28%)	
Language	1 (7%)	
Verbal Fluency	2 (14%)	
Memory	2 (14%)	
Visuospatial	1 (7%)	

EHI (Edinburgh Handedness Inventory)
UMN (Upper Motor Neuron Score)
MRC (Medical Research Council Scale for Muscle Strength)

ECAS results were scored as normal or impaired based on education and age (Pinto-Grau et al., 2017). Four participants with PLS (28%) showed evidence of cognitive impairment based on the total ECAS score. The details are listed in Table 5.1. Abnormal performance in visuospatial domains (7%) were uncommon based on our screening assessment with ECAS.

5.3.2 Comparison of banded and classical CMC

5.3.2.1 Group average banded and classical Corticomuscular coherence (CMC) for all EEG and EMG channels

The group average of Classical CMC spectra (Figure 5.3) is similar to the group average of banded CMC spectra (Stouffer's averaging of p values-based CMC) (Figure 5.2) for both PLS cohort and healthy controls.

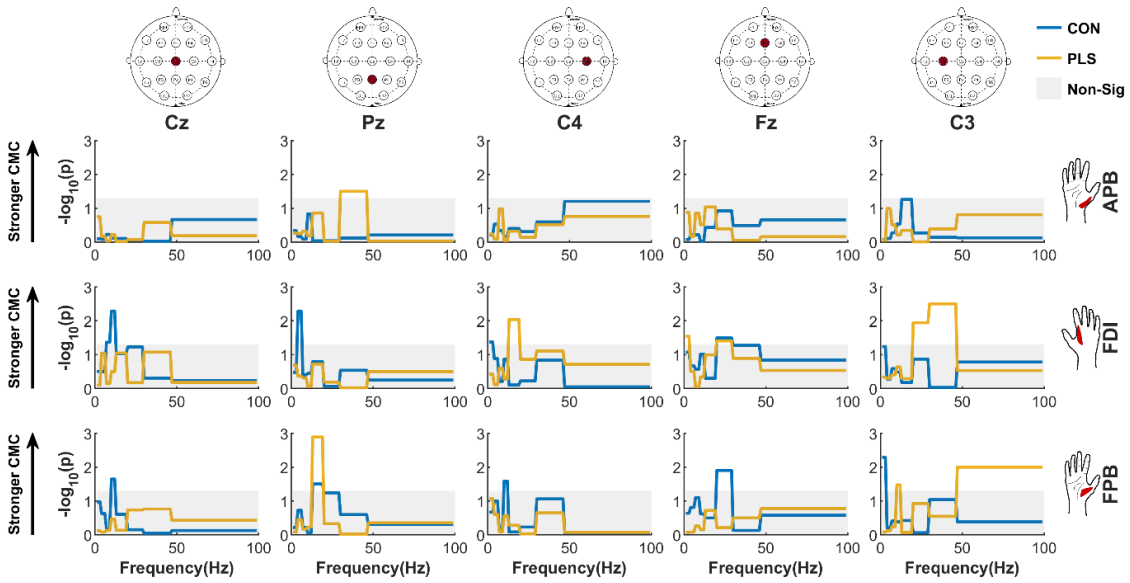

Figure 5.2 Group average banded cortico-muscular coherence (CMC) across 5 selected EEG and 3 selected EMG channels in the PLS cohort vs. healthy controls. *The EEG channels (C3, Cz, C4, Pz, and Fz) are surface Laplacian-referenced and the EMG channels are bipolar surface EMG channels. The CMC were corrected for multiple comparison using adaptive FDR at q = 0.05. The coherence spectra were grouped over pre-defined bands using the spatial median ("pCoh"). The CMC values that were significantly different between PLS and control groups are outlined in Figure 5.8 in this chapter.*

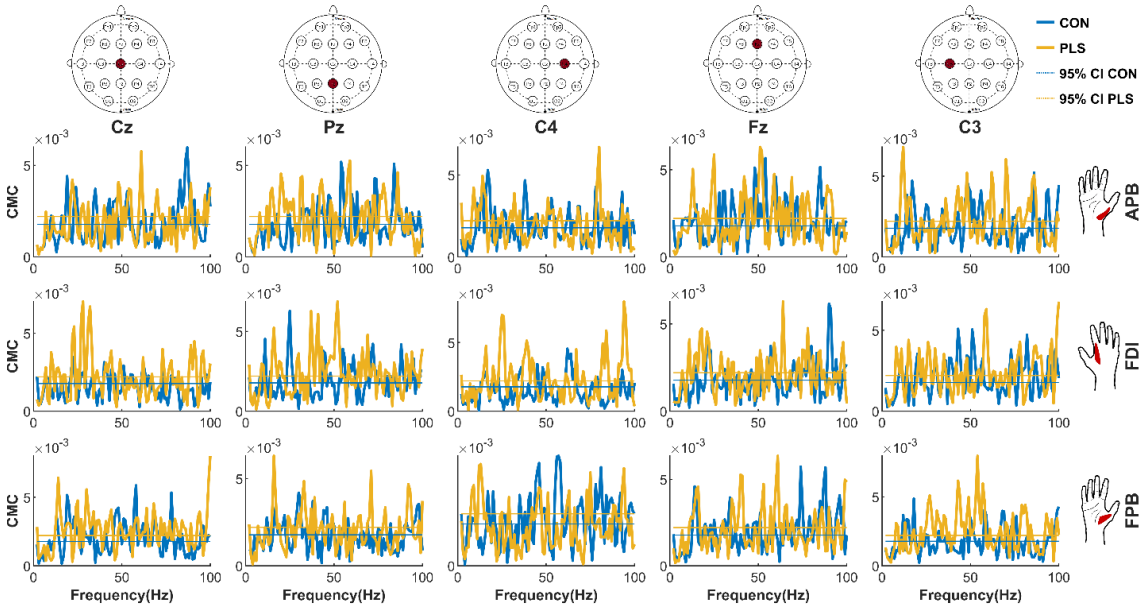

Figure 5.3 Group average classical magnitude-squared CMC across 5 selected EEG and 3 selected EMG channels in the PLS cohort vs. healthy controls. *The EEG channels (C3, Cz, C4, Pz, and Fz) are surface Laplacian-referenced and the EMG channels are bipolar surface EMG channels.*

5.3.2.2 Comparing CMC in the PLS participants using different spectral averaging and banded coherence methods

Both methods (classical and banded) have detected significant CMC in the low-beta (14-20 Hz) and high-gamma (53-97Hz) bands in a PLS participant and the coherence spectra are also similar (Figure 5.4). The banded CMC, however, gave a single value for each frequency band.

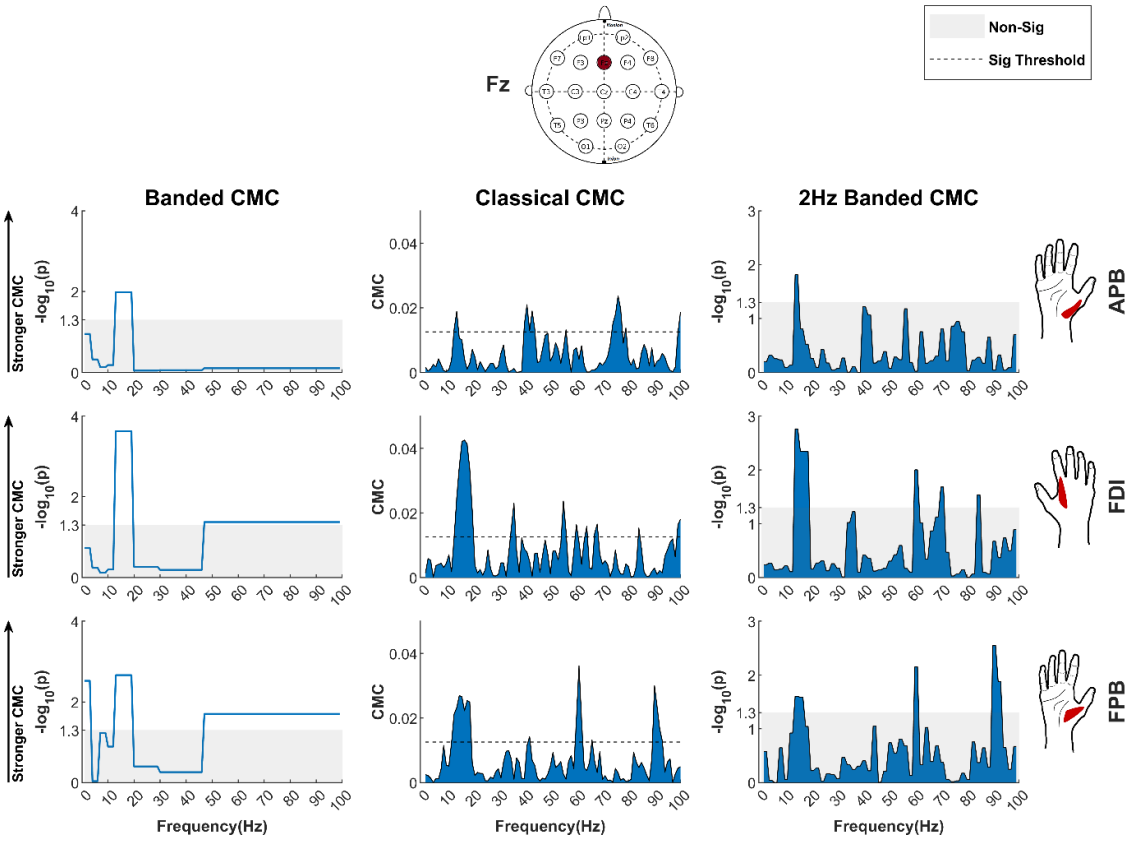

Figure 5.4 Banded and classical magnitude-squared CMC between Fz and 3 EMG channels in a PLS participant.

5.3.2.3 Spatial Topology of beta CMC for Controls

The spatial topology of banded beta "pCoh" CMC between EMG and the five EEG channels showed maximum CMC within the sensorimotor cortices (C3, Cz) and visuomotor processing areas (Pz) in controls (Figure 5.5 top panel). Similar results were observed with classical magnitude-squared CMC (Figure 5.5 bottom panel), however the banded pCoh resulted in more localised CMC patterns.

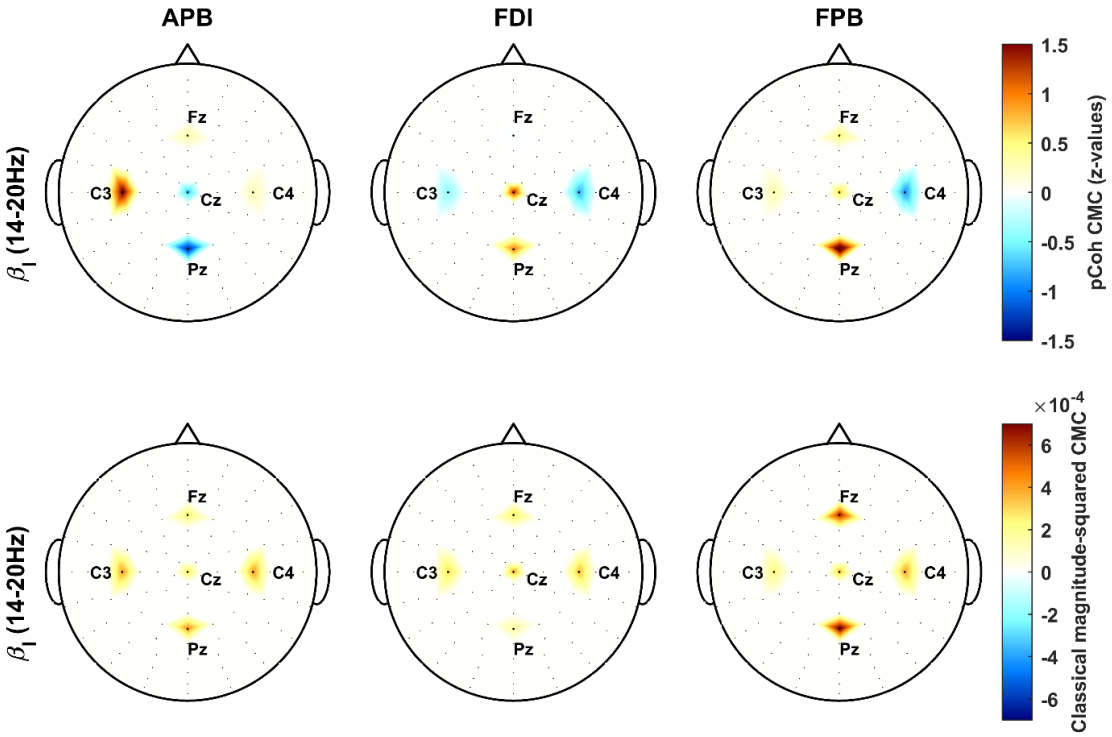

Figure 5.5 The spatial topology of group average beta CMC between 5 EEG (C3, C4, Cz, Fz, Pz) and 3 EMG (APB, FDI, FPB) channels using banded "pCoh" CMC method (top panel) and classical magnitude-squared CMC method in the same band (bottom panel) in healthy controls.

5.3.3 Verification of the task-effect

In our pilot experiments in the control group, the pincer grip task (Experiment 2) generated low levels of beta-band CMC when compared with the precision grip task (Coffey et al., 2021), suggesting that the pincer grip task may be more suitable for studying abnormally increased CMC patterns in patients. The results of the pilot experiments are shown in Figure 5.6, depicting both classical and banded group average CMC in controls for the 10% MVC pincer grip task and the precision grip task. During the precision grip task, the controls showed clear and significant beta CMC peaks at group level.

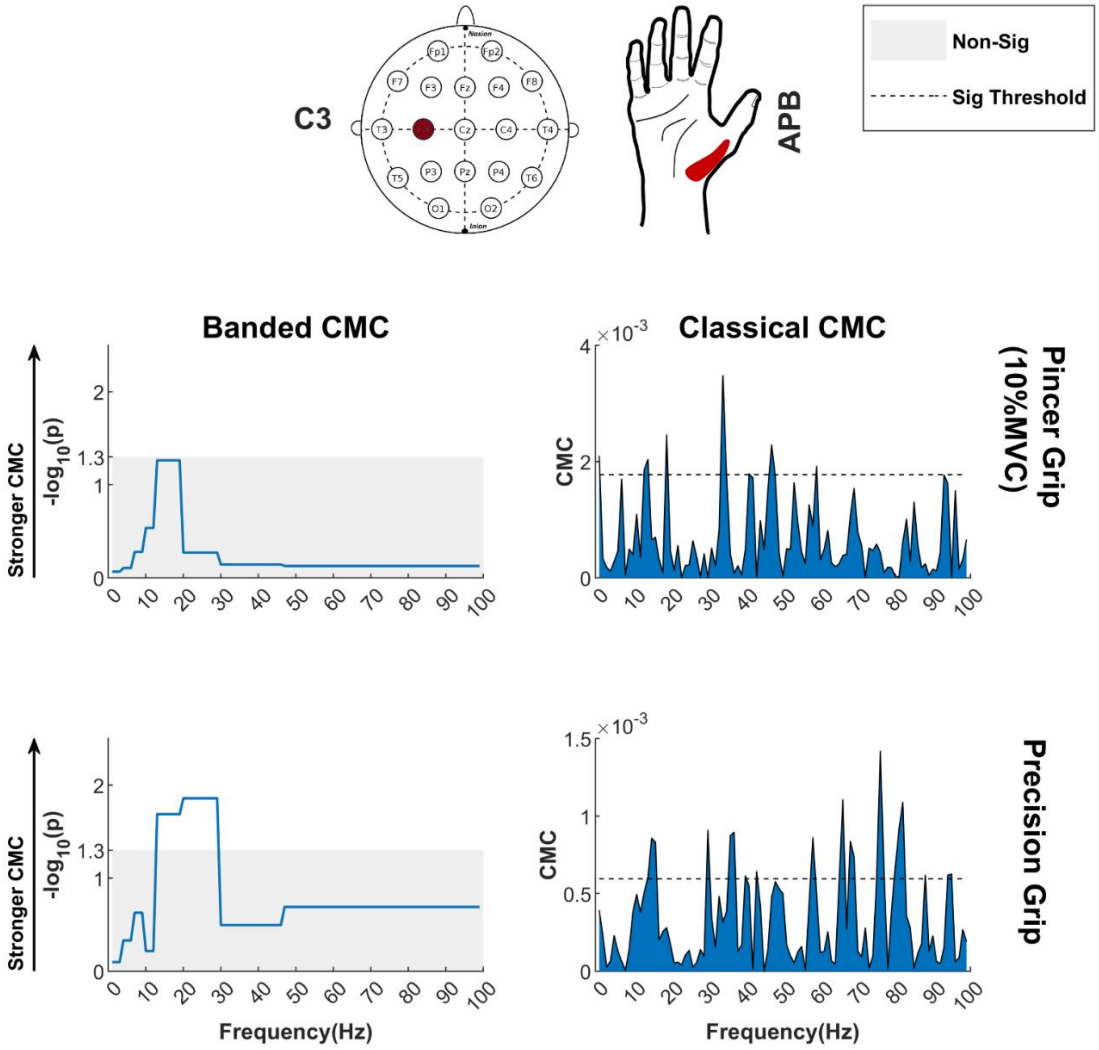

Figure 5.6 Classical and banded group average Corticomuscular coherence (CMC) for healthy controls between C3 (contralateral primary motor cortex) and Abductor Pollicis Brevis (APB) muscle during pincer grip at 10% maximum voluntary contraction (top panel) and precision grip (bottom panel) using thumb and index finger of the right hand. *The comparison confirms that the pincer grip task generates lower typical beta CMC compared to the precision grip task. The pincer grip task was chosen as it was hypothesised that a lower level of beta CMC would facilitate the detection of abnormally increased CMC in the PLS group.*

The 10% MVC pincer grip task exhibited a lower group average CMC peak in the beta-band when compared with CMC during precision grip, Figure 5.6. However, significant beta-band coherence peak was still detected during the pincer grip task in 14 out of 18 control participants using classical coherence (Figure 5.7). The lower CMC observed in the pincer grip task is expected as the force is exerted against a rigid load cell with no digit

displacement and no object flexibility. Previous studies have shown that beta-band CMC is lower for isometric pinch grip contractions against a rigid force transducer when compared with those performed with a compliant, or spring-like load (Kilner et al., 2000).

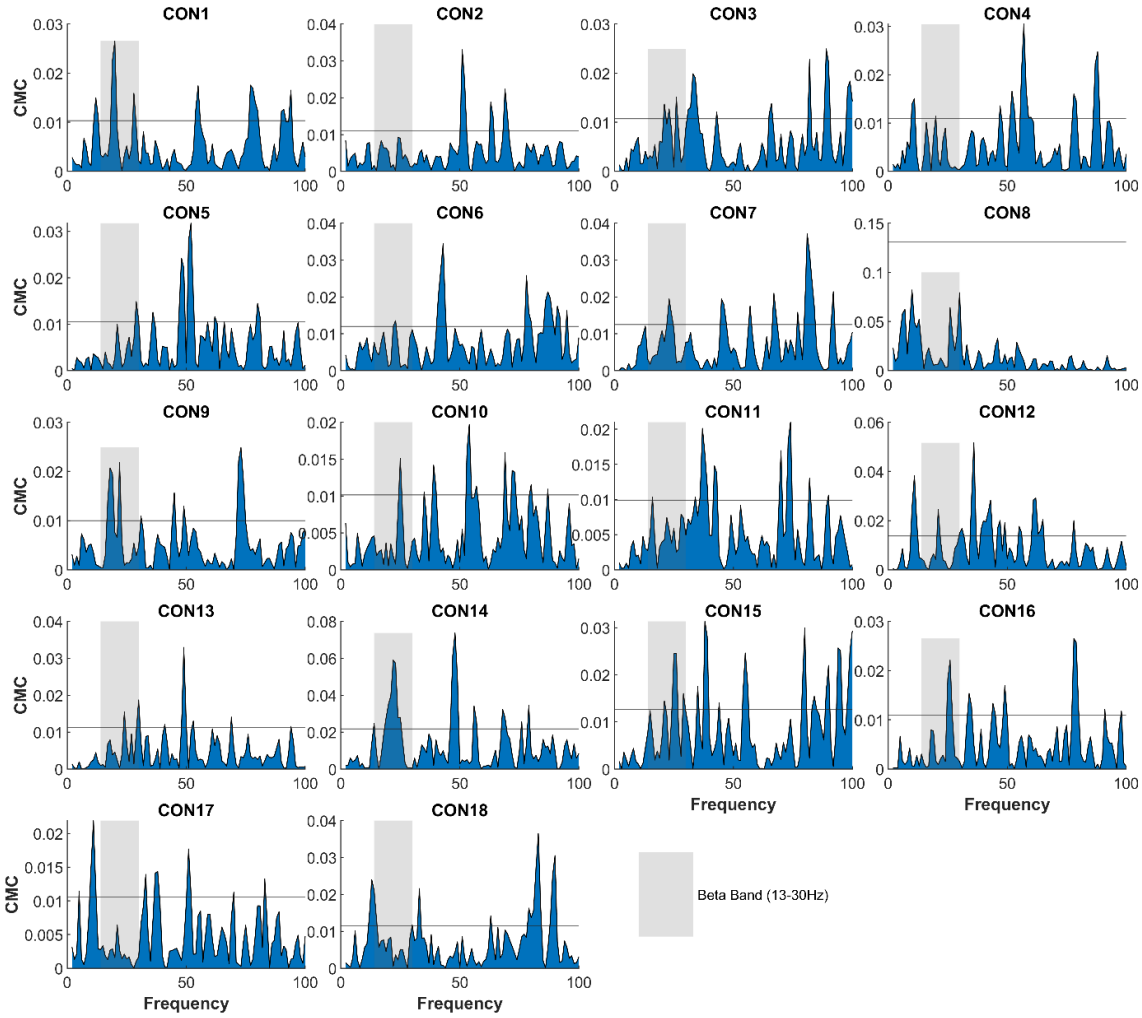

Figure 5.7 Individual classical magnitude squared CMC between C3 (contralateral primary motor cortex) and Flexor Pollicis Brevis (FDI) muscle for pincer grip (10% MVC) task. *The significance threshold or estimate of the upper 95% confidence limit for classical CMC is calculated as* $1 - 0.05^{\frac{1}{(L-1)*0.375}}$ *, where L is the number of trials used to calculate coherence.*

5.3.4 Abnormally high cortico-muscular coherence in PLS

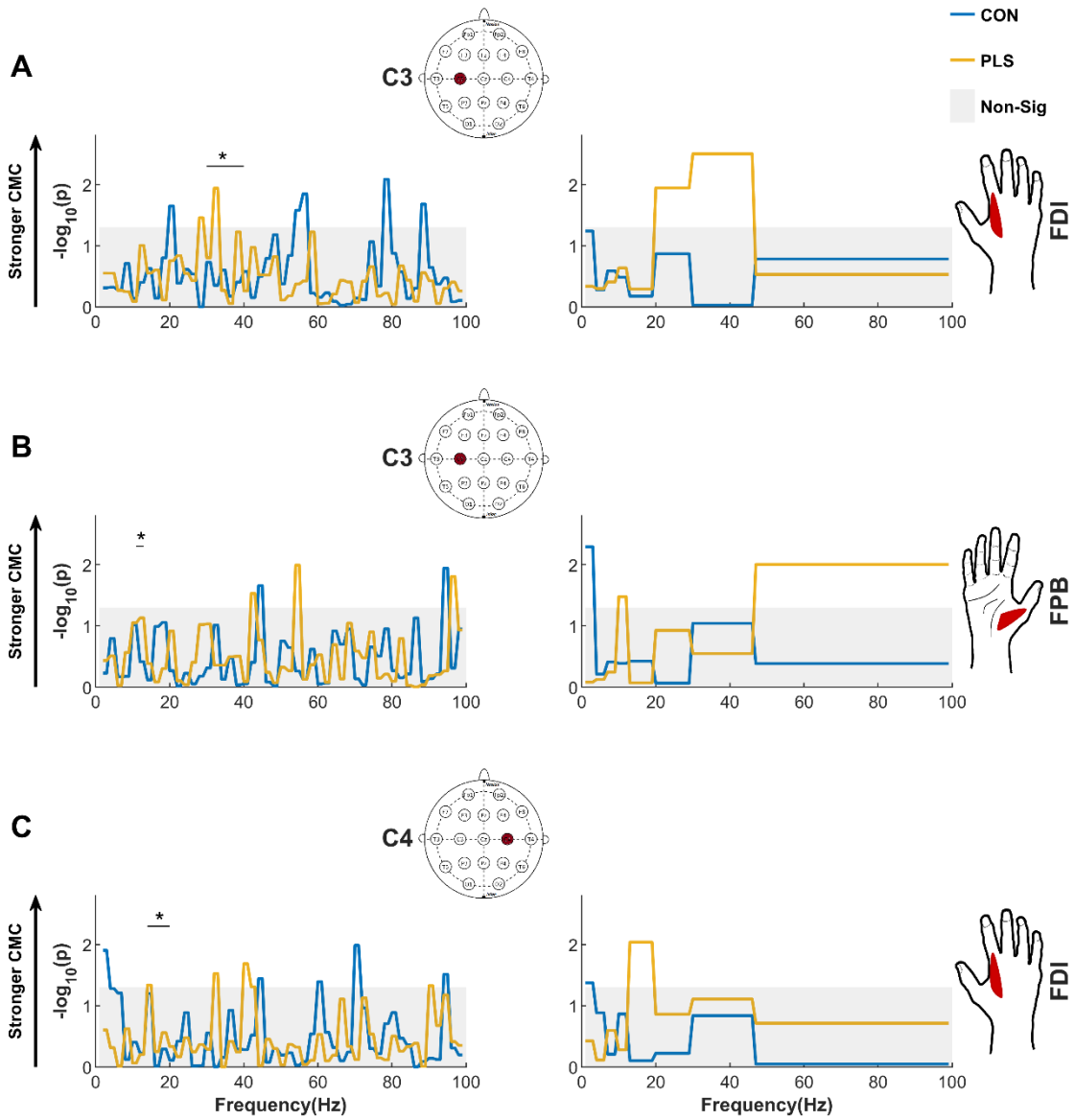

Figure 5.8 Participants with PLS show abnormal Cortico-Muscular (EEG-EMG) Coherence in primary motor areas, and beyond typical beta band during pincer grip task. *The first column displays pCoh grouped over shorter 2 Hz frequency bands and the second column shows the banded coherence ("pCoh") grouped over pre-defined frequency bands. The pCoh spectra show the strength of synchrony of the EEG electrodes over the contralateral primary motor area C3 (A & B) and ipsilateral primary motor area C4 (C) with EMG (First Dorsal Interosseous, FDI; and Flexor Pollicis Brevis, FPB, muscles) in different frequency bands. This figure has been published in Bista et al. (2023) as Figure 3, see appendix 5.1.*

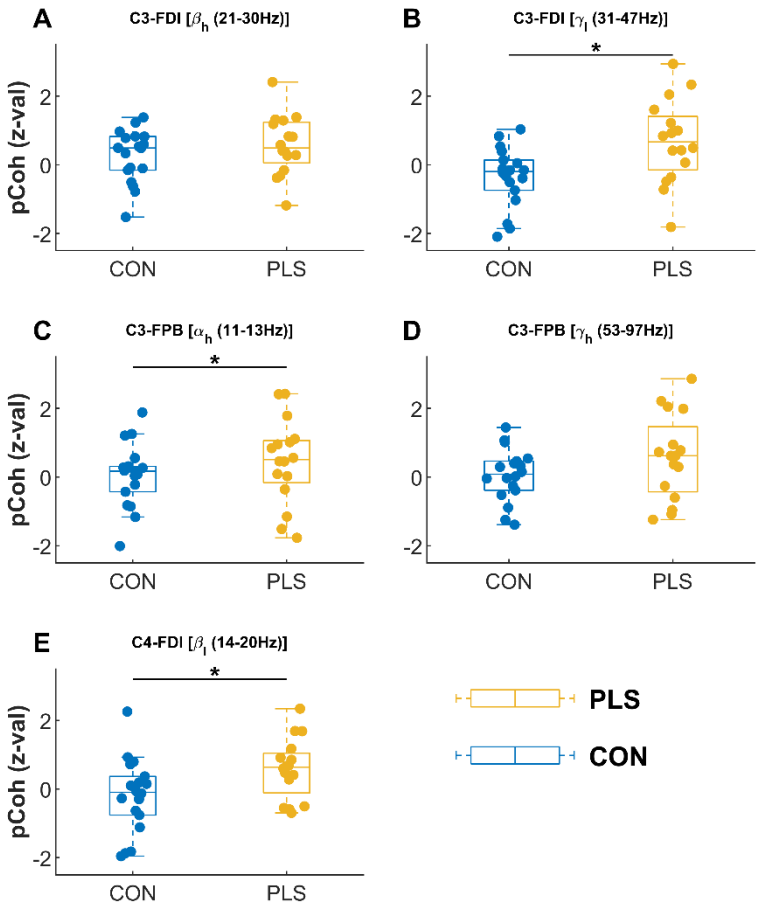

Figure 5.9 Box plot of banded CMC (expressed as z-scores) for the EEG-EMG channel and frequency band combinations that were found to show significant CMC in PLS after FDR correction. *The plots show the CMC for control and PLS participants overlayed with individual values. The groups were compared using the Kolmogorov-Smirnov test. Significant group differences are marked with an asterisk (*p < .05, corrected at FDR q = 0.05). This figure has been published in Bista et al. (2023) as Figure 4, see appendix 5.1.*

The results show that there were statistically significant differences in the frequency, location (EEG-EMG pair), and magnitude of the CMC between healthy controls and the PLS group, Figure 5.8 ($q < 0.05$, with FDR multiple comparison correction). The coherence spectra for all EEG channels and muscles investigated are presented in Figure 5.2 and significant differences between PLS and control groups are summarized in Figure 5.8 and Table 5.2.

Table 5.2 Table showing group average banded Corticomuscular coherence (CMC) values expressed as p values. The CMC measures pertain to selected EEG-EMG channel and frequency band combinations that were significant in the PLS group after FDR correction at q = 0.05. The CMC values are shown for controls and PLS along with group difference p values and effect size. This table has been published as Table 2 in Bista et al. (2023), see appendix 5.1.

EEG/EMG	Frequency	CON Avg pCoh (p)	PLS Avg pCoh (p)	Kolmogorov-Smirnov test (p)	Effect Size Cohen's d
C3-FDI	High Beta	0.135	0.011	0.465	0.381
C3-FDI	Low Gamma	0.093	0.003	0.006	0.987
C3-FPB	High Alpha	0.040	0.033	0.047	0.374
C3-FPB	High Gamma	0.0412	0.009	0.052	0.524
C4-FDI	Low Beta	0.788	0.009	0.015	0.786

Healthy controls did not show strong beta-band CMC peaks over the contralateral motor area when grouped across all participants (C3), likely due to the task selection (pincer grip vs precision grip), Figure 5.6 and Figure 5.8 A-B. However, when examined on an individual basis significant beta-band CMC was detected in 14/18 controls, Figure 5.7. Biological sex had no effect on CMC detected in the PLS cohort ($p > 0.05$, tested using Mann-Whitney U test).

5.3.5 CMC pattern over the contralateral primary motor area

C3-FDI and C3-FPB CMC were significantly higher in the gamma- and alpha-band, respectively, in the PLS group when compared with controls. The coherence was not statistically significant for the control group at the C3 channel location over contralateral motor area (between C3 and for both the FDI and FPB muscles, respectively, Figure 5.8

A-B). It is notable that statistically significant gamma- and alpha- band cortico-muscular coherence was observed in the PLS cohort (Figure 5.8 A-B) as this is not typically observed in healthy subjects during low force muscle contractions.

5.3.6 CMC pattern over the ipsilateral primary motor area

Significant beta-band CMC (β_l) was observed between C4 and the FDI over the ipsilateral motor area in the PLS cohort, and not observed in controls (Figure 5.8 C).

5.3.7 Correlates with UMN dysfunction score show location-specific positivity and negativity

We then conducted a separate analysis to test for significant correlations between CMC and UMN score (calculated for all pre-defined frequency bands and EEG and EMG channels). Several of the CMC measures were significantly correlated with the UMN dysfunction score after FDR correction, Table 5.3, and Figure 5.10. In Table 5.3 and Figure 5.10, a negative correlation between a CMC measure and UMN score indicates that higher UMN-impairment (more severe clinical symptoms) are associated with reduced EEG-EMG synchrony (CMC) in the PLS cohort.

A positive correlation indicates that PLS participants with more severe UMN symptoms exhibited stronger CMC in these muscles/brain regions. Both alpha- and gamma-band CMC between the APB muscle and the contralateral motor cortex (C3) were lower in PLS participants with more severe UMN impairments (significant negative correlation with UMN score). Theta-band CMC coherence between the FDI and the frontal brain region (Fz) was also significantly lower in PLS participants with greater UMN dysfunction. Gamma-band CMC between the APB and the ipsilateral motor area (C4) varied with the degree of upper motor neuron dysfunction. PLS participants with greater UMN

impairments exhibited lower CMC in the high gamma-band (γ_h) but higher CMC in the low gamma-band (γ_l). Finally, PLS participants with greater UMN impairments exhibited greater beta-band CMC between the APB and the parietal brain region (beta-band CMC in the parietal region is not typically observed in healthy controls).

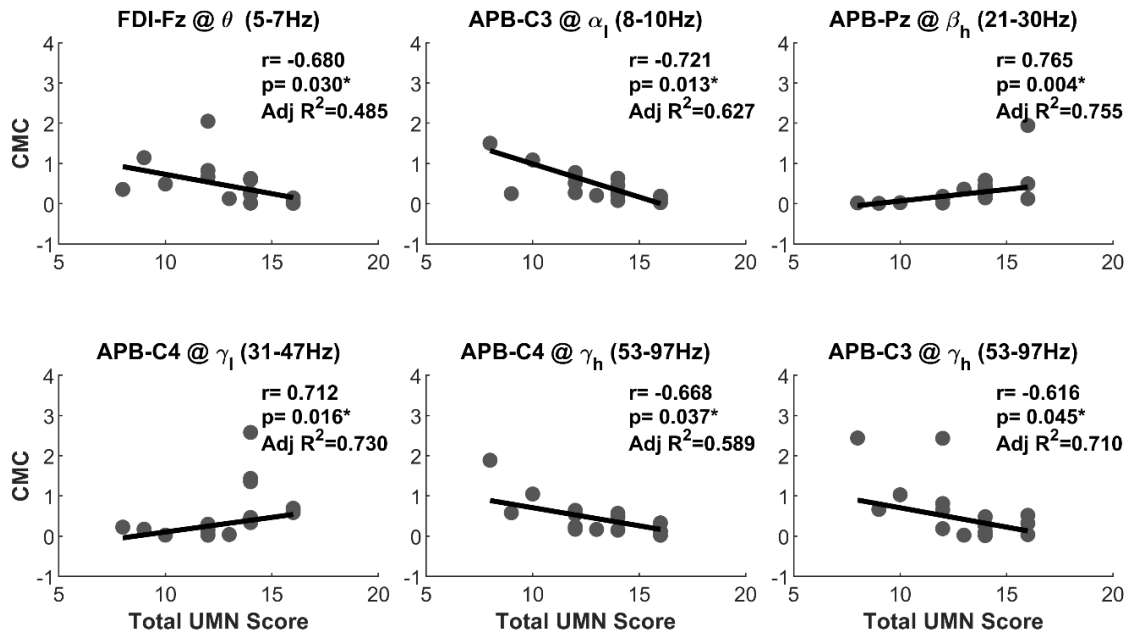

Figure 5.10 Measures of Cortico-Muscular (EEG-EMG) Coherence in PLS show significant strong positive and negative correlations with the clinically defined Upper Motor Neuron (UMN) dysfunction score. *The p-values have been corrected for false discovery rate (FDR) at q = 0.05. Notice that the correlations are partial correlations with the effect of age removed from the inference. This figure has been published as Figure 5 in Bista et al. (2023), see appendix 5.1.*

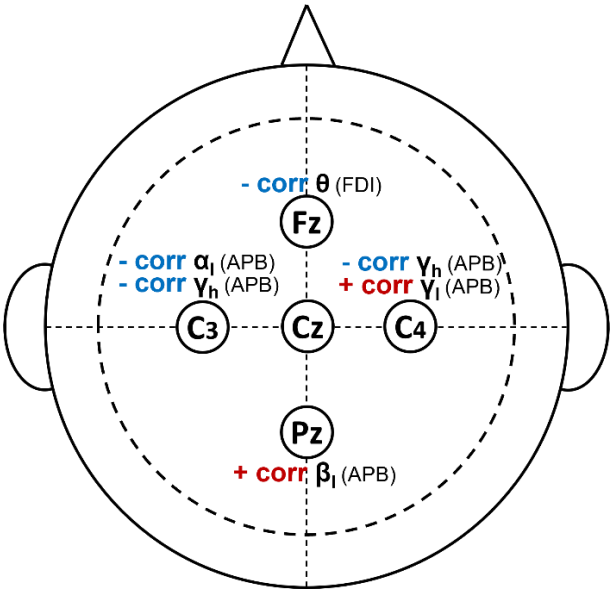

Figure 5.11 Significant correlations of cortico-muscular coherence with clinically defined Upper Motor Neuron (UMN) dysfunction score show location-specific positivity and negativity. *This figure has been published as Figure 6 in Bista et al. (2023), see appendix 5.1.*

Table 5.3 Summary of Cortico-Muscular Coherence (CMC) Measures of Interest.

This table has been published as Table 3 Bista et al. (2023), see appendix 5.1.

CMC Measure	EEG/EMG Location	Frequency Band	Significant Coherence observed in PLS	Significant difference between PLS and Controls	Significant +/- Correlation with UMN Score
1	C3-FDI	High Beta	✓		
2	C3-FDI	Low Gamma	✓	✓	
3	C3-FPB	High Alpha	✓	✓	
4	C3-FPB	High Gamma	✓		
5	C4-FDI	Low Beta	✓	✓	
6	Fz-FDI	Delta			-
7	C3-APB	Low Alpha			-
8	C3-APB	High Gamma			-
9	C4-APB	High Gamma			-
10	C4-APB	Low Gamma			+
11	Pz-APB	Low Beta			+

5.4 Discussion

To date, studies investigating CMC in motor neuron diseases have focused on estimating beta-band CMC between muscles of the hand/arm and M1, as a direct reflection of UMN/LMN pathology (Proudfoot et al., 2018b). However, our recent EEG studies in ALS (Dukic et al., 2019, McMackin et al., 2020) and Post-Polio Syndrome (Coffey et al., 2021) suggest that abnormalities in cortical network activity extend beyond M1 in these conditions, a finding that is also supported by neuroimaging studies (Finegan et al., 2019). We have used CMC to demonstrate how brain activity in participants with PLS differs from that of healthy controls during the performance of a pinch grip motor task. Here we characterised the engagement of different brain regions by the oscillatory functional coupling between signals recorded from brain and muscle, Figure 5.8, and Table 5.2. In PLS, higher CMC at contralateral M1 was observed in the gamma- and alpha-band when compared with controls. Significant beta-band CMC was also detected in ipsilateral M1, which is not typically observed in healthy participants. In each case, the CMC measures were higher in PLS than in controls, suggesting that these observed differences are unlikely to be attributable to muscle wasting or dysfunction (which would typically decrease CMC). We also identified several other CMC measures that were correlated with clinical measures of UMN dysfunction, which were also identified outside of the contralateral primary motor area.

5.4.1 PLS-specific differences in CMC

Higher alpha and gamma-band CMC between contralateral M1 and FDI/FPB was observed in PLS when compared to controls, Figure 5.8 C and B, respectively, with a large difference in gamma-band reported (Cohen's d = 0.987). Altered functional connectivity throughout the sensorimotor cortex has been similarly demonstrated in ALS in resting-state EEG

studies (Nasseroleslami et al., 2017). In the present study, gamma-band CMC was detected in participants with PLS during low force muscle contractions. This is unusual as gamma band CMC is typically only observed in healthy controls during more forceful or dynamic muscle contractions (Omlor et al., 2007, Gwin and Ferris, 2012). Previous literature has shown that gamma- and beta -band CMC are present under different conditions and are often inversely related (i.e., when gamma-band CMC increases, beta-band CMC decreases). For example, gamma-band coherence appears during strong contractions, with a corresponding reduction in beta-band CMC and is thought to reflect a stronger excitation of the motor cortex or greater attention to the task (Brown et al., 1998).

The observed broad increase in CMC in PLS may reflect a combination of pathogenic, adaptive, and/or compensatory increases in the synchronization of neuronal groups in response to upper motor neuron degeneration and dysfunction in the inhibitory inter-neuronal circuitry in PLS (Agarwal et al., 2018). Neuronal loss in M1 in PLS, and the cortical and subcortical changes beyond M1 are likely to disrupt information flow in both local neural circuits and larger scale networks. This may require a rebalancing of inter-regional interactions and a reorganisation of the sensorimotor networks that are engaged in processing and transferring information during movement. This in turn would manifest as changes to the synchronization patterns across the sensorimotor network and alterations in the coupling between cortical/subcortical and spinal regions.

Another key finding was the detection of beta-band CMC in the ipsilateral motor cortex in PLS, with a strong difference reported between PLS and controls (Cohen's d = 0.786). Ipsilateral premotor activity has been previously observed in ALS (specifically in ALS participants that exhibited a greater number of UMN signs relative to LMN symptoms) in an EEG-based investigation of movement-related cortical potentials (Inuggi et al., 2011). It is possible that the increased activation of the ipsilateral sensorimotor cortices is

functionally relevant and aids in the performance of the motor task. Ipsilateral cortical activation is increased in other populations in which elements of the cortical network have been damaged, e.g., in stroke, multiple sclerosis and spinal cord injury (Prak et al., 2021, Lenzi et al., 2007, Ward et al., 2003). Previous studies suggest that ipsilateral M1 aids the contralateral motor cortex in the planning and organization of hand movements (Chen et al., 1997), but it remains unclear whether ipsilateral M1 plays a significant role in mediating the motor command to motoneurons of the hand (Soteropoulos et al., 2011). There is limited evidence to support a monosynaptic pathway to convey direct ipsilateral actions to hand muscles, but it is possible that ipsilateral projections are conveyed through other indirect/polysynaptic pathways (Calvert and Carson, 2022). Though data presented in this study cannot elucidate the precise neural circuits and pathways through which ipsilateral M1 signals influence muscle activity, the results demonstrate for the first time that the contributing brain regions in sensorimotor control are altered in PLS during a motor task. This manifests as a reshaping of synchronous oscillations between cortex and muscle.

5.4.2 Associations between CMC and Clinical Scores

PLS participants with greater clinical impairment exhibited larger CMC in brain regions which are not directly associated with motor execution (positive correlations in Figure 6 between APB and the ipsilateral motor cortex, C4, and the parietal region, Pz). This finding suggests that PLS affects a wider brain network extending beyond M1, as indicated in previous neuroimaging studies (Finegan et al., 2019). Less impaired PLS participants exhibited higher alpha and gamma band coherence in contralateral M1. The significant correlations between CMC and UMN score were primarily observed in the APB muscle (5/6 correlations), though the reason for this is unclear. Previous studies have found no evidence that PLS conforms to the “split-hand plus” feature of ALS, whereby greater

weakness and atrophy is observed in APB relative to other muscles innervated by the median nerve (Menon et al, 2012).

PLS participants with greater motor impairments exhibited higher beta-band CMC in the parietal area (Pz) (Figure 5.11). Studies in non-human primates have shown that activity in posterior parietal sites is modulated by beta-band oscillations from the somatosensory cortex, and that they in turn exert an influence on the motor cortex (Brovelli et al., 2004). Though the majority of corticospinal neurons originate from M1, neuroanatomical and electrophysiological studies in primates have also found evidence of corticospinal projections from the supplementary motor area, somatosensory and parietal cortices (Murray and Coulter, 1981, Maier et al., 2002, Galea and Darian-Smith, 1994). CMC at EEG electrodes over non-M1 cortical areas could thus occur due to an increase in the relative contribution of alternative descending pathways to muscle activation, other than direct M1 projections. These synchronies could also reflect a restructuring of cortico-cortical communication between non-M1 regions and areas such as M1 that have direct projections to the spinal motor pools. For example, the enhanced beta-band coupling between the parietal brain region and muscular activity could reflect an increase in the functional connectivity of these brain networks (Meoded et al., 2015). It is also possible that the chronic loss of corticospinal input to the spinal motoneurons, which is combined with extreme muscle weakness and slowing of movement in PLS, could produce a change in afferent activity. This would in turn influence CMC. Though beta-band CMC is primarily driven by efferent supraspinal structures, there is now evidence to suggest that it can be modulated by sensory receptors that provide afferent feedback to the central nervous system (Witham et al., 2011).

Although the observed CMC differences in PLS could arise from both the direct and indirect effects of UMN degeneration, the increased CMC in more impaired PLS

participants for specific brain regions could potentially suggest that these changes are compensatory/adaptive in nature. Taken together, these results could suggest that the pattern of brain network re-organization in PLS follows a similar trajectory to recovery in stroke, where more impaired PLS participants rely on contributions from the ipsilateral hemisphere but those that are minimally affected can recover function by restructuring the functional connectivity in the contralateral hemisphere (Brancaccio et al., 2022). Future studies are needed to elucidate the pathways through which these wider brain regions could influence muscle activity and determine the exact nature of the observed changes in CMC (pathogenic, adaptive, or compensatory). These network level changes could be further characterised in future longitudinal studies of PLS by examining changes in the CMC measures alongside changes in clinical scores of upper motor neuron impairment.

5.4.3 Banded CMC as a tool for accessing network dysfunction

The differences between more and less impaired PLS participants further suggest that banded CMC has the potential for development as a tool to monitor disease progression or importantly as a measure to assess target engagement in clinical trials (Jeromin and Bowser, 2017). These measures are particularly needed for PLS, as longitudinal progression is difficult to quantify in such a slowly progressing disease. The PLS-specific differences in CMC and the differences between more and less impaired PLS participants reported in this study provide the basis for further development of these markers of motor network dysfunction.

5.5 Conclusion

This study demonstrates the presence of abnormal cortico-muscular coherence in PLS for the first time using the banded coherence method, which we suggest could reflect a restructuring of the cortical network connectivity in response to UMN degeneration. This

observation suggests that PLS affects a sensorimotor brain network extending beyond the primary motor cortex. Correlations showed that higher CMC in specific brain regions was also observed in more impaired PLS participants compared with those with less severe impairments. This may suggest these differences are compensatory/adaptive in nature, though these differences could arise from both the direct and indirect effects of UMN degeneration. The correlations with clinical UMN scores demonstrate the potential for CMC measurements to be used as a tool to identify dysfunction in specific cortical networks during motor tasks, and prompt further development of quantitative neurophysiology-based biomarker candidates in PLS.

5.6 Limitations

The banded coherence method could underestimate the unique coherence value in group average coherence spectra for a broadband frequency band such as the high-gamma band if majority of coherence values are close to zero. For example, in Figure 5.8 A, even though there are four significant peaks in the 2Hz banded group average coherence spectra for controls in the high gamma-band, it is not significant after banding for whole bandwidth because majority of 2Hz banded coherence values within the high-gamma band are close to zero. One possible solution for this problem is to break down the broadband frequency into smaller bandwidths. For example, breaking down the high gamma band (52-97Hz) into high-gamma 1 (52-75Hz) and high-gamma 2 (76-97Hz).

6. Results: Sensor Level Study of EEG Functional Connectivity

Under Review Work List

The work described in this chapter has been submitted in the peer-reviews journal the Journal of Neural Engineering as:

Bista S, Coffey A, Fasano A, et al., Abnormal EEG spectral power and coherence measures during pre-motor stage in Amyotrophic Lateral Sclerosis: Implications for developing biomarker candidates, Journal of Neural Engineering, 2024 (Under review).

6.1 Introduction

ALS is a multi-network dysfunction (Dukic et al., 2021) causing deficits in motor (Cividini et al., 2021, Dukic et al., 2019, Dukic et al., 2021) and cognitive (McMackin et al., 2021, Cividini et al., 2021, Dimond et al., 2017) brain networks. However, understanding the changes in motor networks is important to understand disease pathology because the motor region is predominantly affected by the neurodegeneration. Impairment of sensorimotor and non-motor networks in ALS has been identified from resting state paradigms using EEG (Dukic et al., 2019, Iyer et al., 2015) or fMRI (Agosta et al., 2011, Douaud et al., 2011, Menke et al., 2018, Zhou et al., 2014). However, motor paradigms, involving pre-motor stage or motor execution that can directly access sensorimotor pathways, might be needed to unravel the dynamics of motor network pathology in ALS for biomarker design. Previous electrophysiological studies have reported the manifestation of distinct EEG signatures of cortical sensorimotor activity, such as the Bereitschaftspotential (BP), as early as nearly 2 seconds before a voluntary movement (Pfurtscheller and Berghold, 1989, Deecke, 1996, Shibasaki and Hallett, 2006, Walter et al., 1964, Kornhuber and Deecke, 1965). Depending on the experimental design and the time window investigated, the pre-

movement or pre-motor activity is often associated with preparation (Requin et al., 1990), planning (Nasseroleslami et al., 2014), anticipation (Mauritz and Wise, 1986) or attention (Mannarelli et al., 2014) to upcoming motor execution. During the pre-motor stage and motor execution, there is a decrease in sensorimotor mu or beta power compared to the baseline (rest), known as event-related desynchronization (ERD), signifying cortical activation. Conversely, following execution, there is an increase or rebound in this power, indicating cortical idling or deactivation (Neuper et al., 2006, Pfurtscheller and Lopes da Silva, 1999). Several studies have reported that mu or beta ERDs are altered during pre-motor stage and during motor execution in ALS, however, previous findings have been inconsistent (Riva et al., 2012, Proudfoot et al., 2017, Bizovicar et al., 2014). This is especially important, as this pre-motor activity is associated with the engagement and function of non-primary motor regions such as parietal areas, dorsolateral prefrontal cortex, and pre-motor cortex, that network directly with primary motor areas (M1), and are therefore, most likely to be affected – possibly in a heterogenous manner – in motor system degeneration.

Changes in neural activity and network function can also be investigated using measures that quantify alterations in the spectral content and characteristics of neural activity, such as coherence and Event-Related Spectral Perturbations (ERSPs). While ERDs provide information on the timing and relative neural activity in different brain regions at narrow bands (mu or beta), ERSPs can provide information on the broad band spectral content of this neural activity and how the power of different frequency components (e.g., alpha, beta, gamma) changes over time. In addition, coherence can provide a direct measure of (phase) coupling of non-primary motor cortices with sensorimotor cortices (functional connectivity) which could be key to understanding neuropathophysiological mechanisms in ALS at a network level. We hypothesize that in ALS, the pre-motor activity, as reflected

in ERSPs and the coherence between neural activity in different brain regions, shows abnormal characteristics compared to healthy controls that are distinct from neural activity in motor execution. The rationale is based on the direct effects of motor system degeneration that might affect the connections between primary motor cortex and secondary motor and pre-motor areas, as well as secondary effects such as adaptations, plasticity, or compensatory processes. To examine this, we will compare ERSPs and coherence, between ALS and control groups. More specifically, we will investigate whether particular phases of movement (resting state, pre-movement, motor execution) show larger differences in EEG network connectivity between ALS and controls; and whether the altered EEG networks in ALS show associations with clinical measures of impairment such as ALSFRS-R scores. Lastly, we will test whether these measures are reproducible and show strong effect sizes, which is a prerequisite for developing prospective network-based biomarker candidates in ALS for diagnosis, prognosis, and phenotyping.

6.2 Methods

6.2.1 Ethical Approval

Ethical approval was obtained from Tallaght Hospital/St. James's Hospital Joint Research Ethics Committee for St. James's Hospital, Dublin, Ireland [REC: 2019-07 Chairman's Action (22)], and experiments were conducted under the standards set by the Declaration of Helsinki (2013). All participants provided written informed consent before participating in the experiments.

6.2.2 Participants

6.2.2.1 Inclusion Criteria

Healthy individuals aged between 18 and 65 and all ALS patients fulfilling the revised EL Escorial diagnostic criteria for possible, probable, or definite ALS were included.

6.2.2.2 Exclusion Criteria

Patients diagnosed with primary lateral sclerosis, progressive muscular atrophy, multiple sclerosis, epilepsy, stroke, brain tumours, prior transient ischemic attacks, structural brain disease, psychiatric diseases, medical conditions that affect the nervous system (e.g., diabetes), other neurodegenerative conditions and other terminal conditions, such as human immunodeficiency virus, were excluded. Similarly, people who have previously had (allergic) reactions in similar recording environments (e.g., to recording gels) and pregnant women were also excluded.

6.2.2.3 Clinical and Demographic Profile

Resting state and motor task EEG data were recorded from 22 ALS patients [age: 65.56±9.92 (mean ± std)] and 16 healthy controls [age: 62.67±9.42 (mean ± std)]. The patients and controls were age matched (Mann-Whitney U test, p=0.30). The clinical and demographics data of analysed patients and healthy controls are shown in Table 6.1.

6.2.3 Experiment

6.2.3.1 Experimental paradigm

Participants were comfortably seated on a chair in front of a screen, on which visual cues for the experiment were presented, inside a shielded room (Faraday cage). The screen was positioned at eye level, approximately 1 metre from the participants. Participants were given practice trials to produce and maintain the target force displayed onscreen using their right hand's thumb and index finger (irrespective of their handedness) before starting the

main experiment. The experiment started with a resting-state (eyes open and fixated on a cross on the presentation screen with mind-wandering) recording for 3 blocks of 2 minutes. A motor task followed the resting state recording. Participants were asked to produce a maximum force and hold (for 5 seconds) by pinching the force sensor according to visual cues. Participants were provided with the real-time feedback of the force applied, given by the height of a filled rectangular green bar visible onscreen. Five trials were recorded with 30s rest between the trials, and the average force of the five trials was calculated online and used as the maximal voluntary contraction (MVC). The participants then performed 30 trials of isometric pinch grips at 10% MVC following the target force displayed onscreen. Five seconds after the start of a trial, an empty rectangular box was displayed onscreen as a go cue. The participants pinched the force sensors to increase the height of the green bar to reach the height of the target box and then hold to keep a constant force. After 5 seconds, the box disappeared as a cue for participants to relax. A separate cue for the pre-motor stage was not provided. Each trial lasted for 15s (5s pre-motor, 5s execution, and 5s rest), as shown in Figure 6.1 B.

6.2.3.2 EEG and force acquisition

EEG was recorded with a 128-channel active electrode system (Biosemi ActiveTwo system, Biosemi B.V., Amsterdam, The Netherlands). Eight external electrodes were placed on the scalp and face, and the electrode offset was maintained below ±25µV. The force applied during the pinch grip experiment was measured using two flat resistive force sensors (FlexiForce A201 Sensor, Tekscan, Inc., Boston, MA, USA). The sensor's circular sensing areas (d=9.7mm) were attached to a wooden hexagon prism (edge=30mm, thickness=25mm). An example of force profiles recorded from 30 trials for a healthy participant is shown in Figure 6.1 C.

Table 6.1 The clinical and demographics data of analysed patients and healthy controls.

Group	N	Male	Female	Age (years)[a]	Disease duration (years)[a]	Diagnostic delay (months)[a]	ALSFRS-R[a]
Controls	16	10	6	62.67±9.41			
ALS							
ALL	22	16	6	65.56±9.92	2.37±2.02	20.19±25.02	39.59±5.61
Spinal	19	13	6	65.71±10.51	2.55±2.12	22.24±26.42	40.36±4.69
Bulbar	3	3	0	64.61±6.06	1.20±0.29	7.25±2.00	34.66±9.50
C9ORF72-	21	15	6	65.74±10.13	2.39±2.07	20.40±25.65	39.71±5.71
C9ORF72+	1	1	0	61.77±0.00	1.97±0.00	15.91±0.00	37.00±0.00

Note: Disease duration is the time interval between the estimated symptom onset and the EEG recording. Diagnostic delay is the time interval between the estimated symptom onset and date of diagnosis.

Abbreviations: ALSFRS-R, amyotrophic lateral sclerosis functional rating scale revised; C9ORF72±, presence/absence of the repeat expansion in the Chromosome 9 open reading frame 72; EEG, electroencephalography.

[a] Number shown mean± standard deviation.

6.2.3.3 Disease severity

The revised ALS functional rating scale (ALSFRS-R) scores (Cedarbaum et al., 1999) were obtained from all ALS participants to examine the correlation of EEG connectivity measures with disease severity.

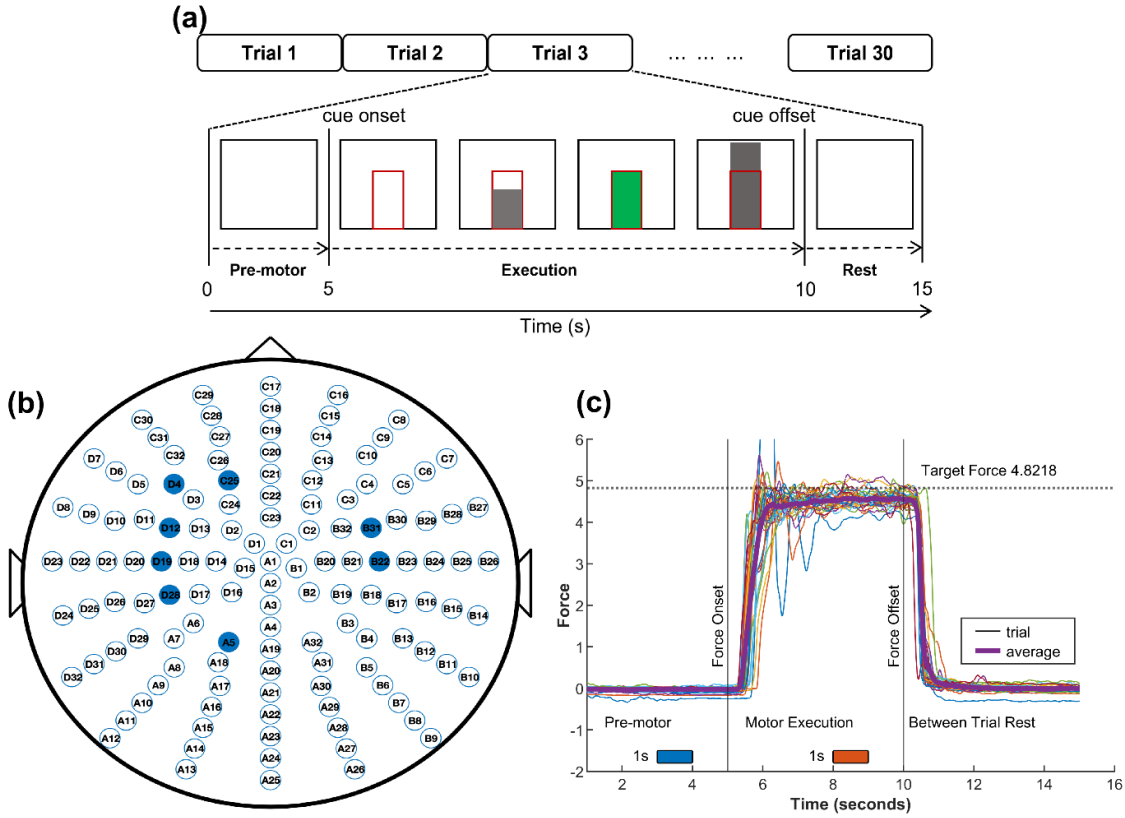

Figure 6.1 EEG channel selection, data format of experiment 2, and force data. *(a) EEG data format showing 30 trials, each trial consisting of 3 phases. Trial 3, for example, is expanded to show the sequence of visual cues and timings of different phases of the task. From left to right: 1. White screen for 5 seconds preceding cue onset where participants take no action: motor planning phase. 2. GO cue, as a red rectangle appears on screen whose height is the target to be matched. 3. Section of 5 seconds during the visual cue: motor execution phase (between trigger 2 and trigger 3), and 5 seconds after the end of the cue: between trial rest phase (between trigger 3 and trigger 1), (b) 2D layout of electrode positions for 128 channel Biosemi system. The blue electrodes are the eight electrodes chosen for analysis, (c) Illustration of the recorded force for all 30 trials and their average for a healthy participant. Target force is 10% of maximum voluntary contraction (MVC). One second time windows were selected for analysis, a blue block (3-4 sec) for pre-motor stage and a red block (8-9 sec) for motor execution.*

6.3 Data analysis

6.3.1 Data Pre-processing

The pre-processing of EEG data was carried out in MATLAB using the Fieldtrip toolbox (fieldtrip.org). The details of the data pre-processing pipeline used in this study are explained in sub-section "4.4.1 Sensor Level Study" of Chapter 4 Materials and Method of this thesis.

Briefly, data analysis involved the extraction of specific segments of EEG data for different conditions. For the resting state, 30 seconds of data from the first block was used. In motor task experiments, "bad trials'' where participants did not achieve the target force within the acceptable range were excluded from analysis. For pre-motor stage, 1-second data between the 3rd and 4th second of good trials were extracted, while for motor execution, 1-second data between the 8th and 9th second of good trials were extracted (see Figure 6.1 c). The bad channels detected by visual inspection were removed and reconstructed using weighted average interpolation of the neighbouring channels (Perrin et al., 1989).

Eight EEG channels A5, B22, B31, C25, D4, D12, D19, and D28 (International 10-10 System equivalent P1, C4, FC4, F1, F3, FC3, C3, and CP3) were chosen a priori for the analysis (Figure 6.1 b). D19/B22 cover left/right primary motor cortex (M1) whereas left/right premotor cortex (PM) is covered by the electrodes D12/B31. The left primary sensory cortex (S1) is covered by D28, and the left superior parietal lobule (SPL) is covered by A5. Similarly, the electrode D4 and C25 covers left dorsolateral prefrontal cortex (DLPFC) and left dorsomedial prefrontal cortex (DMPFC), respectively. The electrodes pertaining to the aforementioned cortical regions were chosen because they are known to be activated during pre-motor activity (Churchland et al., 2006, Riehle, 2005, Pfurtscheller and Berghold, 1989, Glover et al., 2012, Ariani et al., 2015, Papitto et al., 2020) and execution (Hanakawa et al., 2008, Papitto et al., 2020, Lacourse et al., 2005, Alahmadi et

al., 2015, Cisek et al., 2003) of motor tasks in healthy individuals. Additionally, cortical regions such as M1, S1, PM and DLPFC work together to integrate higher-order cognitive processes with sensorimotor functions, facilitating complex movement coordination and task execution based on cognitive demands and goals (Miller and Cohen, 2001). DLPFC is usually associated with the executive control network (Heinonen et al., 2016, Beaty et al., 2015, Shen et al., 2020) or central-executive network (Bressler and Menon, 2010, Bi et al., 2017) whereas M1, S1 and PM are critical parts of sensorimotor networks (Penfield and Boldrey, 1937, Luo et al., 2020). Therefore, the functional interconnection between these brain regions is referred to as the executive sensorimotor network (ESMN). The ESMN enable flexible motor adaptation and cognitive control during various tasks.

The selected channels were (re)referenced using a surface Laplacian spatial filter (see topic "Referencing and Filtering" of sub-section 4.4.1.1 of section 4.4.1 of this thesis for the details of Laplacian filter used) because it helps to minimise the effect of volume conduction in EEG data (Bradshaw and Wikswo, 2001). The Laplacian filtering was followed by dual-pass bandpass filtering between 2-100 Hz and dual-pass bandstop filtering between 49-51 Hz using 4th order Butterworth filters designed using Fieldtrip toolbox. Fieldtrip implemented threshold-based automatic artefact detection, and rejection were used to detect and remove eyeblinks, muscle artefacts, and jump artefacts (see topic "Automatic Artefacts Detection and Rejection" of sub-section 4.4.1.1 of section 4.4.1 of this thesis for the details). The threshold value was fixed such that no more than 20% of trials were rejected as artefactual trials.

6.3.2 Banded Spectral Coherence

The detailed formulation of banded spectral coherence is explained in sub-section 4.4.4.1. Here, a summary of the method is included to avoid repetition. Briefly, the pre-processed

EEG data were converted into the frequency domain using Fourier Transform (Hanning taper, 1 Hz spectral smoothing, 2-100 Hz bandwidth, and 1 Hz frequency resolution). Auto spectra and cross spectra were calculated using the Fieldtrip toolbox for each trial. The 2-100 Hz spectral bandwidth was divided into 8 frequency bands namely delta δ, θ, α_l, α_h, β_l, β_h, γ_l and γ_h excluding the 48-52Hz range to avoid mains power interference. The banded auto- and cross- spectra were calculated for each trial at each frequency band by taking the spatial median of the signal spectra at the specific band frequencies. The banded cross-spectrum was normalised by auto-spectra to obtain a banded spectral coherence estimate for each trial (Nasseroleslami et al., 2019).

6.3.3 Banded Spectral Coherence Statistics

The details of banded spectral coherence statistics are explained in sub-section 4.5.1. Briefly, participant-level statistics (individual p-values) were calculated using one-sample non-parametric rank statistics for spectral coherence (Nasseroleslami et al., 2019). Stouffer's method (Stouffer et al., 1949, Westfall, 2014) was used to combine individual p-values to derive average group p-values. The negative logarithm of the average p-value was used to visualise group average EEG coherence (see equation 4.17). An EEG coherence (C) greater than 1.30 (i.e., $p_{avg} < 0.05$) indicated a significant functional connectivity between two underlying cortical regions (connected by orange lines in result figures). EEG coherence of the patient group was compared with the control group using 2 sample non-parametric rank statistics (Nasseroleslami et al., 2019, Oja and Randles, 2004, Nordhausen and Oja, 2011) with p-value (p_{diff}) corrected for multiple comparisons using adaptive FDR (Benjamini and Hochberg, 2000). Significant differences in EEG coherence values between the patient and control groups (i.e., $C_{ALS} > C_{CONTROLS}$ or $C_{ALS} < C_{CONTROLS}$ and

$p_{diff} < 0.05$), referred to as abnormal EEG connectivity for ALS, are indicated by a bold purple line connecting the underlying cortical regions, Figures 6.3-6.5.

6.3.4 Event Related Spectral Perturbation (ERSP)

See time-frequency analysis (sub-section 4.4.3) for the details of this method. Briefly, the pre-processed time series data of motor experiments (pre-motor and execution), was first averaged over trials to get the event-related potential (ERP). The ERP was then subtracted from every trial of pre-processed data to get non-phase locked (NPL) time series data. The NPL data were decomposed into time-frequency components using wavelet transform (morlet wavelet with 5 cycles, a frequency resolution of 1 Hz, and a time resolution of 0.05 seconds) using the Fieldtrip toolbox. The output time-frequency power was normalised to an inter-trial rest period of 5 seconds of motor task experiment (i.e., -3 to 2 second baseline window). The normalised time-frequency power was averaged over time components to obtain event related spectral perturbations (ERSP). Finally, the ERSP was averaged over participants of each group separately to get the group average ERSP for ALS and healthy controls.

6.3.5 Event Related Spectral Perturbation Statistics

Significant differences (p-values) of ERSP between ALS and healthy controls were calculated using Mann-Whitney U test. Adaptive FDR at q=0.05 was used to correct for multiple comparisons (Benjamini et al., 2006). A 95% confidence interval was also calculated for group average ERSP.

6.3.6 Global Clustering Coefficient

The global clustering coefficient (GCC), which measures the connectedness or network density of the EEG functional network, was calculated for eight frequency band, for both ALS patients and healthy controls, using the Watts and Strogatz method (Watts and

Strogatz, 1998). See sub-section 4.4.5.1 of chapter 4 of this thesis for the details of calculation of GCC.

6.3.7 Classification and Clinical Correlation

A simple machine learning (pattern classification) method was used to assess the level of discrimination provided by the EEG measures from different stages of the task, and to test if any stage provided better discrimination and/or additional information compared to the other stages. A nested 5-fold cross-validated linear support vector machine (LSVM) classification model, designed using MATLAB's Machine Learning Toolbox, was trained, and validated to discriminate patients and healthy controls. The nested cross-validation method was used to avoid feature selection bias and overfitting due to the smaller sample size (Vabalas et al., 2019) by selecting features at threshold value of $q = 0.05$ within the cross-validation loop. To determine the level of discrimination provided by each feature (EEG measure) on the predicted outcome of the LSVM model, we used the Shapley value-based explanation (Lundberg and Lee, 2017). The feature with higher absolute Shapley value is viewed as the most discriminant feature within the classification model (Rodríguez-Pérez and Bajorath, 2020, Ding et al., 2022). We averaged the absolute Shapley value over each fold in the 5-fold cross validation and reported the mean value to avoid biased interpretation based on a single model (Ding et al., 2022).

The association of the ALS abnormal EEG connectivity with their corresponding ALSFRS-R scores was tested using Pearson's correlation coefficients. The p values of correlation coefficients were adjusted for multiple comparisons using adaptive false discovery rate at q = 0.05. A line was fitted to the scatter plot of the data, to visualise the relationship, using the linear least-square fitting method. The degree-of-freedom-adjusted coefficient of determination (Adj R^2) was calculated for the fitted line to assess the goodness of the fit.

6.3.8 Effect Size and Statistical Power

Hedge's g was used to calculate the effect size of the EEG connectivity comparison between healthy controls and ALS patients (See sub-section 4.5.3). Similarly, the area under the curve of the receiver operating characteristic (AUROC), a non-parametric test statistic, was obtained using De Long's method (Zhou et al., 2009) for each connectivity comparison. Empirical Bayesian Inference, implemented using AUROC (Nasseroleslami, 2019), was used to find the statistical power to assess the reproducibility of the group comparison results.

6.4 Results

6.4.1 Spectral power revealed task dependent increase in task-related areas

The EEG channels above contralateral prefrontal and parietal regions (DLPFC and SPL) showed significant increases in spectral power in the θ band (Figure 6.2 A-B) during the pre-motor stage in ALS patients. Similarly, during motor execution, β power was increased in ALS patients compared to healthy controls (i.e., decreased event related desynchronisation) in all pre-selected Laplacian EEG channels (see appendix 6.7), but the difference was statistically significant only in EEG channels over contralateral superior parietal (SPL) and ipsilateral primary motor (M1) regions (Figure 6.2 C-D).

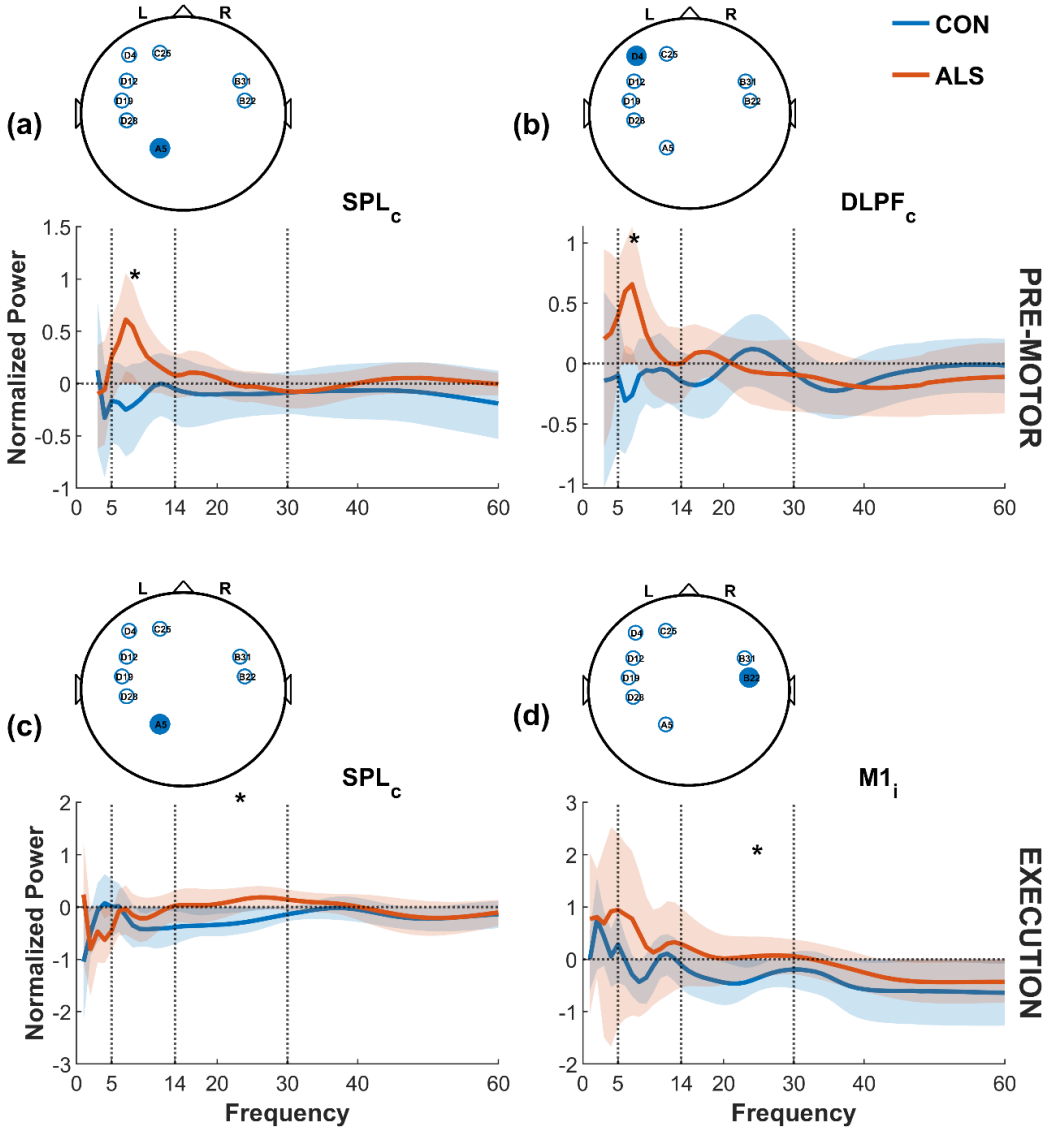

Figure 6.2 Motor task (pre-motor and execution) event related spectral perturbation (ERSP) for channels that exhibited significant differences between the participant groups (p<0.05, corrected for multiple comparisons using adaptive FDR at q = 0.05). *(A, B) Pre-motor ERSP in (A) contralateral superior parietal lobule (SPL) showing significant group difference in the theta (θ, 5-7 Hz) frequency band, and (B) contralateral dorsolateral prefrontal cortex (DLPFC) showing significant group difference in the theta (θ, 5-7 Hz) frequency band. (C, D) Motor execution ERSP in (C) contralateral SPL showing significant group difference in the beta (β, 14-30 Hz) frequency band, and (D) ipsilateral primary motor cortex (M1) showing significant group difference in the beta (β, 14-30 Hz) frequency band. CON: Healthy controls, ALS: people with ALS. The vertical doted lines divide the plots into very-low (delta, 2-4 Hz), low (theta and alpha, 5-13 Hz), high (beta, 14-30) and very-high (gamma, >30) frequency bands.*

6.4.2 EEG connectivity reflects task dependent abnormal motor networks in ALS

6.4.2.1 Sensorimotor network abnormal during resting state

The resting state functional networks for ALS patients and healthy controls for all frequency bands are shown in appendix 6.2. The EEG connectivity between left M1 and left S1 was significantly increased in ALS compared to healthy controls in the θ band (Figure 6.3).

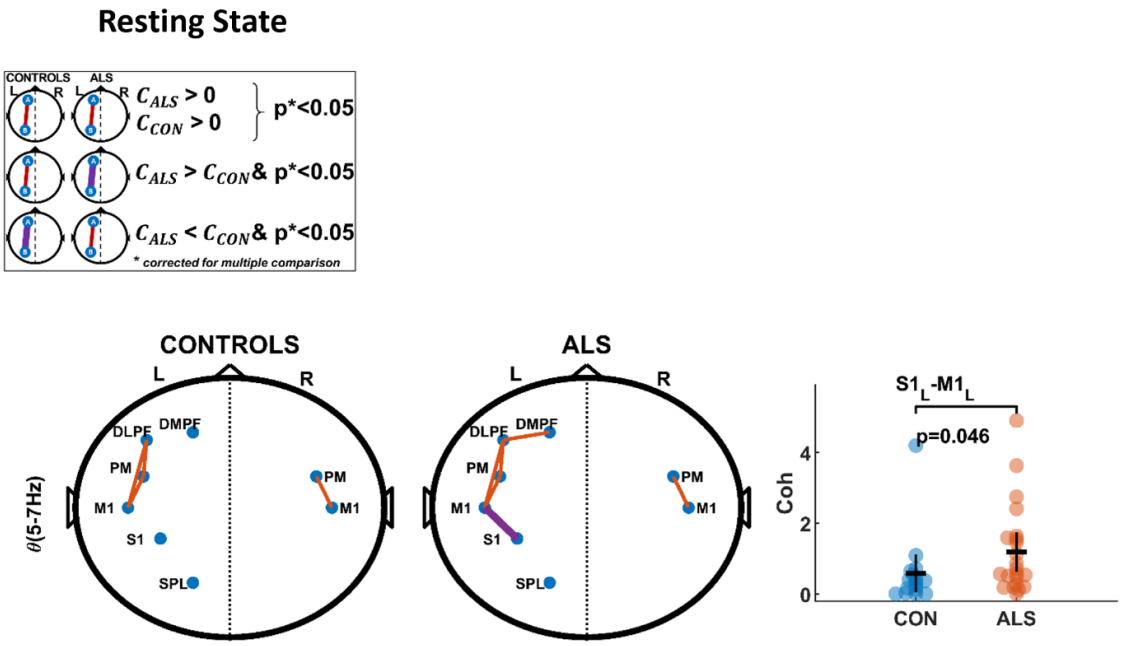

Figure 6.3 Resting state (RS) functional connectivity (FC) network for HC (Left) and ALS patients (Centre) based on the group average corticocortical coherence in the theta (θ) frequency band. *(Right) Distribution of individual M1-S1 corticocortical coherence (Coh) for HC/ALS in the θ frequency band, along with the group difference p-value.*

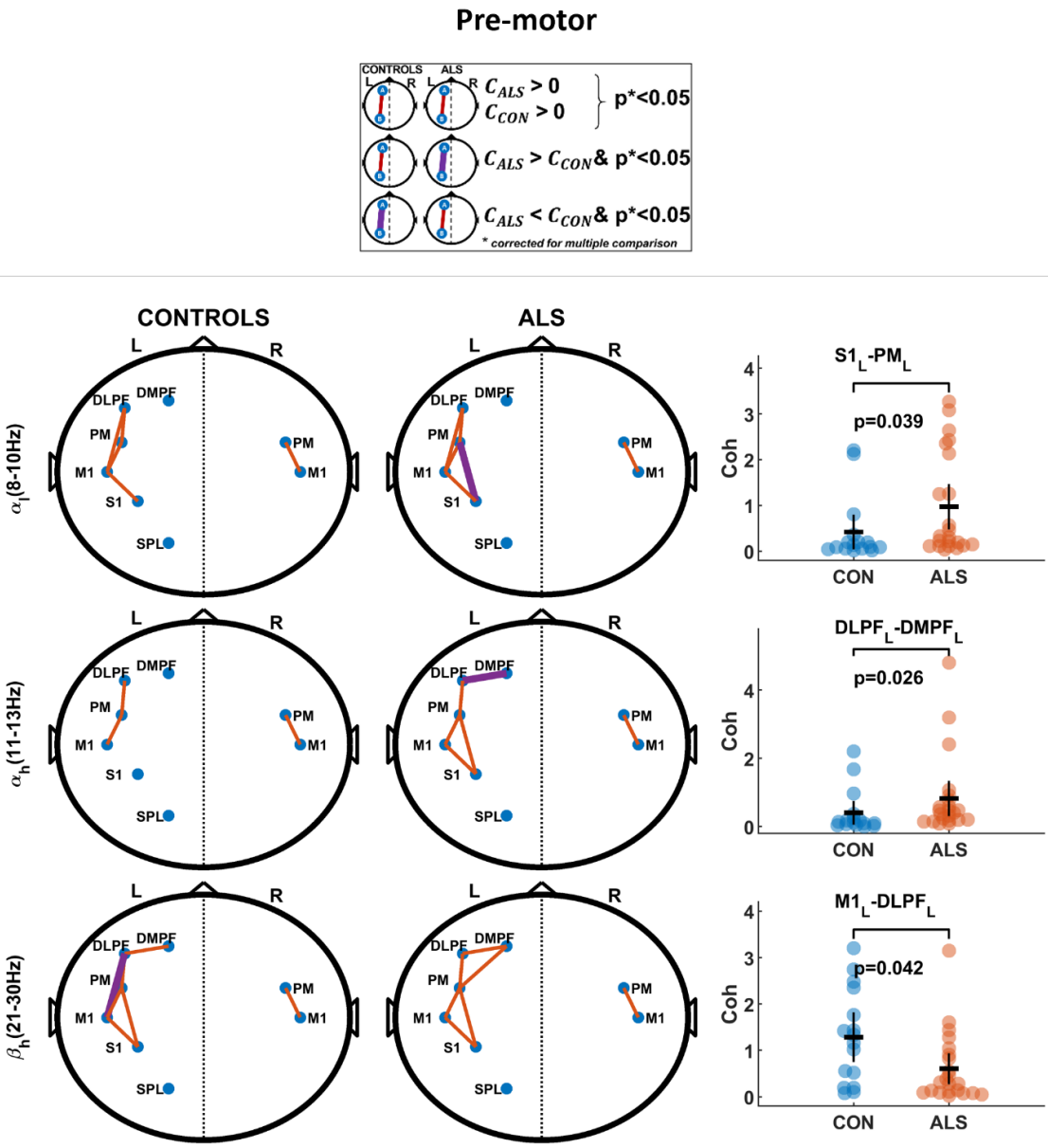

Figure 6.4 Pre-motor stage (PMS) functional connectivity (FC) networks based on the group average corticocortical coherence. *(First column) PMS FC network for healthy controls (HC) in the α_l, α_h, and β_h frequency bands. (Second column) PMS FC network for ALS patients in the α_l, α_h, and β_h frequency bands. (Third column) Distribution of individual PM-S1, DLPF-DMPF, and M1-DLPF corticocortical coherence (Coh) for HC/ALS in the α_l, α_h, and β_h frequency bands, respectively, along with group difference p-values.*

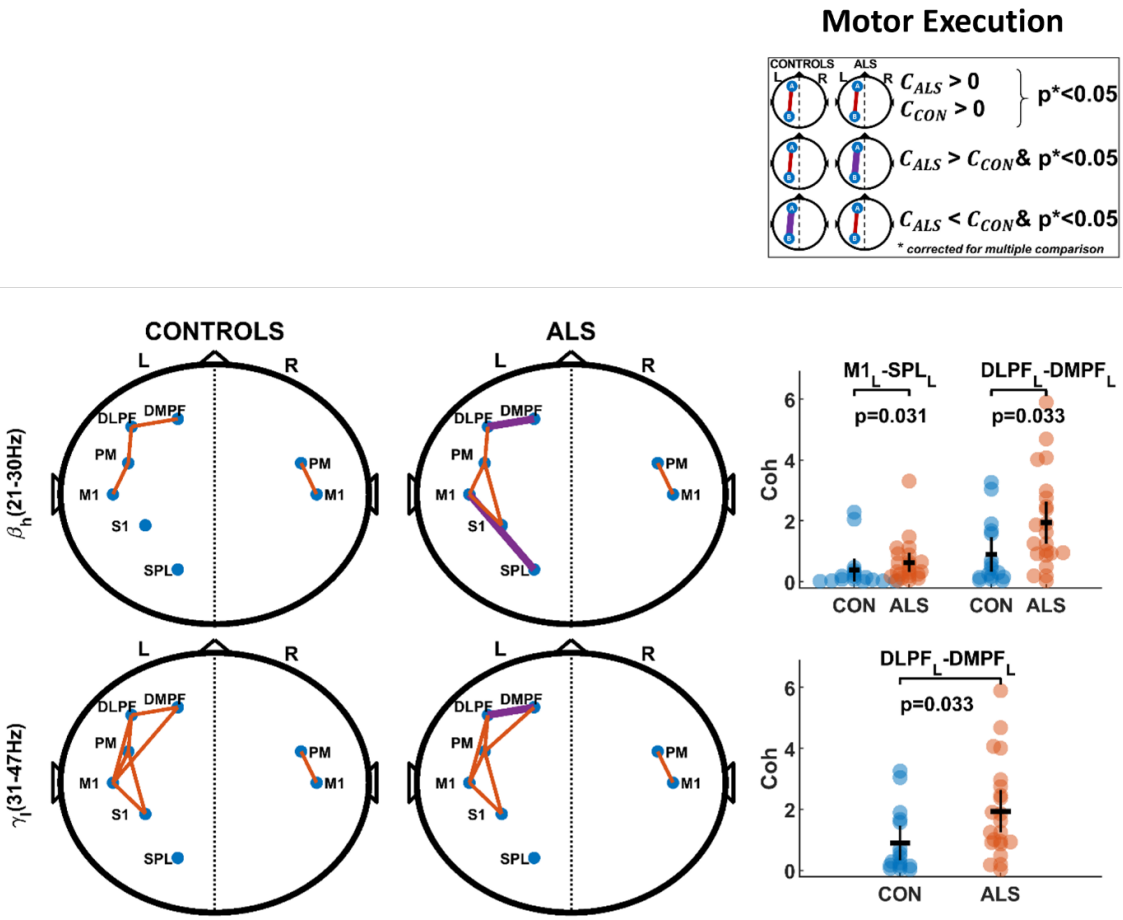

Figure 6.5 Motor execution (ME) functional connectivity (FC) networks based on the group average corticocortical coherence. *(First column) ME FC network for healthy controls (HC) in the β_h, and γ_l frequency bands. (Second column) ME FC network for ALS patients in the β_h and γ_l frequency bands. (Third column) Distribution of individual M1-SPL and DLPFC-DMPFC corticocortical coherence (Coh) for HC/ALS in the β_h, and γ_l frequency bands along with group difference p-values.*

6.4.2.2 Pre(motor) network connectivity abnormal during pre-motor stage

The pre-motor stage functional networks for ALS and healthy controls for all frequency bands are shown in appendix 6.3. The networks involving contralateral primary motor (M1) and premotor (PM) regions were abnormal in ALS during the pre-motor stage. The connectivity between left PM and left S1 in the α_l band was significantly stronger in ALS compared to healthy controls (Figure 6.4 top row). Similarly, the left M1-DLPFC connectivity was significantly weaker in the β_h band (Figure 6.4 middle row). In addition, a frontal network abnormality, i.e., significantly higher DLPFC-DMPFC synchrony in the

α_h band, was observed during the pre-motor stage in ALS patients compared to healthy controls (Figure 6.4 bottom row).

6.4.2.3 Frontoparietal network connectivity abnormal during motor execution

The motor execution functional networks for ALS and healthy controls for all frequency bands are shown in appendix 6.4. ALS patients showed significantly stronger connectivity between the left primary motor (M1) and left parietal (SPL) regions in the β_h frequency band compared to healthy controls (Figure 6.5 top row). Frontal network abnormality, involving DLPFC-DMPFC connectivity in the β_h and γ_l bands, was observed during motor execution (Figure 6.5).

6.4.3 The levels of average closed-path functional connectivity in the executive-sensorimotor network are higher in ALS

In this study, we have reported the EEG-based functional interconnections over primary motor (M1), premotor (PM), primary sensory (S1), and dorsolateral prefrontal (DLPF) cortices as main regions within the executive-sensorimotor network (ESMN) because these cortical regions are key contributors to pre-motor activity and motor execution, and control of voluntary movements. The characteristics of the functional point-to point connections within the selected regions of the ESMN in healthy controls and ALS patients are summarized in Table 6.2. In terms of the number of functional connections between the main nodes of the ESMN, ALS showed a higher number of average point-to-point connections over the frequency spectrum during all three experiments (resting state, pre-motor stage and motor execution) but the difference was not statistically significant.

To further characterise whether these general higher levels of connectivity, pertain to global or scattered increases, or form closed paths and connections, the global clustering coefficient (GCC) values are reported. GCC was increased in ALS in all three experimental

conditions (rest, pre-motor stage, and motor execution), Table 6.3. The most notable increase occurred during resting state and motor execution.

Table 6.2 Comparative summary of executive sensorimotor networks (ESMC) in healthy controls (HC) and ALS during resting state, pre-motor stage and motor execution.

Experiment	ESMN in healthy controls	ESMN in ALS	Remarks
Resting State	observed in α, β, and γ frequency bands, sparse at the θ band, and disappeared in the δ band	observed in all frequency bands except δ, where it was sparse	See figure appendix 6.1
Pre-motor Stage	observed in β and γ bands, sparse in other frequency bands	observed in all frequency bands except δ and θ, where it was sparse	See figure appendix 6.2
Motor Execution	observed in the γ band, sparse in other frequency bands	observed in all frequency bands except δ, where it was sparse	See figure appendix 6.3

Abbreviations: ESMN, executive-sensorimotor network, δ, delta (2-4 Hz); θ, theta (5-7 Hz); α, alpha (8-13Hz); β, beta (14-30 Hz); γ, gamma (31-97 Hz)

Table 6.3 Global clustering coefficient (GCC) for healthy controls (HC) and ALS during resting state, pre-motor stage, and motor execution.

Exp	Group	GCC in different frequency bands								Mean GCC	Group Diff. (p)
		δ	θ	α_l	α_h	β_l	β_h	γ_l	γ_h		
Resting State	HC	0	0.14	0.18	0.18	0.29	0.21	0.25	0.32	0.20	0.023*
	ALS	0.11	0.21	0.29	0.29	0.32	0.36	0.32	0.43	0.29	
Pre-motor Stage	HC	0.11	0.11	0.18	0.11	0.25	0.25	0.29	0.36	0.21	0.062
	ALS	0.11	0.14	0.21	0.21	0.25	0.25	0.32	0.43	0.24	
Motor Execution	HC	0.04	0.11	0.14	0.11	0.14	0.14	0.29	0.46	0.18	0.046*
	ALS	0.11	0.18	0.21	0.21	0.21	0.25	0.29	0.43	0.24	

Abbreviations: δ, delta (2-4 Hz); θ, theta (5-7 Hz); α_l, low alpha (8-10 Hz); α_h, high alpha (8-10 Hz); β_l, low beta (14-20 Hz); β_h, high beta (21-30 Hz); γ_l, low gamma (31-47 Hz); γ_h, high gamma (53-97 Hz).

* p value < 0.05 after correction for multiple comparison using adaptive false discovery rate at q = 0.05.

6.4.4 EEG measure of altered connectivity discriminate ALS patients from healthy controls and reflect uniquely impaired functional networks during pre-motor stage

6.4.4.1 Pre-motor stage abnormal EEG connectivity contributes most to discriminate ALS patients from controls

The abnormal EEG connectivity measures (Table 6.4) were used as features to discriminate patients and healthy controls using a nested k-fold cross-validated LSVM. The classification accuracy of the LSVM was 79.21% with sensitivity of 83.33% and specificity of 71.67%. Amongst the 7 features used for the classification, the features during the pre-motor stage showed a higher contribution to discrimination (as quantified by Shapley values) than the rest and motor execution stages (Figure 6.6). Specifically, the functional connectivity between M1 and DLPFC on the contralateral side in the high-beta band during the pre-motor stage, which was significantly lower in ALS patients compared to healthy controls, showed the highest Shapley value. The resting state functional connectivity between contralateral primary sensorimotor cortices (M1-S1) in the theta band, which was significantly higher in ALS compared to controls, showed the lowest Shapley value amongst the seven connectivity features used. The Shapley values of motor execution features were higher than those during resting state but lower than in the pre-motor stage.

6.4.4.2 Correlation of abnormal EEG connectivity with clinical scores reflects functional impairment in ALS

The correlation between abnormal EEG connectivity in ALS and their ALSFRS-R scores showed that six abnormal EEG connectivity (out of seven) were negatively correlated with the ALSFRS-R scores (see appendix 6.5). However, only two abnormal EEG connectivity were statistically significant ($p<0.05$) after correction for FDR at $q = 0.05$ (Figure 6.7). A negative correlation ($r=-0.378$, $p=0.042$) was obtained between ALSFRS-R scores and

contralateral M1-S1 connectivity in the θ band during rest. Similarly, contralateral M1-SPL connectivity in the β_h band during motor execution showed a significant negative correlation with the ALSFRS-R scores (r=-0.505, p=0.025). The motor planning abnormal EEG connectivity did not show any significant correlations with the ALSFRS-R scores.

Table 6.4 Group average EEG coherence values for healthy controls (HC) and ALS patients in different frequency bands where significant group-level differences were observed.

Exp	Freq Bands	EEG Connectivity	Location	Avg. Coh -log10(pavg)		Group Diff. (p)	Effect Size[a]	Power α=0.05
				HC	ALS			
Resting State	θ	M1-S1	CONT	0.15	6.14	0.046*	0.75 [0.09, 1.43]	0.659
Motor Planning	α_l	PM-S1	CONT	0.03	2.14	0.039*	0.67 [0.02, 1.35]	0.669
	α_h	DLPFC-DMPFC	CONT	0.02	2.32	0.026*	0.70 [0.05, 1.38]	0.734
	β_h	M1-DMPFC	CONT	6.66	0.77	0.042*	-0.79 [-1.48, -0.14]	0.634
Motor Execution	β_h	DLPFC-DMPFC	CONT	1.92	12.00	0.033*	0.69 [0.04, 1.37]	0.702
	β_h	M1-SPL	CONT	0.01	1.41	0.031*	0.84 [0.18, 1.53]	0.682
	γ_l	DLPFC-DMPFC	CONT	6.70	12.00	0.033*	0.89 [0.23, 1.59]	0.709

Abbreviations: θ, theta (5-7 Hz); **α_l**, low alpha (8-10 Hz); **α_h**, high alpha (8-10 Hz); **β_h**, high beta (21-30 Hz); **γ_l**, low gamma (31-47 Hz); **M1**, primary motor cortex, **S1**, primary sensory cortex; **PM**, premotor cortex; **DLPFC**, dorsolateral prefrontal cortex; **DMPFC**, dorsomedial prefrontal cortex; **SPL**, superior parietal lobule; **CONT**, contralateral.

* p value < 0.05 after correction for multiple comparison using adaptive false discovery rate at q = 0.05.

[a]Number in [] shows 95% confidence interval.

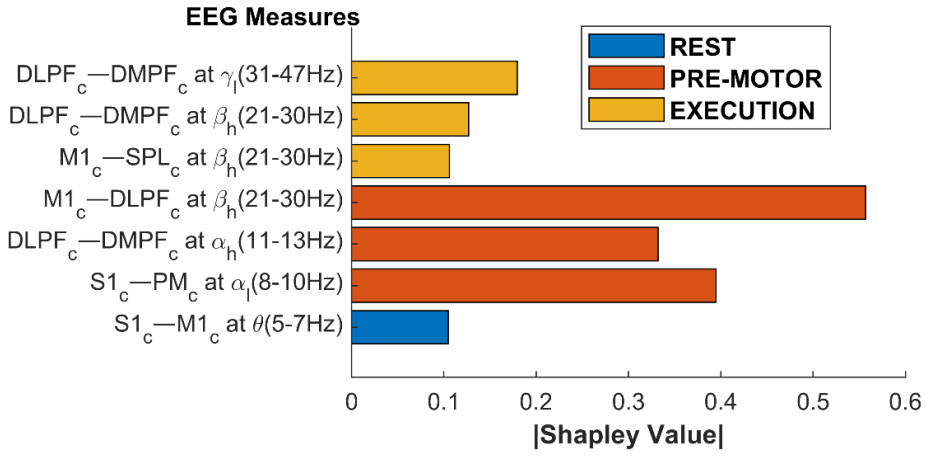

Figure 6.6 Absolute Shapley values for the EEG connectivity measures show the uniquely stronger contribution of the pre-motor stage to discrimination based on the predicted outcome of the nested 5-fold cross-validated linear support vector machines (LSVM) model.

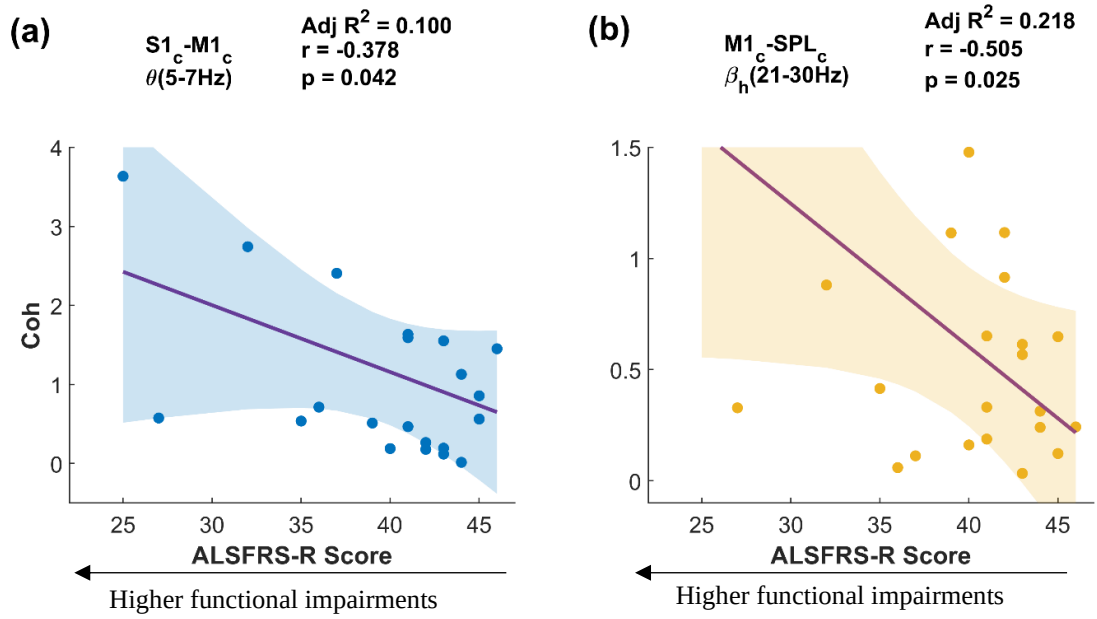

Figure 6.7 Correlation between Amyotrophic lateral sclerosis functional rating scale revised (ALSFRS-R) scores and pairwise corticocortical coherence Coh [-log10(p)]. *(a) Resting-state functional connectivity between left primary motor cortex (M1) and left primary sensory cortex (S1) in the theta band (θ) showed significant negative correlation with the ALSFRS-R scores. (b) Motor execution functional connectivity between left primary motor cortex (M1) and left superior parietal lobule (SPL) in the high-beta band (β_h) showed significant negative correlation with the ALSFRS-R scores. r is Pearson's linear correlation coefficient; p is the level of significance adjusted for multiple comparisons using false discovery rate at q = 0.05. Adj R^2 is the degree of freedom adjusted coefficient of determination for the fitted line using the linear least-squares fitting method.*

6.4.5 EEG measure of connectivity change are meaningful and reliable

The abnormal EEG connectivity observed in ALS in all three experimental conditions reflects meaningful and strong disease-related abnormalities (statistical effect size>0.7 for 6 out of 7 comparisons) and shows acceptable levels of reliability (post-hoc statistical power>0.6), Table 6.4.

6.5 Discussion

6.5.1 Pre-motor networks are impaired in ALS with significant prefrontal and parietal involvement

Neural activity in premotor cortex, primary motor cortex, and supplementary motor area is known to drive several processes, including the successful planning of a motor action during the pre-motor stage, based on invasive studies in non-human primates (Churchland et al., 2006, Li et al., 2015, Shibasaki and Hallett, 2006, Cisek and Kalaska, 2005) and non-invasive EEG study in humans (Nasseroleslami et al., 2014), which leads to faster reaction times (Haith et al., 2016) and more accurate response selection (Wong and Haith, 2017, Ariani and Diedrichsen, 2019). The neural correlates of motor preparation or planning during the pre-movement stage in humans can be studied by the Bereitschaftspotential (BP) or readiness potential (Shibasaki and Hallett, 2006) and the contingent negative variation (CNV) (Walter et al., 1964), as well as the corresponding event related spectral perturbations (ERSPs) that are typically referred to as event-related (de)synchronisation (ERD/ERS) (Pfurtscheller and Berghold, 1989).

Previous studies have reported reduced amplitude of the readiness potential in ALS during preparation of a motor response during pre-movement phase (Thorns et al., 2010, Westphal et al., 1998). However, in terms of β ERD, the results are inconsistent (Bizovicar et al., 2014, Proudfoot et al., 2017, Riva et al., 2012). Our results support the study by Riva et al.

(2012) who reported no significant difference in μ/β ERD in ALS pre-movement in sensorimotor regions. In addition, we looked outside of typical μ/β frequency bands, which is equally important when looking into abnormal activity underpinned by disease pathophysiology and found significant power increases in ALS compared to healthy controls in the prefrontal and the parietal region in the θ band. This suggests that, physiologically, ALS patients tend to put more effort prior to motor activity to prepare or plan a motor task by recruiting neuronal pools over wider cortical areas to overcome the burden of motor neuron degeneration in sensorimotor cortices.

We reported stronger functional connectivity between PM-S1 and DLPFC-DMPFC and weaker functional connectivity between M1-DLPFC the pre-motor stage in ALS compared to healthy controls indicating abnormal involvement of M1, pre-motor, and prefrontal regions in ALS. The functional coupling between these regions is associated with planning of a motor task prior to movement execution (Vesia et al., 2018, Koch et al., 2010). Therefore, the abnormal pre-motor stage spectral power and coherence observed here could be the consequence of abnormal motor planning in ALS. Motor planning is a complex pre-motor neurophysiological process consisting of three sub-processes: abstract kinematics, action selection, and movement-specific transformation of motor goals into the desired movement (Wong et al., 2015). The motor goal is formed by sensory inputs followed by the attention phase to choose an object or action of interest (Wong et al., 2015). In this motor task, the motor goal is predefined, consisting of the pincher grip action of a single object. Thus, the phase for motor goal preparation is brief and may consist of alignment of sensory information from the environment only (i.e., sensory information pertaining to the contacts between fingers and the wooden block). Similarly, the abstract or ambiguous kinematics sub-phase is absent during the planning phase of this task because participants know what movement is required (Cisek et al., 2003, Cisek and Kalaska, 2005). Thus, only

part of the three sub-phases, namely the alignment of sensory information, action selection, and movement specification, might modulate the motor planning networks during pre-movement in our motor task.

The contralateral PM-S1 connectivity was significantly higher in ALS during the pre-motor stage in the α_l frequency band. This could be due to the abnormal involvement of premotor and primary sensory regions in sensorimotor integration during an environment-sensing sub-phase of motor goal formation (Nakayashiki et al., 2021, Koch et al., 2010) in ALS. Similarly, the higher EEG connectivity within the frontal region (DLPFC-DMPFC) in the α_h band in ALS is likely associated with impairment in the action selection phase. Interestingly, significantly reduced EEG connectivity was observed within the contralateral M1-DLPFC at β_h band in ALS. This reduced beta coupling between M1 and DLPFC in ALS could reflect impairment in generation of descending motor commands due to neurodegeneration in the primary motor cortex. These neurophysiological phenomena suggest that pre-motor networks which showed properties of motor planning are impaired in ALS, not only at the level of neuronal oscillations but also at the level of network-level cortical communication, which leads to poor motor performance (task performance accuracy was significantly lower in ALS compared to controls, $p = 0.043$).

The functional activity in the pre-motor stage, while abnormal and affected, is fundamentally different. While resting state and motor execution measures show direct correlation with ALSFRS-R, pre-motor measures do not, suggesting that they reflect a different aspect of network impairment.

6.5.2 Underlying factors for observed changes

6.5.2.1 The potential role of cortical hyperexcitability in abnormal but preserved executive-sensorimotor network connectivity

The EEG network density of closed-loop connections, quantified by mean GCC, was higher in ALS than in healthy controls during all three stages of the experiments (rest, pre-motor stage, and motor execution). This widespread property of the EEG network observed in this study and in other studies on ALS (Iyer et al., 2015, Sorrentino et al., 2018) can potentially reflect cortical hyperexcitability, a well-established signature of ALS (Menon et al., 2015, Vucic et al., 2011). The abnormal contralateral M1-S1 connectivity during rest in ALS agrees with widely-reported impaired sensorimotor networks in ALS by EEG studies (Nasseroleslami et al., 2017) and fMRI studies (Agosta et al., 2011, Zhou et al., 2014, Douaud et al., 2011, Menke et al., 2018). Furthermore, the resting-state sensorimotor network abnormality was negatively correlated with the ALSFRS-R score suggesting that motoric impairment is associated with increased sensorimotor functional coupling in ALS. This corroborates with the increased S1 disinhibition in ALS and negative correlation of S1 excitability with ALSFRS-R scores reported by Höffken et al. (Höffken et al., 2019). Importantly, our finding of abnormal sensorimotor EEG connectivity strengthens the argument that sensorimotor functional connectivity can be captured both at rest and during stages of motor tasks (pre-motor and motor execution), with each stage providing both shared and unique information on network-level dysfunction. Such measures have potential to be used as quantitative neurophysiological biomarker candidates for diagnosis, prognosis, and phenotyping/stratification of ALS (Dukic et al., 2019, Zhou et al., 2014).

Previous studies in healthy participants have shown that contralateral sensorimotor cortices (M1, PM, and S1) along with DLPFC were active during pre-movement or pre-motor

stages (Churchland et al., 2006, Riehle, 2005, Pfurtscheller and Berghold, 1989, Glover et al., 2012, Ariani et al., 2015, Papitto et al., 2020) and motor execution (Hanakawa et al., 2008, Papitto et al., 2020, Lacourse et al., 2005, Alahmadi et al., 2015, Cisek et al., 2003). Beta band cortex-muscle synchrony is a well-known neurophysiological phenomenon involved in the generation and control of sustained motor movements (Conway et al., 1995, Halliday et al., 1998). Gamma band cortex-muscle synchrony is likely due to repetitive force control, which manifests as higher frequency oscillations in cortical regions because of processing of sensory information and sensorimotor integration (Pfurtscheller and Lopes da Silva, 1999, Muthukumaraswamy, 2010). This study demonstrated significant EEG connectivity within contralateral executive-sensorimotor network in healthy controls during both pre-motor and motor execution stages at β and γ frequency bands as expected. Notably, we reported the presence of β and γ ESMN in ALS, similar to healthy controls, during the pre-motor and motor execution stages despite the degeneration of upper motor neurons. This may explain why the control of voluntary movement is preserved in non-weak ALS (10 out of 22 ALS in our study could produce force within mean±1.5sd of force produced by healthy controls, $p=0.44$). Furthermore, EEG connectivity within ESMC during pre-motor and motor execution stages was observed at lower frequency bands in ALS that were not present in healthy controls. The manifestation of a low-frequency ESMC network in ALS may arise as a frequency-based compensation for disrupted high frequency (β or γ) ESMC networks for weak ALS (12 ALS participants in our study unable to produce force within mean±1.5sd of force produced by healthy controls, $p<0.001$). This finding supports the concept of 'motor reserve' in ALS (Bede et al., 2021) and corroborates with the results of Verstraete et al. (2010), who reported that 'although the structural motor network deteriorates in ALS, the functional motor network is preserved.' A longitudinal study on ESMN change over time is required to determine whether the preservation on

ESMN is temporary and disappears over time, or whether it is preserved regardless of disease progression and structural network degeneration.

6.5.2.2 Reduced beta ERD during motor execution

ERD studies in ALS have reported alterations in cortical activity during pre-movement and execution, reflecting the impact of neurodegenerative processes on the motor system (Riva et al., 2012, Bizovicar et al., 2014). Spectral frequency analysis during motor execution revealed the commonly observed β event-related desynchronization (ERD) phenomenon in sensorimotor regions of healthy controls, resulting from task-related cortical inhibition by interneurons (Zaepffel et al., 2013, Ariani et al., 2022, Nasseroleslami et al., 2014). Although no significant differences were found in mu/beta ERD between ALS and healthy controls during the pre-motor stage, ALS patients exhibited significantly reduced β ERD in the ipsilateral motor region and contralateral parietal region during motor execution. This finding is consistent with previous reports of reduced cortical mu/beta ERD in ALS patients during motor execution (Bizovicar et al., 2014). The reduced ERD in ALS during motor execution is likely due to the loss of GABAergic cortical interneurons (Zhou et al., 2013, Poujois et al., 2013, Höffken et al., 2019, Agosta et al., 2011, Fraschini et al., 2016) and imbalances in inhibitory-excitatory neurotransmitters (Foerster et al., 2013).

6.5.2.3 Functional compensation by non-dominant-motor and non-motor regions

The increased β ERSP (i.e., reduced β desynchronisation) in ALS compared to controls in ipsilateral M1 during execution motor task reflects the compensatory role of the non-dominant motor region (Konrad et al., 2002, Schoenfeld et al., 2005, Bede et al., 2021) to overcome the disease burden in the dominant motor region. Similarly, we have shown that, during execution motor task, β ERSP is higher over the contralateral superior parietal region (SPL) along with higher functional coupling with contralateral M1 in the β band.

This is likely to reflect a compensatory role of the superior parietal region in ALS (Poujois et al., 2013, Zhou et al., 2013, Lulé et al., 2007), even though the direct or indirect nature of this contribution needs further investigation. The involvement of frontal and parietal regions in abnormal networks, during motor execution, underpins the abnormal frontoparietal network in ALS (Deligani et al., 2020, Cosottini et al., 2012). In addition, the negative correlation between ALSFRS-R scores and contralateral motor-parietal network connectivity (M1-SPL) during motor execution indicates the increased compensatory role of the parietal cortex in functionally weaker ALS as opposed to those with relatively stronger functionality. This network connectivity appears to counteract the motor control dysfunction resulting from M1 motor neuron degeneration.

6.5.3 Multistate functional network impairments as diagnostic tool

Our result showed that, the abnormal EEG connectivity measures in each stage of the experiment (rest, pre-motor, or execution) contributed to classify ALS from controls. The contribution of the pre-motor stage features during classification was highest followed by motor execution and rest features. This suggests that differences between ALS and controls in functional networks may become more marked during the pre-motor stage enabling the two groups to be more accurately classified. However, the classification power of a standalone stage/experiment/modality is not sufficient to be used as diagnostic tool in clinical settings (Huynh et al., 2016). Combining quantitative EEG features from different battery of analysis has previously been shown to be useful for classifying various neurodegenerative diseases (Garn et al., 2017). This is especially important as the results (Figure 6.3-6.5) indicate that each stage provides unique information on the impairment of specific parts of the ESMN, most notably during the pre-motor stage. Furthermore, combining quantitative EEG and neuropsychology was recommended for differential

diagnosis of Frontotemporal dementia and Alzheimer's disease (Lindau et al., 2003). Our findings suggest that combining features reflecting functional network impairment from multistate experimental paradigms (resting state, pre-motor, and execution) provides the ability to classify between ALS and healthy controls. The inclusion of pre-motor network impairment could be the key to designing quantitative neurophysiological biomarkers of network disruption because, as we have shown, pre-motor stage functional connectivity grabs a fundamentally different type of motor network impairments than motor execution and rest and has the highest contribution for the classification of ALS and healthy controls.

6.6 Conclusion

This study was the first to interrogate the pre-motor networks in ALS based on the alterations in the intensity of task-related neural oscillations and functional connectivity during resting state, the pre-motor stage, and motor execution. Our results highlighted that non-motor or non-primary motor cortical regions less affected by neurodegeneration (i.e., contralateral prefrontal and superior parietal) or non-dominant motor regions (i.e., ipsilateral primary motor) have a distinct - possibly compensatory - role in pre(motor) network function in ALS. Finally, that pre-motor network impairments in ALS are distinct and not an extension of impairment in the primary motor cortex, and therefore can contribute to characterising the disease heterogeneity and developing biomarker candidates of motor networks dysfunction in ALS.

6.7 Limitations

The EEG connectivity calculated using spectral coherence quantifies the neural synchrony or frequency-specific phase-locking and therefore the magnitude of information flow between two underlying cortical regions (functional connectivity) but not the direction of information flow. Incorporating the magnitude and direction of information flow (effective

connectivity) as a classification feature could further increase the accuracy of machine learning models in discriminating between ALS and healthy controls. Source localisation techniques could more accurately detect abnormal motor networks in ALS than Laplacian spatial filtering because they are more robust at reducing volume conduction and can provide information on deeper oscillating cortical sources.

7. Results: Source Level Study of Corticomuscular coherence

7.1 Introduction

Recent electroencephalography (EEG) studies have demonstrated a correspondence between neuroelectric activity and UMN pathology in ALS (McMackin et al., 2019b). The high temporal resolution of EEG is well suited to provide information concerning rhythmic or oscillatory brain activity across a range of frequencies. Previous EEG investigations in people with ALS conducted at rest, have demonstrated altered functional connectivity across brain networks in the theta (4–7 Hz) and gamma (31–60 Hz) frequency bands (Nasseroleslami et al., 2017, Blain-Moraes et al., 2013, Westphal et al., 1998, Dukic et al., 2019). During voluntary contractions, oscillatory signals originating from the sensorimotor cortices are coherent with contralateral muscle signals. This cortex-muscle synchrony can be measured using Corticomuscular coherence (CMC) (Conway et al., 1995). CMC is typically observed as synchrony (in the beta and gamma-bands) between EEG electrodes over M1 and EMG activity (Halliday et al., 1998). It is considered to be indicative of the efferent drive to the spinal motoneurons, while also being subject to the modulating influence of peripheral afference (Witham et al., 2011). The frequency of synchrony between cortex and muscles is modulated by various factors including the type of task and level of contraction force (Kilner et al., 2000, Liu et al., 2019). For low force isometric contractions, the CMC is observed in the beta band (13-30 Hz) whereas in more forceful and dynamic contractions, the CMC shifts to the gamma band (31-97Hz) (Omlor et al., 2007, Gwin and Ferris, 2012, Andrykiewicz et al., 2007).

Recent studies have shown that CMC can provide valuable insights into the pathophysiology of ALS, as well as potential biomarkers for diagnosis and disease progression. Peak beta-band CMC over M1 is reduced in conditions characterised by UMN

degeneration, including stroke (Fang et al., 2009, Aikio et al., 2021) and ALS (Issa et al., 2017, Proudfoot et al., 2018b). This reduction is thought to be due to the progressive loss of motor neurons, which results in a decrease in the number of signals that can be transmitted between the brain and muscles.

Despite its potential as a biomarker for neurodegenerative diseases, CMC analysis is still premature, and there is much that remains to be understood about its relationship with the disease. Our recent CMC study on patients with lower motor neuron dysfunction such as post-polio syndrome (Coffey et al., 2021) and patients with upper motor neuron dysfunction, such as PLS (Bista et al., 2023), found abnormal patterns of brain activity beyond M1 and the beta band during voluntary movement. ALS being the disease where both upper and lower motor neurons are affected, we, therefore, hypothesized that (1) Impaired CMC could be detected beyond the beta frequency band and contralateral sensorimotor cortices in ALS, (2) CMC could be a tool to reveal multiple network dysfunction in ALS.

7.2 Method

7.2.1 Ethics

The study was approved by the Tallaght University Hospital / St. James's Hospital Joint Research Ethics Committee - Dublin [REC Reference: 2019-05 List 17 (01)] and performed in accordance with the Declaration of Helsinki (2013). All participants provided informed written consent to the procedures before undergoing assessment.

7.2.2 Participants

ALS patients were prospectively recruited in this study through the national ALS clinic at Beaumont Hospital. All participants with ALS were clinically diagnosed as possible, probable, or definite ALS (Hardiman et al., 2011). Healthy controls, age-matched to the

ALS cohort, were recruited from a database of healthy controls interested in taking part in the ongoing research studies in the Academic Unit of Neurology, Trinity College Dublin, the University of Dublin.

Participants with a history of major head trauma or other neurological conditions that could affect cognition, alcohol dependence syndrome, current use of neuroleptic medications or high-dose psychoactive medication were excluded. Those with diabetes mellitus, a history of cerebrovascular disease, and those with neuropathy from other causes were also excluded.

7.2.3 Clinical assessment

Disease duration from symptom onset, diagnostic delay, and site of disease onset were recorded. The revised ALS functional rating scale (ALSFRS-R) scores (Cedarbaum et al., 1999) were obtained from ALS cohort. ALSFRS-R is a 48-point validated questionnaire-based clinical scale that ranges from score 0 (severe functional impairment) to 48 (no functional impairment). The 48-point total score can be divided into 4 sub-scales namely bulbar (0-12), fine motor (0-16), gross motor (0-8), and respiratory (0-12) (Cedarbaum et al., 1999). The fine motor and gross motor sub-scales are combined as motor sub-score (0-24) that weigh the level of motor impairment in ALS patients.

The Edinburgh handedness inventory (EHI) (Oldfield, 1971) with 10 questions was performed to assess the handedness of participants.

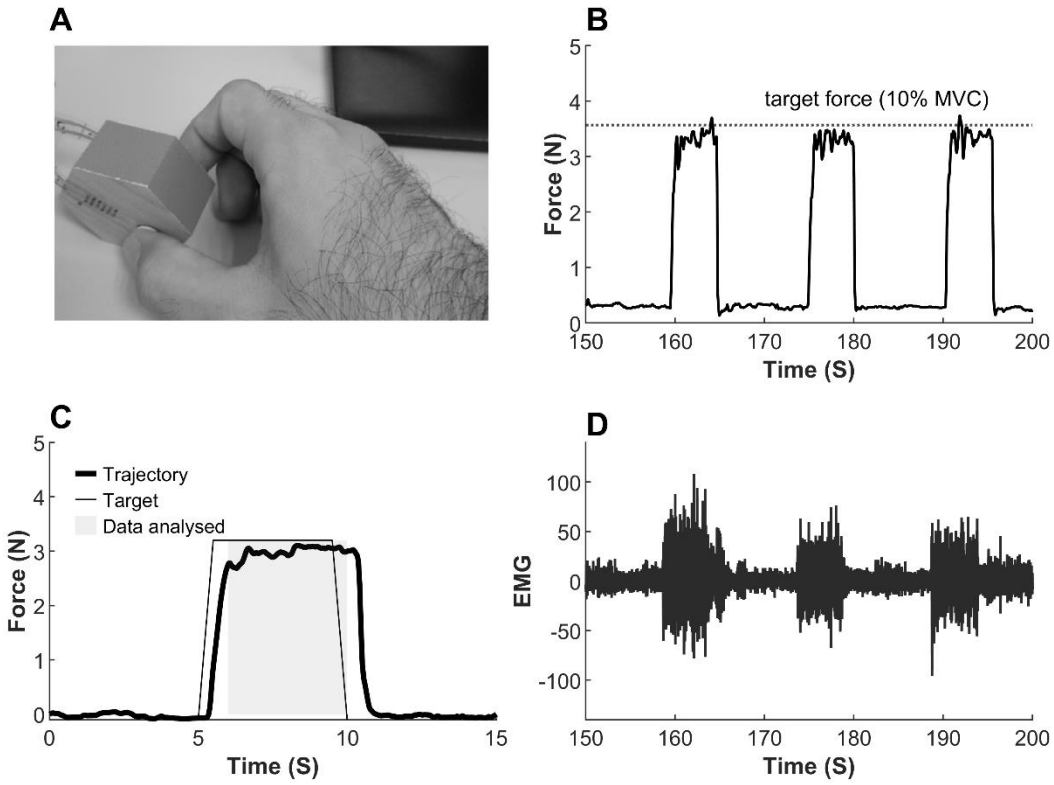

Figure 7.1 Motor task and related electromyography (EMG) and force signals. *(A) Pincher grip motor task performed by thumb and index finger of the right hand, (B) a segment of the force profile of the pincer grip motor task performed at 10% of maximum voluntary contraction (MVC), (C) a force trajectory of the pincer grip motor task averaged over 30 trials, (D) segment of electromyography (EMG) signal recorded from the first dorsal interosseous (FDI) muscle during 10% MVC pincher grip motor task. This figure has been published in Bista et al. (2023) in Figure 1, see appendix 5.1.*

7.2.4 Experimental Paradigm

Assessment was conducted in the same manner for the ALS and control groups, similar to the previously described sensor level study in chapter 6 of this thesis and was also described in Coffey et al. (2021) and Bista et al. (2023). Briefly, participants held a force transducer between the thumb and the index finger of their right hand to measure pincer grip force (Figure 7.1 A). The maximal voluntary contraction (MVC) was determined as the average peak force achieved during three short (5 s) maximal contractions, where the peak force in these attempts lay within 10% of each other. Participants were asked to produce the pincer

grip force at 10% MVC for 5 s with the aid of visual feedback from the force transducer. A 5 s rest period before and after the task was provide (Figure 7.1 C). Participants attempted a total of 30 trials for each task.

7.2.5 Recording of (Neuro-)electro-physiological Signals

All participants were seated in a comfortable seat, EEG data were recorded in a special purpose laboratory, using a 128-channel scalp electrode cap, filtered over the range 0–400 Hz and digitized at 2048 Hz using the BioSemi® ActiveTwo system (BioSemi B.V, Amsterdam, Netherlands). Each participant was fitted with an appropriately sized EEG cap. Surface EMG data were recorded simultaneously with EEG using a bipolar electrode configuration from 8 muscles in the right upper arm, with the electrode pairs placed in accordance with the SENIAM guidelines (Hermens et al., 2000). The online hardware gain and filter settings for the EMG signals during recordings were the same as for the EEG channels, which was followed by further offline pre-processing.

7.2.6 Signal Pre-processing

EEG/EMG data analysis was performed as described in detail in a previous study (Coffey et al., 2021). Briefly, automated artefact rejection routines (Fieldtrip Toolbox) (Oostenveld et al., 2011) were used to discard data contaminated by noise. After visual inspection of the 128-channels recordings, EEG channels with higher levels of noise were removed and reconstructed using weighted average interpolation of neighbouring channels (Perrin et al., 1989). A time window/epoch duration of 4 s (starting 1s after the visual cue) was chosen for analysis. Data epochs where the coefficient of variation of the force produced was above 0.2, or where the mean force was less than 8% or more than 20% MVC, were excluded from further analysis. An average of 7 ± 8 trials (i.e., 28 ± 32 seconds) data were removed across all participants for these reasons. An average of 15±6 trials (i.e., 60±24 seconds) for

the 128 EEG channels were retained for source reconstruction. The EEG data were (re-)referenced using common average referencing. The EMG data (signal amplitude) were normalized with respect to the root mean square EMG amplitude at 100 % MVC. EEG and EMG data were filtered between 1-100Hz and 10-100 Hz, respectively, using a dual-pass 4th order Butterworth bandpass filter. The EMG signals were not rectified. Three EMG signals (First Dorsal Interosseous, FDI; Flexor Pollicis Brevis, FPB and Abductor Pollicis Brevis, APB) were chosen apriori for the cortico-muscular coherence analysis. The target muscles were selected based on their biomechanical involvement in the pincer grip task (Danna-Dos Santos et al., 2010).

7.2.7 Source Reconstruction

The details of source reconstruction are explained in sub-section 4.4.2.2 of chapter 4 of this thesis. Briefly, a template structural MRI was used to compute the forward model. The source reconstruction was done using linearly constrained minimum variance (LCMV) beamformer (Van Veen et al., 1997) using the Fieldtrip toolbox. Ten anatomical brain regions were chosen bilaterally, 5 on each side of the brain, using the automated anatomical labelling (AAL) atlas (Tzourio-Mazoyer et al., 2002). The chosen anatomical brain regions (regions of interest, ROI) were Primary Motor Cortex (M1), Primary Sensory Cortex (S1), Supplementary Motor Area (SMA), Medial Prefrontal Cortex (PFC), and Superior Parietal Lobule (SPL) of both hemispheres. To derive a single time-series for each ROI all the time-series within a ROI were weighted using a Gaussian weighting function with the half width at half maximum set to approximately 17 mm (Dukic et al., 2019, Brookes et al., 2016, Tewarie et al., 2016). Before deriving a single time-series of each ROI, the direction along the maximum power for each region was estimated by using singular vector decomposition on the orientations of the dipoles. Dipoles with the opposite direction (>90

degrees) to the estimated ROI's maximal activity vector were sign-flipped. After completing these steps, we obtained 10 broadband time-series, each representing one ROI. This pipeline was applied to each subject individually.

7.2.8 Spectral Analysis

CMC was examined in eight different frequency bands (Table 4.2) and a single coherence estimate was obtained for each band. The frequency bands were defined based on the typical physiological EEG frequency bands (Sanei and Chambers, 2007) as well as their relevance both in sensorimotor control (Nasseroleslami et al., 2014) and quantifying network dysfunction in motor neuron diseases (Dukic et al., 2019, Dukic et al., 2021).

CMC was estimated based on the spatial median using the procedure as described in sub-section 4.4.4.1 in chapter 4 Materials and Methods of this thesis and in previous studies (Coffey et al., 2021, Bista et al., 2023) . Briefly, the auto- and cross-spectra for each 1 s epoch were calculated for each participant. The spatial median coherence was then estimated from the spatial median of the auto- and cross-spectra across each of the eight defined frequency bands to obtain the banded coherence. The banded spectral cortico-muscular coherence was normalized by dividing the band cross-spectrum by the respective band auto-spectra. To represent the banded CMC as a probability, each coherence value was compared against zero using a non-parametric one-sample test for significant coherence [spatial (signed) ranks (Nordhausen and Oja, 2011, Oja, 2010, Oja and Randles, 2004)]. This procedure yielded individual p-values for each frequency band, for each individual (both ALS and control groups). Stouffer's method was used to combine individual p-values to derive average p-value within each group, i.e. in the healthy group, and in the ALS group (Stouffer et al., 1949, Westfall, 2014). This procedure is similar, but not procedurally equivalent, to the pooled coherence analysis (Amjad et al., 1997). Both

methods can be used to combine information from several participants (or trials). The negative logarithm of the p-values, i.e. -log10(p), was used as a measure of CMC strength to visualize cortico-muscular coherence. The band-specific coherence values, expressed in -log10(p), were used to represent the collective coherence over the range of frequencies within each distinct frequency band.

7.2.9 Statistics

To find significant group differences between the banded CMC values, the band specific CMC values (expressed as p values) were converted into z-scores by taking the inverse of cumulative distribution function (CDF) of $1 - p$. Resulting z-scores of CMC values were compared between healthy controls and ALS patients using a non-parametric 2-sample Wilcoxon rank sum test which reports the test values as z scores. In total 240 comparisons (10 EEG × 3 EMG × 8 Frequency bands) were made. Correction for multiple comparisons was performed using the adaptive false discovery rate at q = 0.05 (Benjamini et al., 2006). The effect size of the CMC differences was also calculated using Cohen's d.

The association of the CMC measures of the ALS cohort with their corresponding ALSFRS-R scores, task performance accuracy, and disease duration was tested using Spearman's rank correlation coefficient. The p values of correlation coefficients were adjusted for multiple comparison (240 comparisons in total, 10 EEG × 3 EMG × 8 Frequency bands) using adaptive false discovery rate at q = 0.05. A line was fitted to the scatter plot of the data, to visualise the relationship, using Robust linear least-square fitting method. The degree-of-freedom-adjusted coefficient of determination (Adj R^2) was calculated for the fitted line to measure the goodness of the fit.

7.3 Results

7.3.1 Clinical Profile

24 ALS (6 females and 18 males, age: 65.33±9.82 [mean ± SD]) were prospectively recruited from the national ALS Clinic based in Beaumont hospital, Dublin. 22 age-matched healthy controls (10 female and 12 male) were recruited (age: 62.27±8.97 [mean ± SD]). Table 7.1 shows the detailed profile of the recruited participants.

Table 7.1 Clinical and demographic data of analysed participants.

	ALS Cohort (n = 24)	**Controls (n=22)**
Age at recording (years)*	65.33±9.82	62.27±8.97
Gender		
Female	6	10
Male	18	12
EHI		
Right	22	21
Left	2	1
Diagnostic delay (months)*	19.04±24.32	
Disease duration (months)*	27.41± 23.43	
Site of onset		
Spinal	22	
Bulbar	2	
Thoracic/Respiratory	0	
ALSFRS-R score (max 48)*	40.40±5.65	
Fine motor sub-score (max 16)*	12.95±2.17	

* Numbers show mean ± standard deviation

EHI (Edinburgh Handedness Inventory)

ALSFRS-R (Amyotrophic Lateral Sclerosis Functional Rating Scale Revised)

7.3.2 Behavioural aspect of task performed

The participants were asked to maintain a sustained contraction (steady force) at 10% MVC for 5 seconds after a visual cue and were provided with visual feedback of the force exerted. Because of the rigid force sensor and low force condition, which makes pincer grip control relatively difficult compared to spring type load or higher force condition (for example 20% MVC or greater), both the control and ALS participants performed the task with periodic adjustment (error correction) of force. Although, the epochs with exerted force not within the acceptable range (i.e., less than 8% MVC and greater than 20% MVC) were rejected, it did not guarantee a smooth force trajectory in individuals (for example see Figure 7.1 B-C). Individually, 14/22 healthy controls and 13/24 ALS patients exhibited significant periodicity (tested by using Fisher's g-statistic) of exerted force at ~0.5 Hz, and 12/22 healthy controls and 7/24 ALS patients exhibited significant periodicity of exerted force at ~0.7 Hz. At the group level (Figure 7.2 A), both healthy controls and ALS patients exhibited a significant spectral power ($p<0.001$) of exerted force at ~0.5 Hz and ~0.7 Hz with no group differences at either frequency ($p = 0.938$ for ~0.5Hz and $p=0.991$ for ~0.7 Hz), Figure 7.2 B. ALS patients made significantly more ($p=0.003$) force exertion errors compared to controls (Figure 7.2 C) i.e., on average, 32.13±27.52 percent of epochs were rejected for ALS patients and 10.60±15.95 percent for healthy controls.

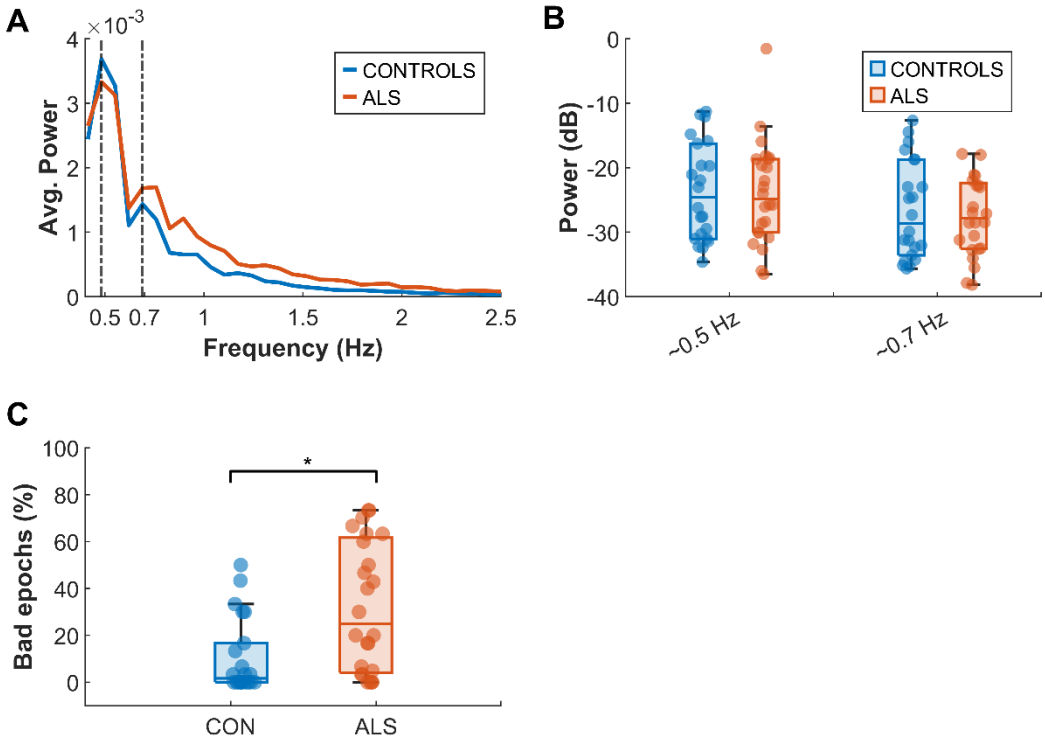

Figure 7.2 Analysis of exerted force during sustained contraction (steady force) task. *(A) Group average (median) power spectra of exerted force at 10% maximal voluntary contraction (MVC) for controls and ALS patients showing significant peaks at ~0.5 Hz and ~0.7 Hz. (B) Boxplot overlayed by scatter plot showing no difference in spectral power of exerted force between controls and ALS at ~0.5 Hz and ~0.7 Hz. (C) Boxplot overlayed by scatter plot of bad epochs (epochs rejected because the exerted force was not in the acceptable range) for controls and ALS patients showing a significant difference between the groups.*

7.3.3 Beta and Gamma sensorimotor CMC during low force pincer grip of rigid object in healthy controls

The CMC results showed that healthy controls exhibited significant synchronization between the cortex and muscles in the beta band (14-30 Hz) during voluntary isometric contraction at 10% MVC. This synchronization occurred between the hand muscles (APB, FDI, FPB) and the contralateral primary sensorimotor cortices (M1/S1) and was observed consistently in all healthy participants in individuals as well as at the group level (Figure 7.3 A-C). In addition to beta CMC, which is a well-known cortex-muscle synchrony associated with generating sustained isometric force at low levels, high-gamma (53-97 Hz)

synchronization was also consistently observed between all three hand muscles and contralateral M1/S1 (Figure 7.3 D-F). Moreover, gamma CMC was also consistently detected between the contracting muscles and the contralateral SMA.

7.3.4 Reduced CMC in Primary Sensorimotor Cortex and beyond in ALS

In the ALS group, there was a significant decrease in CMC compared to the controls between the hand muscles and the primary sensorimotor cortex (M1/S1) and beyond in multiple frequency bands. Specifically, CMC between FDI- ipsilateral S1 at high-alpha (Figure 7.4 A and 7.5 A), FDI- bilateral M1 at low-beta (Figure 7.4 B and 7.5 B-C), FDI- contralateral SPL at low-beta (Figure 7.4 B and 7.5 D), and FDI- ipsilateral SMA at low-beta (Figure 7.4 B and 7.5 E) were significantly lower in ALS patients. Similarly, CMC between APB- contralateral M1/SMA at high-gamma band was also significantly lower in ALS patients (Figure 7.4 C, 7.5 F-G).

7.3.5 Higher CMC in Ipsilateral Prefrontal Cortex in ALS

CMC between FPB and ipsilateral PFC in the low-beta band was significantly higher in ALS patients compared to healthy controls (Figure 7.4 D and 7.5 H).

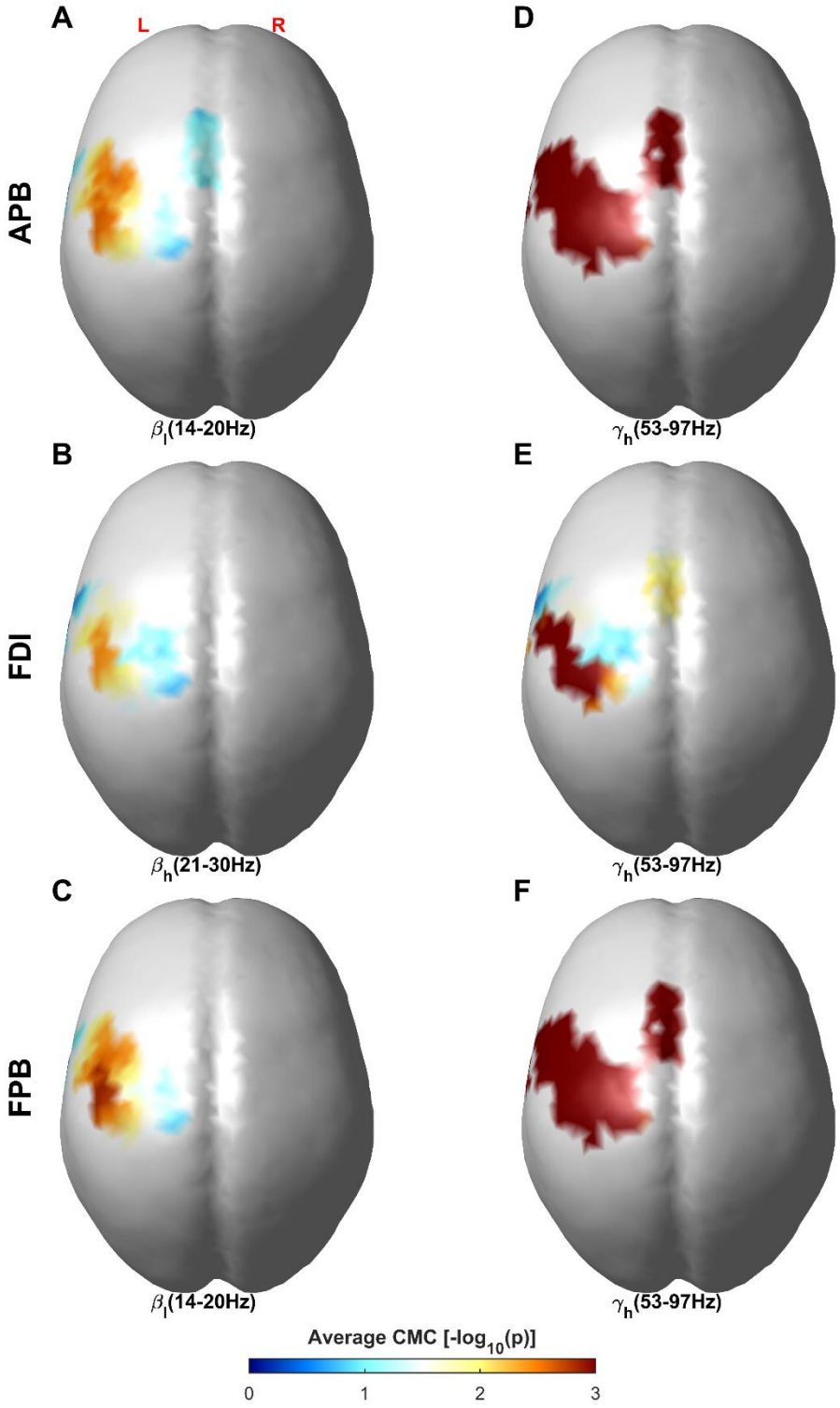

Figure 7.3 Contralateral sensorimotor regions (M1, S1, SMA) in healthy controls show significant (p<0.01) group average Corticomuscular coherence (CMC) with muscles. *(APB, FDI, FPB) in beta (A-C) and gamma bands (D-F) during a low force (10% MVC) pincer grip task of a rigid object. Muscles: Abductor pollicis brevis (APB), First dorsal interosseous (FDI), Flexor pollicis brevis (FPB). Brain regions: Primary motor (M1), Primary sensory (S1), Supplementary motor area (SMA).*

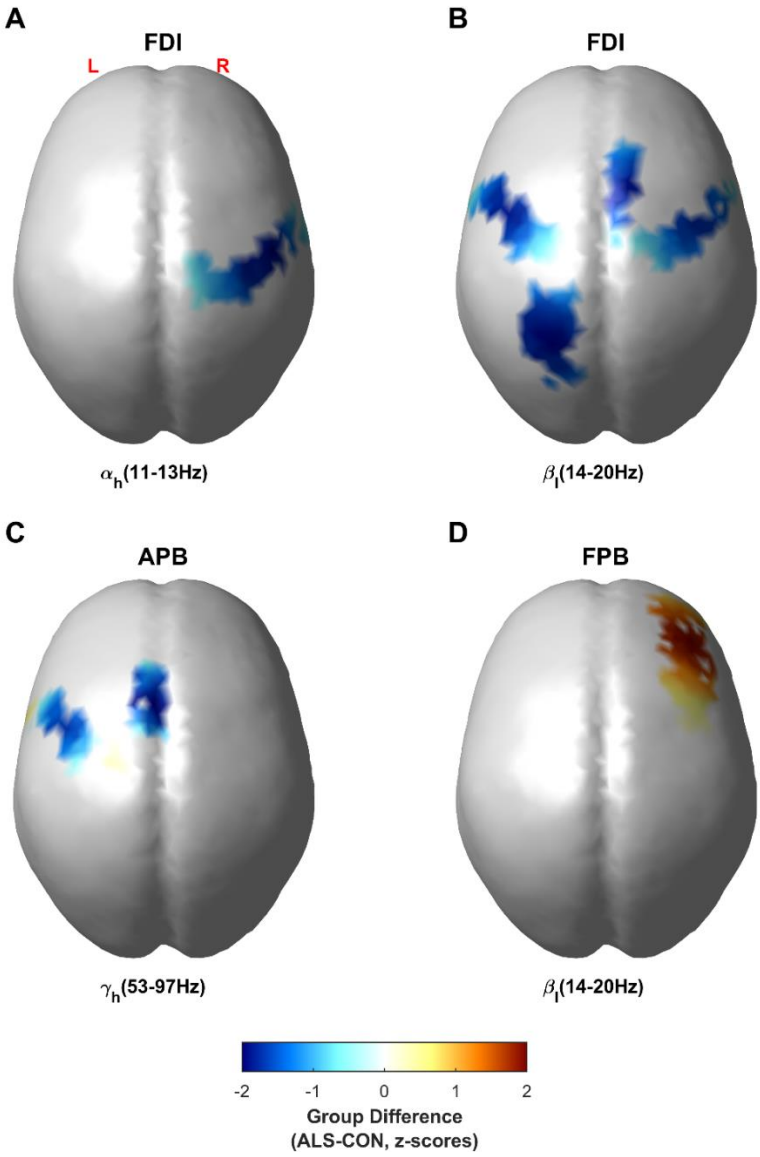

Figure 7.4 Brain regions showing significant group differences (z-scores) in Corticomuscular coherence (CMC) values between ALS patients and controls. *(A) Significantly lower CMC in ALS between the FDI muscle and ipsilateral S1 in the high-alpha band. (B) Significantly lower CMC in ALS patients between the FDI muscle and bilateral M1, ipsilateral SMA, and contralateral SPL in the low-beta band. (C) Significantly lower CMC in ALS patients between the APB muscle and contralateral M1 and contralateral SMA in the high-gamma band. (D) Significantly higher CMC in ALS patients between the FPB muscle and ipsilateral PFC in the low-beta band. Muscles: Abductor pollicis brevis (APB), First dorsal interosseous (FDI), Flexor pollicis brevis (FPB). Brain regions: Primary motor (M1), Primary sensory (S1), Supplementary motor area (SMA), Superior parietal lobule (SPL), Prefrontal cortex (PFC).*

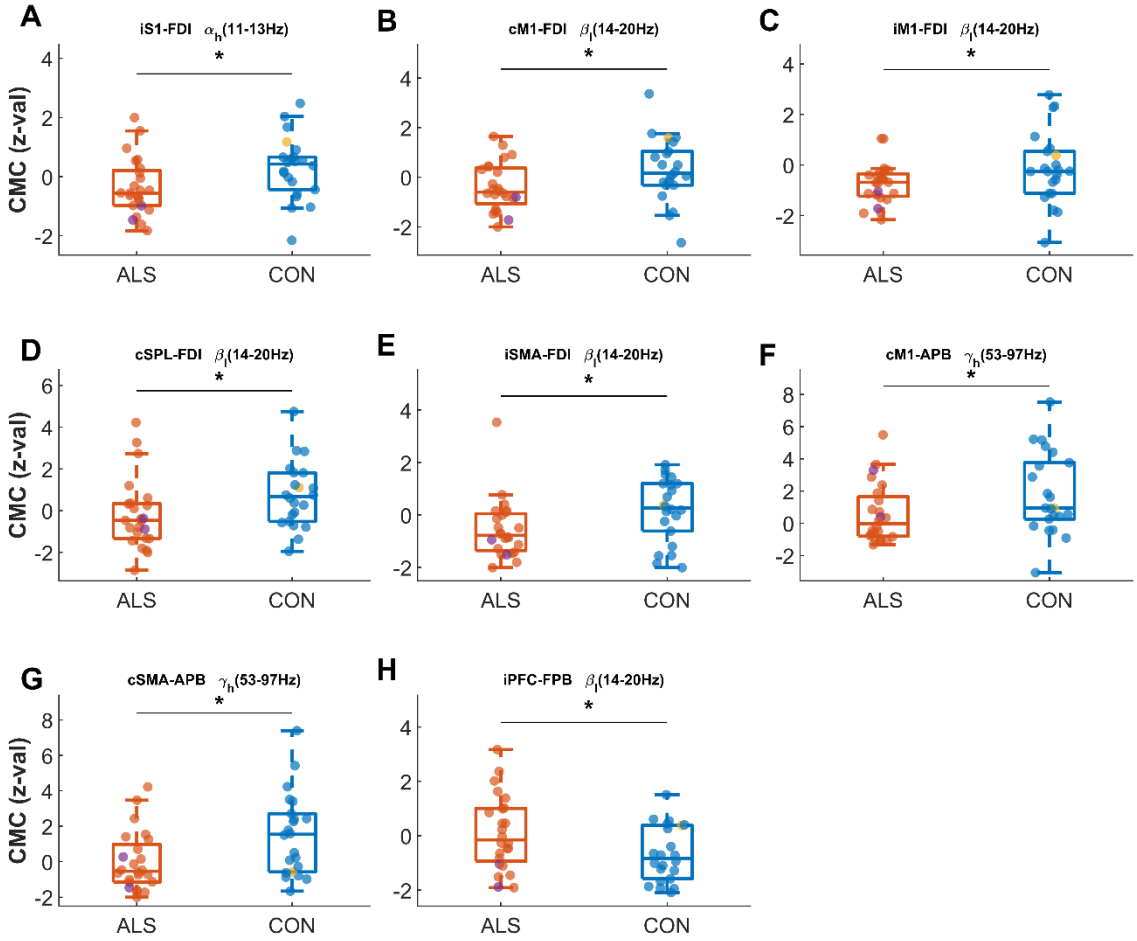

Figure 7.5 Scatter plot overlayed in the box plot of Corticomuscular coherence (CMC) values (z-scores) showing significant group differences (marked by *) between ALS patients and controls. *Significant lower CMC in ALS patients between the FDI and (A) ipsilateral S1 in the high-alpha band, (B, C) bilateral M1 in the low-beta band, (D) contralateral SPL in the low-beta band, and (E) ipsilateral SMA in the low-beta band. Significantly lower CMC in ALS patients between the APB and (F) contralateral M1 in the high-gamma band and (G) contralateral SMA in the high-gamma band. Significantly higher CMC in ALS patients between FPB and (H) ipsilateral PFC in the low-beta band. The purple colour circle in ALS scatter plots represent left-handed ALS participant, similarly the yellow colour circle in controls scatter plots represent left-handed control participant. Muscles:* ***APB*** *Abductor pollicis brevis,* ***FDI*** *First dorsal interosseous,* ***FPB*** *Flexor pollicis brevis (FPB). Brain regions:* ***M1*** *Primary motor,* ***S1*** *Primary sensory,* ***SMA*** *Supplementary motor area,* ***SPL*** *Superior parietal lobule (SPL),* ***PFC*** *Prefrontal cortex. The prefix c/i represents contralateral/ipsilateral side of the brain.*

Table 7.2 Cortex-Muscle pairs where significant group differences in Corticomuscular coherence (CMC) were observed between ALS patients and Controls.

Cortex-Muscle	Location	Frequency	Group Difference (ALS-CON)		
			z-score	p value	Cohen's d
S1-FDI	Ipsilateral	High alpha	-2.27	0.022	0.633
M1-FDI	Contralateral	Low beta	-2.18	0.028	0.610
M1-FDI	Ipsilateral	Low beta	-2.05	0.039	0.553
SMA-FDI	Ipsilateral	Low beta	-2.29	0.021	0.621
SPL-FDI	Contralateral	Low beta	-2.25	0.024	0.574
SMA-APB	Contralateral	High gamma	-2.45	0.014	0.768
M1-APB	Contralateral	High gamma	-2.20	0.027	0.574
PFC-FPB	Ipsilateral	Low beta	2.05	0.039	0.553

SMA: Supplementary motor area, M1: Primary motor cortex, S1: Primary sensory cortex, SPL: Superior parietal lobule, PFC: Prefrontal cortex, FDI: First dorsal interosseous, APB: Abductor pollicis brevis, FPB: Flexor pollicis brevis.

7.3.6 CMC Correlates with Clinical Motor Impairment and Task Performance in ALS patients

Stronger clinical fine motor impairment in ALS, assessed using the ALSFRS-R fine motor sub-scores (lower score means higher impairment), was associated with reduced CMC between FDI muscle and ipsilateral S1 in the delta band (Figure 7.6 A, $r = 0.529$, $p=0.016$) and contralateral S1 in the high-alpha band (Figure 7.6 B, $r = 0.460$, $p = 0.048$). On the other hand, stronger fine motor impairment in ALS was also associated with increased CMC between APB and ipsilateral SPL in the theta band (Figure 7.6 C, $r = -0.473$, $p = 0.039$). Additionally, better task performance accuracy in ALS patients (i.e., the ability to maintain force at an acceptable limit of 10% MVC) was associated with higher CMC

between FDI and contralateral SPL in the low-beta band (Figure 7.6 D, r = 0.562, p = 0.042).

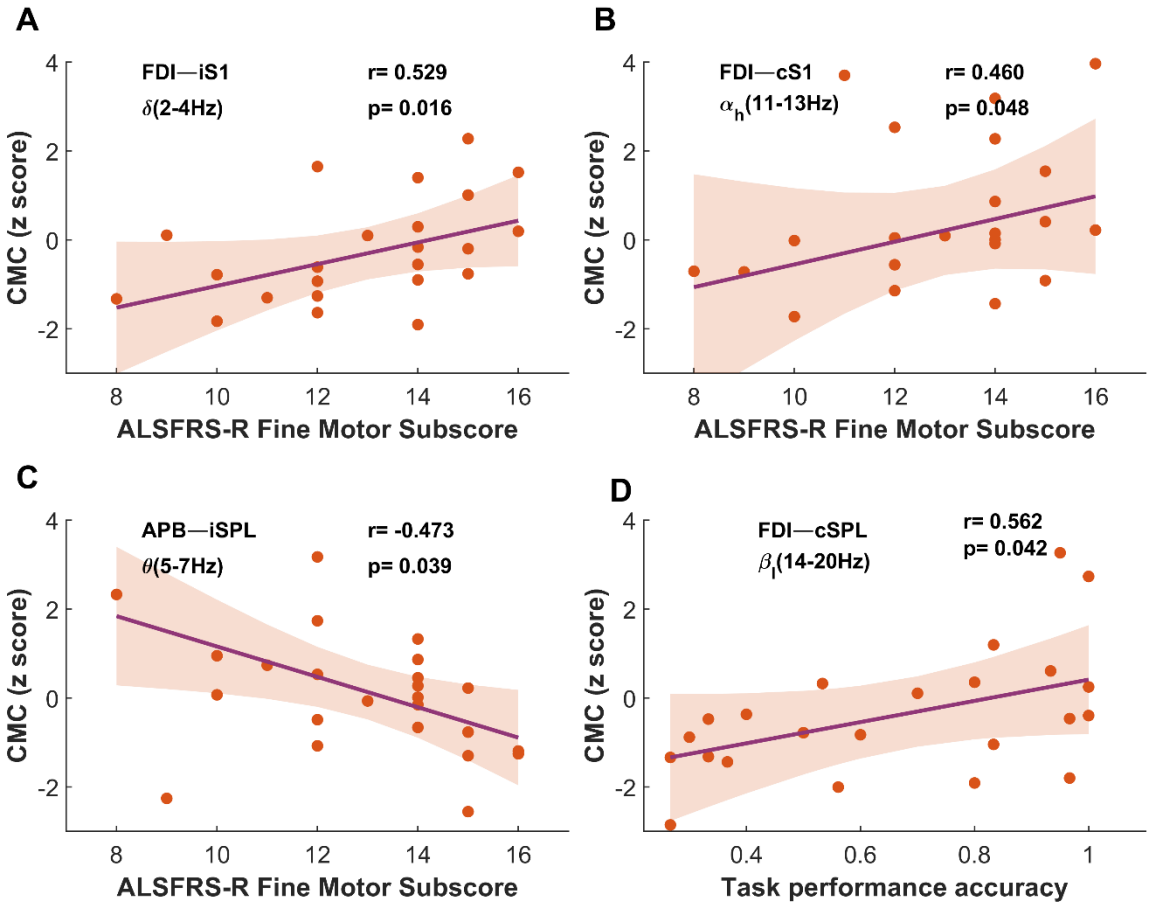

Figure 7.6 Measures of Corticomuscular coherence (CMC) in ALS showed significant strong associations (Spearman's correlation) with the clinically defined ALSFRS-R fine motor sub-scores (A, B, and C) and Task performance accuracy (D). *The fine motor sub-score ranges from 0-16, 16 being normal or no impairment and 0 being severe impairment. The p-values have been corrected for false discovery rate (FDR) at q = 0.05. (A) CMC between the FDI muscle and ipsilateral S1 show significant positive correlation with ALSFRS-R fine motor sub-score in the delta band. (B) CMC between the FDI muscle and contralateral S1 show significant positive correlation with ALSFRS-R fine motor sub-score in the high-alpha band. (C) CMC between the APB muscle and ipsilateral SPL show significant negative correlation with ALSFRS-R fine motor sub-score in the theta band. (D) CMC between the FDI muscle and contralateral SPL show significant positive correlation with task performance accuracy (ratio of number of good epochs to total number of epochs performed) in the low-beta band.*

7.4 Discussion

To date, studies investigating CMC in motor neuron diseases have focused on estimating beta-band CMC between muscles of the hand/arm and M1, as a direct reflection of UMN/LMN pathology (Proudfoot et al., 2018b). However, our recent studies in patients with ALS (Dukic et al., 2019, McMackin et al., 2020), Post-Polio Syndrome (Coffey et al., 2021), and PLS (Bista et al., 2023) suggest that abnormalities in cortical network activity extend beyond M1 in these conditions, a finding that is also supported by neuroimaging studies (Finegan et al., 2019). Here we have used CMC to demonstrate that brain activity in patients with ALS differs from that of healthy controls during the performance of a pinch grip motor task (the engagement of different brain networks is characterised here by the oscillatory coupling between signals recorded from brain and muscle) (Figure 7.4 and Table 7.2). Furthermore, CMC was detected over brain regions and frequency bands distinct from the beta-band CMC that is typically recorded over M1/S1. These observations suggest that ALS affects a wider brain network extending beyond the primary sensorimotor cortex. We also identified several CMC measures that correlated with clinical measures of functional motor dysfunction and motor performance.

7.4.1 Gamma CMC during low force isometric contractions in healthy controls

Beta CMC is dominant during sustained isometric contractions but when the muscle contraction is dynamic, CMC shifts from beta to gamma to account for increased attention to the task and rapid integration of visual, proprioceptive, tactile, and planning information (Andrykiewicz et al., 2007, Gwin and Ferris, 2012, Omlor et al., 2007, Brown et al., 1998). However, beta CMC is not the sole neurophysiological signature of sustained contraction task if additional task parameters are involved. For example, alpha and beta CMC were distinctly observed in mechanically induced physiological tremor in healthy controls

during low force sustained muscle contraction (Halliday et al., 1999, Budini et al., 2014). The observed distinct gamma CMC in addition to beta CMC in healthy controls during our sustained contraction task could be the result of the low frequency periodicity of the exerted force (Figure 7.2 A) which mimics the neurophysiology of a low force dynamic contraction task (Andrykiewicz et al., 2007). In controls, during a low precision (±20% of target) low force (8% MVC) isometric contraction task, gamma CMC in addition to beta CMC has been reported previously by Kristeva-Feige et al. (2002). Similarly, in healthy controls, significant beta and gamma CMC has been reported not only during isometric contraction but also during hand grasping (Tun et al., 2021).

7.4.2 Sensorimotor Dysfunction in ALS

In this study, we compared the CMC between an ALS cohort and age-matched controls for eight frequency bands. The result indicated reduced CMC (except for ipsilateral PFC-FPB in the low-beta band where CMC increases) in the ALS cohort compared to controls in alpha, beta, and gamma frequency bands and in brain regions within and beyond M1. Beta CMC plays an important role in facilitating the efferent/afferent communication between the motor cortex and muscles (Witham et al., 2011), and fine-tuning motor control to adapt to changing task demands (Kilner et al., 2000). CMC in the alpha band is associated with the afferent sensory feedback information from muscles to sensorimotor cortex (Harada et al., 2009) or may reflect the functional connection between M1 and S1(Ohara et al., 2000). Our study showed decreased α/β CMC between primary sensorimotor cortices (M1/S1) and muscle (FDI) in ALS (Figure 7.4 A-B). Previous studies investigating cortex-muscle synchrony using CMC in ALS patients also reported that beta CMC between muscles and sensorimotor areas was significantly reduced in ALS patients compared to controls (Proudfoot et al., 2018b). The reduction of beta CMC was also observed in other

neurodegenerative diseases with movement deficit such as Parkinson's disease (Yokoyama et al., 2020, Zokaei et al., 2021) and neurological disorders that cause motor impairment such as chronic stroke (Meng et al., 2009). Therefore, the observed reduction of α/β CMC in ALS could be attributed to the dysfunction of the corticospinal tract and could be considered a marker of sensorimotor network dysfunction in ALS (Proudfoot et al., 2018b). The reduced CMC for regions other than M1/S1 and/or frequency bands other than α/β could imply broader network impairment in ALS beyond sensorimotor networks (Nasseroleslami et al., 2017, Dukic et al., 2019).

7.4.3 Motor Planning Dysfunction in ALS

The SMA, a motor area with higher-order motor function, plays a crucial role in movement preparation and planning (Shibasaki and Hallett, 2006, Hoshi and Tanji, 2004). Despite very few (about 6%) of corticospinal projections from the SMA to the spinal motor nuclei supplying hand and finger muscles as opposed to more abundant (about 81%) from M1 in non-human primate, the former could contribute to movement preparation and selection by directly influencing the excitability of the spinal circuitry (Maier et al., 2002). Our result showed significant CMC between contralateral SMA and muscles (Figure 7.3) in the γ-band in healthy controls during muscle contraction that may be the result of direct activation of motoneurons to facilitate motor control in addition to the indirect influence through M1 that occurs concurrently (Meng et al., 2008). CMC in the γ-band is associated with dynamic muscle contractions and it is thought to reflect stronger excitation of the motor cortex or greater attention to the task and rapid integration of visual, proprioceptive, tactile, and planning information (Andrykiewicz et al., 2007, Gwin and Ferris, 2012, Omlor et al., 2007, Brown et al., 1998). Previous research has also indicated that γ oscillations act as an online "updating system" for managing motor control (Fries et al., 2007) and γ

oscillations from SMA have been found to be important for sudden changes in the motor plan (Hosaka et al., 2016). Consistent with this idea, it has been reported that γ tACS (transcranial alternating current stimulation) can improve specific components of visuo-motor task execution when sudden changes in the motor plan are required (Santarnecchi et al., 2017). Similarly, γ-band corticospinal coherence between the contralateral motor region and spinal motor neurons has been previously linked to the readiness to respond (Schoffelen et al., 2005). Therefore, significantly lower CMC between SMA and muscles (APB in the γ-band and FDI in the β-band) in ALS patients compared to controls demonstrated by our results (Figure 7.4 B-C) could indicate dysfunctional motor planning networks in ALS (Thorns et al., 2010, Westphal et al., 1998). The reduction of γ-band CMC during initiation of isotonic contraction has previously also been reported in other movement disorders such as cerebral palsy (Riquelme et al., 2014).

7.4.4. Attention Deficit and Cognitive Burden in ALS

Fast or gamma oscillations from M1 have been associated with task engagement in non-human primates (Donoghue et al., 1998). Studies have previously shown that motor performance is enhanced by γ tACS over M1 (Moisa et al., 2016, Joundi et al., 2012), and in turn, observed compensatory neural activity modulation in prefrontal cortex (Moisa et al., 2016). During a dynamic force control task, γ-band CMC between M1 and muscles is linked to higher attention to the task (Andrykiewicz et al., 2007, Omlor et al., 2007, Brown et al., 1998). We have already demonstrated above that although we asked the participants to maintain static (sustained) force, because of the nature of the task, dynamic components were introduced which required increased attention. Therefore, significantly lower γ CMC between contralateral M1 and APB in ALS patients compared to controls (Figure 7.4 C) could be attributed to an attention deficit in ALS (Mannarelli et al., 2014, McMackin et al.,

2019a). Additionally, we have shown that CMC between ipsilateral (right) PFC and FPB muscle in the β band is significantly increased in ALS compared to controls (Figure 7.4 D). This could result from role of prefrontal cortex in compensating for reduced γ CMC between M1 and APB muscle for improving motor performance (Moisa et al., 2016). Furthermore, the increased CMC between right PFC and FPB muscle could be attributed to higher cognitive efforts used by ALS cohort to maintain force at the target level because of cognitive decline (McMackin et al., 2021, Beeldman et al., 2020). High functional connectivity with right PFC in ALS patients has been reported previously by a neuroimaging study (Borgheai et al., 2020) and interpreted as executive dysfunction in ALS patients specifically relating to deficits in task-related working memory processes.

7.4.5 Altered Visuomotor Integration in ALS

The superior parietal lobule (SPL) is involved in various cognitive functions, including visuomotor integration which is the ability to coordinate visual information with motor output. During visuomotor tasks, activity in the SPL is specifically associated with the integration of visual and proprioceptive information, suggesting that the SPL plays a key role in combining sensory information for motor control (Medendorp et al., 2003). Individuals with SPL lesions had difficulty in performing visuomotor tasks that required the integration of visual and proprioceptive information (Pellijeff et al., 2006), which further strengthens the role of the SPL for the integration of sensory information that is critical for motor planning and execution. In ALS, we showed that β CMC between the contralateral SPL and FDI muscle is significantly reduced compared to controls which could be the signature of altered visuomotor integration due to dysfunction of the corticospinal system. Such phenomenon has been previously reported in neurodegenerative diseases such as Alzheimer's disease (Lu et al., 2021). Oculomotor abnormality has been

previously reported in ALS (Rojas et al., 2020, Kang et al., 2018) which further strengthens our interpretation that visuomotor integration could be altered in ALS.

7.4.6 No effect of handedness on the significant CMC differences between ALS patients and controls

The motor task was standardised to be performed by the right hand only, irrespective of left-hand dominance for some participants. Since, we had very few left-hand dominant participants (2 ALS and 1 control) who performed the task using their non-dominant hand, we could not directly compare the effect of handedness on significant CMC differences between ALS patients and healthy controls using statistical test. However, we have visually confirmed by showing a box plot overlayed by scatter plot of CMC measures using different colour (purple for ALS and yellow for controls) for left-handed participants (Figure 7.5), which indicated that those measures were not the outliers (i.e., lie within the standard deviation from the mean). Therefore, we can say that there was no effect of handedness on the significant CMC differences between ALS patients and controls.

7.5 Conclusions

Corticomuscular coherence (CMC) as a tool for investigating motor neuron diseases has traditionally focused on the beta-band CMC between muscles of the hand/arm and M1. However, our recent studies on patients with Post-Polio Syndrome and PLS suggest that abnormalities in cortical network activity extend beyond M1 in these conditions. This study found that the brain activity of ALS patients differed from that of healthy controls during a pinch grip motor task, with CMC detected between brain-muscle pairs and frequency bands distinct from beta-band CMC typically observed between M1/S1 and muscles. These observations suggest that ALS affects a wider brain network directly or indirectly extending

beyond the primary sensorimotor cortex. Additionally, several CMC measures correlated with clinical measures of functional motor dysfunction and motor performance. In ALS patients, there was a reduction of CMC in alpha, beta, and gamma frequency bands, which could be attributed to the dysfunction of the corticospinal tract and could be considered a marker of sensorimotor network dysfunction. The reduction of CMC between muscles and brain regions other than M1/S1 and/or frequency bands other than alpha/beta could imply broader network impairment in ALS beyond sensorimotor networks, potentially contributing to dysfunction of other aspects of motor control such as motor planning, task attention, and visuomotor integration. Overall, these findings suggest that CMC may be a useful tool for studying motor neuron diseases and understanding the underlying neural mechanisms of these conditions.

7.6 Limitations

The CMC studied here using banded spectral coherence doesn't provide directional information. Therefore, the study cannot make inferences whether the corticospinal network dysfunction is driven by descending efferent or ascending afferent pathways.

8. Source Level Study of Effective Connectivity

8.1 Introduction

One promising area of research for early diagnosis of ALS is to find brain network based neurophysiological biomarkers. Directed or non-directed brain networks can be estimated from non-invasive neurophysiological recording or brain imaging technologies such as functional magnetic resonance imaging (fMRI), functional near-infrared spectroscopy (fNIRS), magnetoencephalography (MEG), electroencephalography (EEG) et cetera. Among all brain imaging technologies, EEG is the most cost-effective technology which has already proven its value in brain research. One limitation of EEG is its low spatial resolution, which could be easily overcome by using high-density electrodes with beamforming techniques i.e., estimate source signals from sensor level signals. In addition, source level EEG provides a robust means to identify directional connectivity between brain regions in comparison to fMRI and fNIRS (Anwar et al., 2016).

The network-level changes in brain during rest or on task can be quantified by using brain connectivity measures such as functional connectivity (FC) or effective connectivity (EC). Functional connectivity employs the correlation between the interacting brain regions, and the direction of information flow is not defined (Friston, 2011). So, cortical networks based on functional connectivity lack the causal information such as inflow or outflow which could be crucial for explaining a neurophysiological process in health and in disease. Effective connectivity resolves the issue by providing a causal relationship between the brain regions of interest (Friston, 2011). The effective brain networks can be estimated from the EEG time series by using partial directed coherence (PDC) (Baccalá and Sameshima, 2001), which is a frequency domain version of Granger causality. Other Granger causality-based frequency domain methods such as the direct transfer function

(DTF) (Kaminski and Blinowska, 1991) can be used to find the causal interaction between the brain sources, however, DTF is prone to being affected by alternative interactions or unpredictable factors (Baccalá and Sameshima, 2001). On the other hand, PDC is a widely used method which is proven to be more reliable and faster to quantify causal interactions among multi-channel EEG signals (Huang et al., 2016). Dynamic Causal Modelling (DCM) is another popular method for estimating causal interactions between brain sources, but it requires a prior specification of connectivity linkages (Sato et al., 2009) which is not required with PDC. The asymptotic distribution of PDC is not well known therefore bootstrap-based approaches are commonly used to test for significant connectivity. Variance stabilisation is recommended when it comes to bootstrap-based PDC connectivity approaches (Baccala et al., 2007). Therefore, in this study, we used a normalised version of PDC also called generalised PDC or gPDC. The motivation for choosing gPDC was that it provides variance stabilisation to overcome the lack of scale invariance in PDC (Baccalá and Sameshima, 2021).

Studies using functional connectivity measures have widely reported altered sensorimotor and extra-motor networks in ALS compared to healthy individuals during rest (Agosta et al., 2011, Zhou et al., 2014, Douaud et al., 2011, Menke et al., 2018, Dukic et al., 2019) and tasks (Stanton et al., 2007, Kollewe et al., 2011, Poujois et al., 2013, Cosottini et al., 2012). Similarly, effective connectivity has been widely used to study causal brain networks in neurological disorder such as Alzheimer's disease during rest (Scherr et al., 2021) or task (Agosta et al., 2010b). Although effective connectivity measures could reveal more on ALS neuropathophysiology, the use of the measure to estimate brain network abnormalities in ALS has been rather limited. A resting state fMRI based effective connectivity study on ALS showed altered causal interaction between sensorimotor cortices reflecting damage in motor neurons (Fang et al., 2016). Since, studies have focused

on three cortical regions only (primary motor, primary sensory and supplementary motor), and causal interaction of cortices beyond these sensorimotor regions were not known.

The compensatory mechanism and/or plasticity in ALS, which are well observed phenomena, depend on the functional role of the network. Therefore, we hypothesized that causal network-level changes (motor and extra-motor) can be observed in ALS during different motor tasks (motor planning and motor execution). Our aim for this study was to detect any patterns of changes in causal neuro-electric communication between motor as well as non-motor cortices in ALS during motor tasks.

8.2 Methods

8.2.1 Ethical Approval

Ethical approval was obtained from Tallaght Hospital/St. James's Hospital Joint Research Ethics Committee for St. James's Hospital, Dublin, Ireland [REC: 2019-07 Chairman's Action (22)], and experiments were conducted under the standards set by the Declaration of Helsinki (2013). All participants provided informed written consent before participating in the experiments.

8.2.2 Participants

8.2.2.1 Inclusion Criteria

Healthy individual aged between 18 and 65 and all ALS patient fulfilling the revised EL Escorial diagnostic criteria for possible, probable, or definite ALS were included.

8.2.2.2 Exclusion Criteria

Patients diagnosed with primary lateral sclerosis, progressive muscular atrophy, multiple sclerosis, epilepsy, stroke, brain tumours, prior transient ischemic attacks, structural brain disease, psychiatric diseases, medical conditions that affect the nervous system (e.g., diabetes), other neurodegenerative conditions and other terminal conditions, such as human

immunodeficiency virus, were excluded. Similarly, people who have previously had (allergic) reactions in similar recording environments (e.g., to recording gels) and pregnant women were also excluded.

8.2.2.3 Clinical and Demographic Profile

Motor task EEG data were recorded from 22 ALS patients (mean age: 65.88±10.17) and 16 healthy controls (mean age: 62.67±9.42). The patients and controls were age matched (Mann-Whitney U test, p=0.30). The clinical and demographics data of analysed patients and healthy controls are shown in Table 8.1.

Table 8.1 Clinical and demographics data of analysed ALS patients and healthy controls

	ALS Patients (n=20)	**Healthy Controls (n=19)**
Gender (Male/Female)	15/5	10/9
Age at recording (years)*	64.36±9.61	62.06±8.86
Handedness (Right/Left)	20/0	17/2
Site of Onset (Spinal/Bulbar/Respiratory)	17/3/0	-
Age at onset (years)*	61.99±9.80	-
ALSFRS-R Score (max 48)*	39.35±5.83	-
ALSFRS-R Motor Sub-scores (max 24)*	17.95±3.01	-
C9orf72 Status (Negative/Positive)	19/1	-

* Numbers show mean ± standard deviation

Abbreviations: **ALSFRS-R** amyotrophic lateral sclerosis functional rating scale-revised, **C9orf72** Chromosome 9 open reading frame 72

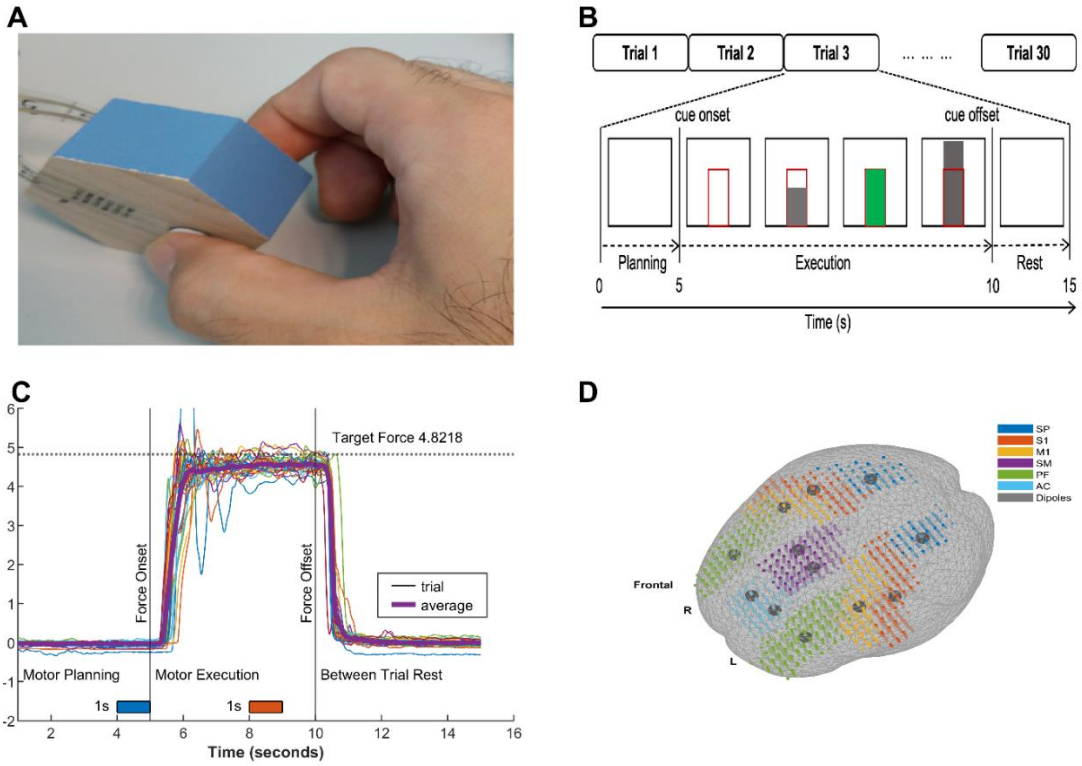

Figure 8.1 Experimental paradigm showing different aspects of task performed and cortical regions of interest for data analysis. ***(A)*** *A pincher grip task using thumb and index finger of the right hand,* ***(B)*** *EEG data format showing 30 trials, each trial consists of 3 phases. Trial 3, for example, is expanded to show the sequence of visual cues and timings of different phases of the task. From left to right: 1. White screen for 5 seconds preceding cue onset where participants take no action: motor planning phase. 2. GO cue, as a red rectangle appears on screen whose height is the target to be matched. 3. Section of 5 seconds motor execution phase showing visual feedback of force applied when the force is incorrectly matched (underfilled). 4. Section of the execution phase showing visual feedback of force applied when the force is correctly matched. 5. Section of execution phase showing visual feedback of force applied when the force is incorrectly matched (overfilled). 5. RELAX cue, white screen for 5 seconds: between trial rest phase,* ***(C)*** *Illustration of the recorded force for all 30 trials and their average for a healthy participant. Target force is 10% of maximum voluntary contraction (MVC). One second time windows were selected for analysis, a blue block (4-5 sec) for motor planning and a red block (8-9 sec) for motor execution,* ***(D)*** *Cortical regions of interest (ROIs) and their dipole current source used for source reconstruction.* ***SP*** *superior parietal lobule,* ***S1*** *primary sensory cortex,* ***M1*** *primary motor cortex,* ***SM*** *supplementary motor area,* ***PF*** *prefrontal cortex,* ***AC*** *anterior cingulate cortex,* ***R*** *right,* ***L*** *left.*

8.2.3 Experimental Paradigm

Assessment was conducted in the same manner for the ALS and control groups, similar to the previously described sensor level study in chapter 6 or source level study in chapter 7 of this thesis and was also described in Coffey et al. (2021) and Bista et al. (2023). Briefly, participants performed 30 trials of isometric pinch grips at 10% MVC using their thumb and index finger of the right hand (Figure 8.1 A), irrespective of their hand dominance, following the target force displayed onscreen. A separate cue for motor planning was not provided. Each trial lasted for 15s (5s planning, 5s execution, and 5s rest), as shown in Figure 8.1 B. An example of force profiles recorded for 30 trials from a healthy participant is shown in Figure 8.1 C.

8.2.4 Clinical measures of disease severity

The revised ALS functional rating scale (ALSFRS-R) scores (Cedarbaum et al., 1999) were obtained from all patients to examine the correlation of EEG effective connectivity measures with disease severity. ALSFRS-R is 48 points validated questionnaire-based clinical scale that ranges from score 0 (severe functional impairment) to 48 (no functional impairment). The 48-point total score can be divided into 4 sub-scales namely bulbar (0-12), fine motor (0-16), gross motor (0-8), and respiratory (0-12) (Cedarbaum et al., 1999). The fine motor and gross motor sub-scales are combined as motor sub-score (0-24) that weigh the level of motor impairment in ALS patients.

8.2.5 Data Analysis

8.2.5.1 Preprocessing

The EEG data was common average referenced followed by 1-100 Hz bandpass filtering using dual-pass 4^{th} order Butterworth filter. A 4^{th} order dual-pass Butterworth band stop filter with stop band of 49-51 Hz was used to remove power line noise. Further, artifacts

such as electrooculogram (EOG), electromyogram (EMG), electrocardiogram (ECG), and jump artifacts were removed automatically using Fieldtrip toolbox. Data epochs where the coefficient of variation of the force produced was above 0.2, or where the mean force was less than 8% or greater than 20% MVC, were excluded from analysis.

8.2.5.2 Source Reconstruction

The details of source reconstruction are explained in sub-section 4.4.2.2 of chapter 4 and in previous chapter of this thesis. Briefly, a template structural MRI data was used to compute the forward model. The source reconstruction was done using linearly constrained minimum variance (LCMV) beamformer (Van Veen et al., 1997) using the Fieldtrip toolbox. Ten anatomical brain regions were chosen bilaterally, 5 on each side of the brain, using the automated anatomical labelling (AAL) atlas (Tzourio-Mazoyer et al., 2002). The chosen anatomical brain regions (regions of interest, ROI) were Primary Motor Cortex (M1), Primary Sensory Cortex (S1), Supplementary Motor Area (SMA), Medial Prefrontal Cortex (PFC), Superior Parietal Lobule (SP), and anterior cingulate cortex (ACC) of both hemispheres.

8.2.5.3 Effective Connectivity using Generalized Partial Directed Coherence

Generalized partial directed coherence (gPDC) was used to evaluate the causal influences or effective connectivity between the ROIs. gPDC is a normalized form of Partial directed coherence (PDC). PDC is a frequency domain multivariate method based on Granger causality which describes the direction of information flow between multivariate time series data based on the decomposition of multivariate partial coherences computed from multivariate autoregressive models (Baccalá and Sameshima, 2001). For the detailed formulation of gPDC see sub-section 4.4.4.2 of Chapter 4.

In this study, gPDC for a bandwidth of 1-100 Hz was calculated using the Fieldtrip toolbox. The 1-100 Hz bandwidth was divided into eight frequency bands (Table 4.2). One gPDC value was calculated for each frequency band by taking the spatial median of the gPDC values at the specified frequencies. For example, the gPDC value for the theta band was the spatial median of gPDC at 5, 6 and 7 Hz.

8.2.5.4 Graph Analysis

Causal inflow (InF) and outflow (OutF) were calculated for both controls and ALS groups from the directed graph representation of effective connectivity. See sub-section 4.4.5.2 of chapter 4 for the details.

8.2.5.5 Statistical Analysis

Gaussian white noise was used for non-parametric bootstrapping (Efron and Tibshirani, 1993) with 2000 repetitions to estimate the null distribution for banded gPDC values. The Empirical Bayesian inference method (Nasseroleslami, 2019) was used to calculate p values for gPDC values. The p values were corrected for multiple comparisons using false discovery rate (FDR) at q=0.05 (Benjamini and Hochberg, 1995). For group analysis, the spatial median of individual gPDC values was taken as group effect whereas the individual p values were combined or averaged using Stouffer's method (Stouffer et al., 1949) to get group level significance of gPDC.

The group level difference (Control versus ALS) for the effective connectivity measure (i.e., gPDC) was calculated by using the non-parametric Wilcoxon rank sum test (Gibbons and Chakraborti, 2003). Similarly, the group level difference between graph measures (i.e., causal inflow and outflow) was calculated by using a parametric 2-sample t-test. The p values obtained from group comparisons were subjected to correction for multiple comparisons using adaptive FDR at q=0.05.

8.2.5.6 Correlation Analysis

The association of the ALS network measures, such as effective connectivity, causal inflow, and causal outflow, with ALSFRS-R motor sub-scores was tested using Spearman's rank correlation coefficients. The p values of the correlation coefficients were adjusted for multiple comparison using adaptive FDR at q = 0.05. A line was fitted to the scatter plot data, to visualise the relationship, using the Robust linear least-square fitting method.

8.3 Results

8.3.1 Weaker motor planning and stronger motor execution effective network patterns in ALS

The causal cortical networks demonstrating significant group differences ($p<0.05$, corrected for multiple comparison using adaptive FDR at $q=0.05$) between healthy controls and ALS patients during motor tasks (planning and execution) are shown in Figure 8.2 and Table 8.2. The group comparison result showed that, motor planning effective networks were weaker in ALS and the frequencies of those networks range from α to γ bands (see Figure 8.2 or 8.3 A). SMA driven contralateral sensorimotor connection (left SMA→ left S1) in the β band wase significantly weaker in ALS patients during motor planning. Similarly, the contralateral SMA received significantly weaker input from ipsilateral S1 (right S1→ left SMA) at α band. Ipsilateral SMA received significantly weaker input from ipsilateral M1 in the γ frequency band.

During execution of the motor task, out of those effective cortical networks that showed significant group differences, all of them were significantly stronger in ALS patients except for a contralateral parieto-frontal connection (left SPL→ left PFC) which was significantly weaker in the α band. In the same frequency band, an interhemispheric parieto-frontal connection (right SPL→ left PFC) was significantly stronger in ALS patients. Importantly,

the interhemispheric motor connection (i.e., right SMA→ left M1) in the β band was significantly stronger in ALS patients during motor execution.

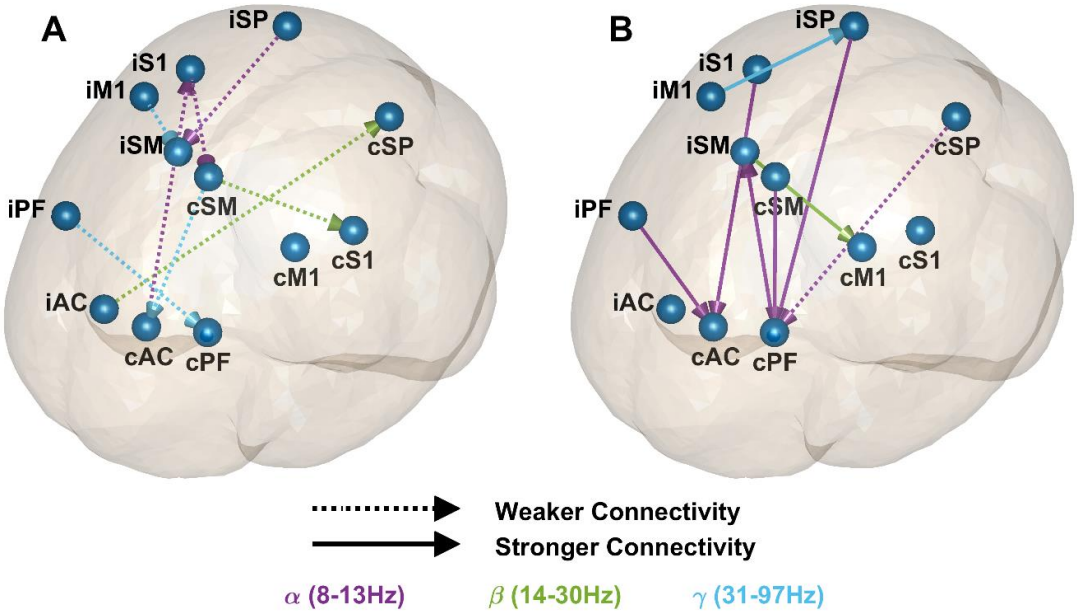

Figure 8.2 Effective connectivity between cortical sources where significant differences were observed between ALS and controls during (A) planning of the motor task and (B) execution of the motor task. *The causal connectivity stronger in ALS is represented by solid arrows and the causal connectivity weaker in ALS is represented by dashed arrows. The frequency band is encoded by the colour of the arrows.* ***M1*** *primary motor cortex,* ***SM*** *supplementary motor area,* ***SP*** *superior parietal lobule,* ***AC*** *anterior cingulate cortex,* ***PF*** *prefrontal cortex,* ***S1*** *primary sensory cortex. The prefix c/i represents contralateral/ipsilateral side of the brain.*

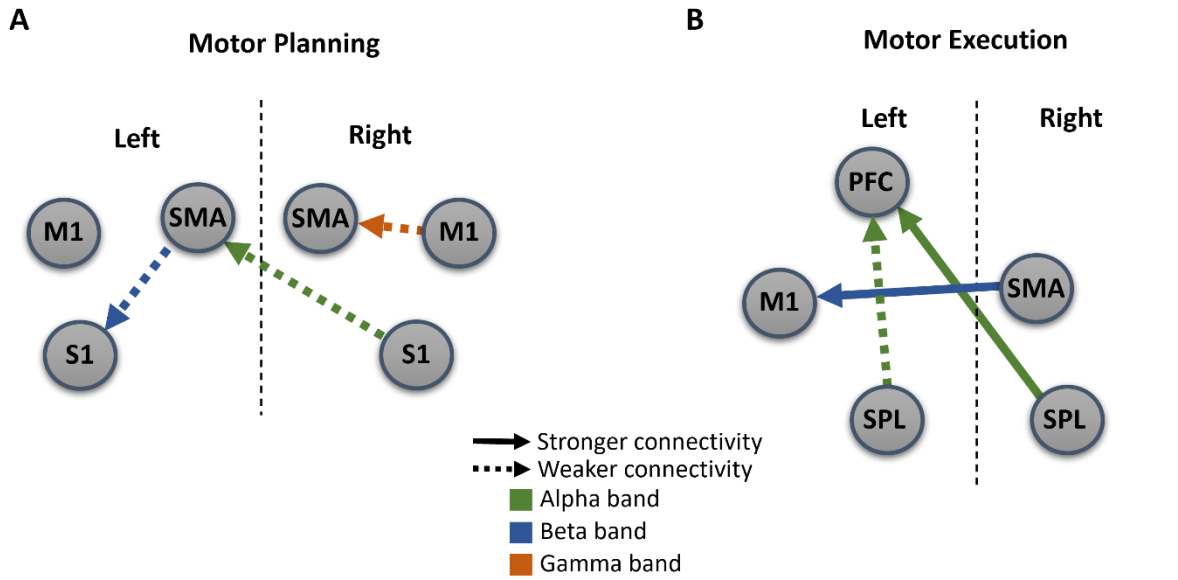

Figure 8.3 Summarized version of figure 8.2 showing most important significant differences observed between ALS patients and controls during (A) planning of the motor task and (B) execution of the motor task. *The causal connectivity stronger in ALS is represented by solid arrows and the causal connectivity weaker in ALS is represented by dashed arrows. The frequency band is encoded by the colour of the arrows.* ***M1*** *primary motor cortex,* ***SMA*** *supplementary motor area,* ***SPL*** *superior parietal lobule,* ***PFC*** *prefrontal cortex,* ***S1*** *primary sensory cortex.*

Table 8.2 Effective connectivity between cortical sources where significant differences were observed between ALS patients and Controls during planning and execution of a motor task.

Motor Task	Connectivity	Frequency	Average Generalised PDC		Group Difference	
			CON	ALS	p value	Cohen's d
Motor Planning	iS1→cSM	Low Alpha	0.243	0.168	0.041	0.974
	iSP→iSM	Low Alpha	0.260	0.172	0.032	0.814
	cAC→iS1	Low Alpha	0.220	0.154	0.027	1.053
	cSM→cS1	Low Beta	0.272	0.185	0.014	1.116
	iAC→cSP	Low Beta	0.279	0.197	0.024	0.908
	iM1→iSM	Low Gamma	0.230	0.191	0.048	0.722
	cSM→cAC	High Gamma	0.228	0.202	0.020	1.026
	iPF→cPF	High Gamma	0.236	0.192	0.009	1.183
Motor Execution	cPF→iSM	Low Alpha	0.161	0.224	0.020	0.981
	iPF→iSM	Low Alpha	0.150	0.217	0.045	0.641
	cSM→cPF	Low Alpha	0.153	0.214	0.035	0.737

	cSP→cPF	Low Alpha	0.201	0.128	0.035	0.903
	iS1→cAC	Low Alpha	0.169	0.241	0.013	1.109
	iSP→cPF	High Alpha	0.174	0.249	0.017	1.030
	iSM→cM1	Low Beta	0.163	0.232	0.032	0.997
	iM1→iSP	High Gamma	0.197	0.219	0.014	1.132

M1 primary motor cortex, **SM** supplementary motor area, **SP** superior parietal lobule, **AC** anterior cingulate cortex, **PF** prefrontal cortex, **S1** primary sensory cortex. The prefix c/i represents contralateral (left)/ipsilateral (right) side of the brain.

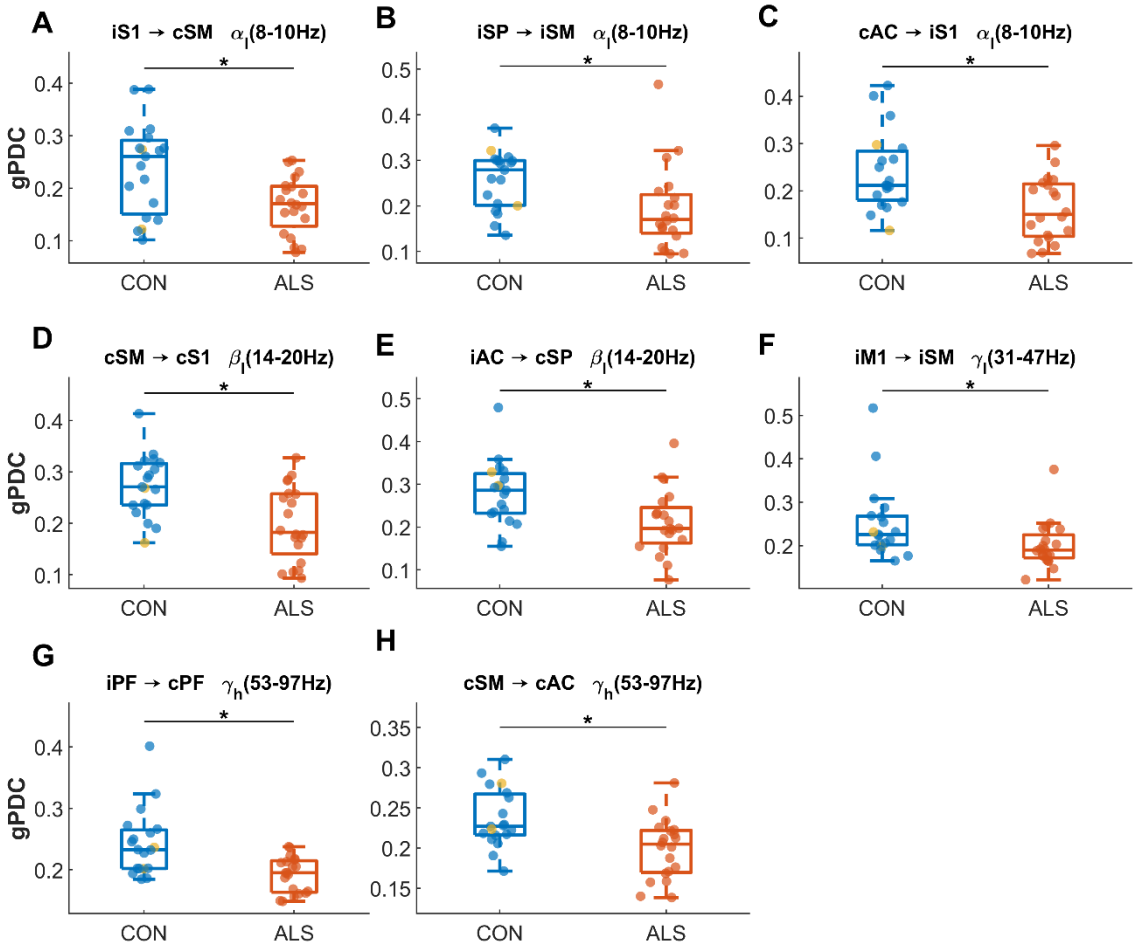

Figure 8.4 Scatter plot overlayed in the box plot of effective connectivity values showing significant group differences (marked by *) between ALS patients and controls during motor planning. → *represents the direction of the connectivity. Yellow colour circle in controls scatter plots represent left-handed control participant. Brain regions:* ***M1*** *Primary motor,* ***S1*** *Primary sensory,* ***SMA*** *Supplementary motor area,* ***SPL*** *Superior parietal lobule (SPL),* ***PFC*** *Prefrontal cortex. The prefix c/i represents contralateral/ipsilateral side of the brain.*

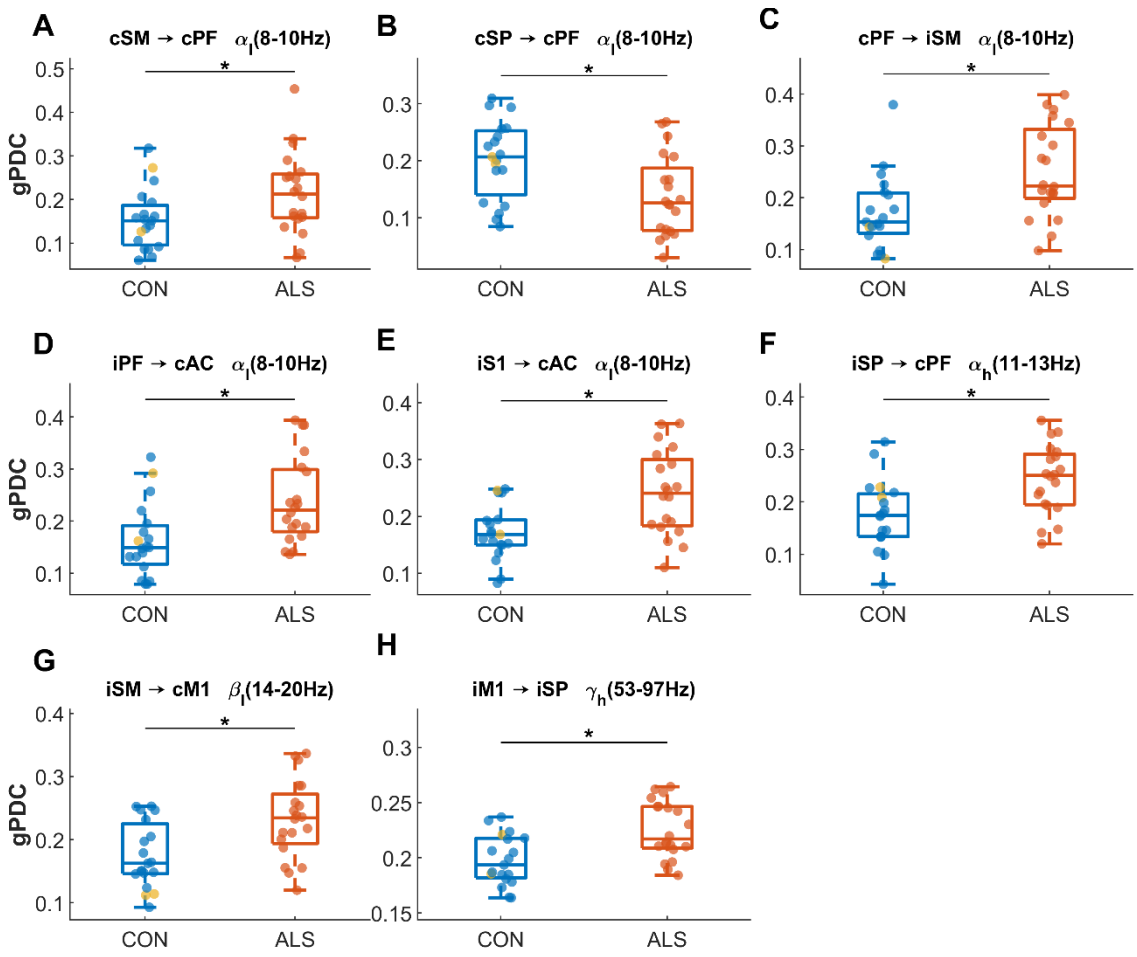

Figure 8.5 Scatter plot overlayed in the box plot of effective connectivity values showing significant group differences (marked by *) between ALS patients and controls during motor execution. *→ represents the direction of the connectivity. Yellow colour circle in controls scatter plots represent left-handed control participant. Brain regions:* ***M1*** *Primary motor,* ***S1*** *Primary sensory,* ***SMA*** *Supplementary motor area,* ***SPL*** *Superior parietal lobule (SPL),* ***PFC*** *Prefrontal cortex. The prefix c/i represents contralateral/ipsilateral side of the brain.*

8.3.2 Cortical network underloading during motor planning and overloading during motor execution in ALS

The brain regions which showed significant differences when their causal flow values were compared between controls and ALS patients during planning and execution for various frequency bands are shown in Figure 8.6 and 8.7, respectively. During motor planning

(Figure 8.6), the signal inflow was significantly reduced towards contralateral S1 in the low α band (Figure 8.6 A), contralateral ACC in the high α band (Figure 8.6 B), and contralateral M1 and ipsilateral ACC in the high β band (Figure 8.6 C). Similarly, a significant reduction in the outflow of oscillatory information from contralateral SMA and ipsilateral PFC in the high β band (Figure 8.6 D) and contralateral ACC and ipsilateral M1 in the low γ band (Figure 8.6 E) was observed in ALS patients compared to controls.

On the other hand, during motor execution (Figure 8.7), the signal inflow was significantly higher in ALS patients compared to controls towards contralateral M1 in the low β band (Figure 8.7 A) and ipsilateral ACC in the high β band (Figure 8.7 B). Similarly, the signal outflow was significantly higher in ALS patients compared to controls from contralateral PFC and ipsilateral SPL in the low α band (Figure 8.7 C).

A significant increase in causal outflow of extra-motor cortical signals was observed in ALS patients during motor execution in the low α band compared to controls. The outflow increase was localized to the contralateral prefrontal region and ipsilateral superior parietal lobule as shown in Figure 8.5 C.

8.3.3 Effective network measures correlate with functional motor impairment in ALS patients within sensorimotor and prefrontal regions

The relationship of effective network measures (gPDC values) with the disease pathology was investigated by correlating them with clinical scores. Several of the effective connectivity measures were significantly correlated with the ALSFRS-R motor sub-scores after FDR correction at q=0.05. In Figure 8.8, a significant negative correlation between an effective connection and the ALSFRS-R motor sub-score indicates that higher motor impairment (more severe clinical symptoms indicated by a reduced ALSFRS-R motor sub-score) is associated with increased causal connectivity in patients. A positive

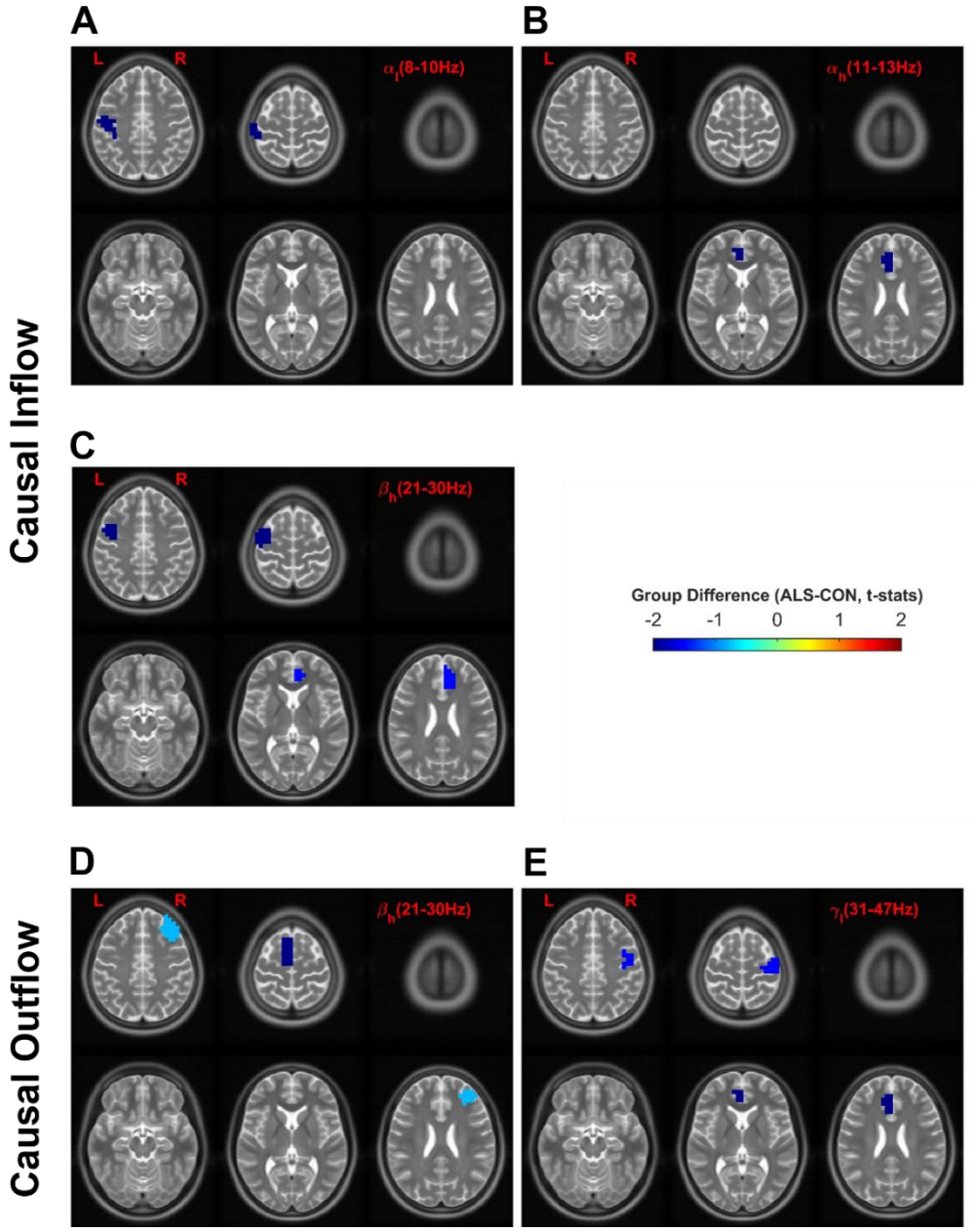

Figure 8.6 Brain regions where significant differences in causal inflow (A, B, C) and outflow (D, E) were observed in ALS patients compared to controls during motor planning. *(A) shows significantly less inflow towards contralateral primary sensory cortex in the low-alpha band in ALS. (B) shows significantly less inflow in ALS towards contralateral anterior cingulate cortex in the high-alpha band. (C) shows significantly less inflow towards contralateral primary motor cortex and ipsilateral anterior cingulate cortex in ALS patients in the high-beta band. (D) shows significantly less outflow from ipsilateral prefrontal cortex and contralateral supplementary motor area in the high-beta band in ALS patients. (E) shows significantly less outflow flow from ipsilateral primary motor cortex and contralateral anterior cingulate cortex in the low-gamma band in ALS patients.*

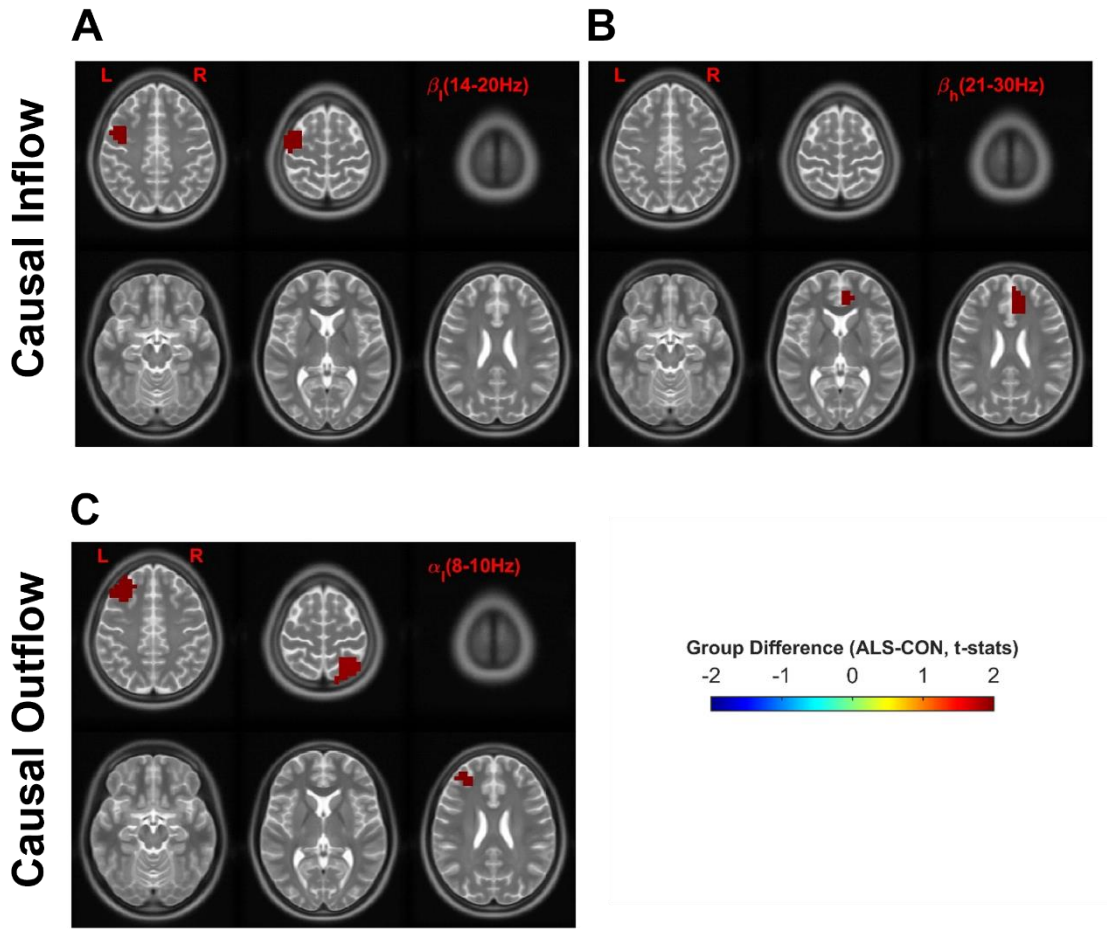

Figure 8.7 Brain regions where significant differences in causal inflow (A, B) and outflow (C) were observed in ALS patients compared to controls during execution of a motor task. *(A) shows significantly more inflow towards contralateral primary motor cortex in the low-beta band in ALS patients. (B) shows significantly more inflow towards ipsilateral anterior cingulate cortex in the high-beta band in ALS patients. (C) shows significantly more outflow from contralateral prefrontal cortex and ipsilateral superior parietal lobule in ALS patients in the low-alpha band.*

correlation indicates that patients with more severe motor symptoms exhibited reduced causal connectivity between the brain regions.

We found that, during motor planning, the ipsilateral causal connectivity from prefrontal region to SMA (iPFC→iSMA) at low α band was weaker in patients with more severe motor impairments (i.e., iPFC→iSMA network showed significant positive correlation with ALSFRS-R motor sub-score) (Figure 8.8 A). The causal inflow or outflow of cortical

ROIs did not show any significant correlation with the motor impairments in ALS patients during motor planning.

During motor execution, interhemispheric effective connections from contralateral M1 to ipsilateral PFC (Figure 8.8 B) and ipsilateral S1 to contralateral S1 (Figure 8.8 D) in the α band were reduced in ALS patients with more severe motor impairment. On the other hand, the causal connectivity from contralateral S1 to contralateral SMA in the high α band was significantly higher in ALS with higher motor impairment during motor execution (Figure 8.8 C). Similarly, the causal inflow of contralateral PFC and SMA was higher in ALS patients with higher motor impairment in the θ and high α bands, respectively (Figure 8.8 E-F). The causal outflow of ROIs did not exhibit any significant correlations with ALSFRS-R motor sub-scores during motor execution.

8.4 Discussion

The motor task was standardised to be performed by the right hand only, irrespective of left-hand dominance for some participants. Since, we had very few left-hand dominant participants (2 healthy controls only) who performed the task using their non-dominant hand, we could not directly compare the effect of handedness on significant connectivity differences between ALS patients and healthy controls using statistical test. However, we have visually confirmed by showing a box plot overlayed by scatter plot of effective connectivity measures using different colour (yellow for controls) for left-handed participants (Figure 8.4 and 8.5), which indicated that those measures were not the outliers (i.e., lie within the standard deviation from the mean). Therefore, we can say that there was no effect of handedness on the significant effective connectivity differences between ALS patients and controls.

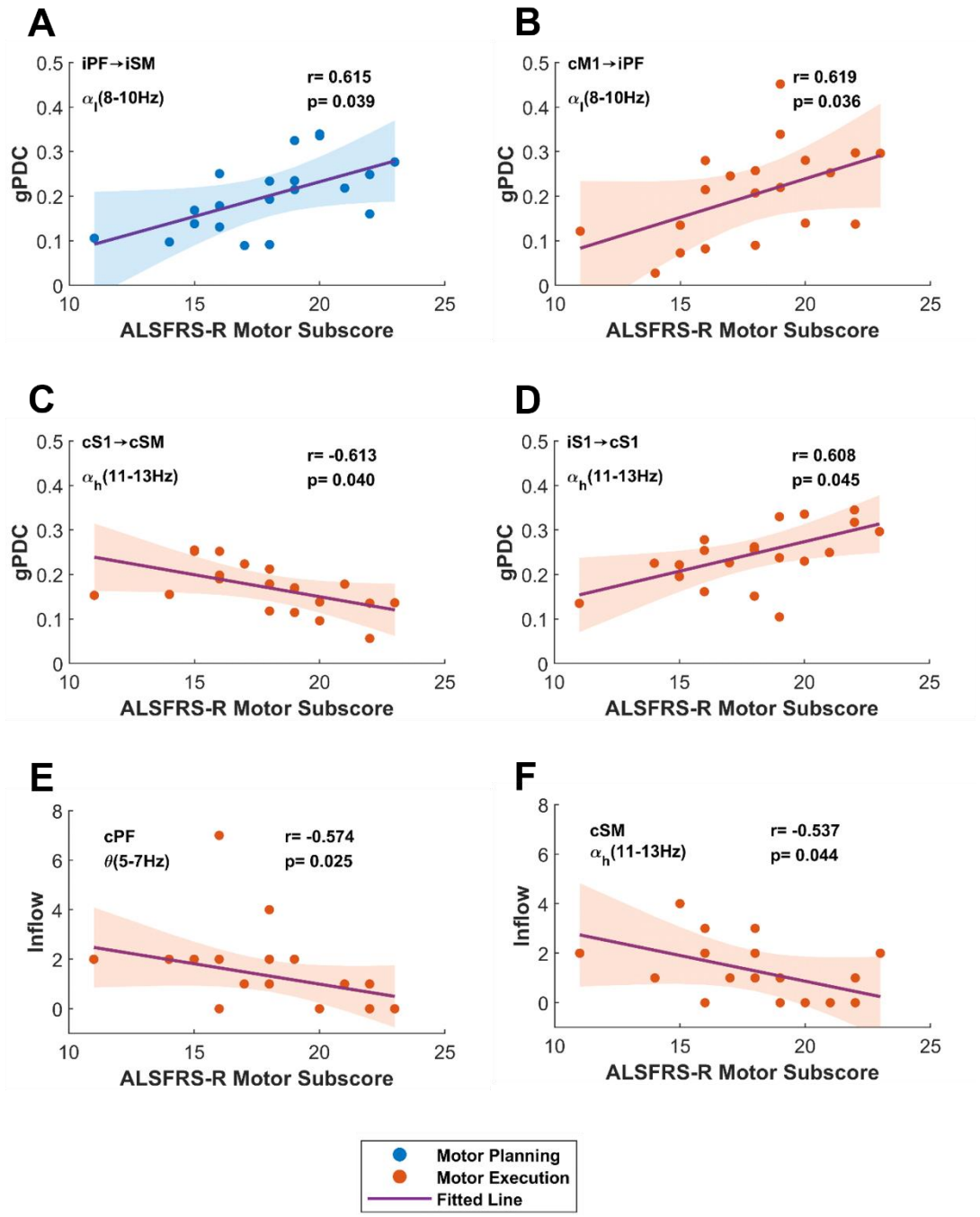

Figure 8.8 Significant correlations between directional connectivity measures (generalised partial directed coherence and causal inflow) and ALSFRS-R motor sub-scores during planning (A) and execution (B, C, D, E, F) of a motor task. ***r*** *is Spearman's correlation coefficient, and the* ***p*** *value is adjusted for multiple comparisons using adaptive FDR at q = 0.05.* ***M1*** *primary motor cortex,* ***SM*** *supplementary motor area,* ***SP*** *superior parietal lobule,* ***AC*** *anterior cingulate cortex,* ***PF*** *prefrontal cortex,* ***S1*** *primary sensory cortex. The prefix c/i represents contralateral/ipsilateral side of the brain.*

8.4.1 Motor planning effective networks are impaired and reflect neurodegeneration in ALS

The present study deciphered several directional network level abnormalities in ALS motor networks compared to healthy controls. In ALS patients, during motor planning, we reported weaker effective networks within and beyond bilateral motor regions (M1 and SMA) compared to controls. Specifically, we showed that an SMA driven sensorimotor network (SMA→S1) at contralateral side in the β band was significantly weaker in ALS compared to controls during motor planning in ALS patients. Previous studies have shown similar weakness in SMA driven sub-cortical networks in ALS patients during movement preparation (Abidi et al., 2020). The pre-movement (motor preparation or planning) alpha/beta event-related de-synchronisation (ERD) of contralateral sensorimotor cortices is a well-known neurophysiological correlate of activated cortical areas (Pfurtscheller and Berghold, 1989). Upper motor neuron degeneration, such as in ALS and primary lateral sclerosis (PLS), causes higher ERD of bilateral sensorimotor regions (Proudfoot et al., 2017). So, the weaker effective connectivity in our results to/from bilateral SMA/S1 and ipsilateral M1, during motor planning, could be the reflection of increased de-synchronous firing patterns of upper motor neurons in ALS as the result of motor neuron degeneration. The effect of motor neuron degeneration in the motor planning circuitry in ALS is also reflected in neuronal firing potential (movement-related potential, MRP). The motor planning/preparation MRP, also called readiness potential, is reduced in ALS patients (Bizovičar et al., 2013, Thorns et al., 2010, Westphal et al., 1998) indicating a reduced number and/or synchrony of active motor neurons due to neurodegeneration. This indicates that neurophysiological signatures of motor planning networks in ALS, including effective

connectivity within sensorimotor networks as demonstrated by this study, are weaker compared to controls and could be directly or indirectly linked to neurodegeneration.

Furthermore, the hypothesis of weaker motor and sensory cortical activation or synchrony in ALS during motor planning as a reflection of neurodegeneration (Bizovičar et al., 2013, Thorns et al., 2010, Westphal et al., 1998, Proudfoot et al., 2017) is supported by the fact that we observed motor and sensory network underloading in ALS compared to controls, meaning a significantly smaller number of incoming connections (inflow) towards contralateral sensorimotor cortices (M1/S1) and outgoing connections (outflow) from contralateral SMA. More importantly, the ipsilateral frontocentral connection at α band (PFC→SMA) showed significant positive correlation with ALSFRS-R motor sub-scores indicating association of severe motor impairment (clinical sign of neurodegeneration) with decreased motor planning effective connectivity in ALS.

8.4.2 SMA compensates for M1 degeneration and facilitates sensorimotor integration in ALS during task execution

The study of effective networks in healthy individuals during motor execution has underpinned significant bidirectional interaction between primary motor (M1), primary sensory (S1), and higher order motor regions such as premotor (PM) and supplementary motor area (SMA) (Grefkes et al., 2008, Kim et al., 2018, Brovelli et al., 2004, Gao et al., 2011, Anwar et al., 2016) contralateral to the limb movement. Additionally, during execution of a unimanual voluntary task, the interhemispheric inhibition causes laterization of motor cortex for motor control (Shibasaki and Hallett, 2006, Welniarz et al., 2015, Duque et al., 2007). The evidence for compensatory and adaptive changes in cortical motor networks are abundant in ALS neurophysiological studies investigating voluntary movements, reporting recruitment of ipsilateral sensorimotor cortices, premotor regions,

and non-motor regions in ALS (Bede et al., 2021, Abidi et al., 2020, Konrad et al., 2002, Inuggi et al., 2011). Our findings showed similar neurophysiological signatures in ALS during motor tasks. We reported stronger causality from ipsilateral SMA to contralateral M1 and higher signal inflow towards contralateral M1 (overloading) in the β band in ALS patients compared to controls, which could reflect two neuropathophysiological mechanisms in ALS. First, the interhemispheric disinhibition between motor regions is increased in ALS as pointed out by various TMS studies (Karandreas et al., 2007, Bos et al., 2019). The interhemispheric pathways are not just limited to M1-M1 interactions but also include the pathway that link higher order motor areas such as PM and SMA to contralateral M1 (Hinder et al., 2012) resulting in stronger connectivity from ipsilateral SMA and contralateral M1 overloading in ALS. Second, the recruitment of ipsilateral SMA and increased signal inflow towards contralateral M1 in ALS patients during motor execution could be to overcome the burden of neurodegeneration in M1.M1 degeneration causes higher demand on motor system in ALS and it has been shown that the motor systems respond to higher motor demand by enhancing information flow between sensorimotor regions of both hemispheres even when the movements are unimanual (Gerloff et al., 1998).

Moreover, we have also reported stronger contralateral S1→SMA effective connectivity and higher causal inflow towards contralateral SMA in the α band for more functionally impaired ALS participants, indicating facilitation of sensorimotor integration and stronger connectedness by higher order motor regions such as the SMA.

8.4.3 Altered fronto-parietal (executive) network in ALS during motor execution

The fronto-parietal network for slower oscillations (θ or α bands) is often associated with executive functions in healthy controls (Sauseng et al., 2005, Marek and Dosenbach, 2018,

Zanto et al., 2011). An abnormal fronto-parietal network has been reported in ALS by resting state EEG studies (Dukic et al., 2019, Dukic et al., 2021, Nasseroleslami et al., 2018). On the one hand, we have reported significantly weaker contralateral fronto-parietal connectivity (left SPL→ left PFC) in the α band in ALS patients compared to controls, on the other hand we have found that the interhemispheric fronto-parietal connection (right SPL→ left PFC) at α band is significantly stronger in ALS patients. This indicates that the ipsilateral SPL compensates for weaker influence of the contralateral SPL on fronto-parietal networks in ALS. This is also reflected in causal outflow of ipsilateral SPL in ALS patients in terms of cortical overloading. Furthermore, the θ band inflow of the contralateral PFC is negatively correlated to ALSFRS-R motor sub-scores i.e., ALS patients with severe motor impairment has higher number of incoming connections towards contralateral PFC. This could be attributed to higher cognitive efforts taken by ALS patients to maintain force at the target level during the execution task. The lateralized effect on the prefrontal network in ALS patients with a higher number of functional connections with the right PFC has been reported previously by a neuroimaging study employing visuo-mental cognitive task (Borgheai et al., 2020) and was interpreted as an executive dysfunction in ALS cohort specifically relating to deficits in task-related working memory processes.

8.4.4 Inter-hemispheric somatosensory interaction during motor execution decreases with disease severity in ALS

In previous studies using sensory evoked potentials (SEP), it has been reported that ALS patients exhibited higher somatosensory disinhibition or cortical hyperexcitability in S1 (Höffken et al., 2019, Machii et al., 2003, Shimizu et al., 2018, Nardone et al., 2020). However, interhemispheric connectivity between S1 areas in ALS has received relatively little attention, despite the observation of reduced functional connectivity between the left

and right M1 as reported in an fMRI study (Jelsone-Swain et al., 2010). We revealed a significant positive correlation between the strength of interhemispheric somatosensory effective connectivity (from ipsilateral S1 to contralateral S1) and functional motor impairments in ALS. Specifically, the strength of this interhemispheric connectivity (right S1→ left S1) was found to be diminished in cases of ALS accompanied by severe functional motoric deficits. Interestingly, a similar neurological pattern has been previously reported in other disorders, such as stroke, which also lead to motor impairments. Post stroke, a reduction in S1-S1 functional connectivity has been identified which was shown to correlate with the degree of motor impairment (Frías et al., 2018).

8.5 Conclusion

The study focused on examining effective network abnormalities related to motor functioning in people with ALS compared to healthy controls. The study identified several disruptions in directional networks within motor systems in ALS with higher order motor regions such as the SMA playing a crucial role. The SMA-driven sensorimotor network was notably weaker on the contralateral side in ALS patients, suggesting impaired motor planning. Stronger SMA-driven effective connectivity may compensate for M1 degeneration during motor execution, with stronger ipsilateral-to-contralateral connections possibly driven by interhemispheric disinhibition and heightened motor demands in ALS. We also reported simultaneous occurrence of pathological and compensatory fronto-parietal connectivity which could be the consequence of executive dysfunction in ALS patients. Additionally, decreased interhemispheric somatosensory interaction during motor execution correlated with disease severity in ALS. These findings contribute to a better understanding of the neurodegenerative processes underlying ALS and how they manifest in motor-related brain networks.

8.6 Limitations

The effective connectivity analysis was based on partial directed coherence (PDC) which is a data driven method unlike dynamic causal modelling (DCM) which is a model driven method. Therefore, we cannot make a direct comparison between ALS patients and controls based on the presence or absence of network causality but must rely on the statistical comparison of causality strength. This limited us from reporting those causal networks which were not statistically different between ALS patients and controls or showed no significant correlation with clinical measures but has neurophysiological importance in health or in disease.

9. Discussions and Conclusion

In this chapter an overall summary and interpretation of the project's results, a discussion of the relevance of results to understanding and quantifying ALS motor network impairments, a consideration of the limitations of the project and the future research that is called for are described. An overall summary of the project results is given in section 9.1. The advantages of using the employed electrophysiological paradigms for investigating motor networks of ALS are described in Section 9.2. The potential impact and clinical applications of this work are mentioned in section 9.3 and the limitations of this work are summarised in section 9.4. Future work that can build upon this project to bring these results towards more sophisticated understanding of the disease and real-world applications are described in section 9.5. Finally, section 9.6 contains a brief conclusion with regards to the entire thesis.

9.1 Summary of the results

9.1.1 Corticomuscular coherence patterns in primary lateral sclerosis

We used CMC to demonstrate how brain activity in participants with PLS differs from that of healthy controls during the performance of a pinch grip motor task. In PLS patients, higher CMC between contralateral M1 and FPB muscle in the alpha band and between contralateral M1 FDI muscle in the gamma band was observed when compared with healthy controls. Significant beta-band CMC was also detected between ipsilateral M1 and FDI muscle, which is not typically observed in healthy participants. We also identified several CMC measures that correlated with clinical measures of UMN dysfunction, which were also identified outside of contralateral M1. PLS participants with greater motor impairments exhibited higher beta-band CMC between parietal area (Pz) and APB muscle whereas less impaired PLS participants exhibited higher alpha- and gamma-band

coherence between contralateral M1 and APB muscle. Although the observed CMC differences in PLS patients could arise from both direct and indirect effects of UMN degeneration, the increased CMC in more impaired PLS participants for specific brain regions could potentially suggest that these changes are compensatory/adaptive in nature. Taken together, these results could suggest that the pattern of brain network re-organization in PLS follows a similar trajectory to recovery in stroke, where more impaired PLS participants rely on contributions from the ipsilateral hemisphere but those that are minimally affected can recover function by restructuring the functional connectivity in the contralateral hemisphere (Brancaccio et al., 2022).

9.1.2 Resting state, pre-movement, motor planning, and motor execution networks

9.1.2.1 Resting state sensorimotor network is abnormal in ALS

Functional assessments of brain networks have the potential to detect and quantify disease specific adaptive and compensatory patterns of network activity. Prior to this study, the functional connectivity differences between ALS patients and age-matched controls during rest have been investigated by our group reporting abnormal sensorimotor networks in ALS (Dukic et al., 2019). We also found that during rest, the functional connectivity between EEG electrodes pertaining to cortical regions M1 and S1 in the θ band was significantly stronger in ALS patients compared to healthy controls. Furthermore, the resting state sensorimotor connectivity (M1-S1) abnormality in the θ band was negatively correlated with the ALSFRS-R score suggesting that motor impairment is associated with increased sensorimotor functional coupling in ALS. This corroborates the increased S1 disinhibition in ALS patients and negative correlation of S1 excitability with ALSFRS-R scores reported by Höffken et al. (Höffken et al., 2019). Importantly, our finding of abnormal sensorimotor EEG connectivity strengthens the argument that sensorimotor functional connectivity at

rest has potential to be a quantitative neurophysiological biomarker candidate for diagnosis and prognosis of ALS (Dukic et al., 2019, Zhou et al., 2014).

9.1.2.2 Cortical hyperexcitability in ALS

We have reported that the EEG functional network density or small-worldness, quantified by the mean global clustering coefficient, was higher in ALS than in healthy controls during rest, pre-movement and motor execution indicating widespread EEG networks. Similar widespread functional brain networks have previously been reported by M/EEG studies using graph analysis in ALS (Iyer et al., 2015, Sorrentino et al., 2018) which reflected cortical hyperexcitability, a well-established pathological finding in ALS (Menon et al., 2015, Vucic et al., 2011).

9.1.2.3 Pre-motor and motor planning networks are impaired in ALS

We studied pre-motor networks in ALS using ERD and functional connectivity in sensor space and motor planning effective connectivity in source space. We reported no significant differences in mu or beta ERD in ALS pre-motor stage in sensorimotor regions, but significantly higher event related spectral perturbations in the prefrontal and the parietal region in the θ band indicating higher attention to the task pre-movement by recruiting a neuron pool distributed over wider cortical areas to overcome the burden of motor neuron degeneration in sensorimotor cortices. In terms of functional network abnormalities during the pre-motor stage, we found that functional connectivity between contralateral premotor and primary sensory cortices (PM-S1) was significantly higher in the alpha-band in ALS patients compared to controls. Similarly, the functional connectivity within the frontal region (DLPFC-DMPFC) in the alpha-band was significantly higher in ALS. Interestingly, significantly reduced EEG functional connectivity was observed within the contralateral M1-DLPF in the beta-band in ALS patients compared to controls. These functional network

abnormalities suggest that that pre-motor activity, which combines attention, preparation, and planning of upcoming motor tasks, is abnormal in ALS not only at the neuronal oscillatory level (Thorns et al., 2010) but also at the cortical network level, which leads to poor motor performance (task performance accuracy was significantly lower in ALS compared to controls, $p = 0.043$).

Using source space analysis, during motor planning, we reported significantly weaker effective connectivity within and beyond bilateral motor regions (M1 and SMA) in ALS patients compared to controls. Specifically, we demonstrated that effective sensorimotor networks involving the SMA, SMA→S1 at the contralateral side at beta-band and ipsilateral S1→ contralateral SMA in the alpha-band, were significantly weaker in ALS compared to controls indicating impaired motor planning in ALS. Previous studies have shown similar weaknesses in the SMA-driven sub-cortical networks in ALS during movement preparation (Abidi et al., 2020). Furthermore, we observed a significantly smaller number of incoming connections (inflow) towards contralateral sensorimotor cortices (M1/S1) in the alpha/beta band and outgoing connections (outflow) from the contralateral SMA in the beta band. This indicated weaker involvement of sensorimotor regions during motor planning due to neurodegeneration as indicated by previous studies (Bizovičar et al., 2013, Thorns et al., 2010, Westphal et al., 1998, Proudfoot et al., 2017).

9.1.2.4 Motor execution networks are impaired in ALS

We studied motor execution networks in ALS using four different EEG measures, namely ERD and functional connectivity in sensor space and corticomuscular coherence and effective connectivity in source space. The CMC patterns in ALS are summarised in the next section.

We reported higher ERSP (reduced beta ERD) in ipsilateral M1 during motor task execution in ALS patients compared to controls. We have also shown that beta ERSP increases (ERD decreases) over the contralateral superior parietal region (SPL). We showed increased functional coupling between M1-SPL in the beta-band which was negatively correlated with ALSFRS-R scores (i.e., higher contralateral M1-SPL coupling for more severe ALS patients). These observations reflect a compensatory role of the non-dominant motor region (Konrad et al., 2002, Schoenfeld et al., 2005, Bede et al., 2021) and non-motor regions (parietal cortex) in ALS to overcome the motor control dysfunction due to neurodegeneration in the dominant motor region (Poujois et al., 2013, Zhou et al., 2013, Lulé et al., 2007).

A potential compensatory mechanism in ALS during motor execution was also observed in our source level study of effective connectivity. We reported stronger effective connectivity from ipsilateral SMA to contralateral M1 and higher signal inflow towards contralateral M1 in the beta-band in ALS patients compared to controls. We have also reported stronger contralateral S1→SMA effective connectivity and higher causal inflow towards contralateral SMA in the α band for more functionally impaired ALS participants. These findings indicate that neurodegeneration in ALS causes a higher demand on the motor system and the motor systems in ALS respond to higher motor demand by enhancing information flow between contralateral primary sensorimotor regions (M1/S1) and bilateral SMA even if the movements are unimanual (Gerloff et al., 1998).

9.2 Advantages of electrophysiological measures to quantify network impairments in ALS

9.2.1 Measuring non-structural network reorganisation

In the presence of neurodegeneration causing structural network atrophy in ALS, non-structural (functional or effective) network reorganisation occurs to compensate for the

structural network degeneration especially in pre-symptomatic or early symptomatic phases of the disease (Bede et al., 2021, Abidi et al., 2020, Konrad et al., 2002, Inuggi et al., 2011). For example, the involvement of cortical regions such as the premotor cortex and SMA, which are largely associated with movement preparation and planning (Churchland et al., 2006, Li et al., 2015, Shibasaki and Hallett, 2006, Glover et al., 2012), during movement execution underlines an alternative strategy for optimizing motor performance in ALS (Konrad et al., 2002). Our study showed similar compensatory mechanisms in ALS i.e., during the performance of a voluntary task, the information flow from ipsilateral SMA to contralateral M1 in the beta band was significantly stronger in ALS patients compared to controls. Another observation of effective network reorganisation in ALS during motor execution was the increased information flow (incoming links or inflow) towards contralateral M1 in the beta band. This suggests that M1 receives effective signal overloading from neighbouring motor and non-motor regions during task execution to compensate for structural atrophy caused by neurodegeneration. We have also found changes in long range fronto-parietal effective connectivity in ALS patients during task execution. The weak contralaterally driven fronto-parietal network (contralateral superior parietal to contralateral prefrontal) was accompanied by strong ipsilaterally driven fronto-parietal network (ipsilateral superior parietal to contralateral prefrontal). The involvement of the parietal region in compensatory mechanisms during motor execution was also observed in functional network analysis, where we found that the functional communication between contralateral M1 and the superior parietal lobule was significantly stronger in ALS. This functional network connectivity strength was more in ALS with higher clinical impairments. This highlights the utility of EEG for detecting non-structural network reorganisation in the presence of structural network atrophy.

9.2.2 Sensor vs source EEG measures

We have used both sensor and source space EEG to study the abnormal brain networks in ALS. The spatial resolution of sensor space EEG is poor because scalp sensors record electrical activity from adjacent and distant cortical and sub-cortical sources, referred to as volume conduction, that affects the coherence analysis causing spurious connectivity (Nunez et al., 1997). However, sensor space analysis is a popular way of analysing M/EEG data because of its convenience (Schaworonkow and Nikulin, 2022). First, we used spatial filtering (surface Laplacian) during sensor space analysis to minimize the effect of volume conduction and improve the spatial resolution of EEG (Bradshaw and Wikswo, 2001). Additionally, we used spatial median based non-parametric rank statistics (Nasseroleslami et al., 2019) to estimate the banded coherence, which is more robust against EEG artefacts (Dukic et al., 2017) and provided more localized coherence measures compared to classical magnitude squared coherence (see chapter 5 for details). Prior research has demonstrated a correlation between network measures derived from EEG sensor space analysis with reduced spurious connectivity and EEG source space analysis (Lai et al., 2018).

In comparison to sensor space EEG measures, source space EEG measures offer higher spatial resolution and reconstruct the true neural sources despite volume conduction, offering a more accurate representation of the underlying brain activity. However, source reconstruction requires head models acquired from individual MRI or template MRI and computationally extensive and complicated inverse modelling. Therefore, to perform source space analysis, one might need special data analysis training and skill sets. In this study we have used source space analysis to investigate functional corticomuscular and effective corticocortical networks during task execution. With sensor space corticomuscular coherence, such as our study in Chapter 5, we must rely on the electrode

position on the scalp to interpret the results. For example, the C3 electrode is usually considered to cover the left primary sensorimotor cortex. Using source space analysis, such as our studies in chapter 7 and 8, we have identified the exact cortical regions that are involved in pathological or compensatory networks in ALS.

9.2.3 Functional vs effectivity connectivity measures

We have used both functional and effective connectivity measures to investigate the network impairments in ALS, each having their own advantages. The functional connectivity measures were based on banded coherence and effective connectivity measures were based on partial directed coherence. Functional connectivity gives a measure of co-activation patterns of brain regions, whereas effective connectivity untangles the directional influence of one brain region to another. Therefore, they can provide answers to different questions. For example, we reported an overall increase of functional coupling between brain regions in ALS during motor execution which could be the result of cortical hyperexcitability (Menon et al., 2015, Vucic et al., 2011). But using effective connectivity we found an increased signal flow towards contralateral M1 from other neighbouring cortical regions during motor execution in ALS suggesting compensatory behaviour of less degenerated cortical regions surrounding severely degenerated motor cortex. This corroborates the fact that neurodegeneration in ALS starts at the motor cortex and progressively spreads outward to non-motor regions (Brettschneider et al., 2013). Additionally, functional connectivity measures captured abnormal connectivity (significantly stronger or weaker compared to controls), such as M1-S1 at rest and M1-SPL during motor execution, that were also significantly correlated with ALSFRS-R scores. Effective connectivity, on the other hand, did not show any overlap between the networks that were significantly different from controls and networks that were correlated to clinical

measures. Therefore, the use of functional and effective connectivity measures in our study elucidated different aspects of network impairments in ALS.

9.2.4 Experimental design and its effect on neurophysiological measures

9.2.4.1 Choice of motor task

We have chosen isometric pincer grip motor task at 10% of MVC for comparison of neurophysiological measures between ALS patients and healthy controls. The choice of the task was based on our previous studies on PPS (Coffey et al., 2021) and PLS (Bista et al., 2023) where we have shown that the task can successfully identify the abnormal corticospinal neural circuitry (increased functional connectivity between cortex and muscles in patient group compared to controls) affected by LMN or UMN degeneration. Furthermore, our preliminary study of two motor tasks, isometric pincer grip at 10 % MVC (force control task) and isometric precision grip (position control task), has demonstrated that the isometric pincer grip task at 10% MVC elicited lower level of beta CMC compared to precision grip task in healthy controls, and therefore, was more sensitive to detect abnormal CMC (increased CMC in patient group compared to controls) in patient groups.

9.2.4.1 Right hand standardisation for motor task

Previous studies using similar motor paradigm have used dominant hand to perform the task, and later flipped the neurophysiological measures for group analysis (Rossiter et al., 2013). For example, beta CMC between right M1 and left-hand muscle for the left-handed participant was considered equivalent to beta CMC between left M1 and right-hand muscle for the right-handed participant during group averaging. Handedness can influence brain organisation (Amunts et al., 1996) and function (Lajtos et al., 2023), with differences observed between left-handed and right-handed individuals. Furthermore, it is important to consider that neural activity in the dominant hemisphere may not always be mirrored

between left- and right-handed individuals, especially in patient groups affected by neurodegeneration and this could ultimately introduce variability in the group results. Therefore, in this thesis, we have standardised right hand, irrespective of the handedness of the participant, to perform the motor task which make our results more consistent across the groups and robust against the potential interference of individual differences in brain lateralisation. We have shown the box plot overlayed by scatter plot of connectivity measures using different colour (purple for ALS and yellow for controls) for left-handed participants (chapter 7 and chapter 8), which indicated that those measures were not the outliers (i.e., within the standard deviation from the mean).

9.3 Impact and future clinical applications

The significance of this project to the understanding of normal and ALS-related network (dys)functioning and the potential applications of the findings of this project to the medical field and further research are summarised in this section.

9.3.1 Spatial median based spectral coherence is a state-of-the-art method for capturing disease specific functional network impairments in motor neurone disease

We have previously proposed a median-based rank statistic for functional connectivity (coherence) (Nasseroleslami et al., 2019) that harnesses the robustness of non-parametric methods (Dukic et al., 2017). We have used the method previously to report abnormal functional connectivity between EEG and EMG (corticomuscular coherence) in people with LMN involvement such as post-polio syndrome (PPS) (Coffey et al., 2021). Here, we have used the method to report abnormal EEG-EMG networks in UMN degeneration such as PLS (see chapter 5), published in Cerebral Cortex (Bista et al., 2023), which established the novelty of the method to capture functional network impairments in people with MND. Therefore, we have extended the use of the method to investigate sensor level EEG-EEG

functional networks (see chapter 6) and source level EEG-EMG functional networks (see chapter 7) in ALS. Studies investigating functional connectivity in health and in disease using coherence usually rely on the maximum value (Aikio et al., 2021) or the area (under the significant coherence spectra) (Tun et al., 2021) to represent the collective connectivity strength with a single value over the range of frequencies within each distinct neurophysiological frequency band. We, on the other hand, used the 2D spatial median (real and imaginary part of normalised cross-spectra as separate dimensions) which provides a balance between overestimating the connectivity using measures such as maximum value or underestimating it, using the area under the significant coherence spectra. More importantly, the new method presents connectivity strengths as p-values so there is no need for separate significance testing such as close form solution or non-parametric bootstrapping as required by other existing connectivity measures. Additionally, this method is robust against the bias introduced by the number of epochs (L) used to estimate functional connectivity (Nasseroleslami et al., 2019). Hence, our method of estimating functional connectivity provides a more powerful detection of network connectivity with a singular value for a frequency band and can identify abnormal network connections in MND or any in other patient group for that matter.

9.3.2 Corticomuscular coherence as a therapeutic outcome measure in MND

In MND, the neurodegeneration disrupts the communication between the brain and muscles, resulting in motor impairments. Those abnormal brain muscles communications can be quantified using Corticomuscular coherence (CMC). We have shown indirectly, using sensor and source level study that PLS and ALS had distinct patterns of abnormal CMC. Specifically, a significant reduction in beta CMC between contralateral M1 and muscle was observed in ALS compared to controls whereas a significant increase in the

beta CMC between ipsilateral M1 and muscle and significant increase in the gamma band CMC between contralateral M1 and muscle was observed in PLS compared to controls. This difference in the pattern of CMC between ALS and PLS compared to controls should be further investigated by comparing these groups directly. Therefore, in future, monitoring changes in the beta/gamma CMC over time can provide insights into the efficacy of therapeutic interventions aimed at preserving or improving motor function. By investigating the magnitude and frequency of brain-muscle synchronization and by associating those measures with clinical motor assessments and behavioural performance of the task, we can track the effects of treatments (Salenius et al., 2002), rehabilitation programs (Delcamp et al., 2022), or assistive devices (Airaksinen et al., 2013). Positive changes in corticomuscular coherence patterns could indicate improved neural control and enhanced motor unit recruitment, reflecting potential therapeutic benefits as indicated by CMC studies in stroke (Krauth et al., 2019, Delcamp et al., 2022) and Parkinson's disease (Salenius et al., 2002, Airaksinen et al., 2013). Therefore, longitudinal studies utilizing corticomuscular coherence as an outcome measure has potential to a better understanding of the disease's progression and the impact of various interventions in MND.

9.3.3 Novel network biomarkers design

9.3.3.1 Diagnostic biomarker design

Studies have argued that the discriminatory power of a standalone experiment or modality is not sufficient to be used as a diagnostic tool for ALS in clinical settings (Huynh et al., 2016). Combining quantitative EEG features from different analyses has previously been shown to be useful for classifying various neurodegenerative diseases (Garn et al., 2017). Similarly, combining quantitative EEG and neuropsychology was recommended for differential diagnosis of Frontotemporal dementia and Alzheimer's disease (Lindau et al.,

2003). We recommend combining functional network impairment measures from multistate experimental paradigm such as resting state, pre-motor stage, and motor execution to design diagnostic biomarkers for ALS because our results have shown that features from different experiments contribute differently for the classification of ALS patients from healthy controls. Furthermore, the inclusion of pre-motor network impairments could be the key to designing quantitative neurophysiological biomarkers of network disruption because, as we have shown, pre-motor activity grabs a fundamentally different type of motor network impairments than motor execution and rest and has the highest contribution for classifying ALS patients from healthy controls. Thus, by training machine learning algorithms with the multistate network abnormalities from large ALS and control datasets, our findings support that this may lead to a novel diagnostic tool that could accurately classify ALS patients from healthy controls.

9.3.3.2 Prognostic biomarker design

Our study has demonstrated abnormal involvement of higher order motor regions such as the SMA and S1 in effective motor networks in ALS. We identified a stronger information flow from S1 to SMA on the contralateral side of the contracted muscle (i.e., S1→SMA effective connectivity) and higher causal inflow toward the contralateral SMA in the alpha band in ALS participants with more severe motor impairment as assessed by the ALSFRS-R motor sub-score. This suggests enhanced sensorimotor integration was facilitated by the SMA in more severe ALS because the alpha oscillations are involved in sensorimotor integration processes, helping to coordinate sensory feedback with motor commands which is crucial for accurate and efficient motor control. Additionally, we found a positive correlation between the strength of interhemispheric somatosensory effective connectivity (from ipsilateral S1 to contralateral S1) and motor impairment in ALS. Specifically, for

more severe motor deficits, the strength of this interhemispheric somatosensory connectivity (iS1→cS1) was notably diminished. A similar neurological pattern has been previously reported in stroke, which also manifests motor impairments. After a stroke, reduced interhemispheric S1-S1 functional connectivity has been identified, exhibiting a correlation with the extent of motor impairment. Even though these effective connections were not significantly different between ALS patients and healthy controls, they are still clinically relevant as a biomarker as they satisfy one property of a biomarker (correlates with clinical scores) and could be combined with other biomarkers for a complete biomarker design. Furthermore, these connectivity measures could provide high sensitivity and specificity compared to the clinical motor assessments such as ALSFRS-R scores. The clinical scores are known to have low sensitivity and specificity and are affected by multidimensionality problems. It requires trained personnel to perform clinical motor assessment, and this might introduce inter-assessor variability in the scores. Therefore, the assessment of two effective connections, namely contralateral S1→SMA and ipsilateral to contralateral S1→S1, that showed positive and negative correlations with motor impairments holds promise for quantifying disease severity and acting as markers for tracking disease progression.

9.3.3.3 Phenotyping biomarker design

We have shown that corticomuscular coherence (CMC) can capture disease specific functional network reorganisation in UMN/LMN involvement. For example, we have previously shown that CMC between muscles and frontal and parietal cortical regions in the gamma band is significantly higher in people with post-polio syndrome which is a LMN disorder (Coffey et al., 2021). In this study, we have shown that CMC between FDI muscle and contralateral M1 in the gamma band and between FDI muscle and ipsilateral M1 in the

beta band are significantly higher in people with PLS which is a UMN disorder (Bista et al., 2023). Similarly, in case of ALS, which entails both UMN and LMN involvement, we have shown that CMC is significantly reduced between contralateral M1 and FDI muscle in the beta band and between contralateral M1 and APB muscle in the gamma band. This indicates that CMC captures three network patterns related to the LMN/UMN involvement, 1. the brain regions involved in network reorganisation, 2. the oscillatory coupling behaviour of those brain regions, and 3. the direction (increase or decrease compared to healthy controls) of functional coupling between brain and muscles. From this indirect comparison, we can argue that the CMC has the potential to segregate people with MND based on LMN/UMN involvement, thus making it a novel candidate for sub-phenotyping motor phenotypes of ALS. However, a direct comparison is needed to validate this argument.

9.4 Limitations

In this section, general limitations which influenced the design of this project or limited the analyses/interpretation of results within this project are discussed along with some measures used to minimize the effects of those limitations.

9.4.1 Participant recruitment and small sample size

The rapid rate of ALS progression and low prevalence of the disease posed a recruitment challenge for this research. The participants needed to attend the data recording session in-person in the hospital setting which limited some people with ALS to participate in the research. For example, some ALS participants had severe decline in motor functions and were unable to use a wheelchair to access the research facility or did not have someone available who could transport them. Additionally, participants were required to have sufficient motor function for the motor tasks. Recruitment was further constrained by the

exclusion criteria of the studies. Participants were excluded if they had co-morbid neuromuscular or psychiatric conditions that could affect the electrophysiological measurements being studied, a common exclusion criterion in this type of research. Some participants were also excluded due to the use of specific medications that affect the central nervous system. Furthermore, the study had a smaller sample size because the participant recruitment and data recording were affected by the Covid-19 pandemic. To take the small sample size into account, we have used non-parametric methods such as rank statistics, bootstrapping etc (Nasseroleslami, 2019, Nasseroleslami et al., 2019) and probabilistic methods such as Empirical Bayesian Inference (Nasseroleslami, 2019) to report the statistical significance and power. Additionally, we have reported effect size and confidence intervals of the network measures along with p-values to highlight that our findings are actual effects rather than some statistical noise.

9.4.2 Exclusion of deeper brain sources

We have used high density EEG (128-channels) to record the brain activity and used the AAL atlas for source reconstruction which allows estimating EEG source activity from 90 brain regions that include cortical, sub-cortical and deeper brain sources. However, for our sensor level study, we have preselected up to 8 channels and for our source level study we have preselected up to 12 cortical brain regions. The channel/source preselection was based on brain regions reported to be activated during voluntary motor control. This has restricted our analysis to frontal, central and parietal cortical regions only, limiting the investigation of temporal, sub-cortical and deeper brain sources which have been shown to have significant effects in network pathophysiology of ALS (Abidi et al., 2020, Dukic et al., 2021).

9.5 Future Work

9.5.1 Continuation of data collection

The EEG/EMG data collection will be continued in the future to make sure we have a reasonable sample size that can provide sufficient power to the analysis. Additionally, longitudinal EEG/EMG data for multiple timepoints (with no fixed interval between the timepoints but separated at least by 3 months) will be collected in the future.

9.5.2 Whole brain network analysis

This work is based on preselection of EEG channels and brain sources which is one of its limitations. In future we will be looking into the whole brain network, including sub-cortical and deeper cortical sources, which will provide more robust evidence of multi-network dysfunction in ALS and the role of deeper brain sources for compensating for abnormal motor networks in ALS.

9.5.3 Direct comparison of CMC between different patient groups

We have indirectly compared the CMC patterns of ALS and PLS with reference to the controls which has provided us new insights about the potential of CMC to capture disease specific functional network impairments. Therefore, in the future we will be comparing different patient groups such as ALS, PLS, and PPS directly using CMC to identify neurophysiological markers that can be used for differential diagnosis.

9.5.4 Directional CMC analysis

Using undirected CMC, we have indirectly identified disease specific functional network dysfunction and reorganisation. However, the CMC based on coherence quantifies the combined effect of efferent motor and afferent sensory pathways in motor control (Witham et al., 2011). In the future, we will be using directional CMC to untangle the contribution of ascending afferent and descending efferent pathways in sensorimotor networks during

different types (force control, position control) and phases (sustained, transient) of motor tasks in healthy people and people with MND. This will help us to understand effects of neurodegeneration on different corticospinal pathways.

9.5.5 Clustering

ALS is a heterogenous disease with motor and non-motor symptoms found to varying degrees within each individual. The resting-state EEG measures have previously identified four sub-phenotypes of ALS using clustering; each sub-phenotype showing distinct network patterns that correlated with clinical measures (Dukic et al., 2021). Furthermore, here we have indirectly shown that CMC during voluntary task execution can capture UMN/LMN specific impairments. Therefore, a combination of network measures during rest and task, which we have identified here, that collectively capture motor, sensory, cognitive, behavioural, and language impairment in ALS could potentially establish a foundation for objectively grouping people with ALS into network-based sub-phenotypes using clustering analyses. These clusters will then be compared to existing criteria for categorizing ALS such as site of symptom onset, degree of UMN/LMN involvement, genetic factor etc to assess their utility in clinical practice for improving ALS prognoses.

9.5.6 Longitudinal analysis

As evidenced by a previous longitudinal study during rest, tracking spectral EEG measures over time offers valuable understanding of the dynamics of network dysfunction in ALS and its associations to disease progression (Nasseroleslami et al., 2017). To enhance the insights from the cross-sectional task based functional and effective connectivity analyses presented here, further investigations are necessary to ascertain whether the network pathophysiology remains consistent or is linked to a particular stage of ALS progression. Longitudinal data collection has been less prioritised but an ongoing aspect of this project.

To date, we have collected 2-time points data from five and a 3rd time point data from one ALS participant. In the future, we will prioritise the longitudinal data collection and subsequent analysis based on the foundation of this study.

9.6 Conclusion

Neurodegeneration in ALS begins in the pyramidal motor system (Brettschneider et al., 2013) causing motor impairments which overtime spread to neighbouring cortical regions by diffusion or to distant cerebral cites mediated by axonal projections. This spreading pathology causes several non-motor impairments such as cognitive and behavioural impairments in ALS (Grossman, 2019). A clear understanding of the multisystem nature of ALS in terms of a network disorder and its association with clinically assessed measures will be vital for improved diagnosis, prognosis, and disease management. However, for early diagnosis, understanding and unravelling the early neurophysiological signatures of pathological changes in motor system is important because motor signs and symptoms appear earliest at the disease onset with various phenotypical heterogeneity, focality, and spread (Ravits and La Spada, 2009). We used voluntary movement related experimental paradigm that can directly access the motor networks in ALS. We have shown that the cortico-cortical and corticospinal motor networks during voluntary movement are impaired in ALS and show associations with clinical measure of functional impairment in ALS such as ALSFRS-R scores. The network impairments underpinned by this study, if further validated by similar studies in a large cohort of patient groups and longitudinal studies, have potential to be candidate biomarkers for clinical diagnostic, prognostic and phenotyping applications or as primary/secondary outcome measure to track network changes in the setting of disease modifying clinical trials.

References

ABIDI, M., DE MARCO, G., COUILLANDRE, A., FERON, M., MSEDDI, E., TERMOZ, N., QUERIN, G., PRADAT, P.-F. & BEDE, P. 2020. Adaptive functional reorganization in amyotrophic lateral sclerosis: coexisting degenerative and compensatory changes. *European Journal of Neurology,* 27**,** 121-128.

ABRAHAMS, S., NEWTON, J., NIVEN, E., FOLEY, J. & BAK, T. H. 2014. Screening for cognition and behaviour changes in ALS. *Amyotroph Lateral Scler Frontotemporal Degener,* 15**,** 9-14.

ACHARD, S., SALVADOR, R., WHITCHER, B., SUCKLING, J. & BULLMORE, E. 2006. A resilient, low-frequency, small-world human brain functional network with highly connected association cortical hubs. *J Neurosci,* 26**,** 63-72.

ACOSTA-CABRONERO, J., WILLIAMS, G. B., PENGAS, G. & NESTOR, P. J. 2010. Absolute diffusivities define the landscape of white matter degeneration in Alzheimer's disease. *Brain,* 133**,** 529-39.

AGARWAL, S., HIGHTON-WILLIAMSON, E., CAGA, J., MATAMALA, J. M., DHARMADASA, T., HOWELLS, J., ZOING, M. C., SHIBUYA, K., GEEVASINGA, N. & VUCIC, S. 2018. Primary lateral sclerosis and the amyotrophic lateral sclerosis–frontotemporal dementia spectrum. *Journal of neurology,* 265**,** 1819-1828.

AGOSTA, F., ALTOMARE, D., FESTARI, C., ORINI, S., GANDOLFO, F., BOCCARDI, M., ARBIZU, J., BOUWMAN, F., DRZEZGA, A., NESTOR, P., NOBILI, F., WALKER, Z. & PAGANI, M. 2018. Clinical utility of FDG-PET in amyotrophic lateral sclerosis and Huntington's disease. *Eur J Nucl Med Mol Imaging,* 45**,** 1546-1556.

AGOSTA, F., FERRARO, P. M., RIVA, N., SPINELLI, E. G., CHIÒ, A., CANU, E., VALSASINA, P., LUNETTA, C., IANNACCONE, S., COPETTI, M., PRUDENTE, E., COMI, G., FALINI, A. & FILIPPI, M. 2016. Structural brain correlates of cognitive and behavioral impairment in MND. *Human Brain Mapping,* 37**,** 1614-1626.

AGOSTA, F., FERRARO, P. M., RIVA, N., SPINELLI, E. G., DOMI, T., CARRERA, P., COPETTI, M., FALZONE, Y., FERRARI, M., LUNETTA, C., COMI, G., FALINI, A., QUATTRINI, A. & FILIPPI, M. 2017. Structural and functional brain signatures of C9orf72 in motor neuron disease. *Neurobiology of Aging,* 57**,** 206-219.

AGOSTA, F., PAGANI, E., PETROLINI, M., SORMANI, M. P., CAPUTO, D., PERINI, M., PRELLE, A., SALVI, F. & FILIPPI, M. 2010a. MRI predictors of long-term evolution in amyotrophic lateral sclerosis. *Eur J Neurosci,* 32**,** 1490-6.

AGOSTA, F., ROCCA, M. A., PAGANI, E., ABSINTA, M., MAGNANI, G., MARCONE, A., FALAUTANO, M., COMI, G., GORNO-TEMPINI, M. L. & FILIPPI, M. 2010b. Sensorimotor network rewiring in mild cognitive impairment and Alzheimer's disease. *Human brain mapping,* 31**,** 515-525.

AGOSTA, F., SALA, S., VALSASINA, P., MEANI, A., CANU, E., MAGNANI, G., CAPPA, S. F., SCOLA, E., QUATTO, P., HORSFIELD, M. A., FALINI, A., COMI, G. & FILIPPI, M. 2013. Brain network connectivity assessed using graph theory in frontotemporal dementia. *Neurology,* 81**,** 134-43.

AGOSTA, F., VALSASINA, P., ABSINTA, M., RIVA, N., SALA, S., PRELLE, A., COPETTI, M., COMOLA, M., COMI, G. & FILIPPI, M. 2011. Sensorimotor Functional Connectivity Changes in Amyotrophic Lateral Sclerosis. *Cerebral Cortex,* 21**,** 2291-2298.

AGOSTA, F., VALSASINA, P., RIVA, N., COPETTI, M., MESSINA, M. J., PRELLE, A., COMI, G. & FILIPPI, M. 2012. The cortical signature of amyotrophic lateral sclerosis. *PLoS One,* 7**,** e42816.

AHMADI, H., FATEMIZADEH, E. & MOTIE-NASRABADI, A. 2023. A Comparative Study of Correlation Methods in Functional Connectivity Analysis Using fMRI Data of Alzheimer's Patients. *J Biomed Phys Eng,* 13**,** 125-134.

AHMED, N., BAKER, M. R. & BASHFORD, J. 2022. The landscape of neurophysiological outcome measures in ALS interventional trials: A systematic review. *Clinical Neurophysiology,* 137**,** 132-141.

AIKIO, R., LAAKSONEN, K., SAIRANEN, V., PARKKONEN, E., ABOU ELSEOUD, A., KUJALA, J. & FORSS, N. 2021. CMC is more than a measure of corticospinal tract integrity in acute stroke patients. *NeuroImage: Clinical,* 32**,** 102818.

AIRAKSINEN, K., MÄKELÄ, J., NURMINEN, J., LUOMA, J., TAULU, S., AHONEN, A. & PEKKONEN, E. 2013. The effect of DBS on cortico-muscular coherence in advanced Parkinson's disease. *Journal of the Neurological Sciences,* 333**,** e107.

AL-CHALABI, A., HARDIMAN, O., KIERNAN, M. C., CHIÒ, A., RIX-BROOKS, B. & VAN DEN BERG, L. H. 2016. Amyotrophic lateral sclerosis: moving towards a new classification system. *The Lancet Neurology,* 15**,** 1182-1194.

ALAHMADI, A. A. S., PARDINI, M., SAMSON, R. S., D'ANGELO, E., FRISTON, K. J., TOOSY, A. T. & GANDINI WHEELER-KINGSHOTT, C. A. M. 2015.

Differential involvement of cortical and cerebellar areas using dominant and nondominant hands: An FMRI study. *Human brain mapping,* 36**,** 5079-5100.

ALEGRE, M., ALONSO-FRECH, F., RODRÍGUEZ-OROZ, M. C., GURIDI, J., ZAMARBIDE, I., VALENCIA, M., MANRIQUE, M., OBESO, J. A. & ARTIEDA, J. 2005. Movement-related changes in oscillatory activity in the human subthalamic nucleus: ipsilateral vs. contralateral movements. *European Journal of Neuroscience,* 22**,** 2315-2324.

ALGAHTANI, H., SHIRAH, B., ALGAHTANI, S., ATTAR, A. & ABUZINADAH, A. R. 2021. Mills' syndrome: Reporting the disease course with a monthly intravenous immunoglobulin program. *Journal of Neuroimmunology,* 355**,** 577562.

ÁLVAREZ, N., DÍEZ, L., AVELLANEDA, C., SERRA, M. & RUBIO, M. 2018. Relevance of the pyramidal syndrome in amyotrophic lateral sclerosis. *Neurologia (Engl Ed),* 33**,** 8-12.

AMJAD, A. M., HALLIDAY, D. M., ROSENBERG, J. R. & CONWAY, B. A. 1997. An extended difference of coherence test for comparing and combining several independent coherence estimates: theory and application to the study of motor units and physiological tremor. *Journal of Neuroscience Methods,* 73**,** 69-79.

AMUNTS, K., SCHLAUG, G., SCHLEICHER, A., STEINMETZ, H., DABRINGHAUS, A., ROLAND, P. E. & ZILLES, K. 1996. Asymmetry in the human motor cortex and handedness. *Neuroimage,* 4**,** 216-22.

ANDICA, C., KAMAGATA, K., HATANO, T., SAITO, Y., OGAKI, K., HATTORI, N. & AOKI, S. 2020. MR Biomarkers of Degenerative Brain Disorders Derived From Diffusion Imaging. *Journal of Magnetic Resonance Imaging,* 52**,** 1620-1636.

ANDRYKIEWICZ, A., PATINO, L., NARANJO, J. R., WITTE, M., HEPP-REYMOND, M. C. & KRISTEVA, R. 2007. Corticomuscular synchronization with small and large dynamic force output. *BMC Neurosci,* 8**,** 101.

ANWAR, A. R., MUTHALIB, M., PERREY, S., GALKA, A., GRANERT, O., WOLFF, S., HEUTE, U., DEUSCHL, G., RAETHJEN, J. & MUTHURAMAN, M. 2016. Effective Connectivity of Cortical Sensorimotor Networks During Finger Movement Tasks: A Simultaneous fNIRS, fMRI, EEG Study. *Brain Topography,* 29**,** 645-660.

ARIANI, G. & DIEDRICHSEN, J. 2019. Sequence learning is driven by improvements in motor planning. *Journal of Neurophysiology,* 121**,** 2088-2100.

ARIANI, G., PRUSZYNSKI, J. A. & DIEDRICHSEN, J. 2022. Motor planning brings human primary somatosensory cortex into action-specific preparatory states. *eLife,* 11**,** e69517.

ARIANI, G., WURM, M. F. & LINGNAU, A. 2015. Decoding Internally and Externally Driven Movement Plans. *The Journal of Neuroscience,* 35**,** 14160-14171.

ARUN, K. M., SMITHA, K. A., SYLAJA, P. N. & KESAVADAS, C. 2020. Identifying Resting-State Functional Connectivity Changes in the Motor Cortex Using fNIRS During Recovery from Stroke. *Brain Topogr,* 33**,** 710-719.

ATASSI, N., XU, M., TRIANTAFYLLOU, C., KEIL, B., LAWSON, R., CERNASOV, P., RATTI, E., LONG, C. J., PAGANONI, S., MURPHY, A., SALIBI, N., SEETHAMRAJU, R., ROSEN, B. & RATAI, E.-M. 2017. Ultra high-field (7tesla) magnetic resonance spectroscopy in Amyotrophic Lateral Sclerosis. *PLOS ONE,* 12**,** e0177680.

AVYARTHANA, D., COLLIN, C. L., ABDULLAH, I., DANIEL, T., OJAS, S., DENNELL, K., PETER, S., CHRIS, H., CHRISTIAN, B., LAWRENCE, K., RICHARD, F., LORNE, Z., SIMON, G., ANGELA, G., HANNAH, B. & SANJAY, K. 2023. Motor cortex functional connectivity is associated with underlying neurochemistry in ALS. *Journal of Neurology, Neurosurgery & Psychiatry,* 94**,** 193.

BABAEEGHAZVINI, P., RUEDA-DELGADO, L. M., GOOIJERS, J., SWINNEN, S. P. & DAFFERTSHOFER, A. 2021. Brain Structural and Functional Connectivity: A Review of Combined Works of Diffusion Magnetic Resonance Imaging and Electro-Encephalography. *Frontiers in Human Neuroscience,* 15.

BACCALÁ, L. A. & SAMESHIMA, K. 2001. Partial directed coherence: a new concept in neural structure determination. *Biological Cybernetics,* 84**,** 463-474.

BACCALÁ, L. A. & SAMESHIMA, K. 2021. Partial directed coherence: twenty years on some history and an appraisal. *Biological Cybernetics,* 115**,** 195-204.

BACCALA, L. A., SAMESHIMA, K. & TAKAHASHI, D. Y. Generalized Partial Directed Coherence. 2007 15th International Conference on Digital Signal Processing, 1-4 July 2007 2007. 163-166.

BAEK, S. H., PARK, J., KIM, Y. H., SEOK, H. Y., OH, K. W., KIM, H. J., KWON, Y. J., SIM, Y., TAE, W. S., KIM, S. H. & KIM, B. J. 2020. Usefulness of diffusion tensor imaging findings as biomarkers for amyotrophic lateral sclerosis. *Sci Rep,* 10**,** 5199.

BAGGIO, H. C., SALA-LLONCH, R., SEGURA, B., MARTI, M. J., VALLDEORIOLA, F., COMPTA, Y., TOLOSA, E. & JUNQUÉ, C. 2014. Functional brain networks and cognitive deficits in Parkinson's disease. *Hum Brain Mapp,* 35**,** 4620-34.

BAKER, K. S., MATTINGLEY, J. B., CHAMBERS, C. D. & CUNNINGTON, R. 2011. Attention and the readiness for action. *Neuropsychologia,* 49**,** 3303-3313.

BALL, T., SCHREIBER, A., FEIGE, B., WAGNER, M., LÜCKING, C. H. & KRISTEVA-FEIGE, R. 1999. The role of higher-order motor areas in voluntary movement as revealed by high-resolution EEG and fMRI. *Neuroimage,* 10**,** 682-94.

BARDEL, B., CHALAH, M. A., CRÉANGE, A., LEFAUCHEUR, J.-P. & AYACHE, S. S. 2022. Motor preparation impairment in multiple sclerosis: Evidence from the Bereitschaftspotential in simple and complex motor tasks. *Neurophysiologie Clinique,* 52**,** 137-146.

BARRY, R. L., BABU, S., ANTERAPER, S. A., TRIANTAFYLLOU, C., KEIL, B., ROWE, O. E., RANGAPRAKASH, D., PAGANONI, S., LAWSON, R., DHEEL, C., CERNASOV, P. M., ROSEN, B. R., RATAI, E. M. & ATASSI, N. 2021. Ultra-high field (7T) functional magnetic resonance imaging in amyotrophic lateral sclerosis: a pilot study. *Neuroimage Clin,* 30**,** 102648.

BASAIA, S., AGOSTA, F., CIVIDINI, C., TROJSI, F., RIVA, N., SPINELLI, E. G., MOGLIA, C., FEMIANO, C., CASTELNOVO, V., CANU, E., FALZONE, Y., MONSURRÒ, M. R., FALINI, A., CHIÒ, A., TEDESCHI, G. & FILIPPI, M. 2020. Structural and functional brain connectome in motor neuron diseases: A multicenter MRI study. *Neurology,* 95**,** e2552-e2564.

BEATY, R. E., BENEDEK, M., BARRY KAUFMAN, S. & SILVIA, P. J. 2015. Default and Executive Network Coupling Supports Creative Idea Production. *Scientific Reports,* 5**,** 10964.

BECKER, W. & KRISTEVA, R. 1980. Cerebral Potentials prior to various Force Deployments**This study was supported by the Deutsche Forschungsgemeinschaft, SFB 70, and by a fellowship of the Deutscher Akademischer Austauschdienst to the second author. *In:* KORNHUBEK, H. H. & DEECKE, L. (eds.) *Progress in Brain Research.* Elsevier.

BEDE, P., BOGDAHN, U., LOPE, J., CHANG, K. M., XIROU, S. & CHRISTIDI, F. 2021. Degenerative and regenerative processes in amyotrophic lateral sclerosis: motor reserve, adaptation and putative compensatory changes. *Neural Regeneration Research,* 16**,** 1208-1209.

BEDE, P., BOKDE, A., ELAMIN, M., BYRNE, S., MCLAUGHLIN, R. L., JORDAN, N., HAMPEL, H., GALLAGHER, L., LYNCH, C., FAGAN, A. J., PENDER, N. & HARDIMAN, O. 2013a. Grey matter correlates of clinical variables in amyotrophic lateral sclerosis (ALS): a neuroimaging study of ALS motor phenotype heterogeneity and cortical focality. *Journal of Neurology, Neurosurgery & Psychiatry,* 84**,** 766-773.

BEDE, P., BOKDE, A. L., BYRNE, S., ELAMIN, M., MCLAUGHLIN, R. L., KENNA, K., FAGAN, A. J., PENDER, N., BRADLEY, D. G. & HARDIMAN, O. 2013b.

Multiparametric MRI study of ALS stratified for the C9orf72 genotype. *Neurology,* 81**,** 361-9.

BEDE, P., MURAD, A. & HARDIMAN, O. 2022. Pathological neural networks and artificial neural networks in ALS: diagnostic classification based on pathognomonic neuroimaging features. *Journal of Neurology,* 269**,** 2440-2452.

BEELDMAN, E., GOVAARTS, R., DE VISSER, M., KLEIN TWENNAAR, M., VAN DER KOOI, A. J., VAN DEN BERG, L. H., VELDINK, J. H., PIJNENBURG, Y. A. L., DE HAAN, R. J., SCHMAND, B. A. & RAAPHORST, J. 2020. Progression of cognitive and behavioural impairment in early amyotrophic lateral sclerosis. *Journal of Neurology, Neurosurgery & Psychiatry,* 91**,** 779-780.

BEHLER, A., MÜLLER, H. P., LUDOLPH, A. C. & KASSUBEK, J. 2023. Diffusion Tensor Imaging in Amyotrophic Lateral Sclerosis: Machine Learning for Biomarker Development. *Int J Mol Sci,* 24.

BENDAT, J. S. & PIERSOL, A. G. 2011. *Random data: analysis and measurement procedures,* John Wiley & Sons.

BENJAMINI, Y. & HOCHBERG, Y. 1995. Controlling the false discovery rate: a practical and powerful approach to multiple testing. *Journal of the Royal statistical society: series B (Methodological),* 57**,** 289-300.

BENJAMINI, Y. & HOCHBERG, Y. 2000. On the Adaptive Control of the False Discovery Rate in Multiple Testing With Independent Statistics. *Journal of Educational and Behavioral Statistics,* 25**,** 60-83.

BENJAMINI, Y., KRIEGER, A. M. & YEKUTIELI, D. 2006. Adaptive linear step-up procedures that control the false discovery rate. *Biometrika,* 93**,** 491-507.

BERGER, A. 2003. How does it work? Positron emission tomography. *Bmj,* 326**,** 1449.

BHARTI, K., S, J. G., BENATAR, M., BRIEMBERG, H., CHENJI, S., DUPRÉ, N., DIONNE, A., FRAYNE, R., GENGE, A., KORNGUT, L., LUK, C., ZINMAN, L. & KALRA, S. 2022. Functional alterations in large-scale resting-state networks of amyotrophic lateral sclerosis: A multi-site study across Canada and the United States. *PLoS One,* 17**,** e0269154.

BI, Y., YUAN, K., YU, D., WANG, R., LI, M., LI, Y., ZHAI, J., LIN, W. & TIAN, J. 2017. White matter integrity of central executive network correlates with enhanced brain reactivity to smoking cues. *Hum Brain Mapp,* 38**,** 6239-6249.

BISTA, S., COFFEY, A., FASANO, A., BUXO, T., MITCHELL, M., GIGLIA, E. R., DUKIC, S., HEVERIN, M., MUTHURAMAN, M., CARSON, R. G., LOWERY,

M., HARDIMAN, O., MCMANUS, L. & NASSEROLESLAMI, B. 2023. Cortico-muscular coherence in primary lateral sclerosis reveals abnormal cortical engagement during motor function beyond primary motor areas. *Cereb Cortex*.

BISWAL, B., ZERRIN YETKIN, F., HAUGHTON, V. M. & HYDE, J. S. 1995. Functional connectivity in the motor cortex of resting human brain using echo-planar mri. *Magnetic Resonance in Medicine,* 34**,** 537-541.

BIZOVICAR, N., DREO, J., KORITNIK, B. & ZIDAR, J. 2014. Decreased movement-related beta desynchronization and impaired post-movement beta rebound in amyotrophic lateral sclerosis. *Clin Neurophysiol,* 125**,** 1689-99.

BIZOVIČAR, N., KORITNIK, B., ZIDAR, I., DREO, J. & ZIDAR, J. 2013. Movement-related cortical potentials in ALS increase at lower and decrease at higher upper motor neuron burden scores. *Amyotroph Lateral Scler Frontotemporal Degener,* 14**,** 380-9.

BLAIN-MORAES, S., MASHOUR, G. A., LEE, H., HUGGINS, J. E. & LEE, U. 2013. Altered cortical communication in amyotrophic lateral sclerosis. *Neurosci Lett,* 543**,** 172-6.

BORGHEAI, S. B., DELIGANI, R. J., MCLINDEN, J., ZISK, A., HOSNI, S. I., ABTAHI, M., MANKODIYA, K. & SHAHRIARI, Y. 2019. Multimodal exploration of non-motor neural functions in ALS patients using simultaneous EEG-fNIRS recording. *J Neural Eng,* 16**,** 066036.

BORGHEAI, S. B., MCLINDEN, J., MANKODIYA, K. & SHAHRIARI, Y. 2020. Frontal Functional Network Disruption Associated with Amyotrophic Lateral Sclerosis: An fNIRS-Based Minimum Spanning Tree Analysis. *Frontiers in Neuroscience,* 14.

BOS, M. V. D., HOWELLS, J., HIGASHIHARA, M., GEEVASINGA, N., KIERNAN, M. & VUCIC, S. 2019. 018 Role of transcallosal inhibition in disease spread in ALS. *Journal of Neurology, Neurosurgery & Psychiatry,* 90**,** A7-A7.

BRADSHAW, L. A. & WIKSWO, J. P. 2001. Spatial Filter Approach for Evaluation of the Surface Laplacian of the Electroencephalogram and Magnetoencephalogram. *Annals of Biomedical Engineering,* 29**,** 202-213.

BRANCACCIO, A., TABARELLI, D. & BELARDINELLI, P. 2022. A new framework to interpret individual inter-hemispheric compensatory communication after stroke. *Journal of Personalized Medicine,* 12**,** 59.

BRESSLER, S. L. & MENON, V. 2010. Large-scale brain networks in cognition: emerging methods and principles. *Trends in Cognitive Sciences,* 14**,** 277-290.

BRETTSCHNEIDER, J., DEL TREDICI, K., TOLEDO, J. B., ROBINSON, J. L., IRWIN, D. J., GROSSMAN, M., SUH, E., VAN DEERLIN, V. M., WOOD, E. M., BAEK, Y., KWONG, L., LEE, E. B., ELMAN, L., MCCLUSKEY, L., FANG, L., FELDENGUT, S., LUDOLPH, A. C., LEE, V. M., BRAAK, H. & TROJANOWSKI, J. Q. 2013. Stages of pTDP-43 pathology in amyotrophic lateral sclerosis. *Ann Neurol,* 74**,** 20-38.

BROMBERG, M. B. & BROWNELL, A. A. 2008. Motor Unit Number Estimation in the Assessment of Performance and Function in Motor Neuron Disease. *Physical Medicine and Rehabilitation Clinics of North America,* 19**,** 509-532.

BROOKES, M. J., HALE, J. R., ZUMER, J. M., STEVENSON, C. M., FRANCIS, S. T., BARNES, G. R., OWEN, J. P., MORRIS, P. G. & NAGARAJAN, S. S. 2011. Measuring functional connectivity using MEG: methodology and comparison with fcMRI. *Neuroimage,* 56**,** 1082-104.

BROOKES, M. J., TEWARIE, P. K., HUNT, B. A. E., ROBSON, S. E., GASCOYNE, L. E., LIDDLE, E. B., LIDDLE, P. F. & MORRIS, P. G. 2016. A multi-layer network approach to MEG connectivity analysis. *NeuroImage,* 132**,** 425-438.

BROOKS, B. R. 1994. El escorial World Federation of Neurology criteria for the diagnosis of amyotrophic lateral sclerosis. *Journal of the Neurological Sciences,* 124**,** 96-107.

BROOKS, B. R., MILLER, R. G., SWASH, M. & MUNSAT, T. L. 2000. El Escorial revisited: Revised criteria for the diagnosis of amyotrophic lateral sclerosis. *Amyotrophic Lateral Sclerosis and Other Motor Neuron Disorders,* 1**,** 293-299.

BROVELLI, A., DING, M., LEDBERG, A., CHEN, Y., NAKAMURA, R. & BRESSLER, S. L. 2004. Beta oscillations in a large-scale sensorimotor cortical network: Directional influences revealed by Granger causality. *Proceedings of the National Academy of Sciences,* 101**,** 9849-9854.

BROWN, P., SALENIUS, S., ROTHWELL, J. C. & HARI, R. 1998. Cortical correlate of the Piper rhythm in humans. *J Neurophysiol,* 80**,** 2911-7.

BRUNS, A., ECKHORN, R., JOKEIT, H. & EBNER, A. 2000. Amplitude envelope correlation detects coupling among incoherent brain signals. *NeuroReport,* 11.

BUCHANAN, C. R., PETTIT, L. D., STORKEY, A. J., ABRAHAMS, S. & BASTIN, M. E. 2015. Reduced structural connectivity within a prefrontal-motor-subcortical network in amyotrophic lateral sclerosis. *Journal of Magnetic Resonance Imaging,* 41**,** 1342-1352.

BUDINI, F., MCMANUS, L. M., BERCHICCI, M., MENOTTI, F., MACALUSO, A., DI RUSSO, F., LOWERY, M. M. & DE VITO, G. 2014. Alpha Band Cortico-

Muscular Coherence Occurs in Healthy Individuals during Mechanically-Induced Tremor. *PLOS ONE,* 9**,** e115012.

BURGH, H. K. V. D., WESTENENG, H.-J., WALHOUT, R., VEENHUIJZEN, K. V., TAN, H. H. G., MEIER, J. M., BAKKER, L. A., HENDRIKSE, J., ES, M. A. V., VELDINK, J. H., HEUVEL, M. P. V. D. & BERG, L. H. V. D. 2020. Multimodal longitudinal study of structural brain involvement in amyotrophic lateral sclerosis. *Neurology,* 94**,** e2592-e2604.

BURLE, B., SPIESER, L., ROGER, C., CASINI, L., HASBROUCQ, T. & VIDAL, F. 2015. Spatial and temporal resolutions of EEG: Is it really black and white? A scalp current density view. *International Journal of Psychophysiology,* 97**,** 210-220.

CALDWELL, S. & ROTHMAN, D. L. 2021. 1H Magnetic Resonance Spectroscopy to Understand the Biological Basis of ALS, Diagnose Patients Earlier, and Monitor Disease Progression. *Frontiers in Neurology,* 12.

CALVERT, G. H. & CARSON, R. G. 2022. Neural mechanisms mediating cross education: With additional considerations for the ageing brain. *Neuroscience & Biobehavioral Reviews,* 132**,** 260-288.

CAO, J., ZHAO, Y., SHAN, X., WEI, H.-L., GUO, Y., CHEN, L., ERKOYUNCU, J. A. & SARRIGIANNIS, P. G. 2022. Brain functional and effective connectivity based on electroencephalography recordings: A review. *Human Brain Mapping,* 43**,** 860-879.

CASTELNOVO, V., CANU, E., CALDERARO, D., RIVA, N., POLETTI, B., BASAIA, S., SOLCA, F., SILANI, V., FILIPPI, M. & AGOSTA, F. 2020. Progression of brain functional connectivity and frontal cognitive dysfunction in ALS. *NeuroImage: Clinical,* 28**,** 102509.

CEDARBAUM, J. M., STAMBLER, N., MALTA, E., FULLER, C., HILT, D., THURMOND, B. & NAKANISHI, A. 1999. The ALSFRS-R: a revised ALS functional rating scale that incorporates assessments of respiratory function. *Journal of the Neurological Sciences,* 169**,** 13-21.

CHANG, F., LI, H., LI, N., ZHANG, S., LIU, C., ZHANG, Q. & CAI, W. 2022. Functional near-infrared spectroscopy as a potential objective evaluation technique in neurocognitive disorders after traumatic brain injury. *Frontiers in Psychiatry,* 13.

CHEAH, B. C., VUCIC, S., KRISHNAN, A. V., BOLAND, R. A. & KIERNAN, M. C. 2011. Neurophysiological index as a biomarker for ALS progression: Validity of mixed effects models. *Amyotrophic Lateral Sclerosis,* 12**,** 33-38.

CHEN, R., GERLOFF, C., HALLETT, M. & COHEN, L. G. 1997. Involvement of the ipsilateral motor cortex in finger movements of different complexities. *Annals of*

Neurology: Official Journal of the American Neurological Association and the Child Neurology Society, 41**,** 247-254.

CHEN, Z. Y., LIU, M. Q. & MA, L. 2018. Cortical Thinning Pattern of Bulbar- and Spinal-onset Amyotrophic Lateral Sclerosis: a Surface-based Morphometry Study. *Chin Med Sci J,* 33**,** 100-106.

CHEW, S. & ATASSI, N. 2019. Positron Emission Tomography Molecular Imaging Biomarkers for Amyotrophic Lateral Sclerosis. *Frontiers in Neurology,* 10.

CHIÒ, A., CALVO, A., MOGLIA, C., MAZZINI, L. & MORA, G. 2011. Phenotypic heterogeneity of amyotrophic lateral sclerosis: a population based study. *J Neurol Neurosurg Psychiatry,* 82**,** 740-6.

CHIÒ, A., HAMMOND, E. R., MORA, G., BONITO, V. & FILIPPINI, G. 2015. Development and evaluation of a clinical staging system for amyotrophic lateral sclerosis. *J Neurol Neurosurg Psychiatry,* 86**,** 38-44.

CHIÒ, A., MOGLIA, C., CANOSA, A., MANERA, U., D'OVIDIO, F., VASTA, R., GRASSANO, M., BRUNETTI, M., BARBERIS, M., CORRADO, L., D'ALFONSO, S., IAZZOLINO, B., PEOTTA, L., SARNELLI, M. F., SOLARA, V., ZUCCHETTI, J. P., DE MARCHI, F., MAZZINI, L., MORA, G. & CALVO, A. 2020. ALS phenotype is influenced by age, sex, and genetics: A population-based study. *Neurology,* 94**,** e802-e810.

CHIÒ, A., MOGLIA, C., CANOSA, A., MANERA, U., VASTA, R., BRUNETTI, M., BARBERIS, M., CORRADO, L., D'ALFONSO, S., BERSANO, E., SARNELLI, M. F., SOLARA, V., ZUCCHETTI, J. P., PEOTTA, L., IAZZOLINO, B., MAZZINI, L., MORA, G. & CALVO, A. 2019. Cognitive impairment across ALS clinical stages in a population-based cohort. *Neurology,* 93**,** e984-e994.

CHIÒ, A., PAGANI, M., AGOSTA, F., CALVO, A., CISTARO, A. & FILIPPI, M. 2014. Neuroimaging in amyotrophic lateral sclerosis: insights into structural and functional changes. *The Lancet Neurology,* 13**,** 1228-1240.

CHUGH, A., SHAHBAZI, M. & LANGE, D. 2013. Hemiplegic Form of Amyotrophic Lateral Sclerosis (ALS) with Cognitive Changes: An Autopsy Study (P02.176). *Neurology,* 80**,** P02.176-P02.176.

CHURCHLAND, M. M., SANTHANAM, G. & SHENOY, K. V. 2006. Preparatory activity in premotor and motor cortex reflects the speed of the upcoming reach. *Journal of neurophysiology,* 96**,** 3130-3146.

CISEK, P., CRAMMOND, D. J. & KALASKA, J. F. 2003. Neural activity in primary motor and dorsal premotor cortex in reaching tasks with the contralateral versus ipsilateral arm. *Journal of neurophysiology,* 89**,** 922-942.

CISEK, P. & KALASKA, J. F. 2005. Neural Correlates of Reaching Decisions in Dorsal Premotor Cortex: Specification of Multiple Direction Choices and Final Selection of Action. *Neuron,* 45**,** 801-814.

CISTARO, A., PAGANI, M., MONTUSCHI, A., CALVO, A., MOGLIA, C., CANOSA, A., RESTAGNO, G., BRUNETTI, M., TRAYNOR, B. J., NOBILI, F., CARRARA, G., FANIA, P., LOPIANO, L., VALENTINI, M. C. & CHIÒ, A. 2014. The metabolic signature of C9ORF72-related ALS: FDG PET comparison with nonmutated patients. *European Journal of Nuclear Medicine and Molecular Imaging,* 41**,** 844-852.

CIVIDINI, C., BASAIA, S., SPINELLI, E. G., CANU, E., CASTELNOVO, V., RIVA, N., CECCHETTI, G., CASO, F., MAGNANI, G., FALINI, A., FILIPPI, M. & AGOSTA, F. 2021. Amyotrophic Lateral Sclerosis-Frontotemporal Dementia: Shared and Divergent Neural Correlates Across the Clinical Spectrum. *Neurology,* 98**,** e402-15.

CLARK, J. A., SOUTHAM, K. A., BLIZZARD, C. A., KING, A. E. & DICKSON, T. C. 2016. Axonal degeneration, distal collateral branching and neuromuscular junction architecture alterations occur prior to symptom onset in the SOD1G93A mouse model of amyotrophic lateral sclerosis. *Journal of Chemical Neuroanatomy,* 76**,** 35-47.

COFFEY, A., BISTA, S., FASANO, A., BUXO, T., MITCHELL, M., GIGLIA, E. R., DUKIC, S., FENECH, M., BARRY, M., WADE, A., HEVERIN, M., MUTHURAMAN, M., CARSON, R. G., LOWERY, M., HARDIMAN, O. & NASSEROLESLAMI, B. 2021. Altered supraspinal motor networks in survivors of poliomyelitis: A cortico-muscular coherence study. *Clin Neurophysiol,* 132**,** 106-113.

COHEN, D. 1972. Magnetoencephalography: Detection of the brain's electrical activity with a superconducting magnetometer. *Science,* 175**,** 664-666.

COHEN, J. 1988. *Statistical power analysis for the behavioral sciences,* New York. NY, Lawrence Erlbaum Associates.

COMPSTON, A. 2010. Aids to the Investigation of Peripheral Nerve Injuries. Medical Research Council: Nerve Injuries Research Committee. His Majesty's Stationery Office: 1942; pp. 48 (iii) and 74 figures and 7 diagrams; with Aids to the Examination of the Peripheral Nervous System. By Michael O'Brien for the Guarantors of Brain. Saunders Elsevier: 2010; pp. [8] 64 and 94 Figures. *Brain,* 133**,** 2838-2844.

CONSONNI, M., DALLA BELLA, E., CONTARINO, V. E., BERSANO, E. & LAURIA, G. 2020. Cortical thinning trajectories across disease stages and cognitive impairment in amyotrophic lateral sclerosis. *Cortex,* 131**,** 284-294.

CONWAY, B. A., HALLIDAY, D. M., FARMER, S. F., SHAHANI, U., MAAS, P., WEIR, A. I. & ROSENBERG, J. R. 1995. Synchronization between motor cortex and spinal motoneuronal pool during the performance of a maintained motor task in man. *The Journal of Physiology,* 489**,** 917-924.

CORRELL, J., MELLINGER, C., MCCLELLAND, G. H. & JUDD, C. M. 2020. Avoid Cohen's 'Small', 'Medium', and 'Large' for Power Analysis. *Trends in Cognitive Sciences,* 24**,** 200-207.

COSOTTINI, M., PESARESI, I., PIAZZA, S., DICIOTTI, S., CECCHI, P., FABBRI, S., CARLESI, C., MASCALCHI, M. & SICILIANO, G. 2012. Structural and functional evaluation of cortical motor areas in Amyotrophic Lateral Sclerosis. *Exp Neurol,* 234**,** 169-80.

CROSSLEY, N. A., MECHELLI, A., SCOTT, J., CARLETTI, F., FOX, P. T., MCGUIRE, P. & BULLMORE, E. T. 2014. The hubs of the human connectome are generally implicated in the anatomy of brain disorders. *Brain,* 137**,** 2382-95.

CUI, R. Q. & DEECKE, L. 1999. High resolution DC-EEG of the Bereitschaftspotential preceding anatomically congruent versus spatially congruent bimanual finger movements. *Brain Topogr,* 12**,** 117-27.

CUNNINGTON, R., WINDISCHBERGER, C. & MOSER, E. 2005. Premovement activity of the pre-supplementary motor area and the readiness for action: Studies of time-resolved event-related functional MRI. *Human Movement Science,* 24**,** 644-656.

DAI, Z., YAN, C., LI, K., WANG, Z., WANG, J., CAO, M., LIN, Q., SHU, N., XIA, M., BI, Y. & HE, Y. 2014. Identifying and Mapping Connectivity Patterns of Brain Network Hubs in Alzheimer's Disease. *Cerebral Cortex,* 25**,** 3723-3742.

DANNA-DOS SANTOS, A., POSTON, B., JESUNATHADAS, M., BOBICH, L. R., HAMM, T. M. & SANTELLO, M. 2010. Influence of fatigue on hand muscle coordination and EMG-EMG coherence during three-digit grasping. *Journal of neurophysiology,* 104**,** 3576-3587.

DE CARVALHO, M., BENTES, C., EVANGELISTA, T. & LUÍS, M. L. S. 1999. Fibrillation and sharp-waves: Do we need them to diagnose ALS? *Amyotrophic Lateral Sclerosis and Other Motor Neuron Disorders,* 1**,** 29-32.

DE CARVALHO, M., DENGLER, R., EISEN, A., ENGLAND, J. D., KAJI, R., KIMURA, J., MILLS, K., MITSUMOTO, H., NODERA, H., SHEFNER, J. & SWASH, M. 2008. Electrodiagnostic criteria for diagnosis of ALS. *Clinical Neurophysiology,* 119**,** 497-503.

DE CARVALHO, M., SCOTTO, M., LOPES, A. & SWASH, M. 2003. Clinical and neurophysiological evaluation of progression in amyotrophic lateral sclerosis. *Muscle Nerve,* 28**,** 630-3.

DE VOS, K. J. & HAFEZPARAST, M. 2017. Neurobiology of axonal transport defects in motor neuron diseases: Opportunities for translational research? *Neurobiol Dis,* 105**,** 283-299.

DEECKE, L. 1987. Bereitschaftspotential as an indicator of movement preparation in supplementary motor area and motor cortex. *Ciba Found Symp,* 132**,** 231-50.

DEECKE, L. 1996. Planning, preparation, execution, and imagery of volitional action. *Cognitive Brain Research,* 3**,** 59-64.

DELCAMP, C., CORMIER, C., CHALARD, A., AMARANTINI, D. & GASQ, D. 2022. Botulinum toxin combined with rehabilitation decrease corticomuscular coherence in stroke patients. *Clinical Neurophysiology,* 136**,** 49-57.

DELIGANI, R. J., HOSNI, S. I., BORGHEAI, S. B., MCLINDEN, J., ZISK, A. H., MANKODIYA, K. & SHAHRIARI, Y. 2020. Electrical and Hemodynamic Neural Functions in People With ALS: An EEG-fNIRS Resting-State Study. *IEEE Trans Neural Syst Rehabil Eng,* 28**,** 3129-3139.

DELORENZO, C., DELLAGIOIA, N., BLOCH, M., SANACORA, G., NABULSI, N., ABDALLAH, C., YANG, J., WEN, R., MANN, J. J., KRYSTAL, J. H., PARSEY, R. V., CARSON, R. E. & ESTERLIS, I. 2015. In vivo ketamine-induced changes in [^{11}C]ABP688 binding to metabotropic glutamate receptor subtype 5. *Biol Psychiatry,* 77**,** 266-275.

DIECKMANN, N., ROEDIGER, A., PRELL, T., SCHUSTER, S., HERDICK, M., MAYER, T. E., WITTE, O. W., STEINBACH, R. & GROSSKREUTZ, J. 2022. Cortical and subcortical grey matter atrophy in Amyotrophic Lateral Sclerosis correlates with measures of disease accumulation independent of disease aggressiveness. *Neuroimage Clin,* 36**,** 103162.

DIMOND, D., ISHAQUE, A., CHENJI, S., MAH, D., CHEN, Z., SERES, P., BEAULIEU, C. & KALRA, S. 2017. White matter structural network abnormalities underlie executive dysfunction in amyotrophic lateral sclerosis. *Hum Brain Mapp,* 38**,** 1249-1268.

DING, H., DROBY, A., ANWAR, A. R., BANGE, M., HAUSDORFF, J. M., NASSEROLESLAMI, B., MIRELMAN, A., MAIDAN, I., GROPPA, S. & MUTHURAMAN, M. 2022. Treadmill training in Parkinson's disease is underpinned by the interregional connectivity in cortical-subcortical network. *npj Parkinson's Disease,* 8**,** 153.

DONOGHUE, J. P., SANES, J. N., HATSOPOULOS, N. G. & GAÁL, G. 1998. Neural Discharge and Local Field Potential Oscillations in Primate Motor Cortex During Voluntary Movements. *Journal of Neurophysiology,* 79**,** 159-173.

DOUAUD, G., FILIPPINI, N., KNIGHT, S., TALBOT, K. & TURNER, M. R. 2011. Integration of structural and functional magnetic resonance imaging in amyotrophic lateral sclerosis. *Brain,* 134**,** 3470-9.

DU, Y., FU, Z. & CALHOUN, V. D. 2018. Classification and Prediction of Brain Disorders Using Functional Connectivity: Promising but Challenging. *Frontiers in Neuroscience,* 12.

DUKIC, S., IYER, P. M., MOHR, K., HARDIMAN, O., LALOR, E. C. & NASSEROLESLAMI, B. 2017. Estimation of coherence using the median is robust against EEG artefacts. *Annu Int Conf IEEE Eng Med Biol Soc,* 2017**,** 3949-3952.

DUKIC, S., MCMACKIN, R., BUXO, T., FASANO, A., CHIPIKA, R., PINTO-GRAU, M., COSTELLO, E., SCHUSTER, C., HAMMOND, M., HEVERIN, M., COFFEY, A., BRODERICK, M., IYER, P. M., MOHR, K., GAVIN, B., PENDER, N., BEDE, P., MUTHURAMAN, M., LALOR, E. C., HARDIMAN, O. & NASSEROLESLAMI, B. 2019. Patterned functional network disruption in amyotrophic lateral sclerosis. *Human Brain Mapping,* 40**,** 4827-4842.

DUKIC, S., MCMACKIN, R., COSTELLO, E., METZGER, M., BUXO, T., FASANO, A., CHIPIKA, R., PINTO-GRAU, M., SCHUSTER, C., HAMMOND, M., HEVERIN, M., COFFEY, A., BRODERICK, M., IYER, P. M., MOHR, K., GAVIN, B., MCLAUGHLIN, R., PENDER, N., BEDE, P., MUTHURAMAN, M., VAN DEN BERG, L. H., HARDIMAN, O. & NASSEROLESLAMI, B. 2021. Resting-state EEG reveals four subphenotypes of amyotrophic lateral sclerosis. *Brain,* 145**,** 621-631.

DUQUE, J., MURASE, N., CELNIK, P., HUMMEL, F., HARRIS-LOVE, M., MAZZOCCHIO, R., OLIVIER, E. & COHEN, L. G. 2007. Intermanual Differences in Movement-related Interhemispheric Inhibition. *Journal of Cognitive Neuroscience,* 19**,** 204-213.

EFRON, B. & TIBSHIRANI, R. J. 1993. An introduction to the bootstrap Chapman & Hall. *New York,* 436.

EICKHOFF, S. B. & MÜLLER, V. I. 2015. Functional Connectivity. *In:* TOGA, A. W. (ed.) *Brain Mapping.* Waltham: Academic Press.

EISEN, A. 2021. The Dying Forward Hypothesis of ALS: Tracing Its History. *Brain Sci,* 11.

FALCÃO DE CAMPOS, C., GROMICHO, M., UYSAL, H., GROSSKREUTZ, J., KUZMA-KOZAKIEWICZ, M., OLIVEIRA SANTOS, M., PINTO, S., PETRI, S., SWASH, M. & DE CARVALHO, M. 2023. Trends in the diagnostic delay and pathway for amyotrophic lateral sclerosis patients across different countries. *Frontiers in Neurology,* 13.

FANG, T., AL KHLEIFAT, A., STAHL, D. R., LAZO LA TORRE, C., MURPHY, C., YOUNG, C., SHAW, P. J., LEIGH, P. N. & AL-CHALABI, A. 2017. Comparison of the King's and MiToS staging systems for ALS. *Amyotroph Lateral Scler Frontotemporal Degener,* 18**,** 227-232.

FANG, X., ZHANG, Y., WANG, Y., ZHANG, Y., HU, J., WANG, J., ZHANG, J. & JIANG, T. 2016. Disrupted effective connectivity of the sensorimotor network in amyotrophic lateral sclerosis. *Journal of neurology,* 263**,** 508-516.

FANG, Y., DALY, J. J., SUN, J., HVORAT, K., FREDRICKSON, E., PUNDIK, S., SAHGAL, V. & YUE, G. H. 2009. Functional corticomuscular connection during reaching is weakened following stroke. *Clinical Neurophysiology,* 120**,** 994-1002.

FATIMA, M., TAN, R., HALLIDAY, G. M. & KRIL, J. J. 2015. Spread of pathology in amyotrophic lateral sclerosis: assessment of phosphorylated TDP-43 along axonal pathways. *Acta Neuropathologica Communications,* 3**,** 47.

FELDMAN, E. L., GOUTMAN, S. A., PETRI, S., MAZZINI, L., SAVELIEFF, M. G., SHAW, P. J. & SOBUE, G. 2022. Amyotrophic lateral sclerosis. *The Lancet,* 400**,** 1363-1380.

FERRARI, M. & QUARESIMA, V. 2012. A brief review on the history of human functional near-infrared spectroscopy (fNIRS) development and fields of application. *NeuroImage,* 63**,** 921-935.

FERREA, S., JUNKER, F., KORTH, M., GRUHN, K., GREHL, T. & SCHMIDT-WILCKE, T. 2021. Cortical Thinning of Motor and Non-Motor Brain Regions Enables Diagnosis of Amyotrophic Lateral Sclerosis and Supports Distinction between Upper- and Lower-Motoneuron Phenotypes. *Biomedicines,* 9.

FILIPPI, M., SPINELLI, E. G., CIVIDINI, C. & AGOSTA, F. 2019. Resting State Dynamic Functional Connectivity in Neurodegenerative Conditions: A Review of Magnetic Resonance Imaging Findings. *Frontiers in Neuroscience,* 13.

FINEGAN, E., CHIPIKA, R. H., SHING, S. L. H., HARDIMAN, O. & BEDE, P. 2019. Primary lateral sclerosis: a distinct entity or part of the ALS spectrum? *Amyotrophic Lateral Sclerosis and Frontotemporal Degeneration,* 20**,** 133-145.

FISCHL, B. & DALE, A. M. 2000. Measuring the thickness of the human cerebral cortex from magnetic resonance images. *Proc Natl Acad Sci U S A,* 97**,** 11050-5.

FISHER, K. M., ZAAIMI, B., WILLIAMS, T. L., BAKER, S. N. & BAKER, M. R. 2012. Beta-band intermuscular coherence: a novel biomarker of upper motor neuron dysfunction in motor neuron disease. *Brain,* 135**,** 2849-64.

FOERSTER, B. R., CALLAGHAN, B. C., PETROU, M., EDDEN, R. A., CHENEVERT, T. L. & FELDMAN, E. L. 2012a. Decreased motor cortex γ-aminobutyric acid in amyotrophic lateral sclerosis. *Neurology,* 78**,** 1596-600.

FOERSTER, B. R., DWAMENA, B. A., PETROU, M., CARLOS, R. C., CALLAGHAN, B. C. & POMPER, M. G. 2012b. Diagnostic Accuracy Using Diffusion Tensor Imaging in the Diagnosis of ALS: A Meta-analysis. *Academic Radiology,* 19**,** 1075-1086.

FOERSTER, B. R., POMPER, M. G., CALLAGHAN, B. C., PETROU, M., EDDEN, R. A. E., MOHAMED, M. A., WELSH, R. C., CARLOS, R. C., BARKER, P. B. & FELDMAN, E. L. 2013. An Imbalance Between Excitatory and Inhibitory Neurotransmitters in Amyotrophic Lateral Sclerosis Revealed by Use of 3-T Proton Magnetic Resonance SpectroscopyExcitatory and Inhibitory Neurotransmitters in ALS. *JAMA Neurology,* 70**,** 1009-1016.

FONTANA, A., MARIN, B., LUNA, J., BEGHI, E., LOGROSCINO, G., BOUMÉDIENE, F., PREUX, P. M., COURATIER, P. & COPETTI, M. 2021. Time-trend evolution and determinants of sex ratio in Amyotrophic Lateral Sclerosis: a dose-response meta-analysis. *J Neurol,* 268**,** 2973-2984.

FORAN, E. & TROTTI, D. 2009. Glutamate transporters and the excitotoxic path to motor neuron degeneration in amyotrophic lateral sclerosis. *Antioxid Redox Signal,* 11**,** 1587-602.

FORTANIER, E., GRAPPERON, A.-M., LE TROTER, A., VERSCHUEREN, A., RIDLEY, B., GUYE, M., ATTARIAN, S., RANJEVA, J.-P. & ZAARAOUI, W. 2019. Structural Connectivity Alterations in Amyotrophic Lateral Sclerosis: A Graph Theory Based Imaging Study. *Frontiers in Neuroscience,* 13.

FOURNIER, C. N., BEDLACK, R., QUINN, C., RUSSELL, J., BECKWITH, D., KAMINSKI, K. H., TYOR, W., HERTZBERG, V., JAMES, V., POLAK, M. & GLASS, J. D. 2020. Development and Validation of the Rasch-Built Overall Amyotrophic Lateral Sclerosis Disability Scale (ROADS). *JAMA Neurol,* 77**,** 480-488.

FOURNIER, C. N., JAMES, V. & GLASS, J. D. 2023. Clinically meaningful change: evaluation of the Rasch-built Overall Amyotrophic Lateral Sclerosis Disability Scale (ROADS) and the ALSFRS-R. *Amyotrophic Lateral Sclerosis and Frontotemporal Degeneration,* 24**,** 311-316.

FOX, M. D. & RAICHLE, M. E. 2007. Spontaneous fluctuations in brain activity observed with functional magnetic resonance imaging. *Nature Reviews Neuroscience,* 8**,** 700-711.

FRANCHIGNONI, F., MORA, G., GIORDANO, A., VOLANTI, P. & CHIÒ, A. 2013. Evidence of multidimensionality in the ALSFRS-R Scale: a critical appraisal on its measurement properties using Rasch analysis. *J Neurol Neurosurg Psychiatry,* 84**,** 1340-5.

FRASCHINI, M., DEMURU, M., HILLEBRAND, A., CUCCU, L., PORCU, S., DI STEFANO, F., PULIGHEDDU, M., FLORIS, G., BORGHERO, G. & MARROSU, F. 2016. EEG functional network topology is associated with disability in patients with amyotrophic lateral sclerosis. *Scientific Reports,* 6**,** 38653.

FRÍAS, I., STARRS, F., GISIGER, T., MINUK, J., THIEL, A. & PAQUETTE, C. 2018. Interhemispheric connectivity of primary sensory cortex is associated with motor impairment after stroke. *Scientific Reports,* 8**,** 12601.

FRIES, P., NIKOLIĆ, D. & SINGER, W. 2007. The gamma cycle. *Trends Neurosci,* 30**,** 309-16.

FRISTON, K. J. 2011. Functional and effective connectivity: a review. *Brain connectivity,* 1**,** 13-36.

FUJIMOTO, H., MIHARA, M., HATTORI, N., HATAKENAKA, M., KAWANO, T., YAGURA, H., MIYAI, I. & MOCHIZUKI, H. 2014. Cortical changes underlying balance recovery in patients with hemiplegic stroke. *NeuroImage,* 85**,** 547-554.

FUKADA, K., MATSUI, T., FURUTA, M., HIROZAWA, D., MATSUI, M., KAJIYAMA, Y., SHIMIZU, M., KINOSHITA, M., MOCHIZUKI, H., SAWADA, J.-I. & HAZAMA, T. 2016. The Motor Unit Number Index of Subclinical Abnormality in Amyotrophic Lateral Sclerosis. *Journal of Clinical Neurophysiology,* 33.

GALEA, M. P. & DARIAN-SMITH, I. 1994. Multiple Corticospinal Neuron Populations in the Macaque Monkey Are Specified by Their Unique Cortical Origins, Spinal Terminations, and Connections. *Cerebral Cortex,* 4**,** 166-194.

GALVIN, M., RYAN, P., MAGUIRE, S., HEVERIN, M., MADDEN, C., VAJDA, A., NORMAND, C. & HARDIMAN, O. 2017. The path to specialist multidisciplinary care in amyotrophic lateral sclerosis: A population- based study of consultations, interventions and costs. *PLOS ONE,* 12**,** e0179796.

GAO, Q., DUAN, X. & CHEN, H. 2011. Evaluation of effective connectivity of motor areas during motor imagery and execution using conditional Granger causality. *NeuroImage,* 54**,** 1280-1288.

GARN, H., CORONEL, C., WASER, M., CARAVIAS, G. & RANSMAYR, G. 2017. Differential diagnosis between patients with probable Alzheimer's disease, Parkinson's disease dementia, or dementia with Lewy bodies and frontotemporal dementia, behavioral variant, using quantitative electroencephalographic features. *Journal of Neural Transmission,* 124**,** 569-581.

GAWEL, M., KUZMA-KOZAKIEWICZ, M., SZMIDT-SALKOWSKA, E. & KAMIŃSKA, A. 2014. Are we really closer to improving the diagnostic sensitivity in ALS patients with Awaji criteria? *Amyotrophic Lateral Sclerosis and Frontotemporal Degeneration,* 15**,** 257-261.

GERLOFF, C., RICHARD, J., HADLEY, J., SCHULMAN, A. E., HONDA, M. & HALLETT, M. 1998. Functional coupling and regional activation of human cortical motor areas during simple, internally paced and externally paced finger movements. *Brain,* 121**,** 1513-1531.

GESER, F., BRANDMEIR, N. J., KWONG, L. K., MARTINEZ-LAGE, M., ELMAN, L., MCCLUSKEY, L., XIE, S. X., LEE, V. M. & TROJANOWSKI, J. Q. 2008. Evidence of multisystem disorder in whole-brain map of pathological TDP-43 in amyotrophic lateral sclerosis. *Arch Neurol,* 65**,** 636-41.

GEWEKE, J. 1982. Measurement of Linear Dependence and Feedback between Multiple Time Series. *Journal of the American Statistical Association,* 77**,** 304-313.

GIBBONS, J. D. & CHAKRABORTI, S. 2003. *Nonparametric statistical inference,* New York, NY 10016, Marcel Dekker, Inc.

GLOVER, G. H. 2011. Overview of functional magnetic resonance imaging. *Neurosurg Clin N Am,* 22**,** 133-9, vii.

GLOVER, S., WALL, M. B. & SMITH, A. T. 2012. Distinct cortical networks support the planning and online control of reaching-to-grasp in humans. *Eur J Neurosci,* 35**,** 909-15.

GOOCH, C. L., DOHERTY, T. J., CHAN, K. M., BROMBERG, M. B., LEWIS, R. A., STASHUK, D. W., BERGER, M. J., ANDARY, M. T. & DAUBE, J. R. 2014. Motor unit number estimation: a technology and literature review. *Muscle Nerve,* 50**,** 884-93.

GOUTMAN, S. A., HARDIMAN, O., AL-CHALABI, A., CHIÓ, A., SAVELIEFF, M. G., KIERNAN, M. C. & FELDMAN, E. L. 2022. Emerging insights into the complex

genetics and pathophysiology of amyotrophic lateral sclerosis. *Lancet Neurol,* 21**,** 465-479.

GOVAARTS, R., BEELDMAN, E., FRASCHINI, M., GRIFFA, A., ENGELS, M. M. A., VAN ES, M. A., VELDINK, J. H., VAN DEN BERG, L. H., VAN DER KOOI, A. J., PIJNENBURG, Y. A. L., DE VISSER, M., STAM, C. J., RAAPHORST, J. & HILLEBRAND, A. 2022. Cortical and subcortical changes in resting-state neuronal activity and connectivity in early symptomatic ALS and advanced frontotemporal dementia. *NeuroImage: Clinical,* 34**,** 102965.

GREFKES, C., EICKHOFF, S. B., NOWAK, D. A., DAFOTAKIS, M. & FINK, G. R. 2008. Dynamic intra- and interhemispheric interactions during unilateral and bilateral hand movements assessed with fMRI and DCM. *NeuroImage,* 41**,** 1382-1394.

GREICIUS, M. D., KRASNOW, B., REISS, A. L. & MENON, V. 2003. Functional connectivity in the resting brain: A network analysis of the default mode hypothesis. *Proceedings of the National Academy of Sciences of the United States of America,* 100**,** 253-258.

GROSS, J., KUJALA, J., HAMALAINEN, M., TIMMERMANN, L., SCHNITZLER, A. & SALMELIN, R. 2001. Dynamic imaging of coherent sources: Studying neural interactions in the human brain. *Proc Natl Acad Sci U S A,* 98**,** 694-9.

GROSSMAN, M. 2019. Amyotrophic lateral sclerosis — a multisystem neurodegenerative disorder. *Nature Reviews Neurology,* 15**,** 5-6.

GROUP, B. D. W. 2001. Biomarkers and surrogate endpoints: preferred definitions and conceptual framework. *Clin Pharmacol Ther,* 69**,** 89-95.

GWIN, J. T. & FERRIS, D. P. 2012. Beta- and gamma-range human lower limb corticomuscular coherence. *Frontiers in human neuroscience,* 6**,** 258-258.

HAITH, A. M., PAKPOOR, J. & KRAKAUER, J. W. 2016. Independence of Movement Preparation and Movement Initiation. *The Journal of Neuroscience,* 36**,** 3007-3015.

HALLIDAY, D. M., CONWAY, B. A., FARMER, S. F. & ROSENBERG, J. R. 1998. Using electroencephalography to study functional coupling between cortical activity and electromyograms during voluntary contractions in humans. *Neurosci Lett,* 241**,** 5-8.

HALLIDAY, D. M., CONWAY, B. A., FARMER, S. F. & ROSENBERG, J. R. 1999. Load-independent contributions from motor-unit synchronization to human physiological tremor. *J Neurophysiol,* 82**,** 664-75.

HALLIDAY, D. M. & ROSENBERG, J. R. 1999. Time and Frequency Domain Analysis of Spike Train and Time Series Data. *In:* WINDHORST, U. & JOHANSSON, H. (eds.) *Modern Techniques in Neuroscience Research.* Berlin, Heidelberg: Springer Berlin Heidelberg.

HÄMÄLÄINEN, M., HARI, R., ILMONIEMI, R. J., KNUUTILA, J. & LOUNASMAA, O. V. 1993. Magnetoencephalography---theory, instrumentation, and applications to noninvasive studies of the working human brain. *Reviews of Modern Physics,* 65**,** 413-497.

HAMANO, T., LÜDERS, H. O., IKEDA, A., COLLURA, T. F., COMAIR, Y. G. & SHIBASAKI, H. 1997. The cortical generators of the contingent negative variation in humans: A study with subdural electrodes. *Electroencephalography and Clinical Neurophysiology - Evoked Potentials,* 104**,** 257-268.

HAN, J. & MA, L. 2010. Study of the features of proton MR spectroscopy ((1)H-MRS) on amyotrophic lateral sclerosis. *J Magn Reson Imaging,* 31**,** 305-8.

HANAGASI, H. A., GURVIT, I. H., ERMUTLU, N., KAPTANOGLU, G., KARAMURSEL, S., IDRISOGLU, H. A., EMRE, M. & DEMIRALP, T. 2002. Cognitive impairment in amyotrophic lateral sclerosis: evidence from neuropsychological investigation and event-related potentials. *Brain Res Cogn Brain Res,* 14**,** 234-44.

HANAKAWA, T., DIMYAN, M. A. & HALLETT, M. 2008. Motor Planning, Imagery, and Execution in the Distributed Motor Network: A Time-Course Study with Functional MRI. *Cerebral Cortex,* 18**,** 2775-2788.

HANNAFORD, A., PAVEY, N., VAN DEN BOS, M., GEEVASINGA, N., MENON, P., SHEFNER, J. M., KIERNAN, M. C. & VUCIC, S. 2021. Diagnostic Utility of Gold Coast Criteria in Amyotrophic Lateral Sclerosis. *Annals of Neurology,* 89**,** 979-986.

HARADA, T., MIYAI, I., SUZUKI, M. & KUBOTA, K. 2009. Gait capacity affects cortical activation patterns related to speed control in the elderly. *Exp Brain Res,* 193**,** 445-54.

HARDIMAN, O., VAN DEN BERG, L. H. & KIERNAN, M. C. 2011. Clinical diagnosis and management of amyotrophic lateral sclerosis. *Nature Reviews Neurology,* 7**,** 639-649.

HATAZAWA, J., BROOKS, R. A., DALAKAS, M. C., MANSI, L. & DI CHIRO, G. 1988. Cortical motor-sensory hypometabolism in amyotrophic lateral sclerosis: a PET study. *J Comput Assist Tomogr,* 12**,** 630-6.

HEDGES, L. V. & OLKIN, I. 1985. *Statistical Methods for Meta-Analysis,* Elsevier Science.

HEINONEN, J., NUMMINEN, J., HLUSHCHUK, Y., ANTELL, H., TAATILA, V. & SUOMALA, J. 2016. Default Mode and Executive Networks Areas: Association with the Serial Order in Divergent Thinking. *PLoS One,* 11**,** e0162234.

HERMENS, H. J., FRERIKS, B., DISSELHORST-KLUG, C. & RAU, G. 2000. Development of recommendations for SEMG sensors and sensor placement procedures. *Journal of Electromyography and Kinesiology,* 10**,** 361-374.

HINDER, M. R., FUJIYAMA, H. & SUMMERS, J. J. 2012. Premotor-Motor Interhemispheric Inhibition Is Released during Movement Initiation in Older but Not Young Adults. *PLOS ONE,* 7**,** e52573.

HLAVÁČKOVÁ-SCHINDLER, K., PALUŠ, M., VEJMELKA, M. & BHATTACHARYA, J. 2007. Causality detection based on information-theoretic approaches in time series analysis. *Physics Reports,* 441**,** 1-46.

HÖFFKEN, O., SCHMELZ, A., LENZ, M., GRUHN, K., GREHL, T., TEGENTHOFF, M. & SCZESNY-KAISER, M. 2019. Excitability in somatosensory cortex correlates with motoric impairment in amyotrophic lateral sclerosis. *Amyotrophic Lateral Sclerosis and Frontotemporal Degeneration,* 20**,** 192-198.

HOLASEK, S. S., WENGENACK, T. M., KANDIMALLA, K. K., MONTANO, C., GREGOR, D. M., CURRAN, G. L. & PODUSLO, J. F. 2005. Activation of the stress-activated MAP kinase, p38, but not JNK in cortical motor neurons during early presymptomatic stages of amyotrophic lateral sclerosis in transgenic mice. *Brain Res,* 1045**,** 185-98.

HOLLAND, P. W. & WELSCH, R. E. 1977. Robust regression using iteratively reweighted least-squares. *Communications in Statistics - Theory and Methods,* 6**,** 813-827.

HOSAKA, R., NAKAJIMA, T., AIHARA, K., YAMAGUCHI, Y. & MUSHIAKE, H. 2016. The Suppression of Beta Oscillations in the Primate Supplementary Motor Complex Reflects a Volatile State During the Updating of Action Sequences. *Cereb Cortex,* 26**,** 3442-3452.

HOSHI, E. & TANJI, J. 2004. Differential Roles of Neuronal Activity in the Supplementary and Presupplementary Motor Areas: From Information Retrieval to Motor Planning and Execution. *Journal of Neurophysiology,* 92**,** 3482-3499.

HU, Z., LIU, G., DONG, Q. & NIU, H. 2020. Applications of Resting-State fNIRS in the Developing Brain: A Review From the Connectome Perspective. *Front Neurosci,* 14**,** 476.

HUANG, D., REN, A., SHANG, J., LEI, Q., ZHANG, Y., YIN, Z., LI, J., VON DENEEN, K. M. & HUANG, L. 2016. Combining Partial Directed Coherence and Graph

Theory to Analyse Effective Brain Networks of Different Mental Tasks. *Frontiers in Human Neuroscience,* 10.

HUYNH, W., DHARMADASA, T., VUCIC, S. & KIERNAN, M. C. 2019. Functional Biomarkers for Amyotrophic Lateral Sclerosis. *Frontiers in Neurology,* 9.

HUYNH, W., SIMON, N. G., GROSSKREUTZ, J., TURNER, M. R., VUCIC, S. & KIERNAN, M. C. 2016. Assessment of the upper motor neuron in amyotrophic lateral sclerosis. *Clinical Neurophysiology,* 127**,** 2643-2660.

IKEDA, A., LÜDERS, H. O., COLLURA, T. F., BURGESS, R. C., MORRIS, H. H., HAMANO, T. & SHIBASAKI, H. 1996. Subdural potentials at orbitofrontal and mesial prefrontal areas accompanying anticipation and decision making in humans: A comparison with Bereitschaftspotential1. *Electroencephalography and Clinical Neurophysiology,* 98**,** 206-212.

INCE, R. A. A., GIORDANO, B. L., KAYSER, C., ROUSSELET, G. A., GROSS, J. & SCHYNS, P. G. 2017. A statistical framework for neuroimaging data analysis based on mutual information estimated via a gaussian copula. *Human Brain Mapping,* 38**,** 1541-1573.

INUGGI, A., RIVA, N., GONZÁLEZ-ROSA, J. J., AMADIO, S., AMATO, N., FAZIO, R., DEL CARRO, U., COMI, G. & LEOCANI, L. 2011. Compensatory movement-related recruitment in amyotrophic lateral sclerosis patients with dominant upper motor neuron signs: an EEG source analysis study. *Brain Res,* 1425**,** 37-46.

ISSA, N. P., FRANK, S., ROOS, R. P., SOLIVEN, B., TOWLE, V. L. & REZANIA, K. 2017. Intermuscular coherence in amyotrophic lateral sclerosis: A preliminary assessment. *Muscle Nerve,* 55**,** 862-868.

IYER, P. M., EGAN, C., PINTO-GRAU, M., BURKE, T., ELAMIN, M., NASSEROLESLAMI, B., PENDER, N., LALOR, E. C. & HARDIMAN, O. 2015. Functional Connectivity Changes in Resting-State EEG as Potential Biomarker for Amyotrophic Lateral Sclerosis. *PloS one,* 10**,** e0128682-e0128682.

JACOBSEN, A. B., BOSTOCK, H. & TANKISI, H. 2019. Following disease progression in motor neuron disorders with 3 motor unit number estimation methods. *Muscle & Nerve,* 59**,** 82-87.

JELSONE-SWAIN, L., FLING, B., SEIDLER, R., HOVATTER, R., GRUIS, K. & WELSH, R. 2010. Reduced Interhemispheric Functional Connectivity in the Motor Cortex during Rest in Limb-Onset Amyotrophic Lateral Sclerosis. *Frontiers in Systems Neuroscience,* 4.

JEONG, Y., PARK, K. C., CHO, S. S., KIM, E. J., KANG, S. J., KIM, S. E., KANG, E. & NA, D. L. 2005. Pattern of glucose hypometabolism in frontotemporal dementia with motor neuron disease. *Neurology,* 64**,** 734-6.

JEROMIN, A. & BOWSER, R. 2017. Biomarkers in Neurodegenerative Diseases. *In:* BEART, P., ROBINSON, M., RATTRAY, M. & MARAGAKIS, N. J. (eds.) *Neurodegenerative Diseases: Pathology, Mechanisms, and Potential Therapeutic Targets.* Cham: Springer International Publishing.

JOHNSEN, B., PUGDAHL, K., FUGLSANG-FREDERIKSEN, A., KOLLEWE, K., PARACKA, L., DENGLER, R., CAMDESSANCHÉ, J. P., NIX, W., LIGUORI, R., SCHOFIELD, I., MADERNA, L., CZELL, D., NEUWIRTH, C., WEBER, M., DRORY, V. E., ABRAHAM, A., SWASH, M. & DE CARVALHO, M. 2019. Diagnostic criteria for amyotrophic lateral sclerosis: A multicentre study of inter-rater variation and sensitivity. *Clinical Neurophysiology,* 130**,** 307-314.

JOHNSON, S. A., BURKE, K. M., SCHEIER, Z. A., KEEGAN, M. A., CLARK, A. P., CHAN, J., FOURNIER, C. N. & BERRY, J. D. 2022. Longitudinal comparison of the self-entry Amyotrophic Lateral Sclerosis Functional Rating Scale-Revised (ALSFRS-RSE) and Rasch-Built Overall Amyotrophic Lateral Sclerosis Disability Scale (ROADS) as outcome measures in people with amyotrophic lateral sclerosis. *Muscle & Nerve,* 66**,** 495-502.

JONES, D. K. & CERCIGNANI, M. 2010. Twenty-five pitfalls in the analysis of diffusion MRI data. *NMR in Biomedicine,* 23**,** 803-820.

JOUNDI, R. A., JENKINSON, N., BRITTAIN, J. S., AZIZ, T. Z. & BROWN, P. 2012. Driving oscillatory activity in the human cortex enhances motor performance. *Curr Biol,* 22**,** 403-7.

JOYCE, N. C. & CARTER, G. T. 2013. Electrodiagnosis in persons with amyotrophic lateral sclerosis. *Pm r,* 5**,** S89-95.

KALRA, S. 2019. Magnetic Resonance Spectroscopy in ALS. *Frontiers in Neurology,* 10.

KALRA, S., MÜLLER, H. P., ISHAQUE, A., ZINMAN, L., KORNGUT, L., GENGE, A., BEAULIEU, C., FRAYNE, R., GRAHAM, S. J. & KASSUBEK, J. 2020. A prospective harmonized multicenter DTI study of cerebral white matter degeneration in ALS. *Neurology,* 95**,** e943-e952.

KAMINSKI, M. J. & BLINOWSKA, K. J. 1991. A new method of the description of the information flow in the brain structures. *Biological Cybernetics,* 65**,** 203-210.

KANG, B. H., KIM, J. I., LIM, Y. M. & KIM, K. K. 2018. Abnormal Oculomotor Functions in Amyotrophic Lateral Sclerosis. *J Clin Neurol,* 14**,** 464-471.

KARANDREAS, N., PAPADOPOULOU, M., KOKOTIS, P., PAPAPOSTOLOU, A., TSIVGOULIS, G. & ZAMBELIS, T. 2007. Impaired interhemispheric inhibition in amyotrophic lateral sclerosis. *Amyotroph Lateral Scler,* 8**,** 112-8.

KASSUBEK, J., MÜLLER, H. P., DEL TREDICI, K., LULÉ, D., GORGES, M., BRAAK, H. & LUDOLPH, A. C. 2018. Imaging the pathoanatomy of amyotrophic lateral sclerosis in vivo: targeting a propagation-based biological marker. *J Neurol Neurosurg Psychiatry,* 89**,** 374-381.

KAUR, C., SINGH, P., BISHT, A., JOSHI, G. & AGRAWAL, S. 2022. Recent Developments in Spatio-Temporal EEG Source Reconstruction Techniques. *Wireless Personal Communications,* 122**,** 1531-1558.

KENT-BRAUN, J. A., WALKER, C. H., WEINER, M. W. & MILLER, R. G. 1998. Functional significance of upper and lower motor neuron impairment in amyotrophic lateral sclerosis. *Muscle & Nerve,* 21**,** 762-768.

KIERNAN, M. C., VUCIC, S., CHEAH, B. C., TURNER, M. R., EISEN, A., HARDIMAN, O., BURRELL, J. R. & ZOING, M. C. 2011. Amyotrophic lateral sclerosis. *The Lancet,* 377**,** 942-955.

KILNER, J. M., BAKER, S. N., SALENIUS, S., HARI, R. & LEMON, R. N. 2000. Human Cortical Muscle Coherence Is Directly Related to Specific Motor Parameters. *The Journal of Neuroscience,* 20**,** 8838-8845.

KIM, Y. K., PARK, E., LEE, A., IM, C. H. & KIM, Y. H. 2018. Changes in network connectivity during motor imagery and execution. *PLoS One,* 13**,** e0190715.

KING, A. E., WOODHOUSE, A., KIRKCALDIE, M. T. K. & VICKERS, J. C. 2016. Excitotoxicity in ALS: Overstimulation, or overreaction? *Experimental Neurology,* 275**,** 162-171.

KITAMURA, J., SHIBASAKI, H. & KONDO, T. 1993. A cortical slow potential is larger before an isolated movement of a single finger than simultaneous movement of two fingers. *Electroencephalogr Clin Neurophysiol,* 86**,** 252-8.

KLINE, R. B. 2004. *Beyond significance testing: Reforming data analysis methods in behavioral research,* Washington, DC, US, American Psychological Association.

KLOSTERMANN, F., NIKULIN, V. V., KÜHN, A. A., MARZINZIK, F., WAHL, M., POGOSYAN, A., KUPSCH, A., SCHNEIDER, G. H., BROWN, P. & CURIO, G. 2007. Task-related differential dynamics of EEG alpha- and beta-band synchronization in cortico-basal motor structures. *Eur J Neurosci,* 25**,** 1604-15.

KOCH, G., CERCIGNANI, M., PECCHIOLI, C., VERSACE, V., OLIVERI, M., CALTAGIRONE, C., ROTHWELL, J. & BOZZALI, M. 2010. In vivo definition of parieto-motor connections involved in planning of grasping movements. *NeuroImage,* 51**,** 300-312.

KOENRAADT, K. L. M., ROELOFSEN, E. G. J., DUYSENS, J. & KEIJSERS, N. L. W. 2014. Cortical control of normal gait and precision stepping: An fNIRS study. *NeuroImage,* 85**,** 415-422.

KOLLEWE, K., MÜNTE, T. F., SAMII, A., DENGLER, R., PETRI, S. & MOHAMMADI, B. 2011. Patterns of cortical activity differ in ALS patients with limb and/or bulbar involvement depending on motor tasks. *J Neurol,* 258**,** 804-10.

KONRAD, C., HENNINGSEN, H., BREMER, J., MOCK, B., DEPPE, M., BUCHINGER, C., TURSKI, P., KNECHT, S. & BROOKS, B. 2002. Pattern of cortical reorganization in amyotrophic lateral sclerosis: a functional magnetic resonance imaging study. *Exp Brain Res,* 143**,** 51-6.

KORNHUBER, H. H. & DEECKE, L. 1965. Hirnpotentialänderungen bei Willkürbewegungen und passiven Bewegungen des Menschen: Bereitschaftspotential und reafferente Potentiale. *Pflüger's Archiv für die gesamte Physiologie des Menschen und der Tiere,* 284**,** 1-17.

KRAUTH, R., SCHWERTNER, J., VOGT, S., LINDQUIST, S., SAILER, M., SICKERT, A., LAMPRECHT, J., PERDIKIS, S., CORBET, T., MILLÁN, J. D. R., HINRICHS, H., HEINZE, H.-J. & SWEENEY-REED, C. M. 2019. Cortico-Muscular Coherence Is Reduced Acutely Post-stroke and Increases Bilaterally During Motor Recovery: A Pilot Study. *Frontiers in Neurology,* 10.

KRISTEVA-FEIGE, R., FRITSCH, C., TIMMER, J. & LÜCKING, C.-H. 2002. Effects of attention and precision of exerted force on beta range EEG-EMG synchronization during a maintained motor contraction task. *Clinical Neurophysiology,* 113**,** 124-131.

KURUVILLA, M. S., GREEN, J. R., AYAZ, H. & MURMAN, D. L. 2013. Neural correlates of cognitive decline in ALS: an fNIRS study of the prefrontal cortex. *Cogn Neurosci,* 4**,** 115-21.

LACOURSE, M. G., ORR, E. L., CRAMER, S. C. & COHEN, M. J. 2005. Brain activation during execution and motor imagery of novel and skilled sequential hand movements. *Neuroimage,* 27**,** 505-19.

LAI, M., DEMURU, M., HILLEBRAND, A. & FRASCHINI, M. 2018. A comparison between scalp- and source-reconstructed EEG networks. *Scientific Reports,* 8**,** 12269.

LAJTOS, M., BARRADAS-CHACÓN, L. A. & WRIESSNEGGER, S. C. 2023. Effects of handedness on brain oscillatory activity during imagery and execution of upper limb movements. *Frontiers in Psychology,* 14.

LAKENS, D. 2013. Calculating and reporting effect sizes to facilitate cumulative science: a practical primer for t-tests and ANOVAs. *Frontiers in psychology,* 4**,** 863-863.

LANG, E. W., TOMÉ, A. M., KECK, I. R., GÓRRIZ-SÁEZ, J. M. & PUNTONET, C. G. 2012. Brain connectivity analysis: a short survey. *Comput Intell Neurosci,* 2012**,** 412512.

LATIF, L. A. 2018. 40 - Motor Neuron Diseases. *In:* CIFU, D. X. & LEW, H. L. (eds.) *Braddom's Rehabilitation Care: A Clinical Handbook.* Elsevier.

LENZI, D., CONTE, A., MAINERO, C., FRASCA, V., FUBELLI, F., TOTARO, P., CARAMIA, F., INGHILLERI, M., POZZILLI, C. & PANTANO, P. 2007. Effect of corpus callosum damage on ipsilateral motor activation in patients with multiple sclerosis: a functional and anatomical study. *Human brain mapping,* 28**,** 636-644.

LESKO, L. J. & ATKINSON, A. J., JR. 2001. Use of biomarkers and surrogate endpoints in drug development and regulatory decision making: criteria, validation, strategies. *Annu Rev Pharmacol Toxicol,* 41**,** 347-66.

LI, J., PAN, P., SONG, W., HUANG, R., CHEN, K. & SHANG, H. 2012. A meta-analysis of diffusion tensor imaging studies in amyotrophic lateral sclerosis. *Neurobiology of Aging,* 33**,** 1833-1838.

LI, N., CHEN, T. W., GUO, Z. V., GERFEN, C. R. & SVOBODA, K. 2015. A motor cortex circuit for motor planning and movement. *Nature,* 519**,** 51-6.

LI, W., WEI, Q., HOU, Y., LEI, D., AI, Y., QIN, K., YANG, J., KEMP, G. J., SHANG, H. & GONG, Q. 2021. Disruption of the white matter structural network and its correlation with baseline progression rate in patients with sporadic amyotrophic lateral sclerosis. *Translational Neurodegeneration,* 10**,** 35.

LIAO, G., TANG, Y., YU, J. & HU, S. 2020. The metabolism pattern of brain FDG-PET in amyotrophic lateral sclerosis. *Journal of Nuclear Medicine,* 61**,** 1543-1543.

LINDAU, M., JELIC, V., JOHANSSON, S. E., ANDERSEN, C., WAHLUND, L. O. & ALMKVIST, O. 2003. Quantitative EEG Abnormalities and Cognitive Dysfunctions in Frontotemporal Dementia and Alzheimer's Disease. *Dementia and Geriatric Cognitive Disorders,* 15**,** 106-114.

LIU, J., SHENG, Y. & LIU, H. 2019. Corticomuscular Coherence and Its Applications: A Review. *Frontiers in human neuroscience,* 13**,** 100-100.

LIU, J. & WANG, F. 2017. Role of Neuroinflammation in Amyotrophic Lateral Sclerosis: Cellular Mechanisms and Therapeutic Implications. *Front Immunol,* 8**,** 1005.

LIZIER, J. T., HEINZLE, J., HORSTMANN, A., HAYNES, J.-D. & PROKOPENKO, M. 2011. Multivariate information-theoretic measures reveal directed information structure and task relevant changes in fMRI connectivity. *Journal of Computational Neuroscience,* 30**,** 85-107.

LU, K., NICHOLAS, J. M., WESTON, P. S. J., STOUT, J. C., O'REGAN, A. M., JAMES, S.-N., BUCHANAN, S. M., LANE, C. A., PARKER, T. D., KEUSS, S. E., KESHAVAN, A., MURRAY-SMITH, H., CASH, D. M., SUDRE, C. H., MALONE, I. B., COATH, W., WONG, A., RICHARDS, M., HENLEY, S. M. D., FOX, N. C., SCHOTT, J. M. & CRUTCH, S. J. 2021. Visuomotor integration deficits are common to familial and sporadic preclinical Alzheimer's disease. *Brain Communications,* 3.

LULÉ, D., DIEKMANN, V., KASSUBEK, J., KURT, A., BIRBAUMER, N., LUDOLPH, A. C. & KRAFT, E. 2007. Cortical Plasticity in Amyotrophic Lateral Sclerosis: Motor Imagery and Function. *Neurorehabilitation and Neural Repair,* 21**,** 518-526.

LUNA, J., COURATIER, P., LAHMADI, S., LAUTRETTE, G., FONTANA, A., TORTELLI, R., LOGROSCINO, G., PREUX, P. M., COPETTI, M. & BENOIT, M. 2021. Comparison of the ability of the King's and MiToS staging systems to predict disease progression and survival in amyotrophic lateral sclerosis. *Amyotroph Lateral Scler Frontotemporal Degener,* 22**,** 478-485.

LUNDBERG, S. M. & LEE, S.-I. A Unified Approach to Interpreting Model Predictions. *In:* GUYON, I., LUXBURG, U. V., BENGIO, S., WALLACH, H., FERGUS, R., VISHWANATHAN, S. & GARNETT, R., eds., 2017 2017. Curran Associates, Inc.

LUO, N., SUI, J., ABROL, A., CHEN, J., TURNER, J. A., DAMARAJU, E., FU, Z., FAN, L., LIN, D., ZHUO, C., XU, Y., GLAHN, D. C., RODRIGUE, A. L., BANICH, M. T., PEARLSON, G. D. & CALHOUN, V. D. 2020. Structural Brain Architectures Match Intrinsic Functional Networks and Vary across Domains: A Study from 15 000+ Individuals. *Cerebral Cortex,* 30**,** 5460-5470.

MACHII, K., UGAWA, Y., KOKUBO, Y., SASAKI, R. & KUZUHARA, S. 2003. Somatosensory evoked potential recovery in kii amyotrophic lateral sclerosis/parkinsonism-dementia complex (kii AlS/PDC). *Clin Neurophysiol,* 114**,** 564-8.

MACHTS, J., BITTNER, V., KASPER, E., SCHUSTER, C., PRUDLO, J., ABDULLA, S., KOLLEWE, K., PETRI, S., DENGLER, R., HEINZE, H.-J., VIELHABER, S., SCHOENFELD, M. A. & BITTNER, D. M. 2014. Memory deficits in amyotrophic lateral sclerosis are not exclusively caused by executive dysfunction: a comparative

neuropsychological study of amnestic mild cognitive impairment. *BMC neuroscience,* 15**,** 83-83.

MACHTS, J., KEUTE, M., KAUFMANN, J., SCHREIBER, S., KASPER, E., PETRI, S., PRUDLO, J., VIELHABER, S. & SCHOENFELD, M. A. 2020. Longitudinal clinical and neuroanatomical correlates of memory impairment in motor neuron disease. *NeuroImage. Clinical,* 29**,** 102545-102545.

MACKENZIE, T. N., BAILEY, A. Z., MI, P. Y., TSANG, P., JONES, C. B. & NELSON, A. J. 2016. Human area 5 modulates corticospinal output during movement preparation. *Neuroreport,* 27**,** 1056-60.

MAIER, M. A., ARMAND, J., KIRKWOOD, P. A., YANG, H. W., DAVIS, J. N. & LEMON, R. N. 2002. Differences in the corticospinal projection from primary motor cortex and supplementary motor area to macaque upper limb motoneurons: an anatomical and electrophysiological study. *Cereb Cortex,* 12**,** 281-96.

MANNARELLI, D., PAULETTI, C., LOCURATOLO, N., VANACORE, N., FRASCA, V., TREBBASTONI, A., INGHILLERI, M. & FATTAPPOSTA, F. 2014. Attentional processing in bulbar- and spinal-onset amyotrophic lateral sclerosis: Insights from event-related potentials. *Amyotrophic Lateral Sclerosis and Frontotemporal Degeneration,* 15**,** 30-38.

MAREK, S. & DOSENBACH, N. U. F. 2018. The frontoparietal network: function, electrophysiology, and importance of individual precision mapping. *Dialogues Clin Neurosci,* 20**,** 133-140.

MARIN, B., BOUMÉDIENE, F., LOGROSCINO, G., COURATIER, P., BABRON, M. C., LEUTENEGGER, A. L., COPETTI, M., PREUX, P. M. & BEGHI, E. 2017. Variation in worldwide incidence of amyotrophic lateral sclerosis: a meta-analysis. *Int J Epidemiol,* 46**,** 57-74.

MARIN, B., FONTANA, A., ARCUTI, S., COPETTI, M., BOUMÉDIENE, F., COURATIER, P., BEGHI, E., PREUX, P. M. & LOGROSCINO, G. 2018. Age-specific ALS incidence: a dose-response meta-analysis. *Eur J Epidemiol,* 33**,** 621-634.

MARZETTI, L., BASTI, A., CHELLA, F., D'ANDREA, A., SYRJÄLÄ, J. & PIZZELLA, V. 2019. Brain Functional Connectivity Through Phase Coupling of Neuronal Oscillations: A Perspective From Magnetoencephalography. *Front Neurosci,* 13**,** 964.

MASUDA, N., SAKAKI, M., EZAKI, T. & WATANABE, T. 2018. Clustering Coefficients for Correlation Networks. *Frontiers in Neuroinformatics,* 12.

MAURITZ, K. H. & WISE, S. P. 1986. Premotor cortex of the rhesus monkey: neuronal activity in anticipation of predictable environmental events. *Experimental Brain Research,* 61**,** 229-244.

MCCOMAS, A. J., FAWCETT, P. R. W., CAMPBELL, M. J. & SICA, R. E. P. 1971. Electrophysiological estimation of the number of motor units within a human muscle. *Journal of Neurology, Neurosurgery & Psychiatry,* 34**,** 121-131.

MCCOMBE, P. A. & HENDERSON, R. D. 2010. Effects of gender in amyotrophic lateral sclerosis. *Gender Medicine,* 7**,** 557-570.

MCFARLAND, D. J., MCCANE, L. M., DAVID, S. V. & WOLPAW, J. R. 1997. Spatial filter selection for EEG-based communication. *Electroencephalography and Clinical Neurophysiology,* 103**,** 386-394.

MCKAY, K. A., SMITH, K. A., SMERTINAITE, L., FANG, F., INGRE, C. & TAUBE, F. 2021. Military service and related risk factors for amyotrophic lateral sclerosis. *Acta Neurol Scand,* 143**,** 39-50.

MCMACKIN, R., DUKIC, S., BRODERICK, M., IYER, P. M., PINTO-GRAU, M., MOHR, K., CHIPIKA, R., COFFEY, A., BUXO, T., SCHUSTER, C., GAVIN, B., HEVERIN, M., BEDE, P., PENDER, N., LALOR, E. C., MUTHURAMAN, M., HARDIMAN, O. & NASSEROLESLAMI, B. 2019a. Dysfunction of attention switching networks in amyotrophic lateral sclerosis. *NeuroImage: Clinical,* 22**,** 101707.

MCMACKIN, R., DUKIC, S., COSTELLO, E., PINTO-GRAU, M., FASANO, A., BUXO, T., HEVERIN, M., REILLY, R., MUTHURAMAN, M., PENDER, N., HARDIMAN, O. & NASSEROLESLAMI, B. 2020. Localization of Brain Networks Engaged by the Sustained Attention to Response Task Provides Quantitative Markers of Executive Impairment in Amyotrophic Lateral Sclerosis. *Cereb Cortex,* 30**,** 4834-4846.

MCMACKIN, R., DUKIC, S., COSTELLO, E., PINTO-GRAU, M., MCMANUS, L., BRODERICK, M., CHIPIKA, R., IYER, P. M., HEVERIN, M., BEDE, P., MUTHURAMAN, M., PENDER, N., HARDIMAN, O. & NASSEROLESLAMI, B. 2021. Cognitive network hyperactivation and motor cortex decline correlate with ALS prognosis. *Neurobiology of Aging,* 104**,** 57-70.

MCMACKIN, R., MUTHURAMAN, M., GROPPA, S., BABILONI, C., TAYLOR, J.-P., KIERNAN, M. C., NASSEROLESLAMI, B. & HARDIMAN, O. 2019b. Measuring network disruption in neurodegenerative diseases: New approaches using signal analysis. *Journal of Neurology, Neurosurgery & Psychiatry,* 90**,** 1011-1020.

MEDAGLIA, J. D. 2017. Graph Theoretic Analysis of Resting State Functional MR Imaging. *Neuroimaging Clin N Am,* 27**,** 593-607.

MEDENDORP, W. P., GOLTZ, H. C., VILIS, T. & CRAWFORD, J. D. 2003. Gaze-centered updating of visual space in human parietal cortex. *J Neurosci,* 23**,** 6209-14.

MEHTA, P. R., IACOANGELI, A., OPIE-MARTIN, S., VAN VUGT, J. J. F. A., AL KHLEIFAT, A., BREDIN, A., OSSHER, L., ANDERSEN, P. M., HARDIMAN, O., MEHTA, A. R., FRATTA, P., TALBOT, K., CONSORTIUM, P. M. A. S. & AL-CHALABI, A. 2022. The impact of age on genetic testing decisions in amyotrophic lateral sclerosis. *Brain,* 145**,** 4440-4447.

MENG, F., TONG, K.-Y., CHAN, S.-T., WONG, W.-W., LUI, K.-H., TANG, K.-W., GAO, X. & GAO, S. 2008. Study on connectivity between coherent central rhythm and electromyographic activities. *Journal of Neural Engineering,* 5**,** 324.

MENG, F., TONG, K. Y., CHAN, S. T., WONG, W. W., LUI, K. H., TANG, K. W., GAO, X. & GAO, S. 2009. Cerebral plasticity after subcortical stroke as revealed by cortico-muscular coherence. *IEEE Trans Neural Syst Rehabil Eng,* 17**,** 234-43.

MENKE, R., PROUDFOOT, M., TALBOT, K. & TURNER, M. 2018. The two-year progression of structural and functional cerebral MRI in amyotrophic lateral sclerosis. *NeuroImage: Clinical,* 17**,** 953-961.

MENKE, R. A. L., AGOSTA, F., GROSSKREUTZ, J., FILIPPI, M. & TURNER, M. R. 2017. Neuroimaging Endpoints in Amyotrophic Lateral Sclerosis. *Neurotherapeutics,* 14**,** 11-23.

MENON, P., HIGASHIHARA, M., VAN DEN BOS, M., GEEVASINGA, N., KIERNAN, M. C. & VUCIC, S. 2020. Cortical hyperexcitability evolves with disease progression in ALS. *Ann Clin Transl Neurol,* 7**,** 733-741.

MENON, P., KIERNAN, M. C. & VUCIC, S. 2015. Cortical hyperexcitability precedes lower motor neuron dysfunction in ALS. *Clinical Neurophysiology,* 126**,** 803-809.

MEODED, A., MORRISSETTE, A. E., KATIPALLY, R., SCHANZ, O., GOTTS, S. J. & FLOETER, M. K. 2015. Cerebro-cerebellar connectivity is increased in primary lateral sclerosis. *Neuroimage Clin,* 7**,** 288-96.

METWALLI, N. S., BENATAR, M., NAIR, G., USHER, S., HU, X. & CAREW, J. D. 2010. Utility of axial and radial diffusivity from diffusion tensor MRI as markers of neurodegeneration in amyotrophic lateral sclerosis. *Brain Research,* 1348**,** 156-164.

MILLER, E. K. & COHEN, J. D. 2001. An Integrative Theory of Prefrontal Cortex Function. *Annual Review of Neuroscience,* 24**,** 167-202.

MOISA, M., POLANIA, R., GRUESCHOW, M. & RUFF, C. C. 2016. Brain Network Mechanisms Underlying Motor Enhancement by Transcranial Entrainment of Gamma Oscillations. *J Neurosci,* 36**,** 12053-12065.

MÜLLER, H.-P., TURNER, M. R., GROSSKREUTZ, J., ABRAHAMS, S., BEDE, P., GOVIND, V., PRUDLO, J., LUDOLPH, A. C., FILIPPI, M. & KASSUBEK, J. 2016. A large-scale multicentre cerebral diffusion tensor imaging study in amyotrophic lateral sclerosis. *Journal of Neurology, Neurosurgery & Psychiatry,* 87**,** 570-579.

MURPHY, N. A., ARTHUR, K. C., TIENARI, P. J., HOULDEN, H., CHIÒ, A. & TRAYNOR, B. J. 2017. Age-related penetrance of the C9orf72 repeat expansion. *Sci Rep,* 7**,** 2116.

MURRAY, E. A. & COULTER, J. D. 1981. Organization of corticospinal neurons in the monkey. *J Comp Neurol,* 195**,** 339-65.

MUTHUKUMARASWAMY, S. D. 2010. Functional Properties of Human Primary Motor Cortex Gamma Oscillations. *Journal of Neurophysiology,* 104**,** 2873-2885.

NAKAYASHIKI, K., TOJIKI, H., HAYASHI, Y., YANO, S. & KONDO, T. 2021. Brain Processes Involved in Motor Planning Are a Dominant Factor for Inducing Event-Related Desynchronization. *Frontiers in Human Neuroscience,* 15.

NANDEDKAR, S. D., NANDEDKAR, D. S., BARKHAUS, P. E. & STALBERG, E. V. 2004. Motor unit number index (MUNIX). *IEEE Transactions on Biomedical Engineering,* 51**,** 2209-2211.

NARDONE, R., GOLASZEWSKI, S., THOMSCHEWSKI, A., SEBASTIANELLI, L., VERSACE, V., BRIGO, F., ORIOLI, A., SALTUARI, L., HÖLLER, Y. & TRINKA, E. 2020. Disinhibition of sensory cortex in patients with amyotrophic lateral sclerosis. *Neuroscience Letters,* 722**,** 134860.

NASSEROLESLAMI, B. 2019. An Implementation of Empirical Bayesian Inference and Non-Null Bootstrapping for Threshold Selection and Power Estimation in Multiple and Single Statistical Testing. *bioRxiv***,** 342964.

NASSEROLESLAMI, B., DUKIC, S., BRODERICK, M., MOHR, K., SCHUSTER, C., GAVIN, B., MCLAUGHLIN, R., HEVERIN, M., VAJDA, A., IYER, P., PENDER, N., BEDE, P., LALOR, E. & HARDIMAN, O. 2018. Decreased EEG Spectral Power and Increased Cortico-Cortical Connectivity Correlate with Structural MRI Changes in Amyotrophic Lateral Sclerosis (P2.036). *Neurology,* 90**,** P2.036.

NASSEROLESLAMI, B., DUKIC, S., BRODERICK, M., MOHR, K., SCHUSTER, C., GAVIN, B., MCLAUGHLIN, R., HEVERIN, M., VAJDA, A., IYER, P. M., PENDER, N., BEDE, P., LALOR, E. C. & HARDIMAN, O. 2017. Characteristic Increases in EEG Connectivity Correlate With Changes of Structural MRI in Amyotrophic Lateral Sclerosis. *Cerebral Cortex,* 29**,** 27-41.

NASSEROLESLAMI, B., DUKIC, S., BUXO, T., COFFEY, A., MCMACKIN, R., MUTHURAMAN, M., HARDIMAN, O., LOWERY, M. M. & LALOR, E. C. 2019. Non-Parametric Rank Statistics for Spectral Power and Coherence. *bioRxiv***,** 818906.

NASSEROLESLAMI, B., LAKANY, H. & CONWAY, B. A. 2014. EEG signatures of arm isometric exertions in preparation, planning and execution. *Neuroimage,* 90**,** 1-14.

NEUPER, C., WÖRTZ, M. & PFURTSCHELLER, G. 2006. ERD/ERS patterns reflecting sensorimotor activation and deactivation. *In:* NEUPER, C. & KLIMESCH, W. (eds.) *Progress in Brain Research.* Elsevier.

NIINIMAA, A. & OJA, H. 2014. Multivariate Median. *Encyclopedia of Statistical Sciences.* Wiley StatsRef: Statistics Reference Online.

NOLTE, G., BAI, O., WHEATON, L., MARI, Z., VORBACH, S. & HALLETT, M. 2004. Identifying true brain interaction from EEG data using the imaginary part of coherency. *Clinical neurophysiology,* 115**,** 2292-2307.

NORDHAUSEN, K. & OJA, H. 2011. Multivariate L1 Statistical Methods: The Package MNM. *Journal of Statistical Software,* 43**,** 1 - 28.

NUNEZ, P. L. 1995. Neocortical dynamics and human EEG rhythms. *(No Title).*

NUNEZ, P. L. & SRINIVASAN, R. 2006. *Electric fields of the brain: the neurophysics of EEG,* Oxford University Press, USA.

NUNEZ, P. L., SRINIVASAN, R., WESTDORP, A. F., WIJESINGHE, R. S., TUCKER, D. M., SILBERSTEIN, R. B. & CADUSCH, P. J. 1997. EEG coherency: I: statistics, reference electrode, volume conduction, Laplacians, cortical imaging, and interpretation at multiple scales. *Electroencephalography and Clinical Neurophysiology,* 103**,** 499-515.

NZWALO, H., DE ABREU, D., SWASH, M., PINTO, S. & DE CARVALHO, M. 2014. Delayed diagnosis in ALS: The problem continues. *Journal of the Neurological Sciences,* 343**,** 173-175.

OGAKI, K., LI, Y., ATSUTA, N., TOMIYAMA, H., FUNAYAMA, M., WATANABE, H., NAKAMURA, R., YOSHINO, H., YATO, S., TAMURA, A., NAITO, Y., TANIGUCHI, A., FUJITA, K., IZUMI, Y., KAJI, R., HATTORI, N. & SOBUE, G. 2012. Analysis of C9orf72 repeat expansion in 563 Japanese patients with amyotrophic lateral sclerosis. *Neurobiol Aging,* 33**,** 2527.e11-6.

OGAWA, S., LEE, T. M., KAY, A. R. & TANK, D. W. 1990. Brain magnetic resonance imaging with contrast dependent on blood oxygenation. *Proc Natl Acad Sci U S A,* 87**,** 9868-72.

OHARA, S., MIMA, T., BABA, K., IKEDA, A., KUNIEDA, T., MATSUMOTO, R., YAMAMOTO, J., MATSUHASHI, M., NAGAMINE, T., HIRASAWA, K., HORI, T., MIHARA, T., HASHIMOTO, N., SALENIUS, S. & SHIBASAKI, H. 2001. Increased synchronization of cortical oscillatory activities between human supplementary motor and primary sensorimotor areas during voluntary movements. *J Neurosci,* 21**,** 9377-86.

OHARA, S., NAGAMINE, T., IKEDA, A., KUNIEDA, T., MATSUMOTO, R., TAKI, W., HASHIMOTO, N., BABA, K., MIHARA, T., SALENIUS, S. & SHIBASAKI, H. 2000. Electrocorticogram–electromyogram coherence during isometric contraction of hand muscle in human. *Clinical Neurophysiology,* 111**,** 2014-2024.

OISHI, K., MIELKE, M. M., ALBERT, M., LYKETSOS, C. G. & MORI, S. 2011. DTI analyses and clinical applications in Alzheimer's disease. *J Alzheimers Dis,* 26 Suppl 3**,** 287-96.

OJA, H. 2010. Multivariate signs and ranks. *In:* OJA, H. (ed.) *Multivariate Nonparametric Methods with R: An approach based on spatial signs and ranks.* New York, NY: Springer New York.

OJA, H. & RANDLES, R. H. 2004. Multivariate Nonparametric Tests. *Statistical Science,* 19**,** 598-605, 8.

OLDFIELD, R. C. 1971. The assessment and analysis of handedness: The Edinburgh inventory. *Neuropsychologia,* 9**,** 97-113.

OMLOR, W., PATINO, L., HEPP-REYMOND, M. C. & KRISTEVA, R. 2007. Gamma-range corticomuscular coherence during dynamic force output. *Neuroimage,* 34**,** 1191-8.

OOSTENVELD, R., FRIES, P., MARIS, E. & SCHOFFELEN, J.-M. 2011. FieldTrip: Open Source Software for Advanced Analysis of MEG, EEG, and Invasive Electrophysiological Data. *Computational Intelligence and Neuroscience,* 2011**,** 156869.

OSTWALD, D. & BAGSHAW, A. P. 2011. Information theoretic approaches to functional neuroimaging. *Magnetic Resonance Imaging,* 29**,** 1417-1428.

PAPITTO, G., FRIEDERICI, A. D. & ZACCARELLA, E. 2020. The topographical organization of motor processing: An ALE meta-analysis on six action domains and the relevance of Broca's region. *NeuroImage,* 206**,** 116321.

PARAKH, S. & ATKIN, J. D. 2016. Protein folding alterations in amyotrophic lateral sclerosis. *Brain Res,* 1648**,** 633-649.

PASSOW, S., SPECHT, K., ADAMSEN, T. C., BIERMANN, M., BREKKE, N., CRAVEN, A. R., ERSLAND, L., GRÜNER, R., KLEVEN-MADSEN, N., KVERNENES, O. H., SCHWARZLMÜLLER, T., OLESEN, R. A. & HUGDAHL, K. 2015. Default-mode network functional connectivity is closely related to metabolic activity. *Hum Brain Mapp,* 36**,** 2027-38.

PELLIJEFF, A., BONILHA, L., MORGAN, P. S., MCKENZIE, K. & JACKSON, S. R. 2006. Parietal updating of limb posture: An event-related fMRI study. *Neuropsychologia,* 44**,** 2685-2690.

PENDER, N., PINTO-GRAU, M. & HARDIMAN, O. 2020. Cognitive and behavioural impairment in amyotrophic lateral sclerosis. *Current Opinion in Neurology,* 33**,** 649-654.

PENFIELD, W. & BOLDREY, E. 1937. Somatic motor and sensory representation in the cerebral cortex of man as studied by electrical stimulation. *Brain,* 60**,** 389-443.

PERRIN, F., PERNIER, J., BERTRAND, O. & ECHALLIER, J. F. 1989. Spherical splines for scalp potential and current density mapping. *Electroencephalography and Clinical Neurophysiology,* 72**,** 184-187.

PETER, J., FERRAIOLI, F., MATHEW, D., GEORGE, S., CHAN, C., ALALADE, T., SALCEDO, S. A., SAED, S., TATTI, E., QUARTARONE, A. & GHILARDI, M. F. 2022. Movement-related beta ERD and ERS abnormalities in neuropsychiatric disorders. *Frontiers in neuroscience,* 16.

PFURTSCHELLER, G. & BERGHOLD, A. 1989. Patterns of cortical activation during planning of voluntary movement. *Electroencephalography and Clinical Neurophysiology,* 72**,** 250-258.

PFURTSCHELLER, G. & LOPES DA SILVA, F. H. 1999. Event-related EEG/MEG synchronization and desynchronization: basic principles. *Clinical Neurophysiology,* 110**,** 1842-1857.

PHILIPS, T. & ROTHSTEIN, J. D. 2014. Glial cells in amyotrophic lateral sclerosis. *Exp Neurol,* 262 Pt B**,** 111-20.

PINTI, P., TACHTSIDIS, I., HAMILTON, A., HIRSCH, J., AICHELBURG, C., GILBERT, S. & BURGESS, P. W. 2020. The present and future use of functional near-infrared spectroscopy (fNIRS) for cognitive neuroscience. *Annals of the New York Academy of Sciences,* 1464**,** 5-29.

PINTO-GRAU, M., BURKE, T., LONERGAN, K., MCHUGH, C., MAYS, I., MADDEN, C., VAJDA, A., HEVERIN, M., ELAMIN, M., HARDIMAN, O. & PENDER, N. 2017. Screening for cognitive dysfunction in ALS: validation of the Edinburgh Cognitive and Behavioural ALS Screen (ECAS) using age and education adjusted normative data. *Amyotroph Lateral Scler Frontotemporal Degener,* 18**,** 99-106.

PISHARADY, P. K., EBERLY, L. E., ADANYEGUH, I. M., MANOUSAKIS, G., GULIANI, G., WALK, D. & LENGLET, C. 2023. Multimodal MRI improves diagnostic accuracy and sensitivity to longitudinal change in amyotrophic lateral sclerosis. *Communications Medicine,* 3**,** 84.

POUJOIS, A., SCHNEIDER, F., FAILLENOT, I., CAMDESSANCHÉ, J.-P., VANDENBERGHE, N., THOMAS-ANTÉRION, C. & ANTOINE, J.-C. 2013. Brain plasticity in the motor network is correlated with disease progression in amyotrophic lateral sclerosis. *Human brain mapping,* 34.

PRAK, R. F., MARSMAN, J.-B. C., RENKEN, R., TEPPER, M., THOMAS, C. K. & ZIJDEWIND, I. 2021. Increased Ipsilateral M1 Activation after Incomplete Spinal Cord Injury Facilitates Motor Performance. *Journal of Neurotrauma,* 38**,** 2988-2998.

PROUDFOOT, M., BEDE, P. & TURNER, M. R. 2019. Imaging Cerebral Activity in Amyotrophic Lateral Sclerosis. *Frontiers in neurology,* 9**,** 1148-1148.

PROUDFOOT, M., COLCLOUGH, G. L., QUINN, A., WUU, J., TALBOT, K., BENATAR, M., NOBRE, A. C., WOOLRICH, M. W. & TURNER, M. R. 2018a. Increased cerebral functional connectivity in ALS. *A resting-state magnetoencephalography study,* 90**,** e1418-e1424.

PROUDFOOT, M., ROHENKOHL, G., QUINN, A., COLCLOUGH, G. L., WUU, J., TALBOT, K., WOOLRICH, M. W., BENATAR, M., NOBRE, A. C. & TURNER, M. R. 2017. Altered cortical beta-band oscillations reflect motor system degeneration in amyotrophic lateral sclerosis. *Human Brain Mapping,* 38**,** 237-254.

PROUDFOOT, M., VAN EDE, F., QUINN, A., COLCLOUGH, G. L., WUU, J., TALBOT, K., BENATAR, M., WOOLRICH, M. W., NOBRE, A. C. & TURNER, M. R. 2018b. Impaired corticomuscular and interhemispheric cortical beta

oscillation coupling in amyotrophic lateral sclerosis. *Clin Neurophysiol,* 129**,** 1479-1489.

PUGDAHL, K., CAMDESSANCHÉ, J. P., CENGIZ, B., DE CARVALHO, M., LIGUORI, R., ROSSATTO, C., OLIVEIRA SANTOS, M., VACCHIANO, V. & JOHNSEN, B. 2021. Gold Coast diagnostic criteria increase sensitivity in amyotrophic lateral sclerosis. *Clin Neurophysiol,* 132**,** 3183-3189.

RADDA, G. K., RAJAGOPALAN, B. & TAYLOR, D. J. 1989. Biochemistry in vivo: an appraisal of clinical magnetic resonance spectroscopy. *Magn Reson Q,* 5**,** 122-51.

RAICHLE, M. E. 1998. Behind the scenes of functional brain imaging: a historical and physiological perspective. *Proc Natl Acad Sci U S A,* 95**,** 765-72.

RAICHLE, M. E., MACLEOD, A. M., SNYDER, A. Z., POWERS, W. J., GUSNARD, D. A. & SHULMAN, G. L. 2001. A default mode of brain function. *Proc Natl Acad Sci U S A,* 98**,** 676-82.

RAICHLE, M. E. & MINTUN, M. A. 2006. BRAIN WORK AND BRAIN IMAGING. *Annual Review of Neuroscience,* 29**,** 449-476.

RAVITS, J. M. & LA SPADA, A. R. 2009. ALS motor phenotype heterogeneity, focality, and spread: deconstructing motor neuron degeneration. *Neurology,* 73**,** 805-11.

RENGA, V. 2022. Brain Connectivity and Network Analysis in Amyotrophic Lateral Sclerosis. *Neurol Res Int,* 2022**,** 1838682.

REQUIN, J., LECAS, J.-C. & VITTON, N. 1990. A comparison of preparation-related neuronal activity changes in the prefrontal, premotor, primary motor and posterior parietal areas of the monkey cortex: preliminary results. *Neuroscience Letters,* 111**,** 151-156.

RICHARDS, D., MORREN, J. A. & PIORO, E. P. 2020. Time to diagnosis and factors affecting diagnostic delay in amyotrophic lateral sclerosis. *Journal of the Neurological Sciences,* 417.

RIEHLE, A. 2005. Preparation for action: one of the key functions of the motor cortex. *Motor cortex in voluntary movements: A distributed system for distributed functions,* 33**,** 213-240.

RIQUELME, I., CIFRE, I., MUÑOZ, M. A. & MONTOYA, P. 2014. Altered corticomuscular coherence elicited by paced isotonic contractions in individuals with cerebral palsy: A case-control study. *Journal of Electromyography and Kinesiology,* 24**,** 928-933.

RIVA, N., FALINI, A., INUGGI, A., GONZALEZ-ROSA, J. J., AMADIO, S., CERRI, F., FAZIO, R., DEL CARRO, U., COMOLA, M., COMI, G. & LEOCANI, L. 2012. Cortical activation to voluntary movement in amyotrophic lateral sclerosis is related to corticospinal damage: electrophysiological evidence. *Clin Neurophysiol,* 123**,** 1586-92.

ROBERTS, R. E., ANDERSON, E. J. & HUSAIN, M. 2013. White matter microstructure and cognitive function. *Neuroscientist,* 19**,** 8-15.

ROCHE, J. C., ROJAS-GARCIA, R., SCOTT, K. M., SCOTTON, W., ELLIS, C. E., BURMAN, R., WIJESEKERA, L., TURNER, M. R., LEIGH, P. N., SHAW, C. E. & AL-CHALABI, A. 2012. A proposed staging system for amyotrophic lateral sclerosis. *Brain,* 135**,** 847-52.

RODRÍGUEZ-PÉREZ, R. & BAJORATH, J. 2020. Interpretation of machine learning models using shapley values: application to compound potency and multi-target activity predictions. *Journal of Computer-Aided Molecular Design,* 34**,** 1013-1026.

ROEDER, L., BOONSTRA, T. W. & KERR, G. K. 2020. Corticomuscular control of walking in older people and people with Parkinson's disease. *Scientific Reports,* 10**,** 2980.

ROJAS, P., RAMÍREZ, A. I., FERNÁNDEZ-ALBARRAL, J. A., LÓPEZ-CUENCA, I., SALOBRAR-GARCÍA, E., CADENA, M., ELVIRA-HURTADO, L., SALAZAR, J. J., DE HOZ, R. & RAMÍREZ, J. M. 2020. Amyotrophic Lateral Sclerosis: A Neurodegenerative Motor Neuron Disease With Ocular Involvement. *Frontiers in Neuroscience,* 14.

ROMANO, A., TROSI LOPEZ, E., LIPAROTI, M., POLVERINO, A., MININO, R., TROJSI, F., BONAVITA, S., MANDOLESI, L., GRANATA, C., AMICO, E., SORRENTINO, G. & SORRENTINO, P. 2022. The progressive loss of brain network fingerprints in Amyotrophic Lateral Sclerosis predicts clinical impairment. *NeuroImage: Clinical,* 35**,** 103095.

ROSSITER, H. E., EAVES, C., DAVIS, E., BOUDRIAS, M.-H., PARK, C.-H., FARMER, S., BARNES, G., LITVAK, V. & WARD, N. S. 2013. Changes in the location of cortico-muscular coherence following stroke. *NeuroImage: Clinical,* 2**,** 50-55.

ROWE, J. B., STEPHAN, K. E., FRISTON, K., FRACKOWIAK, R. S. J. & PASSINGHAM, R. E. 2004. The Prefrontal Cortex shows Context-specific Changes in Effective Connectivity to Motor or Visual Cortex during the Selection of Action or Colour. *Cerebral Cortex,* 15**,** 85-95.

RUBINOV, M. & BULLMORE, E. 2013. Schizophrenia and abnormal brain network hubs. *Dialogues Clin Neurosci,* 15**,** 339-49.

RUIZ-GÓMEZ, S. J., HORNERO, R., POZA, J., MATURANA-CANDELAS, A., PINTO, N. & GÓMEZ, C. 2019. Computational modeling of the effects of EEG volume conduction on functional connectivity metrics. Application to Alzheimer's disease continuum. *Journal of Neural Engineering,* 16**,** 066019.

RYAN, M., HEVERIN, M., DOHERTY, M. A., DAVIS, N., CORR, E. M., VAJDA, A., PENDER, N., MCLAUGHLIN, R. & HARDIMAN, O. 2018. Determining the incidence of familiality in ALS: A study of temporal trends in Ireland from 1994 to 2016. *Neurol Genet,* 4**,** e239.

RYAN, M., HEVERIN, M., MCLAUGHLIN, R. L. & HARDIMAN, O. 2019. Lifetime Risk and Heritability of Amyotrophic Lateral Sclerosis. *JAMA Neurol,* 76**,** 1367-1374.

SADAGHIANI, S., BROOKES, M. J. & BAILLET, S. 2022. Connectomics of human electrophysiology. *Neuroimage,* 247**,** 118788.

SAGE, C. A., VAN HECKE, W., PEETERS, R., SIJBERS, J., ROBBERECHT, W., PARIZEL, P., MARCHAL, G., LEEMANS, A. & SUNAERT, S. 2009. Quantitative diffusion tensor imaging in amyotrophic lateral sclerosis: revisited. *Hum Brain Mapp,* 30**,** 3657-75.

SALENIUS, S., AVIKAINEN, S., KAAKKOLA, S., HARI, R. & BROWN, P. 2002. Defective cortical drive to muscle in Parkinson's disease and its improvement with levodopa. *Brain,* 125**,** 491-500.

SANDER, C. Y. & HESSE, S. 2017. News and views on in-vivo imaging of neurotransmission using PET and MRI. *Q J Nucl Med Mol Imaging,* 61**,** 414-428.

SANEI, S. & CHAMBERS, J. A. 2007. Introduction to EEG. *EEG Signal Processing.*

SANTARNECCHI, E., BIASELLA, A., TATTI, E., ROSSI, A., PRATTICHIZZO, D. & ROSSI, S. 2017. High-gamma oscillations in the motor cortex during visuo-motor coordination: A tACS interferential study. *Brain Res Bull,* 131**,** 47-54.

SARICA, A., CERASA, A., VALENTINO, P., YEATMAN, J., TROTTA, M., BARONE, S., GRANATA, A., NISTICÒ, R., PERROTTA, P., PUCCI, F. & QUATTRONE, A. 2017. The corticospinal tract profile in amyotrophic lateral sclerosis. *Human Brain Mapping,* 38**,** 727-739.

SARICA, A., CERASA, A., VASTA, R., PERROTTA, P., VALENTINO, P., MANGONE, G., GUZZI, P. H., ROCCA, F., NONNIS, M., CANNATARO, M. & QUATTRONE, A. 2014. Tractography in amyotrophic lateral sclerosis using a novel probabilistic tool: A study with tract-based reconstruction compared to voxel-based approach. *Journal of Neuroscience Methods,* 224**,** 79-87.

SATO, J. R., TAKAHASHI, D. Y., ARCURI, S. M., SAMESHIMA, K., MORETTIN, P. A. & BACCALÁ, L. A. 2009. Frequency domain connectivity identification: an application of partial directed coherence in fMRI. *Human brain mapping,* 30**,** 452-461.

SAUSENG, P., KLIMESCH, W., SCHABUS, M. & DOPPELMAYR, M. 2005. Fronto-parietal EEG coherence in theta and upper alpha reflect central executive functions of working memory. *Int J Psychophysiol,* 57**,** 97-103.

SCHAWORONKOW, N. & NIKULIN, V. V. 2022. Is sensor space analysis good enough? Spatial patterns as a tool for assessing spatial mixing of EEG/MEG rhythms. *NeuroImage,* 253**,** 119093.

SCHERR, M., UTZ, L., TAHMASIAN, M., PASQUINI, L., GROTHE, M. J., RAUSCHECKER, J. P., GRIMMER, T., DRZEZGA, A., SORG, C. & RIEDL, V. 2021. Effective connectivity in the default mode network is distinctively disrupted in Alzheimer's disease-A simultaneous resting-state FDG-PET/fMRI study. *Human brain mapping,* 42**,** 4134-4143.

SCHIEL, K. A. 2021. A beneficial role for elevated extracellular glutamate in Amyotrophic Lateral Sclerosis and cerebral ischemia. *BioEssays,* 43**,** 2100127.

SCHMIDT, R., VERSTRAETE, E., DE REUS, M. A., VELDINK, J. H., VAN DEN BERG, L. H. & VAN DEN HEUVEL, M. P. 2014. Correlation between structural and functional connectivity impairment in amyotrophic lateral sclerosis. *Hum Brain Mapp,* 35**,** 4386-95.

SCHOENFELD, M. A., TEMPELMANN, C., GAUL, C., KÜHNEL, G. R., DÜZEL, E., HOPF, J. M., FEISTNER, H., ZIERZ, S., HEINZE, H. J. & VIELHABER, S. 2005. Functional motor compensation in amyotrophic lateral sclerosis. *Journal of Neurology,* 252**,** 944-952.

SCHOFFELEN, J. M. & GROSS, J. 2009. Source connectivity analysis with MEG and EEG. *Hum Brain Mapp,* 30**,** 1857-65.

SCHOFFELEN, J. M., OOSTENVELD, R. & FRIES, P. 2005. Neuronal coherence as a mechanism of effective corticospinal interaction. *Science,* 308**,** 111-3.

SCHOONHOVEN, D. N., BRIELS, C. T., HILLEBRAND, A., SCHELTENS, P., STAM, C. J. & GOUW, A. A. 2022. Sensitive and reproducible MEG resting-state metrics of functional connectivity in Alzheimer's disease. *Alzheimer's Research & Therapy,* 14**,** 38.

SCHREIBER, T. 2000. Measuring Information Transfer. *Physical Review Letters,* 85**,** 461-464.

SCHUSTER, C., HARDIMAN, O. & BEDE, P. 2017. Survival prediction in Amyotrophic lateral sclerosis based on MRI measures and clinical characteristics. *BMC Neurology,* 17**,** 73.

SERKOVA, N. J. & BROWN, M. S. 2012. Quantitative analysis in magnetic resonance spectroscopy: from metabolic profiling to in vivo biomarkers. *Bioanalysis,* 4**,** 321-341.

SETH, A. K., BARRETT, A. B. & BARNETT, L. 2015. Granger Causality Analysis in Neuroscience and Neuroimaging. *The Journal of Neuroscience,* 35**,** 3293-3297.

SHAHBAZI, F., EWALD, A., ZIEHE, A. & NOLTE, G. Constructing Surrogate Data to Control for Artifacts of Volume Conduction for Functional Connectivity Measures. *In:* SUPEK, S. & SUŠAC, A., eds. 17th International Conference on Biomagnetism Advances in Biomagnetism – Biomag2010, 2010// 2010 Berlin, Heidelberg. Springer Berlin Heidelberg, 207-210.

SHAHRIZAILA, N., SOBUE, G., KUWABARA, S., KIM, S. H., BIRKS, C., FAN, D. S., BAE, J. S., HU, C. J., GOURIE-DEVI, M., NOTO, Y., SHIBUYA, K., GOH, K. J., KAJI, R., TSAI, C., CUI, L., TALMAN, P., HENDERSON, R. D., VUCIC, S. & KIERNAN, M. C. 2016. Amyotrophic lateral sclerosis and motor neuron syndromes in Asia. *Journal of Neurology, Neurosurgery & Psychiatry,* 87**,** 821-830.

SHEFNER, J. M., AL-CHALABI, A., BAKER, M. R., CUI, L.-Y., DE CARVALHO, M., EISEN, A., GROSSKREUTZ, J., HARDIMAN, O., HENDERSON, R., MATAMALA, J. M., MITSUMOTO, H., PAULUS, W., SIMON, N., SWASH, M., TALBOT, K., TURNER, M. R., UGAWA, Y., VAN DEN BERG, L. H., VERDUGO, R., VUCIC, S., KAJI, R., BURKE, D. & KIERNAN, M. C. 2020. A proposal for new diagnostic criteria for ALS. *Clinical Neurophysiology,* 131**,** 1975-1978.

SHEN, D., YANG, X., WANG, Y., HE, D., SUN, X., CAI, Z., LI, J., LIU, M. & CUI, L. 2021. The Gold Coast criteria increases the diagnostic sensitivity for amyotrophic lateral sclerosis in a Chinese population. *Translational Neurodegeneration,* 10**,** 28.

SHEN, K.-K., WELTON, T., LYON, M., MCCORKINDALE, A. N., SUTHERLAND, G. T., BURNHAM, S., FRIPP, J., MARTINS, R. & GRIEVE, S. M. 2020. Structural core of the executive control network: A high angular resolution diffusion MRI study. *Human Brain Mapping,* 41**,** 1226-1236.

SHI, F., YAP, P. T., GAO, W., LIN, W., GILMORE, J. H. & SHEN, D. 2012. Altered structural connectivity in neonates at genetic risk for schizophrenia: a combined study using morphological and white matter networks. *Neuroimage,* 62**,** 1622-33.

SHIBASAKI, H. & HALLETT, M. 2006. What is the Bereitschaftspotential? *Clinical Neurophysiology,* 117**,** 2341-2356.

SHIMIZU, T., BOKUDA, K., KIMURA, H., KAMIYAMA, T., NAKAYAMA, Y., KAWATA, A., ISOZAKI, E. & UGAWA, Y. 2018. Sensory cortex hyperexcitability predicts short survival in amyotrophic lateral sclerosis. *Neurology,* 90**,** e1578-e1587.

SORRENTINO, P., RUCCO, R., JACINI, F., TROJSI, F., LARDONE, A., BASELICE, F., FEMIANO, C., SANTANGELO, G., GRANATA, C., VETTOLIERE, A., MONSURRÒ, M. R., TEDESCHI, G. & SORRENTINO, G. 2018. Brain functional networks become more connected as amyotrophic lateral sclerosis progresses: a source level magnetoencephalographic study. *Neuroimage Clin,* 20**,** 564-571.

SOTEROPOULOS, D. S., EDGLEY, S. A. & BAKER, S. N. 2011. Lack of Evidence for Direct Corticospinal Contributions to Control of the Ipsilateral Forelimb in Monkey. *The Journal of Neuroscience,* 31**,** 11208-11219.

SPORNS, O., TONONI, G. & KÖTTER, R. 2005. The human connectome: A structural description of the human brain. *PLoS Comput Biol,* 1**,** e42.

STAGG, C. J., KNIGHT, S., TALBOT, K., JENKINSON, M., MAUDSLEY, A. A. & TURNER, M. R. 2013. Whole-brain magnetic resonance spectroscopic imaging measures are related to disability in ALS. *Neurology,* 80**,** 610-5.

STAM, C. J., DE HAAN, W., DAFFERTSHOFER, A., JONES, B. F., MANSHANDEN, I., VAN CAPPELLEN VAN WALSUM, A. M., MONTEZ, T., VERBUNT, J. P. A., DE MUNCK, J. C., VAN DIJK, B. W., BERENDSE, H. W. & SCHELTENS, P. 2008. Graph theoretical analysis of magnetoencephalographic functional connectivity in Alzheimer's disease. *Brain,* 132**,** 213-224.

STAM, C. J., NOLTE, G. & DAFFERTSHOFER, A. 2007. Phase lag index: assessment of functional connectivity from multi channel EEG and MEG with diminished bias from common sources. *Hum Brain Mapp,* 28**,** 1178-93.

STANTON, B. R., WILLIAMS, V. C., LEIGH, P. N., WILLIAMS, S. C., BLAIN, C. R., JAROSZ, J. M. & SIMMONS, A. 2007. Altered cortical activation during a motor task in ALS. Evidence for involvement of central pathways. *J Neurol,* 254**,** 1260-7.

STOKES, P. R., MYERS, J. F., KALK, N. J., WATSON, B. J., ERRITZOE, D., WILSON, S. J., CUNNINGHAM, V. J., RIANO BARROS, D., HAMMERS, A., TURKHEIMER, F. E., NUTT, D. J. & LINGFORD-HUGHES, A. R. 2014. Acute increases in synaptic GABA detectable in the living human brain: a [^{11}C]Ro15-4513 PET study. *Neuroimage,* 99**,** 158-65.

STOUFFER, S. A., SUCHMAN, E. A., DEVINNEY, L. C., STAR, S. A. & WILLIAMS JR, R. M. 1949. *The American soldier: Adjustment during army life. (Studies in social psychology in World War II), Vol. 1*, Oxford, England, Princeton Univ. Press.

STRONG, M. J. 2017. Revisiting the concept of amyotrophic lateral sclerosis as a multisystems disorder of limited phenotypic expression. *Curr Opin Neurol,* 30**,** 599-607.

STRONG, M. J., ABRAHAMS, S., GOLDSTEIN, L. H., WOOLLEY, S., MCLAUGHLIN, P., SNOWDEN, J., MIOSHI, E., ROBERTS-SOUTH, A., BENATAR, M., HORTOBÁGYI, T., ROSENFELD, J., SILANI, V., INCE, P. G. & TURNER, M. R. 2017. Amyotrophic lateral sclerosis - frontotemporal spectrum disorder (ALS-FTSD): Revised diagnostic criteria. *Amyotroph Lateral Scler Frontotemporal Degener,* 18**,** 153-174.

SUN, C., FOURNIER, C. N., YE, S., ZHANG, N., MA, Y. & FAN, D. 2021. Chinese validation of the Rasch-Built Overall Amyotrophic Lateral Sclerosis Disability Scale. *European Journal of Neurology,* 28**,** 1876-1883.

SWASH, M. & DE CARVALHO, M. 2004. The Neurophysiological Index in ALS. *Amyotrophic Lateral Sclerosis and Other Motor Neuron Disorders,* 5**,** 108-110.

TAE, W. S., HAM, B. J., PYUN, S. B., KANG, S. H. & KIM, B. J. 2018. Current Clinical Applications of Diffusion-Tensor Imaging in Neurological Disorders. *J Clin Neurol,* 14**,** 129-140.

TAHEDL, M., MURAD, A., LOPE, J., HARDIMAN, O. & BEDE, P. 2021. Evaluation and categorisation of individual patients based on white matter profiles: Single-patient diffusion data interpretation in neurodegeneration. *Journal of the Neurological Sciences,* 428**,** 117584.

TEWARIE, P., BRIGHT, M. G., HILLEBRAND, A., ROBSON, S. E., GASCOYNE, L. E., MORRIS, P. G., MEIER, J., VAN MIEGHEM, P. & BROOKES, M. J. 2016. Predicting haemodynamic networks using electrophysiology: The role of non-linear and cross-frequency interactions. *NeuroImage,* 130**,** 273-292.

THIVARD, L., PRADAT, P. F., LEHÉRICY, S., LACOMBLEZ, L., DORMONT, D., CHIRAS, J., BENALI, H. & MEININGER, V. 2007. Diffusion tensor imaging and voxel based morphometry study in amyotrophic lateral sclerosis: Relationships with motor disability. *Journal of Neurology, Neurosurgery and Psychiatry,* 78**,** 889-892.

THOMPSON, B. 2007. Effect sizes, confidence intervals, and confidence intervals for effect sizes. *Psychology in the Schools,* 44**,** 423-432.

THORNS, J., WIERINGA, B. M., MOHAMMADI, B., HAMMER, A., DENGLER, R. & MÜNTE, T. F. 2010. Movement initiation and inhibition are impaired in amyotrophic lateral sclerosis. *Experimental Neurology,* 224**,** 389-394.

TRAYNOR, B. J., CODD, M. B., CORR, B., FORDE, C., FROST, E. & HARDIMAN, O. M. 2000. Clinical Features of Amyotrophic Lateral Sclerosis According to the El Escorial and Airlie House Diagnostic Criteria: A Population-Based Study. *Archives of Neurology,* 57**,** 1171-1176.

TROJSI, F., DI NARDO, F., D'ALVANO, G., PASSANITI, C., SHARBAFSHAAER, M., CANALE, F., RUSSO, A., SILVESTRO, M., LAVORGNA, L., CIRILLO, M., ESPOSITO, F., TEDESCHI, G. & SICILIANO, M. 2023. Cognitive, behavioral, and brain functional connectivity correlates of fatigue in amyotrophic lateral sclerosis. *Brain and Behavior,* 13**,** e2931.

TUN, N. N., SANUKI, F. & IRAMINA, K. 2021. Electroencephalogram-Electromyogram Functional Coupling and Delay Time Change Based on Motor Task Performance. *Sensors,* 21**,** 4380.

TÜRKER, K. S. 1993. Electromyography: Some Methodological Problems and Issues. *Physical Therapy,* 73**,** 698-710.

TURNER, M. R., BAROHN, R. J., CORCIA, P., FINK, J. K., HARMS, M. B., KIERNAN, M. C., RAVITS, J., SILANI, V., SIMMONS, Z., STATLAND, J., BERG, L. H. V. D., CONFERENCE, D. O. T. N. I. P. & MITSUMOTO, H. 2020. Primary lateral sclerosis: consensus diagnostic criteria. *Journal of Neurology, Neurosurgery & Psychiatry,* 91**,** 373-377.

TZOURIO-MAZOYER, N., LANDEAU, B., PAPATHANASSIOU, D., CRIVELLO, F., ETARD, O., DELCROIX, N., MAZOYER, B. & JOLIOT, M. 2002. Automated anatomical labeling of activations in SPM using a macroscopic anatomical parcellation of the MNI MRI single-subject brain. *Neuroimage,* 15**,** 273-89.

TZVETANOV, P., LISICHKOV, I., ROUSSEFF, R. T., HEGDE, V. & KOSTADINOV, S. 2022. Abnormality of Contingent Negative Variation Correlates with Parkinson's Disease Severity. *Innov Clin Neurosci,* 19**,** 71-76.

VABALAS, A., GOWEN, E., POLIAKOFF, E. & CASSON, A. J. 2019. Machine learning algorithm validation with a limited sample size. *PLOS ONE,* 14**,** e0224365.

VALERIE, S. L. W., JONES, L. V. & TUKEY, J. W. 1999. Controlling Error in Multiple Comparisons, with Examples from State-to-State Differences in Educational Achievement. *Journal of Educational and Behavioral Statistics,* 24**,** 42-69.

VAN DEN BOSCH, L., VAN DAMME, P., BOGAERT, E. & ROBBERECHT, W. 2006. The role of excitotoxicity in the pathogenesis of amyotrophic lateral sclerosis.

Biochimica et Biophysica Acta (BBA) - Molecular Basis of Disease, 1762**,** 1068-1082.

VAN DEN HEUVEL, M. P., SPORNS, O., COLLIN, G., SCHEEWE, T., MANDL, R. C., CAHN, W., GOÑI, J., HULSHOFF POL, H. E. & KAHN, R. S. 2013. Abnormal rich club organization and functional brain dynamics in schizophrenia. *JAMA Psychiatry,* 70**,** 783-92.

VAN DER BURGH, H. K., WESTENENG, H. J., WALHOUT, R., VAN VEENHUIJZEN, K., TAN, H. H. G., MEIER, J. M., BAKKER, L. A., HENDRIKSE, J., VAN ES, M. A., VELDINK, J. H., VAN DEN HEUVEL, M. P. & VAN DEN BERG, L. H. 2020. Multimodal longitudinal study of structural brain involvement in amyotrophic lateral sclerosis. *Neurology,* 94**,** e2592-e2604.

VAN EIJK, R. P. A., DE JONGH, A. D., NIKOLAKOPOULOS, S., MCDERMOTT, C. J., EIJKEMANS, M. J. C., ROES, K. C. B. & VAN DEN BERG, L. H. 2021. An old friend who has overstayed their welcome: the ALSFRS-R total score as primary endpoint for ALS clinical trials. *Amyotroph Lateral Scler Frontotemporal Degener,* 22**,** 300-307.

VAN VEEN, B. D., VAN DRONGELEN, W., YUCHTMAN, M. & SUZUKI, A. 1997. Localization of brain electrical activity via linearly constrained minimum variance spatial filtering. *IEEE Transactions on biomedical engineering,* 44**,** 867-880.

VERSTRAETE, E., VAN DEN HEUVEL, M. P., VELDINK, J. H., BLANKEN, N., MANDL, R. C., HULSHOFF POL, H. E. & VAN DEN BERG, L. H. 2010. Motor Network Degeneration in Amyotrophic Lateral Sclerosis: A Structural and Functional Connectivity Study. *PLOS ONE,* 5**,** e13664.

VERSTRAETE, E., VELDINK, J. H., HENDRIKSE, J., SCHELHAAS, H. J., HEUVEL, M. P. V. D. & BERG, L. H. V. D. 2012. Structural MRI reveals cortical thinning in amyotrophic lateral sclerosis. *Journal of Neurology, Neurosurgery & Psychiatry,* 83**,** 383-388.

VERSTRAETE, E., VELDINK, J. H., MANDL, R. C. W., VAN DEN BERG, L. H. & VAN DEN HEUVEL, M. P. 2011. Impaired Structural Motor Connectome in Amyotrophic Lateral Sclerosis. *PLOS ONE,* 6**,** e24239.

VERSTRAETE, E., VELDINK, J. H., VAN DEN BERG, L. H. & VAN DEN HEUVEL, M. P. 2014. Structural brain network imaging shows expanding disconnection of the motor system in amyotrophic lateral sclerosis. *Hum Brain Mapp,* 35**,** 1351-61.

VESIA, M., CULHAM, J. C., JEGATHEESWARAN, G., ISAYAMA, R., LE, A., DAVARE, M. & CHEN, R. 2018. Functional interaction between human dorsal premotor cortex and the ipsilateral primary motor cortex for grasp plans: a dual-site TMS study. *Neuroreport,* 29**,** 1355-1359.

VICENTE, R., WIBRAL, M., LINDNER, M. & PIPA, G. 2011. Transfer entropy—a model-free measure of effective connectivity for the neurosciences. *Journal of Computational Neuroscience,* 30**,** 45-67.

VILLRINGER, A., PLANCK, J., STODIECK, S., BÖTZEL, K., SCHLEINKOFER, L. & DIRNAGL, U. 1994. Noninvasive assessment of cerebral hemodynamics and tissue oxygenation during activation of brain cell function in human adults using near infrared spectroscopy. *Adv Exp Med Biol,* 345**,** 559-65.

VINCK, M., OOSTENVELD, R., VAN WINGERDEN, M., BATTAGLIA, F. & PENNARTZ, C. M. A. 2011. An improved index of phase-synchronization for electrophysiological data in the presence of volume-conduction, noise and sample-size bias. *NeuroImage,* 55**,** 1548-1565.

VUCIC, S., CHEAH, B. C., YIANNIKAS, C. & KIERNAN, M. C. 2011. Cortical excitability distinguishes ALS from mimic disorders. *Clinical Neurophysiology,* 122**,** 1860-1866.

VUCIC, S. & KIERNAN, M. C. 2006. Novel threshold tracking techniques suggest that cortical hyperexcitability is an early feature of motor neuron disease. *Brain,* 129**,** 2436-46.

VUCIC, S. & KIERNAN, M. C. 2017. Transcranial Magnetic Stimulation for the Assessment of Neurodegenerative Disease. *Neurotherapeutics : the journal of the American Society for Experimental NeuroTherapeutics,* 14**,** 91-106.

VUCIC, S., NICHOLSON, G. A. & KIERNAN, M. C. 2008. Cortical hyperexcitability may precede the onset of familial amyotrophic lateral sclerosis. *Brain,* 131**,** 1540-50.

WALHOUT, R., WESTENENG, H.-J., VERSTRAETE, E., HENDRIKSE, J., VELDINK, J. H., HEUVEL, M. P. V. D. & BERG, L. H. V. D. 2015. Cortical thickness in ALS: towards a marker for upper motor neuron involvement. *Journal of Neurology, Neurosurgery & Psychiatry,* 86**,** 288-294.

WALTER, W. G., COOPER, R., ALDRIDGE, V. J., MCCALLUM, W. C. & WINTER, A. L. 1964. Contingent Negative Variation : An Electric Sign of Sensori-Motor Association and Expectancy in the Human Brain. *Nature,* 203**,** 380-384.

WARD, N., BROWN, M., THOMPSON, A. & FRACKOWIAK, R. 2003. Neural correlates of outcome after stroke: a cross-sectional fMRI study. *Brain,* 126**,** 1430-1448.

WARREN, D. E., POWER, J. D., BRUSS, J., DENBURG, N. L., WALDRON, E. J., SUN, H., PETERSEN, S. E. & TRANEL, D. 2014. Network measures predict

neuropsychological outcome after brain injury. *Proc Natl Acad Sci U S A,* 111**,** 14247-52.

WATABE, T. & HATAZAWA, J. 2019. Evaluation of Functional Connectivity in the Brain Using Positron Emission Tomography: A Mini-Review. *Front Neurosci,* 13**,** 775.

WATTS, D. J. & STROGATZ, S. H. 1998. Collective dynamics of 'small-world' networks. *Nature,* 393**,** 440-442.

WEERSINK, J. B., DE JONG, B. M., HALLIDAY, D. M. & MAURITS, N. M. 2021. Intermuscular coherence analysis in older adults reveals that gait-related arm swing drives lower limb muscles via subcortical and cortical pathways. *J Physiol,* 599**,** 2283-2298.

WEI, L., BAEKEN, C., LIU, D., ZHANG, J. & WU, G. R. 2022a. Functional connectivity-based prediction of global cognition and motor function in riluzole-naive amyotrophic lateral sclerosis patients. *Netw Neurosci,* 6**,** 161-174.

WEI, P., BAO, R. & FAN, Y. 2022b. Comparing the reliability of different ICA algorithms for fMRI analysis. *PLOS ONE,* 17**,** e0270556.

WEISZFELD, E. 1937. Sur le point pour lequel la somme des distances de n points donnés est minimum. *Tohoku Mathematical Journal, First Series,* 43**,** 355-386.

WELNIARZ, Q., DUSART, I., GALLEA, C. & ROZE, E. 2015. One hand clapping: lateralization of motor control. *Frontiers in Neuroanatomy,* 9.

WESTFALL, P. H. 2014. Combining P-values. Wiley StatsRef: Statistics Reference Online.

WESTPHAL, K. P., HEINEMANN, H. A., GRÖZINGER, B., KOTCHOUBEY, B. J., DIEKMANN, V., BECKER, W. & KORNHUBER, H. H. 1998. Bereitschaftspotential in amyotrophic lateral sclerosis (ALS): lower amplitudes in patients with hyperreflexia (spasticity). *Acta Neurologica Scandinavica,* 98**,** 15-21.

WIJESEKERA, L. C. & LEIGH, P. N. 2009. Amyotrophic lateral sclerosis. *Orphanet journal of rare diseases,* 4**,** 3-3.

WIJESEKERA, L. C., MATHERS, S., TALMAN, P., GALTREY, C., PARKINSON, M. H., GANESALINGAM, J., WILLEY, E., AMPONG, M. A., ELLIS, C. M., SHAW, C. E., AL-CHALABI, A. & LEIGH, P. N. 2009. Natural history and clinical features of the flail arm and flail leg ALS variants. *Neurology,* 72**,** 1087-94.

WILLIAMS, K. L., FIFITA, J. A., VUCIC, S., DURNALL, J. C., KIERNAN, M. C., BLAIR, I. P. & NICHOLSON, G. A. 2013. Pathophysiological insights into ALS with C9ORF72 expansions. *J Neurol Neurosurg Psychiatry,* 84**,** 931-5.

WIRTH, A. M., KHOMENKO, A., BALDARANOV, D., KOBOR, I., HSAM, O., GRIMM, T., JOHANNESEN, S., BRUUN, T.-H., SCHULTE-MATTLER, W., GREENLEE, M. W. & BOGDAHN, U. 2018. Combinatory Biomarker Use of Cortical Thickness, MUNIX, and ALSFRS-R at Baseline and in Longitudinal Courses of Individual Patients With Amyotrophic Lateral Sclerosis. *Frontiers in Neurology,* 9.

WITHAM, C. L., RIDDLE, C. N., BAKER, M. R. & BAKER, S. N. 2011. Contributions of descending and ascending pathways to corticomuscular coherence in humans. *J Physiol,* 589**,** 3789-800.

WONG, A. L. & HAITH, A. M. 2017. Motor planning flexibly optimizes performance under uncertainty about task goals. *Nature Communications,* 8**,** 14624.

WONG, A. L., HAITH, A. M. & KRAKAUER, J. W. 2015. Motor Planning. *The Neuroscientist,* 21**,** 385-398.

WU, Z., CHEN, X., GAO, M., HONG, M., HE, Z., HONG, H. & SHEN, J. 2021. Effective Connectivity Extracted from Resting-State fMRI Images Using Transfer Entropy. *IRBM,* 42**,** 457-465.

XU, L., LIU, T., LIU, L., YAO, X., CHEN, L., FAN, D., ZHAN, S. & WANG, S. 2020. Global variation in prevalence and incidence of amyotrophic lateral sclerosis: a systematic review and meta-analysis. *J Neurol,* 267**,** 944-953.

YAZAWA, S., NAKAO, K., SUGIMOTO, A., YAGI, K., TSURUTA, K. & MATSUHASHI, M. 2017. Altered cerebral motor execution mechanism in amyotrophic lateral sclerosis: An MEG study. *Journal of the Neurological Sciences,* 381**,** 1099.

YOKOYAMA, H., YOSHIDA, T., ZABJEK, K., CHEN, R. & MASANI, K. 2020. Defective corticomuscular connectivity during walking in patients with Parkinson's disease. *Journal of Neurophysiology,* 124**,** 1399-1414.

ZAEPFFEL, M., TRACHEL, R., KILAVIK, B. E. & BROCHIER, T. 2013. Modulations of EEG beta power during planning and execution of grasping movements. *PloS one,* 8**,** e60060.

ZANTO, T. P., RUBENS, M. T., THANGAVEL, A. & GAZZALEY, A. 2011. Causal role of the prefrontal cortex in top-down modulation of visual processing and working memory. *Nat Neurosci,* 14**,** 656-61.

ZEINEH, M. M., HOLDSWORTH, S., SKARE, S., ATLAS, S. W. & BAMMER, R. 2012. Ultra-high resolution diffusion tensor imaging of the microscopic pathways of the medial temporal lobe. *Neuroimage,* 62**,** 2065-82.

ZHANG, L., ULUĞ, A. M., ZIMMERMAN, R. D., LIN, M. T., RUBIN, M. & BEAL, M. F. 2003. The diagnostic utility of FLAIR imaging in clinically verified amyotrophic lateral sclerosis. *Journal of Magnetic Resonance Imaging,* 17**,** 521-527.

ZHAO, J., WANG, X., HUO, Z., CHEN, Y., LIU, J., ZHAO, Z., MENG, F., SU, Q., BAO, W., ZHANG, L., WEN, S., WANG, X., LIU, H. & ZHOU, S. 2022. The Impact of Mitochondrial Dysfunction in Amyotrophic Lateral Sclerosis. *Cells,* 11.

ZHOU, F., GONG, H., LI, F., ZHUANG, Y., ZANG, Y., XU, R. & WANG, Z. 2013. Altered motor network functional connectivity in amyotrophic lateral sclerosis: a resting-state functional magnetic resonance imaging study. *NeuroReport,* 24**,** 657-662.

ZHOU, F., XU, R., DOWD, E., ZANG, Y., GONG, H. & WANG, Z. 2014. Alterations in regional functional coherence within the sensory-motor network in amyotrophic lateral sclerosis. *Neuroscience letters,* 558**,** 192-196.

ZHOU, W., YU, S. & CHEN, B. 2022. Causality detection with matrix-based transfer entropy. *Information Sciences,* 613**,** 357-375.

ZHOU, X.-H., MCCLISH, D. K. & OBUCHOWSKI, N. A. 2009. *Statistical methods in diagnostic medicine,* John Wiley & Sons.

ZOKAEI, N., QUINN, A. J., HU, M. T., HUSAIN, M., VAN EDE, F. & NOBRE, A. C. 2021. Reduced cortico-muscular beta coupling in Parkinson's disease predicts motor impairment. *Brain Communications,* 3.

ZOU, Z. Y., ZHOU, Z. R., CHE, C. H., LIU, C. Y., HE, R. L. & HUANG, H. P. 2017. Genetic epidemiology of amyotrophic lateral sclerosis: a systematic review and meta-analysis. *J Neurol Neurosurg Psychiatry,* 88**,** 540-549.

Appendices

Appendix chapter 4

Appendix 4.1 Ethical approval letter

REC Reference: 2019-05 List 17 (01)
Previous REC Reference: 2015-01 Chairman's Action (1)
(Please quote reference on all correspondence)

EudraCT Number: N/A

Date of Valid Submission to REC: 26.03.2019
Date of Ethical Review: 08.05.2019
R&I application Number: N/A

Dear Ms Coffey,

Thank you for your correspondence in which you submitted an amendment for the above named study.

The Chairman has reviewed the documentation you submitted and approved this amendment. The following documents were reviewed:

- Non-clinical Amendment Request Form, dated 22.03.2019
- PIL & CF
- Protocol
- DPIA
- EMG Electrodes booklet
- Medical history form

Applicants must submit an annual report for ongoing projects and an end of project report upon completion of the study. It is the responsibility of the researcher/research team to ensure all aspects of the study are executed in compliance with the General Data Protection regulation (GDPR), Health Research Regulations and the Data Protection Act 2018. ***Additionally, please note for documents submitted for GDPR purposes that the REC and the Chair are not confirming that you're documents are GDPR compliant, they are approving the document from an ethical perspective.***

Yours sincerely,

Sadhbh O'Neill

REC Officer – Dr Sadhbh O'Neill - SJH/TUH Research Ethics Committee

Ospidéal na hOllscoile, Tamhlacht
Tamhlacht, Baile Átha Cliath, D24 NR0A, Éire
Príomhlíne: +353 1 414 2000
www.tuh.ie

Tallaght University Hospital
Tallaght, Dublin, D24 NR0A, Ireland
Tel: +353 1 414 2000
www.tuh.ie

Tallaght University Hospital is a registered business name of 'The Adelaide and Meath Hospital, Dublin Incorporating The National Children's Hospital'.

Appendix 4.2 Control consent form

SRH / AMNCH RESEARCH ETHICS COMMITTEE.
CONTROL CONSENT FORM

Study title: "Impairments of Neuro-muscular Communication in Motor-Neuron Disease: A Bio-Marker for Early and Personalised Diagnosis"

I have read and understood the Control Information Leaflet about this research project. The information has been fully explained to me and I have been able to ask questions, all of which have been answered to my satisfaction.	Yes ☐	No ☐
I understand that I don't have to take part in this study and that I can opt out at any time. I understand that I don't have to give a reason for opting out and I understand that opting out won't affect my future medical care.	Yes ☐	No ☐
I am aware of the potential risks, benefits, and alternatives of this research study.	Yes ☐	No ☐
I give permission for researchers with delegated authority from Professor Hardiman and her research team to look at my medical records to get information. I have been assured that information about me will be kept private and confidential.	Yes ☐	No ☐
I have been given a copy of the Information Leaflets and this completed consent form for my records. I understand that a copy is maintained in my medical records and a copy will be sent to the principal investigator.	Yes ☐	No ☐
I consent to take part in this research study having been fully informed of the risks, benefits, and alternatives.	Yes ☐	No ☐
I give informed explicit consent to have my data processed as part of this research study.	Yes ☐	No ☐
I consent to be contacted by researchers as part of this research study.	Yes ☐	No ☐

FUTURE CONTACT [please choose one or more as you see fit]		
OPTION 1: I consent to be re-contacted by researchers about possible future MND research related to the current study for which I may be eligible.	Yes ☐	No ☐
OPTION 2: I consent to be re-contacted by researchers about possible future MND research unrelated to the current study for which I may be eligible.	Yes ☐	No ☐

STORAGE AND FUTURE USE OF INFORMATION		
RETENTION OF RESEARCH MATERIAL IN THE FUTURE		
PLEASE TICK YES FOR EITHER OPTION 1 OR OPTION 2 OR NEITHER		
OPTION 1: I give permission for material/data to be stored for *possible future research related* to the current study *only if consent is obtained* at the time of the future research but only if the research is approved by a Research Ethics Committee.	Yes ☐	No ☐
OPTION 2: I give permission for material/data to be stored for *possible future research related* to the current study *without further consent being required* but only if the research is approved by a Research Ethics Committee.	Yes ☐	No ☐
PLEASE TICK YES FOR EITHER OPTION 3 OR OPTION 4 OR NEITHER		
OPTION 3: I give permission for material/data to be stored for *possible future research unrelated* to the current study *only if consent is obtained* at the time of the future research but only if the research is approved by a Research Ethics Committee.	Yes ☐	No ☐
OPTION 4: I give permission for material/data to be stored for *possible future research unrelated* to the current study *without further consent* being required but only if the research is approved by a Research Ethics Committee (As detailed in "*Consent to Future Uses'* in the information leaflet.	Yes ☐	No ☐
YOU MAY TICK YES FOR OPTION 5 AND/OR 6 OR NEITHER		
OPTION 5: I agree that some future research projects may be carried out by researchers working for commercial/pharmaceutical companies.	Yes ☐	No ☐
OPTION 6: I understand I will not be entitled to a share of any profits that may arise from the future use of my material/data or products derived from it.	Yes ☐	No ☐

PARTICIPANT'S NAME: _____

PARTICIPANT'S SIGNATURE: _____

DATE: _____

Statement of responsibility of the Principal Investigator's or his/her nominated experimenter's: I have taken the time to explain the nature, purpose, procedures, benefits, and risks of this research study to the above patient in a way they could understand. I have offered to answer any questions about any aspect of the study that concerns them and fully answered such questions. I believe that the participant understands my explanation and has freely given informed consent.

Experimenter's Name: _____

Experimenter's signature: _____

Date: _____

The 3 copies needed: 1 original for the participant's medical records in hospital, 1 copy for the participant, 1 copy for the investigator's records.

Appendix 4.3 Patient consent form

SIH / AMNCH RESEARCH ETHICS COMMITTEE.
PATIENT CONSENT FORM

Study title: "Impairments of Neuro-muscular Communication in Motor-Neuron Disease: A Bio-Marker for Early and Personalised Diagnosis"

I have read and understood the Patient Information Leaflet about this research project. The information has been fully explained to me and I have been able to ask questions, all of which have been answered to my satisfaction.	Yes ☐	No ☐
I understand that I don't have to take part in this study and that I can opt out at any time. I understand that I don't have to give a reason for opting out and I understand that opting out won't affect my future medical care.	Yes ☐	No ☐
I am aware of the potential risks, benefits, and alternatives of this research study.	Yes ☐	No ☐
I give permission for researchers with delegated authority from Professor Hardiman and her research team to look at my medical records to get information. I have been assured that information about me will be kept private and confidential.	Yes ☐	No ☐
I have been given a copy of the Information Leaflets and this completed consent form for my records. I understand that a copy is maintained in my medical records and a copy will be sent to the principal investigator.	Yes ☐	No ☐
I consent to take part in this research study having been fully informed of the risks, benefits, and alternatives.	Yes ☐	No ☐
I give informed explicit consent to have my data processed as part of this research study.	Yes ☐	No ☐
I consent to be contacted by researchers as part of this research study.	Yes ☐	No ☐

FUTURE CONTACT [please choose one or more as you see fit]		
OPTION 1: I consent to be re-contacted by researchers about possible future MND research related to the current study for which I may be eligible.	Yes ☐	No ☐
OPTION 2: I consent to be re-contacted by researchers about possible future MND research unrelated to the current study for which I may be eligible.	Yes ☐	No ☐

STORAGE AND FUTURE USE OF INFORMATION		
RETENTION OF RESEARCH MATERIAL IN THE FUTURE		
PLEASE TICK YES FOR EITHER OPTION 1 OR OPTION 2 OR NEITHER		
OPTION 1: I give permission for material/data to be stored for *possible future research related* to the current study *only if consent is obtained* at the time of the future research but only if the research is approved by a Research Ethics Committee.	Yes ☐	No ☐
OPTION 2: I give permission for material/data to be stored for *possible future research related* to the current study *without further consent being required* but only if the research is approved by a Research Ethics Committee.	Yes ☐	No ☐
PLEASE TICK YES FOR EITHER OPTION 3 OR OPTION 4 OR NEITHER		
OPTION 3: I give permission for material/data to be stored for *possible future research unrelated* to the current study *only if consent is obtained* at the time of the future research but only if the research is approved by a Research Ethics Committee.	Yes ☐	No ☐
OPTION 4: I give permission for material/data to be stored for *possible future research unrelated* to the current study *without further consent* being required but only if the research is approved by a Research Ethics Committee (As detailed in "*Consent to Future Uses*" in the information leaflet.	Yes ☐	No ☐
YOU MAY TICK YES FOR OPTION 5 AND/OR 6 OR NEITHER		
OPTION 5: I agree that some future research projects may be carried out by researchers working for commercial/pharmaceutical companies.	Yes ☐	No ☐
OPTION 6: I understand I will not be entitled to a share of any profits that may arise from the future use of my material/data or products derived from it.	Yes ☐	No ☐

PARTICIPANT'S NAME: _____

PARTICIPANT'S SIGNATURE: _____

DATE: _____

Where the participant is incapable of comprehending the nature, significance and scope of the consent required, the form must be signed by a person competent to give consent to his or her participation in the research study (other than a person who applied to undertake or conduct the study). If the subject is a minor (under 18 years old) the signature of parent or guardian must be obtained: -

NAME OF CONSENTOR, PARENT or GUARDIAN: _____

SIGNATURE: _____

RELATION TO PARTICIPANT: _____

Where the participant can comprehend the nature, significance and scope of the consent required, but is physically unable to sign written consent, signatures of two witnesses present when consent was given by the participant to a registered medical practitioner treating him or her for the illness.

NAME OF FIRST WITNESS: _____ SIGNATURE: _____

NAME OF SECOND WITNESS: _____ SIGNATURE: _____

Statement of responsibility of the Principal Investigator's or his/her nominated experimenter's: I have taken the time to explain the nature, purpose, procedures, benefits, and risks of this research study to the above patient in a way they could understand. I have offered to answer any questions about any aspect of the study that concerns them and fully answered such questions. I believe that the participant understands my explanation and has freely given informed consent.

Experimenter's Name: _____

Experimenter's signature: _____

Date: _____

The 3 copies needed: 1 original for the participant's medical records in hospital, 1 copy for the participant, 1 copy for the investigator's records.

Appendix 4.4 Patient Information Leaflet

Patient Information Leaflet

Study title: **"Impairments of Neuro**-muscular Communication in Motor-Neuron Disease: A Bio-**Marker for Early and Personalised Diagnosis"**

Principal investigator's name:	Prof Orla Hardiman
Principal investigator's title:	Professor, Academic Unit of Neurology, Trinity College Dublin Consultant Neurologist, Beaumont Hospital, Dublin
Contact of principal investigator:	+353 1 896 4496
Co-investigator's :	Dr Colin Doherty
Co-investigator's title:	Consultant Neurologist, **Neurology Dept., St.James' Hospital,** Dublin.
Data Controller's Identity:	The Academic Unit of Neurology, Trinity College Dublin
Data Controller's Contact Details:	Address: Academic Unit of Neurology Room 5.43, Trinity Biomedical Sciences Inst. Trinity College Dublin 152-160 Pearse Street Dublin 2 Phone: +353 1 896 4376
Data Protection Officer's Identity:	Trinity College Dublin Data Protection Officer
Data Protection Officer's Contact Details:	Address: Data Protection Officer **Secretary's Office,** Trinity College Dublin, Dublin 2, Ireland. Email: dataprotection@tcd.ie.

You are being invited to take part in a research study to be carried out at the Wellcome HRB **Clinical Research Facility (CRF) at St. James's Hospital** by the academic Unit of Neurology, Trinity College Dublin.

Before you decide whether or not you wish to take part, you should read the information provided below carefully and, if you wish, discuss it with your family, friends or GP (doctor). Take time to ask questions – **don't feel rushed and don't feel under pressure to make a quick** decision.

You should clearly understand the risks and benefits of taking part in this study so that you can make a decision that is right for you. **This process is known as 'Informed Consent'.**

You don't have to take part in this study. If you decide not to take part, **it won't affect your** future medical care

You can change your mind about taking part in the study any time you like. Even if the study has started, you can still opt out. You don't have to give us a reason. If you do opt out, rest assured it won't affect the quality of treatment you get in the future.

Why is this study being done?

Earlier diagnosis of Motor neuron disease (MND) or ALS will help toward better care and finding potential future treatments. We are aiming to find a new way to diagnose MND and its sub-categories earlier and with greater accuracy. In this new method we look at how the brain and muscles talk to each other.

In doing so we are trying to find out more about how the disease affects the brain and signals in movement with new ways to diagnose ALS and its sub-categories.

We are also looking at how spinal muscular atrophy (SMA), primary lateral sclerosis (PLS), post-polio syndrome (PPS) and multiple sclerosis (MS) affect these parts of brain signalling to improve the ability to distinguish between these diseases and ALS, while also helping us understand more about these diseases themselves and improve our ability in diagnosing them.

We will measure brain activity using a procedure called Electroencephalography (EEG) as well as the signalling networks involved in hand movement via surface electromyography (EMG). This is **described under 'What will happen to me if I agree to take part?'**

Why am I being asked to take part?

You have been invited to take part in this study because you are over the age of 18 years and have been diagnosed with ALS, PLS, PPS, SMA or MS.
We will be recruiting 200 participants with ALS, PLS, SMA, MS or PPS and 100 participants without these conditions as controls.

Who should NOT attend the study (exclusion criteria)?

If you have any of the following, you will not be able to participate in this study:

1. Psychiatric condition
2. Anyone taking psychiatric medications or illicit drugs
3. Medical condition that affect the nervous system (e.g., uncontrolled diabetes, seizure disorders)
4. Previous (allergic) reactions in similar recording environments, e.g., to recording gels
5. Pregnancy

What will happen to me if I agree to take part?

If you agree to participate, you will be asked to attend the Clinical Research Facility in St James's Hospital for a recording session. The session will last approximately 3.5 hours. You may withdraw from the study at any time, including before, during and after the session. We will ask you to attend up to 3 sessions at 4-month intervals, to monitor changes in the brain over time. However, **participation in all 3 sessions is not required to contribute to this study**.

When you arrive you, the contents of this leaflet will be revised with you by a member of the research team. The details of what you will be asked to do and what you will experience will be described again and you will be offered the chance to ask any questions or address any concerns you may have before agreeing to participate.

If you agree to participate, you will be asked to sign a consent form. Once completed you will be asked a series of questions to determine handedness and recent caffeine consumption. These questions are used to ensure that the experiment will be successfully performed, and the results are appropriately interpreted.
A neurological examination will be performed to determine aspects such as power, reflexes and muscle tone of the upper limbs.
We will also ask you to tell us of any medications you are currently taking or if you have/have had any serious medical problems, so we can maximise your care should you require medical attention for any reason. **This information will be destroyed at the end of the session.**

Next, you will be asked to participate in EEG and EMG recording sessions.

In each recording session, we will put 16 electrodes on your right hand and forearm these are the electromyography (EMG) electrodes, which will allow us to record muscle activity of the right arm.
we will also place a cap on your head. Electrodes will be placed into holes in the cap over your scalp to record the activity of your brain. 8 electrodes will be placed around the ears and eyes

to record background activity. We will use some conductive gel when attaching the electrodes to your skin. This is called **electroencephalography** (EEG)
We will then do the recording while you are at rest, when you do some simple right hand/finger movements such as pressing a wooden block. The experimenter will tell you the details of the instructions of the task in advance.

You may need to wash your hand/head after the experiment to remove the conductive gels. Showering facilities are available on site. You may also use a towel to wipe away the gel and subsequently wash it completely away after you leave if you prefer to do so.

These techniques are non-invasive, i.e., there are no needles involved and all electrodes are placed on the surface of the skin. You may feel bored, restless or stiff from sitting in a chair for 3.5 hours. You may move while seated in the chair between recording periods, however due to the number of cables which connect the electrodes to the recording device, we will ask you to stay seated for the duration of the session once we begin applying the equipment. If you wish to withdraw from the study at any time this equipment can be quickly removed by a member of the research team so that you can leave the chair.

Your responsibilities as a participant:
If you agree to participate in this study, we request that you cooperate to the best of your ability. You can withdraw from the study at any stage without justifying your decision and your future treatment will not be affected.

Our responsibilities to you as investigators:
Alleviating any discomfort is important to us during this recording, both to ensure your own comfort is maximised and to improve the quality of the data we collect, which is best when the muscles are relaxed. Therefore, please alert one of the research team during the session if at any time you feel uncomfortable or tense, if you wish to change position in the chair of if you would like a pillow to support your arm or back.
All data will be maintained in a strictly confidential manner. The information that you provide will be stored in a way that it cannot be accessed except by the study team.

What are the benefits?

There is no direct benefit to you for taking part in this study.
Your participation, however, helps scientific and clinical research and postgraduate researchers undertaking this research as part of a higher degree. Your participation may also benefit those affected by neurological diseases in future.

What are the risks?

There is no risk involved in taking part in this study, as the procedure and devices are safe and commonly used. In the unlikely event that you show allergic reactions to the gels, the experiment will stop, and we will provide medical advice to treat the reaction.

However, there may be discomforts for you while taking part in the experiment. The experiment may be boring, tiring and fatiguing as it includes sitting in a position for 3-3.5 hours. The conductive gel used to attach the electrodes to your skin may feel cold or warm, cause wet and mild itching

sensation, and will need washing to remove after the experiment. The removal of tape on hand and forearm may be slightly painful or uncomfortable for some patients. If at any time you feel that your participation in this study has become unduly stressful, you are free to discontinue. This will not affect in any way the quality of care that you receive.

There is no intention to look for diseases using the recorded data. In case of incidental findings in the EEG and EMG recordings that may be an indirect sign of a previously unknown disease, you will be asked for permission to discuss the findings a neurologist, your GP or other doctors for follow up care.

What if something goes wrong when I'm taking part in this study?

If for any reason you feel unwell, please alert a member of the research team and the study can be halted immediately. If you require medical attention there are nurses on site at the Wellcome Trust Clinical Research Facility who are on hand to provide any necessary care/assistance. Any leads/cables connecting the electrodes can be easily removed by the experimenter. Once these are removed you can stand, leave the room, go to the bathroom or elsewhere.

If you feel uncomfortable or for any reason wish to pause/stop the session, alert a member of the research team and we will do so immediately. You do not need to provide an explanation to the study team.

Who is organising and funding this study?

This research is being conducted by The Academic Unit of Neurology, Trinity College Dublin. The research is funded by academic grants provided by The Irish Research Council, The Health Research Board and Science Foundation Ireland in addition to charities such as Research Motor Neurone.

Members of the research team are undertaking postgraduate research at The Academic Unit of Neurology, including PhD candidates who are researching ALS, PLS, PPS and/or MS.

Is the study confidential?

Your participation in this study will only be known to members of the Academic Unit of Neurology, Trinity College Dublin. Members of Academic Unit of Neurology, Trinity College Dublin who may provide/have provided medical care to you that is separate from this study, such as Prof. Orla Hardiman, may be made aware of your participation in this study. Your participation will not be disclosed to others in your healthcare or the public. We will not contact your GP to inform them of your participation in this study, unless you request us to do so.

All the information obtained from participating individuals will be treated in a strictly confidential manner. All of the personal and clinical information obtained will be stored on a secure password-protected computer database to which only the study team will have access. Each individual entered on the database will be assigned a unique numeric (code). Therefore, the data will be **"coded", i.e.**, your name will not appear on the database. A code will be used instead of your name.

The link between your name and this code will be maintained in a separate password-protected encrypted database with access limited to named researchers from the study team.
All paper records, including your consent form will be stored in a limited-access, secure storage space.

What Personal Data will be collected?
To help answer the research questions, the study team will collect Personal Data about you so that they can understand your medical history and your brain activity responses. The following are examples of Personal Data that may be collected during this session:

- Name
- Date of birth
- Diagnosis of ALS, PLS, PPS, SMA or MS diagnosis
- Handedness (using a test called the Edinburgh Handedness Scale)
- Neurological examination recorded on day of the study
- Signals from your brain and hand muscles and details of the task that was ongoing while these signals were recorded.

To help us understand how the signals we measure relate to other aspects of the brain's activity or structure, we may also investigate the relationship between the signals we collect and data you have provided to the Academic Unit of Neurology, Trinity College Dublin during other research studies the Unit performs. The following are examples of Personal Data that may be collected from other studies performed by the Academic Unit of Neurology:

- Neuropsychological test scores
- MRI scans of your brain
- MUNIX data

Your participation in other such studies is voluntary, you do not need to provide this information to us during this session or participate in these other studies to complete participation in this study.

If you have a diagnosis of ALS, we may also gather information relating to your diagnosis from the National ALS Register, to investigate how these signals relate to different symptoms or subgroups of the disease. The following are examples of Personal Data that may be collected from the National ALS Register:

- Symptoms you experience
- Genetic risk factors you do/do not have

Contribution of your data to the National ALS Register is voluntary, you do not need to provide this information to us during this session or contribute data to the National ALS Register to complete participation in this study. Such information about your disease will only be obtained from the

National ALS Register upon approval of a justifiable request to a manager of the ALS register. We will not collect or store unnecessary information about your disease from the Register, only that which is used to help us better understand the signals we measure in this study.

How will my Personal Data be used?
If you agree to take part in this study, your Personal Data will be used:

- To determine if you can take part in the study
- To measure how your brain and muscle signals responds during the study and compare this to other study participants
- To learn more about the disease and to help develop new diagnostic tests
- To provide you with treatment in the event of a study related injury
- To develop new analysis methods to improve the study of neurological diseases.

The research team at St James's Hospital and Trinity College Dublin use your health data for research only based on your consent.
Your Coded Data may also be used in continued medical research projects investigating Motor Neuron Disease, Post-Polio Syndrome, Multiple Sclerosis and the development of new research methods that can be used to study these diseases. This is optional and you will be asked to consent for future use of your Coded Data for related research projects. Further information is provided in the "Consent to Future Uses" section below.

Who will receive my Personal Data?
The Academic Unit of Neurology research team will have access to your coded data. The key which links your name to the code associated with this data can only be accessed by a limited number of people within the Academic Unit of Neurology. Your name is maintained only for the purposes of relating data you have provided here to other data you may have provided to the Academic Unit of Neurology (described in "What Personal Data will be collected?" above).

The results of this study and optional future research may be published in study reports, scientific presentations and publications. Information that could reasonably identify you will not be included in such publications. Your results will not be sent to you or your GP, consultant or other healthcare providers, unless you request us to do so.

We will store the coded files and a separately stored file which relates your name to your study code for up to 5 years after the study of brain function in ALS, PLS, PPS and MS by the Academic Unit of Neurology has been completed. Thereafter your data will be fully anonymised, by destroying the link between your name and the study code, so that the data can no longer be attributed to/associated with you. This fully anonymised data may be used for future research and may be provided to other research teams or made available online to maximise the information learned from it.

In order to ensure that the study has been conducted carefully national or international agencies (e.g., Department of Health, Irish Research Council, Health Research Board, American ALS Association etc.) may require access to the data we collect for this study: you hereby give

permission to the investigators to provide information obtained as a result of your participation in this study (muscle and brain signals) to such bodies. Your name or personal contact details will not be provided, only your coded data files.

Data Protection

This section addresses the protection of your Personal Data. Personal Data means any information relating to an identified or identifiable living person. Sensitive Personal Data includes biological/health measurements.

We will be using your Sensitive Personal Data in our research to help us study how neurodegenerative diseases (ALS, PLS, PPS and MS) affect the brain's function and how any changes in brain function relate to different symptoms or subtypes of these diseases. This may improve our ability to diagnose these diseases or their subtypes, predict how the disease will progress in different individuals with these diseases, and test new medications for these diseases.

Here we address questions you may have related to how your data will be protected in compliance with Irish and European law, including the General Data Protection Regulation 2016 (GDPR):

What is the legal basis under which we are processing your data?
The legal basis under which we will process the collected data is for reasons of public interest in the area of public health (Article 6(1)e and Article 9(2)j of the General Data Protection Regulation 2016).

Who is the recipient of your data?
The Academic Unit of Neurology research team will have access to your coded data. The key which links your name to the code associated with this data can only be accessed by a limited number of people within the Academic Unit of Neurology. Further information is provided in the "Is This Study Confidential?" section.

How long will your data be stored for?
These data will be kept for 5 years after the end of the study of brain function in ALS, MS and PPS in the Academic Unit of Neurology. After this, the collected data will be anonymised so that it can no longer be attributed to you by any means. Your data may also be fully anonymised before this time.

Is there any risks which might arise from processing your data?
There are low risks with remote likelihood of harm which might arise from processing your data. Such risks include hacking of computers holding your data, loss of coded data files by experimenters, loss of paper consent/handedness files, failure to destroy medical history information and unconsented/non-GDPR compliant data sharing.

In order to minimise the potential for these risks to occur we have implemented the following measures:

- All computers storing data are password protected.

- The hard drive and remotely accessible computer are encrypted and locked in an office (on Trinity College Dublin's campus). This hard drive is not removed from the office.
- The spreadsheet storing the key to your pseudoanonymised data encrypted and is only stored on a password protected remotely accessible computer and an additional password protected computer locked on Trinity's campus. This file is only accessible by a limited number of the research team members.
- Your coded data files are directly transferred from the CRF where the session takes place to the remotely accessible computer by a secure, password protected connection.
- Files are not otherwise transferred to personal devices.
- The research team have will be carefully instructed how to handle participants information noted on the paper forms and have undergone GDPR training
- Any future backup/archiving of your data with a third-party vendor will be subject to a Data Sharing Agreement approved by Trinity College Dublin's Data Protection Officer to ensure the data is stored in compliance with GDPR and is not misused

How can you withdraw from this study?

You have a right to withdraw consent at any time. This can be done before, during or after the recording session in person by telling a member of the research team or using the contact details provided at the end of this leaflet.

How can you file a complaint?

If you would like to lodge a complaint regarding our data policy, you may do so by contacting Data Protection Commissioner in Trinity College Dublin (contact details are on the first page of this leaflet)

What rights do you have regarding your data?

Under the General Data Protection Regulation from 2016 you have the following rights:

- Right to access (Article 15): You have a right to request access to your data and a copy of it.
- Right to rectification (Article 16): You have a right to have any inaccurate information about you corrected or deleted.
- Right to erasure (Article 17): You have a right to have your personal data deleted.
- Right to restriction of processing (Article 18): You have a right to restrict or object to processing of your personal data.
- Right to data portability (Article 20): You have a right to move your personal data that we have collected to another in a readable format (e.g., CD or USB).
- Right to object automated processing (Article 21-22): We will be applying automated methods on the collected data to sub-categorize patients into groups that might be used to facilitate more patient-specific future clinical trials. You have a right to object this.

As data processing is being performed on the legal basis of public interest and personal health, we may not fulfil some of these rights, according to Article 89 of General Data Protection Regulations 2016 ("Safeguards and derogations relating to processing for archiving purposes in the public interest, scientific or historical research purposes or statistical purposes").

Namely, in the future you may be unable to restricted processing, object to automated processing or request erasure of data we have already collected with your consent. This is because loss of this collected data may lead to us having insufficient information for performing the analysis required for this research.

Will your personal data be processed further after this study? If so, could your data leave the EU?

We would like to maximise the amount of information that can be learned from your data, by utilising it in future research. Consenting to the future use of your data beyond this project is optional and will be restricted to use for specific aims, with data sharing agreements in place to **safeguard your rights. This is described in more detail below in the section "Consent to Future Use".**

Consent to Future Uses

We wish to maximise the amount of information that can be learned from the data you provide during this study. We therefore ask for your consent to use this data for further research of neurological diseases. **Consenting to future uses of your data beyond this study is optional.** Such further research is for the purposes of one or more of the following:

- Improving understanding of neurological disorders
- Improving the ability to diagnose neurological disorders
- Improving the prediction of how neurological disorders will progress.
- Developing new analysis methods, measurements or tools which can be used for purposes 1-3.

This research may be performed by research groups or commercial entities other than The Academic Unit of Neurology, Trinity College Dublin, and may be within or outside the EU/EEA. Commercial entities such as pharmaceutical companies may wish to investigate the data, we collect in order to develop new tools for use in medical practice or drug testing. Any research/commercial groups will only be provided with coded files. The key which links your name to this data to make it identifiable will not be accessible to anyone other than a limited number of team members within The Academic Unit of Neurology, Trinity College Dublin.

Furthermore, if you consent to the future use of your data by another research group/commercial entity, data will only be provided to them if a Data Sharing Agreement has been produced and approved by the Data Protection Officer of Trinity College Dublin to ensure your data protection rights are maintained. If this group is outside of the EU a Cross Border Transfer Agreement approved by the Data Protection Officer of Trinity College Dublin will also be in place to protect your rights.

Where can I get further information?

If you have any further questions about the study or if you want to opt out of the study, you can rest assured it won't affect the quality of treatment you get in the future.
If you need any further information now or at any time in the future, please contact:

Saroj Bista

Address: Room 5.43,
Trinity Biomedical Sciences Institute,
152-160 Pearse St.,
Trinity College Dublin,
Dublin 2,
Ireland.
Phone No: +353 1 896 4497
Email: sbista@tcd.ie

Appendix chapter 5

Appendix 5.1 Bista et al., 2023

OXFORD

Cerebral Cortex, 2023, 1–12
https://doi.org/10.1093/cercor/bhad152
Original Article

Cortico-muscular coherence in primary lateral sclerosis reveals abnormal cortical engagement during motor function beyond primary motor areas

Saroj Bista[1,†,*], Amina Coffey[1,†], Antonio Fasano[1], Teresa Buxo[1], Matthew Mitchell[1], Eileen Rose Giglia[1], Stefan Dukic[1,2], Mark Heverin[1], Muthuraman Muthuraman[3], Richard G. Carson[4,5], Madeleine Lowery[6], Orla Hardiman[1,7], Lara McManus[1,‡], Bahman Nasseroleslami[1,‡]

[1]Academic Unit of Neurology, Trinity Biomedical Science Institute, Trinity College Dublin, Dublin 2, Ireland,
[2]Department of Neurology, University Medical Centre Utrecht Brain Centre, Utrecht University, Utrecht 3584 CG, The Netherlands,
[3]Neural Engineering with Signal Analytics and Artificial Intelligence, Department of Neurology, University Hospital Würzburg, Würzburg 97080, Germany,
[4]Trinity College Institute of Neuroscience and School of Psychology, Trinity College Dublin,, Dublin 2, Ireland,
[5]School of Psychology, Queen's University Belfast, Belfast BT71NN, UK,
[6]School of Electrical and Electronic Engineering, University College Dublin, Dublin 4, Ireland,
[7]Beaumont Hospital, Dublin 9, Ireland

*Corresponding author: Email: sbista@tcd.ie
†Joint First Authors
‡Joint Last Authors

Primary lateral sclerosis (PLS) is a slowly progressing disorder, which is characterized primarily by the degeneration of upper motor neurons (UMNs) in the primary motor area (M1). It is not yet clear how the function of sensorimotor networks beyond M1 are affected by PLS. The aim of this study was to use cortico-muscular coherence (CMC) to characterize the oscillatory drives between cortical regions and muscles during a motor task in PLS and to examine the relationship between CMC and the level of clinical impairment. We recorded EEG and EMG from hand muscles in 16 participants with PLS and 18 controls during a pincer-grip task. In PLS, higher CMC was observed over contralateral-M1 (α- and γ-band) and ipsilateral-M1 (β-band) compared with controls. Significant correlations between clinically assessed UMN scores and CMC measures showed that higher clinical impairment was associated with lower CMC over contralateral-M1/frontal areas, higher CMC over parietal area, and both higher and lower CMC (in different bands) over ipsilateral-M1. The results suggest an atypical engagement of both contralateral and ipsilateral M1 during motor activity in PLS, indicating the presence of pathogenic and/or adaptive/compensatory alterations in neural activity. The findings demonstrate the potential of CMC for identifying dysfunction within the sensorimotor networks in PLS.

Key words: primary lateral sclerosis (PLS); cortico-muscular coherence; upper motor neuron; neurodegeneration EEG; EMG.

Introduction

Primary lateral sclerosis (PLS) is a slowly progressive disorder of upper motor neuron (UMN) degeneration (Finegan et al. 2019). A definite diagnosis of PLS requires clinical signs of UMN dysfunction, a disease duration of at least 3 years, and an absence of the significant lower motor neuron (LMN) degeneration that differentiates it from amyotrophic lateral sclerosis (ALS) (Turner et al. 2020). PLS is also characterized by cortical and subcortical changes beyond primary motor area (M1) and the corticospinal tracts (Finegan et al. 2019). These widespread structural changes in the sensorimotor network are likely to, in turn, impact the function and neural communication between different parts of this network. Such potential differences in the interactions between different parts of the sensorimotor network during motor tasks can be best assessed by quantifying the fast oscillatory interactions between neuroelectric signal recordings (Coffey et al. 2020; Dukic et al. 2021).

Recent electroencephalogram (EEG) studies have demonstrated a correspondence between neuroelectric activity and UMN pathology in ALS (McMackin et al. 2019). The high temporal resolution of EEG is well suited to provide information concerning rhythmic or oscillatory brain activity across a range of frequencies. Previous EEG investigations in people with ALS, conducted at rest, have demonstrated an altered functional connectivity across brain networks in the theta (4–7 Hz) and gamma (31–60 Hz) frequency bands (Westphal et al. 1998; Blain-Moraes et al. 2013; Nasseroleslami et al. 2017; Dukic et al. 2019). The UMN pathology of ALS is similar to that of PLS, though ALS has both UMN and LMN pathology. This suggests that cortico-cortical communication is also similarly altered in PLS, and this is supported, in part, by magnetic resonance imaging (MRI) studies (Agosta et al. 2014; Meoded et al. 2015).

The functional significance of abnormal cortical communication can be better understood by examining cortical

Received: November 1, 2022. Revised: April 13, 2023. Accepted: April 18, 2023

engagement during active motor tasks. More specifically, the cortical regions engaged in the execution of motor tasks can be assessed by calculating the coherence between ensemble neural activity recorded over cortex (measured with EEG) and the collective activity of spinal motor neurons recorded from the contracting muscle (EMG) (Conway et al. 1995; Halliday et al. 1998). Cortico-muscular coherence (CMC) is typically observed as synchrony (in the beta and gamma bands) between EEG electrodes over M1 and EMG activity. It is considered to be indicative of the efferent drive to the spinal motoneurons while also being subject to the modulating influence of peripheral afference (Witham et al. 2011). Peak beta-band CMC over M1 is reduced in conditions characterized by UMN degeneration, including stroke (Fang et al. 2009; Aikio et al. 2021) and ALS (Issa et al. 2017; Proudfoot et al. 2018). In principle, CMC also provides a method of investigating whether changes in the engagement of other cortical regions during movement accompany the PLS-induced neuronal loss in M1. It might be anticipated that the loss of fast-conducting corticospinal axons in PLS will be accompanied by pathogenic, adaptive, and/or compensatory changes throughout the sensorimotor network, given the redundancy in the sensorimotor system (Neilson and Neilson 2005; Ajemian et al. 2013; MacKinnon 2018). This may involve the engagement of cortical regions beyond M1 (Bede et al. 2021).

Here, we used EEG and EMG signals recorded during the performance of a motor task to test the hypothesis that, in PLS, CMC can be detected over brain regions extending beyond M1. We also sought to determine whether the variations in CMC are correlated with the clinical measures of UMN dysfunction.

Materials and methods

Ethics

The study was approved by the "Tallaght University Hospital/St. James's Hospital Joint Research Ethics Committee—Dublin," REC Reference: 2019-05 List 17 (01), and was performed in accordance with the Declaration of Helsinki. All participants provided informed written consent to the procedures before undergoing assessment.

PLS cohort

The PLS cohort were prospectively recruited in this cross-sectional study between June 2017 and August 2019 through the national ALS clinic at Beaumont Hospital. All participants with PLS fulfilled the clinical criteria for PLS (Turner et al. 2020). Healthy controls, age-matched to the PLS cohort, were recruited from a database of healthy controls interested in taking part in the ongoing research studies in the Academic Unit of Neurology, Trinity College Dublin, the University of Dublin.

Subjects with a history of major head trauma or other neurological conditions that could affect cognition, alcohol dependence syndrome, current use of neuroleptic medications, or high-dose psychoactive medication were excluded. Those with diabetes mellitus, a history of cerebrovascular disease, and those with neuropathy from other causes were also excluded. All of the PLS cohort underwent nerve conduction studies and EMG to exclude other concurrent peripheral nerve disorders that could interfere with CMC analyses.

Clinical assessment

On the day of EEG recording, the PLS cohort underwent an extensive clinical assessment. Disease duration from the symptom onset and the site of disease onset were recorded. Muscle strength was assessed using the Medical Research Council ("MRC") score (Compston 2010) in 9 bilateral (i.e. 18) upper limb muscles, including deltoid, triceps, biceps, wrist flexors and extensors, fingers flexors and extensors, and abductors of the index fingers and thumbs. The degree of clinical UMN involvement in the upper limbs was graded by a UMN score (de Carvalho et al. 2003). An adapted UMN score based on Kent-Braun et al. (1998) was calculated using reflex and UMN signs assessment. Reflexes were assessed at 3 sites in the upper limbs (biceps, triceps, and brachioradialis). The UMN score ranges from 0 (normal) to 16 (reflecting hyperreflexia [0–6], hypertonia [0–4], clonus [0–2], Babinski [0–2], and Hoffmann sign [0–2]). The Edinburgh Cognitive ALS Screen (ECAS), which evaluates cognitive performance across language, verbal fluency, executive, memory, and visuospatial domains (Abrahams et al. 2014), was performed on 14 of the 16 PLS participants (2 declined). Edinburgh handedness inventory (Oldfield 1971) with 10 questionnaires was performed to assess the handedness of the participant.

HD-EEG and bipolar surface EMG were subsequently recorded in all participants for the calculation of CMC during motor tasks.

Experimental paradigm

Assessment was conducted in the same manner for the PLS and control groups, similar to previous work carried out by our group, and as described in detail by Coffey et al. (2020), with additional notes in Supplementary files. Participants held a force transducer between the thumb and the index finger of their right hand to measure the pincer grip force (Fig. 1A). The maximal voluntary contraction (MVC) was determined as the average peak force achieved during 3 short (5 s) maximal contractions, where the peak force in these attempts lay within 10% of each other. Similar to our previous study, participants were asked to produce a force at 10% MVC for 5 s, while holding the force transducer in pincer grip, guided by visual force feedback on screen (pincer grip task). In a second task, participants were also asked to hold the force transducer for 5 s (precision grip task). Preliminary analysis showed that participants exhibited lower beta-band CMC during the pincer grip task compared with precision grip (Supplementary Fig. S1). The present study focused on the pincer grip task, as the preliminary CMC analysis at the sensor level indicated greater differences between PLS and controls during this task. Participants attempted a total of 30 trials for each task.

Recording of (neuro-)electro-physiological signals

All participants were seated comfortably, and the EEG data were recorded in a special-purpose laboratory, using 128-channel scalp electrode cap, filtered over the range of 0–400 Hz and digitized at 2,048 Hz using the BioSemi ActiveTwo system (BioSemi B.V, Amsterdam, Netherlands). Each participant was fitted with an appropriately sized EEG cap.

Surface EMG data were recorded using a bipolar electrode configuration from 8 muscles in the right upper arm, with the electrode pairs placed in accordance with the SENIAM guidelines (Hermens et al. 2000). The online hardware gain and filter settings for the EMG signals during recordings were the same as EEG channels, which was followed by further offline preprocessing. Five EEG channels (Cz, Pz, C4, Fz, and C3) and 3 EMG signals (first dorsal interosseous [FDI], flexor pollicis brevis [FPB], and abductor pollicis brevis [APB]) were chosen a priori for the CMC analysis. The EEG electrodes were chosen due to their representative coverage of the cortical motor network. The C3, Cz, and C4 cover the contralateral hand area, central, and ipsilateral

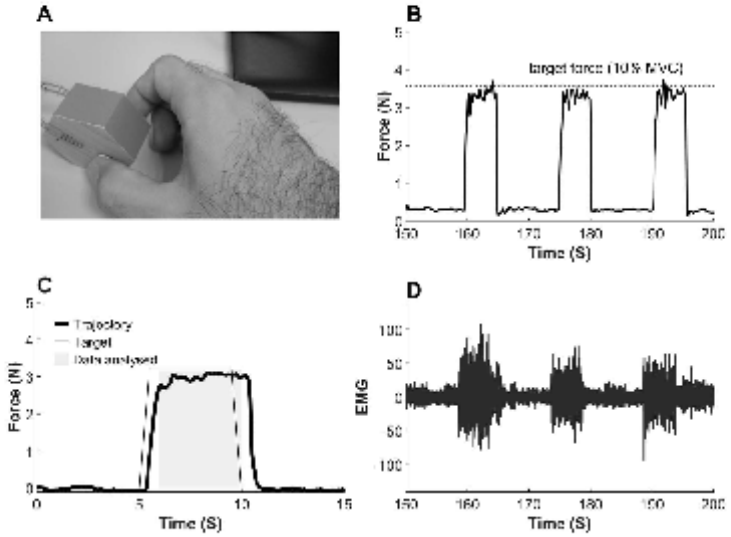

Fig. 1. A) Pincher grip motor task performed by thumb and index finger of right hand. B) A segment of force profile of pincher grip motor task performed at 10% of maximal voluntary contraction (MVC). C) A force trajectory of the pincher grip motor task averaged over 30 trials. D) Segment of EMG signal recorded from the FDI muscle during 10% MVC pincher grip motor task.

hand sensorimotor regions for the chosen tasks. Fz pertains to the frontal areas that reflect the activity from supplementary motor regions (and, to some extent, premotor areas). Finally, Pz reflects the activity from parietal areas that play important roles in visuomotor tasks (Nasseroleslami et al. 2014). Importantly, these regions have minimal spatial overlaps and allow the activity of more distinct regions to be assessed. The target muscles were selected based on their biomechanical involvement in the pincer grip task (Danna-Dos Santos et al. 2010).

Signal preprocessing and spectral analysis

EEG/EMG data analysis (Fig. 2) was performed as described in detail in a previous study (Coffey et al. 2020). Briefly, automated artifact rejection routines (Fieldtrip Toolbox) (Oostenveld et al. 2011) were used to discard data contaminated by noise. After visual inspection of the 128-ch recordings, EEG channels with higher levels of noise were removed and were reconstructed using weighted average interpolation of neighboring channels (Perrin et al. 1989). An average of 22 ± 6 trials (i.e. 88 ± 24 s) for the 5 target EEG channels were retained for the corticomuscular coherence calculation across all participants. A time window/epoch duration of 4 s (starting 1 s after the visual cue) was chosen for analysis. Data epochs, where the coefficient of variation of the force produced was >0.2, or where the mean force was <8% or >20% MVC, were excluded from further analysis. An average of 3 ± 6 trials (i.e. 12 ± 24 s) data were removed across all participants for these reasons. The raw EEG data were (re-)referenced using surface Laplacian spatial filter (McFarland et al. 1997; Bradshaw and Wikswo 2001), which served to provide signals that are more spatially specific to each EEG electrode. The EMG data (signal amplitude) were normalized with respect to root mean square EMG amplitude at 100% MVC. EEG and EMG data were filtered between 1–100 and 10–100 Hz, respectively, using a dual-pass fourth-order Butterworth bandpass filter. The auto-spectrum of each EEG/EMG signal, and the cross-spectrum between all combinations of EEG–EMG signals (frequency resolution: 1 Hz, bandwidth: 2–100 Hz) were calculated using Fieldtrip toolbox (Hanning taper and frequency smoothing at 1 Hz, nonoverlapping windows of 1 s). EMG signals were not rectified.

Estimation of coherence spectrum and banded coherence

Coherence is presented based on equivalent z-scores and P-values at both subject and group levels. This approach prevents bias by eliminating the dependence on the number of trials for the coherence analysis.

CMC was examined in 8 different frequency bands, and a single coherence estimate was obtained for each band—delta (2–4 Hz), theta (5–7 Hz), low alpha (8–10 Hz), high alpha (11–13 Hz), low beta (14–20 Hz), high beta (21–30 Hz), low gamma (31–47 Hz), and high gamma (53–97 Hz, excluding the 48–52 Hz range to avoid mains power noise). The frequency bands were defined based on the typical physiological EEG frequency bands (Sanei and Chambers 2007) as well as their relevance both in sensorimotor control (Nasseroleslami et al. 2014) and quantifying network dysfunction in motor neuron diseases (Dukic et al. 2019, 2021).

CMC was estimated based on the spatial median using the following procedure. Coherence was estimated using the median value of the auto- and cross-spectra represented by their real and imaginary components in the 2D space calculated across epochs (Weiszfeld 1937; Niinimaa and Oja 2014) and Figure 2 in Nasseroleslami et al. (2019). This contrasts with classical coherence estimates which are based on the expected value or arithmetic mean of the spectra. The auto- and cross-spectra for each 1-s epoch were calculated for each participant. The spatial median coherence was then estimated from the spatial median of the auto- and cross-spectra with a resolution of 2 Hz, Fig. 2F, and across each of the 8 defined frequency bands to obtain

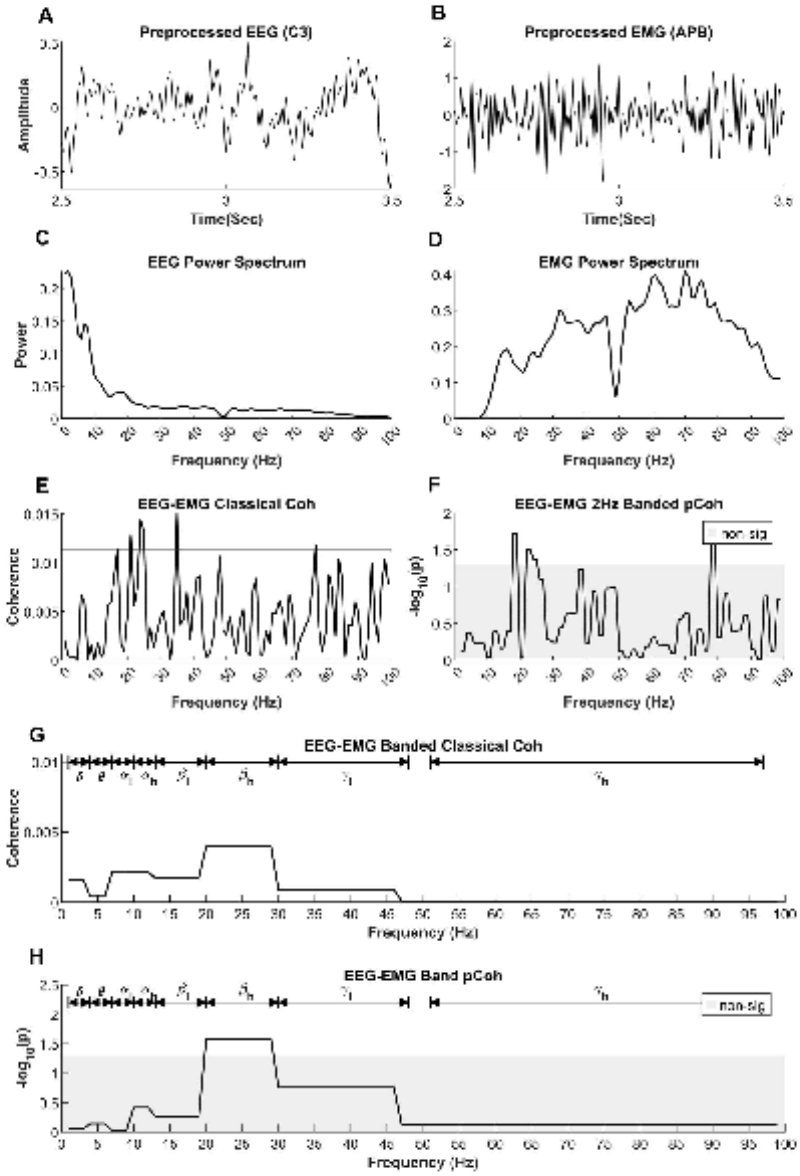

Fig. 2. Example showing the estimation of CMC using data from a healthy control participant (CON13 in Supplementary Fig. S2). A) Preprocessed EEG signal recorded from C3 electrode. B) Preprocessed EMG signal recorded from APB muscle during the same time. C) Power spectrum of EEG signal. D) Power spectrum of EMG signal in the frequency range of interest. E) CMC estimated using the magnitude squared coherence with spectral smoothing ("classical coherence"). F) CMC calculated using the spatial median to estimate the auto- and cross-spectra of the EEG and EMG data ("pCoh"). Here, the spatial median was used to group the coherence spectra over bands with a 2-Hz interval to facilitate the comparison of pCoh with classical coherence. G) Conversion of classical magnitude squared coherence into banded CMC values. Here, the spatial median method is used to group the classical coherence spectra so that there is 1 coherence value for each of the predefined bands. H) pCoh CMC calculated using the spatial median method to group coherence spectra over predefined bands. Note that images (F) and (H) use the same coherence methodology, with the only difference being the bandwidth of the frequency bands used for grouping the coherence spectra. Frequency bands: delta (δ), theta (θ), low alpha (α_l), high alpha (α_h), low beta (β_l), high beta (β_h), low gamma (γ_l), and high gamma (γ_h).

the "banded coherence," Fig. 2H. The banded spectral CMC was normalized by dividing the band cross-spectrum by the respective band auto-spectra. The strength of coherence was subsequently presented using the equivalent P-value as -log(P), which we denote as "pCoh."

To represent the banded CMC as a probability, each coherence value was compared against 0 using a nonparametric 1-sample test for significant coherence (spatial [signed] ranks; Hannu Oja and Randles 2004; Hannu Oja 2010; Nordhausen and Oja 2011). This procedure yielded individual P-values for each frequency band for each individual (both PLS and control groups). Stouffer's method was used to combine individual P-values to derive average P-value within each group, i.e. in the healthy group and in the PLS group (Stouffer et al. 1949; Westfall 2014). This procedure is similar, but not procedurally equivalent, to the pooled coherence analysis (Amjad et al. 1997). Both methods can be used to combine information from several participants (or trials). The negative logarithm of the P-values, i.e. $-\log_{10}(P)$, was used as a measure of CMC strength to visualize CMC. The band-specific coherence values, expressed in $-\log_{10}(P)$, were used to represent the collective coherence over the range of frequencies within each distinct frequency band (Fig. 2H).

For comparison, the magnitude squared coherence, referred to here as "classical coherence," was also estimated in the frequency range of 2–100 Hz in addition to the banded coherence. Spectral smoothing of the auto- and cross-spectrum was done using a Hanning filter. The significance threshold (upper 95% confidence limit) was calculated as $1 - 0.05^{1/(L \cdot 0.375)}$, where L is the number of segments used to calculate coherence and the factor 0.375 is correction for spectral smoothing using Hanning filter (Halliday and Rosenberg 1999).

Statistics

To find significant group differences between the banded CMC values, the band-specific CMC values (expressed as P-values) were converted into z-scores by taking inverse of cumulative distribution function of 1 − P. The resulting z-scores of CMC values were compared between controls and PLS using a nonparametric 2-sample Kolmogorov–Smirnov test (Massey 1951), which compares the shapes of 2 distributions rather the central tendency (mean and median). In total, 120 comparisons (5 EEG × 3 EMG × 8 frequency bands) were made. Correction for multiple comparisons was performed using the adaptive false discovery rate (FDR) at $q = 0.05$ (Benjamini et al. 2006). The effect size of the CMC differences was calculated using Cohen's d.

Correlation of the CMC measures with clinically assessed UMN scores was calculated for all the predefined frequency bands and the preselected EEG and EMG channels (i.e. 120 CMC measures in total, 5 × 3 EEG–EMG combinations × 8 frequency bands). The association of the CMC measures, expressed in $-\log_{10}(P)$, in the PLS cohort with their corresponding UMN scores was tested using Spearman's rank correlation coefficient. For this purpose, partial correlations were used to remove the potential effects of age from the inference (range: 46.39–77.43 years). The P-values of correlation coefficients were adjusted for multiple comparison (120 comparisons in total, 5 EEG × 3 EMG × 8 frequency bands) using adaptive FDR at $q = 0.05$. A line was fitted to the correlation data to visualize the relationship using the robust linear least-square fitting method. The degrees-of-freedom-adjusted coefficient of determination (Adj R^2) was calculated for the fitted line to measure the goodness of the fit.

Table 1. Clinical and demographic data of the analyzed PLS and control groups.

	PLS	Controls
Biological sex (female/male)	7/9	7/11
Average age at recording (years)	62.7 ± 8.7	62.5 ± 8.9
EHI (right/left)	14/2	16/2
Disease duration (years)	7.6 ± 6.01	–
UMN score (max 16)	12.8 ± 2.3	
Spasticity score (upper limb) (max 4)	3.5 ± 1.09	
MRC (upper limb) (max 100)	71.6 ± 4.08	
ECAS total abnormal score n (%)	4 (28%)	
Language	1 (7%)	
Verbal fluency	2 (14%)	
Memory	2 (14%)	
Visuospatial	1 (7%)	

EHI, Edinburgh Handedness Inventory; UMN, Upper Motor Neuron Score; MRC, Medical Research Council Scale for Muscle Strength; ECAS, Edinburgh Cognitive ALS Screen.

Results

Clinical profile

Sixteen participants with PLS (7 females and 9 males, age: 62.7 ± 8.7 [mean ± SD]) with PLS were prospectively recruited from the national ALS Clinic based at Beaumont hospital, Dublin. All participants with PLS were diagnosed with definite PLS, fulfilling the consensus criteria (Turner et al. 2020) defined as the absence of LMN degeneration 4 or more years from symptom onset; 18 healthy controls (7 female) were recruited (age: 62.5 ± 8.97 [mean ± SD]). Table 1 shows the detailed profile of the recruited participants.

ECAS results were scored as normal or impaired based on education and age (Pinto-Grau et al. 2017). Four participants with PLS (28%) showed evidence of cognitive impairment based on the total ECAS score. The details are listed in Table 1. Abnormal performance in visuospatial domains (7%) were uncommon based on our screening assessment with ECAS.

Abnormally high CMC in PLS

The results show that there were statistically significant differences in the frequency, location, and magnitude of the CMC between healthy controls and the PLS group, Fig. 3 ($q < 0.05$, with FDR multiple comparison correction). The coherence spectra for all EEG channels and muscles investigated are presented in Supplementary Fig. S3, and the significant differences between PLS and control groups are summarized in Fig. 4 and Table 2. Healthy controls did not show strong beta-band CMC peaks over the contralateral motor area when grouped across all participants (C3), likely due to the task selection (pincer grip vs. precision grip). Supplementary Fig. S1 and Fig. 3A and B. However, when examined on an individual basis, significant beta-band CMC was detected in 14/18 controls (Supplementary Fig. S2). Biological sex had no effect on the CMC detected in the PLS cohort ($P > 0.05$, tested using Mann–Whitney U test).

CMC pattern over contralateral primary motor area

CMC was significantly higher in the gamma and alpha bands in the PLS group when compared with controls. The coherence was not statistically significant for the control group at the C3 channel location over contralateral motor area (between C3 and for both the FDI and FPB muscles, respectively, Fig. 3A and B). It is notable that statistically significant gamma- and alpha-band CMC was

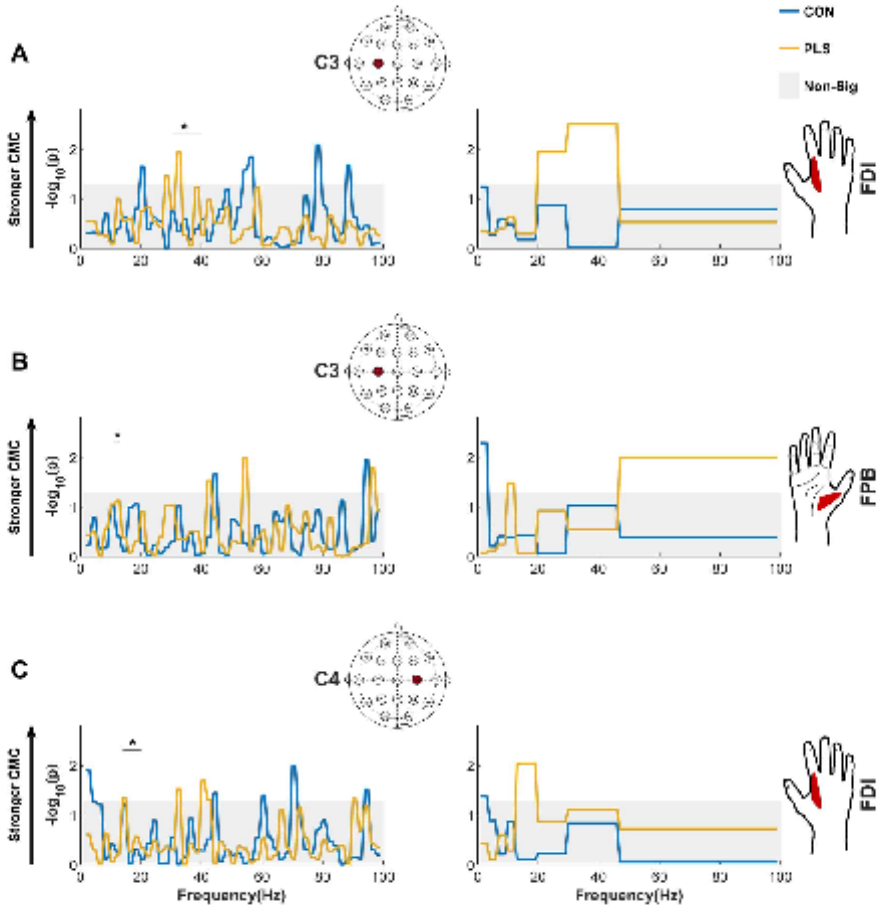

Fig. 3. Participants with PLS show abnormal cortico-muscular (EEG–EMG) coherence in primary motor areas and abnormal frequency bands. The first column displays pCoh grouped over shorter 2-Hz frequency bands, and the second column shows the banded coherence ("pCoh") grouped over predefined frequency bands. The pCoh spectra show the strength of synchrony of the EEG electrodes over the contralateral primary motor area C3 (A and B) and ipsilateral primary motor area C4 (C) with EMG (FDI and FPB muscles) in different frequency bands. The shaded area corresponds to the nonsignificant values at $\alpha = 0.05$ threshold for P-values (corrected for multiple comparison, 120 comparisons in total, using FDR at $q = 0.05$). In PLS, CMC between C3-FDI was present in the gamma band instead of the typical beta-band CMC observed in healthy controls during this type of task. The PLS cohort also exhibited CMC between ipsilateral C4-FDI in the beta band which was not present in controls.

observed in the PLS cohort, as this is not typically observed in healthy subjects during low-force muscle contractions.

CMC pattern over ipsilateral primary motor area

Significant beta-band CMC (β1) was observed between C4 and the FDI over the ipsilateral motor area in the PLS cohort and was not observed in controls (Fig. 3C).

Correlates with UMN dysfunction score show location-specific positivity and negativity

We then conducted a separate analysis to test for significant correlations between CMC and UMN score (calculated for all predefined frequency bands and EEG and EMG channels). Several of the CMC measures were significantly correlated with the UMN dysfunction score after FDR correction (Table 3 and Fig. 5). In Table 3 and Fig. 5, a negative correlation between a CMC measure and UMN score indicates that higher UMN impairment (more severe clinical symptoms) are associated with reduced EEG–EMG synchrony (CMC) in the PLS cohort. A positive correlation indicates that PLS participants with more severe UMN symptoms exhibited stronger CMC in these muscles/brain regions. Both alpha- and gamma-band CMC between the APB muscle and the contralateral motor cortex were lower in PLS participants with more severe UMN impairments (significant negative correlation with UMN score). Theta-band CMC coherence between the FDI and the frontal brain region (Fz) was also significantly lower in

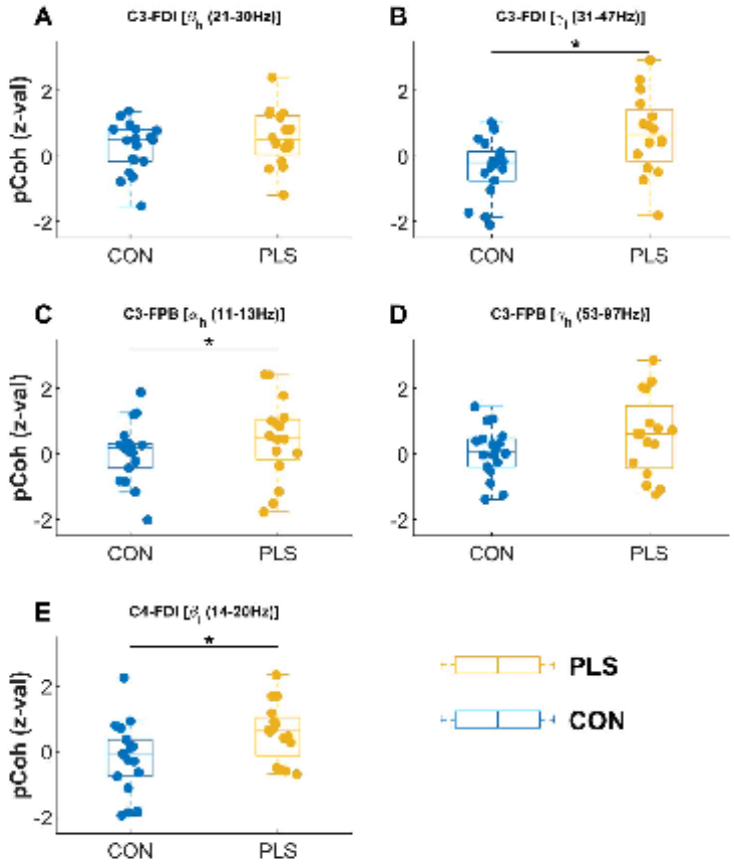

Fig. 4. Box plot of banded CMC (expressed as z-scores) for the EEG–EMG channel and frequency band combinations that were found to show significant CMC in PLS after FDR correction (based on Table 2, see Fig. 3 and Supplementary Fig. S3). The plots show the CMC, between EEG electrodes over the contralateral primary motor area C3 (A, B, C and D) and ipsilateral primary motor area C4 (E) with EMG (FDI and FPB muscles) in different frequency bands, for control and PLS participants overlayed with individual values. The groups were compared using Kolmogorov–Smirnov test. Significant group difference is marked with an asterisk (*$P < 0.05$, corrected at FDR $q = 0.05$).

PLS participants with greater UMN dysfunction. Gamma-band CMC between the APB and the ipsilateral motor area (C4) varied with the degree of UMN dysfunction. PLS participants with greater UMN impairments exhibited lower CMC in the high gamma band (γ_h) but higher CMC in the low gamma band (γ_l). Finally, PLS participants with greater UMN impairments exhibited greater beta-band CMC between the APB and the parietal brain region (beta-band CMC in the parietal region is not typically observed in healthy controls).

Discussion

To date, studies investigating CMC in motor neuron diseases have focused on estimating beta-band CMC between muscles of the hand/arm and M1 as a direct reflection of UMN/LMN pathology (Proudfoot et al. 2018). However, our recent EEG studies in ALS (Dukic et al. 2019; McMackin et al. 2020) and Post-Polio Syndrome (Coffey et al. 2020) suggest that abnormalities in the cortical network activity extend beyond M1 in these conditions, a finding that is also supported by neuroimaging studies (Finegan et al. 2019). We have used CMC to demonstrate how brain activity in participants with PLS differs from that of healthy controls during the performance of a pinch grip motor task. Here, we characterized the engagement of different brain regions by the oscillatory functional coupling between signals recorded from brain and muscle (Fig. 3, and Table 2). In PLS, higher CMC at the contralateral M1 was observed in the gamma and alpha bands when compared with controls. Significant beta-band CMC was also detected in ipsilateral M1, which is not typically observed in healthy participants. In each case, the CMC measures were higher in PLS than in controls, suggesting that these observed differences are unlikely to be attributable to muscle wasting or dysfunction (which would typically decrease

Table 2. Table showing group average banded Corticomuscular coherence (CMC) values expressed as P-values. The CMC measures pertain to selected EEG–EMG channel and frequency band combinations that were significant in the PLS group after FDR correction at $q = 0.05$ (based on Fig. 3 and Supplementary Fig. S3). The CMC values are shown for controls and PLS along with group difference P-values and effect size.

EEG/EMG	Frequency	CON Avg pCoh (*P*)	PLS Avg pCoh (*P*)	Kolmogorov–Smirnov test (*P*)	Effect size Cohen's *d*
C3-FDI	High beta	0.135	0.011	0.465	0.381
C3-FDI	**Low gamma**	**0.093**	**0.003**	**0.006**	**0.987**
C3-FPB	**High alpha**	**0.040**	**0.033**	**0.047**	**0.374**
C3-FPB	High gamma	0.0412	0.009	0.052	0.524
C4-FDI	**Low beta**	**0.788**	**0.009**	**0.015**	**0.786**

The bold values in Table 2 indicate the CMC comparison between controls and PLS marked by an asterisk (*) in Figure 4.

Table 3. Summary of cortico-muscular coherence (CMC) measures of interest.

CMC measure	EEG/EMG location	Frequency band	Significant coherence observed in PLS	Significant difference between PLS and controls	Significant +/− correlation with UMN score
1	C3-FDI	High beta	✓		
2	C3-FDI	Low gamma	✓	✓	
3	C3-FPB	High alpha	✓	✓	
4	C3-FPB	High gamma	✓		
5	C4-FDI	Low beta	✓	✓	
6	Fz-FDI	Delta			−
7	C3-APB	Low alpha			−
8	C3-APB	High gamma			−
9	C4-APB	High gamma			−
10	C4-APB	Low gamma			+
11	Pz-APB	Low beta			+

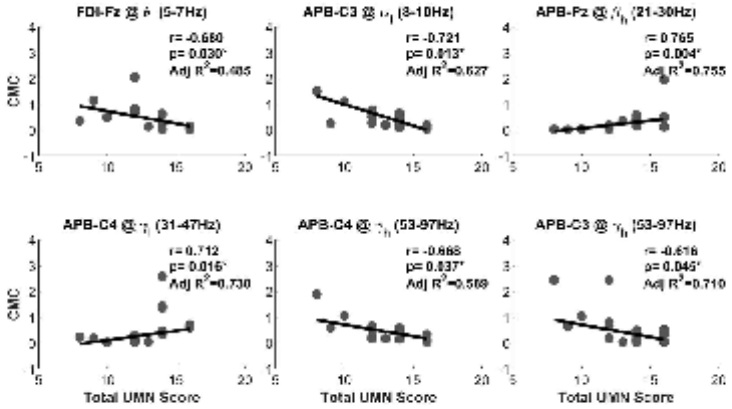

Fig. 5. Measures of cortico-muscular (EEG–EMG) coherence in PLS shows significant strong positive and negative associations with the clinically defined UMN dysfunction score (i.e. Spearman's rho between 0.6 and 0.8 or between −0.8 and −0.6 for each correlation). The P-values have been corrected for FDR at $q = 0.05$. Notice that the correlations are partial correlations with the effect of age removed from the inference.

CMC). We also identified several CMC measures that were correlated with clinical measures of UMN dysfunction, which were also identified outside of the contralateral primary motor area.

PLS-specific differences in CMC

Higher alpha- and gamma-band CMC between contralateral M1 and FDI/FPB was observed in PLS when compared to controls, Fig. 4B and C, respectively, with a large difference reported in the gamma band (Cohen's $d = 0.987$). Altered functional connectivity throughout the sensorimotor cortex has been similarly demonstrated in ALS in resting-state EEG studies (Nasseroleslami et al. 2017). In the present study, gamma-band CMC was detected in participants with PLS during the low-force muscle contractions. This is unusual as the gamma-band CMC is typically only observed in healthy controls during more forceful or dynamic muscle contractions (Omlor et al. 2007; Gwin and Ferris 2012). Previous literature has shown that gamma- and beta-band CMC are present under different conditions and are often inversely related (i.e. when gamma-band CMC increases, beta-band CMC decreases). For example, gamma band coherence

appears during strong contractions, with a corresponding reduction in the beta-band CMC and is thought to reflect a stronger excitation of the motor cortex or greater attention to the task (Brown et al. 1998).

The observed broad increase in CMC in PLS may reflect a combination of pathogenic, adaptive, and/or compensatory increases in the synchronization of neuronal groups in response to UMN degeneration and dysfunction in the inhibitory interneuronal circuitry in PLS (Agarwal et al. 2018). Neuronal loss in M1 in PLS and the cortical and subcortical changes beyond M1 are likely to disrupt information flow in both local neural circuits and larger-scale networks. This may require a rebalancing of interregional interactions and a reorganization of the sensorimotor networks that are engaged in processing and transferring information during movement. This, in turn, would manifest as changes to the synchronization patterns across the sensorimotor network and alterations in the coupling between the cortico/subcortical and spinal regions.

Another key finding was the detection of beta-band CMC in the ipsilateral motor cortex in PLS, with a strong difference reported between PLS and controls (Cohen's $d = 0.786$). Ipsilateral premotor activity has been previously observed in ALS (specifically, in ALS participants who exhibited a greater number of UMN signs relative to LMN symptoms) in an EEG-based investigation of movement-related cortical potentials (Inuggi et al. 2011). It is possible that the increased activation of the ipsilateral sensorimotor cortices is functionally relevant and aids in the performance of the motor task. Ipsilateral cortical activation is increased in other populations in which elements of the cortical network have been damaged, e.g. in stroke, multiple sclerosis, and spinal cord injury (Ward et al. 2003; Lenzi et al. 2007; Prak et al. 2021). Previous studies suggest that ipsilateral M1 aids the contralateral motor cortex in the planning and organization of hand movements (Chen et al. 1997), but it remains unclear whether ipsilateral M1 plays a significant role in mediating the motor command to motoneurons of the hand (Soteropoulos et al. 2011). There is limited evidence to support a monosynaptic pathway to convey direct ipsilateral actions to hand muscles, but it is possible that ipsilateral projections are conveyed through other indirect/polysynaptic pathways (Calvert and Carson 2022). Though data presented in this study cannot elucidate the precise neural circuits and pathways through which ipsilateral M1 signals influence muscle activity, the results demonstrate for the first time that the contributing brain regions in the sensorimotor control are altered in PLS during a motor task. This manifests as a reshaping of synchronous oscillations between cortex and muscle.

Associations between CMC and clinical scores

PLS participants with greater clinical impairment exhibited larger CMC in brain regions which are not directly associated with motor execution (positive correlations in Fig. 6 between APB and the ipsilateral motor cortex, C4, and the parietal region, Pz). This finding suggests that PLS affects a wider brain network extending beyond M1, as indicated in previous neuroimaging studies (Finegan et al. 2019). Less-impaired PLS participants exhibited higher alpha- and gamma-band coherence in contralateral M1. The significant correlations between CMC and UMN score were primarily observed in the APB muscle (5/6 correlations), though the reason for this is unclear. Previous studies have found no evidence that PLS conforms to the "split-hand plus" feature of ALS, whereby greater weakness and atrophy is observed in APB relative to other muscles innervated by the median nerve (Menon et al. 2013).

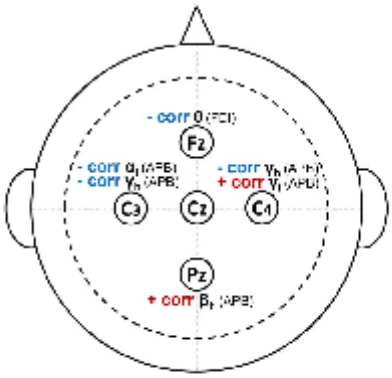

Fig. 6. Significant correlations of the CMC with clinically defined UMN dysfunction score show location-specific positivity and negativity.

PLS participants with greater motor impairments exhibited higher beta-band CMC in the parietal area (Pz) (Fig. 6). Studies in nonhuman primates have shown that activity in the posterior parietal sites is modulated by beta-band oscillations from the somatosensory cortex and that they, in turn, exert an influence on the motor cortex (Brovelli et al. 2004). Though the majority of corticospinal neurons originate from M1, the neuroanatomical and electrophysiological studies in primates have also found evidence of corticospinal projections from the supplementary motor area and somatosensory and parietal cortices (Murray and Coulter 1981; Galea and Darian-Smith 1994; Maier et al. 2002). CMC at EEG electrodes over non-M1 cortical areas could thus occur due to an increase in the relative contribution of alternative descending pathways to muscle activation, other than direct M1 projections. These synchronies could also reflect a restructuring of cortico-cortical communication between non-M1 regions and areas such as M1 that have direct projections to the spinal motor pools. For example, the enhanced beta-band coupling between the parietal brain region and muscular activity could reflect an increase in the functional connectivity of these brain networks (Meoded et al. 2015). It is also possible that the chronic loss of corticospinal input to the spinal motoneurons, which is combined with extreme muscle weakness and slowing of movement in PLS, could produce a change in afferent activity. This would in turn influence CMC. Though beta-band CMC is primarily driven by efferent supraspinal structures, there is now evidence to suggest that it can be modulated by sensory receptors that provide afferent feedback to the central nervous system (Witham et al. 2011).

Although the observed CMC differences in PLS could arise from both the direct and indirect effects of UMN degeneration, the increased CMC in more-impaired PLS participants for specific brain regions could potentially suggest that these changes are compensatory/adaptive in nature. Taken together, these results could suggest that the pattern of brain network reorganization in PLS follows a similar trajectory to recovery in stroke, where more-impaired PLS participants rely on contributions from the ipsilateral hemisphere, but those who are minimally affected can recover function by restructuring the functional connectivity in the contralateral hemisphere (Brancaccio et al. 2022). Future studies are needed to elucidate the pathways through which these wider brain regions could influence muscle activity and determine the exact nature of the observed changes in

CMC (pathogenic, adaptive, or compensatory). These network-level changes could be further characterized in the future longitudinal studies of PLS by examining the changes in the CMC measures alongside changes in the clinical scores of UMN impairment.

Future directions

The novel findings of this study identify distinct differences in the CMC patterns found in PLS. Though the data presented in the current study cannot determine the exact mechanism and/or neuroanatomical pathways through which cortical signals originating outside of contralateral M1 influence muscle activity, we suggest several possible mechanisms through which abnormal CMC in PLS could arise.

Future studies could also examine whether these CMC patterns can discriminate PLS from more rapidly progressive ALS phenotypes. There is a clear need for quantitative measures to support diagnosis, as people with PLS currently have long periods of diagnostic uncertainty and face exclusion from ALS clinical trials (people with restricted UMN symptoms and suspected PLS typically do not meet inclusion criteria) (Brooks et al. 2000; D'Amico et al. 2013). The differences between more- and less-impaired PLS participants further suggest that CMC has the potential for development as a tool to monitor disease progression or importantly as a measure to assess target engagement in clinical trials (Jeromin and Bowser 2017). These measures are particularly needed for PLS, as longitudinal progression is difficult to quantify in such a slowly progressing disease. The PLS-specific differences in CMC and the differences between more- and less-impaired PLS participants reported in this study provide the basis for further development of these markers of motor network dysfunction.

Conclusion

This study demonstrates the presence of abnormal corticomuscular coherence in PLS for the first time, which we suggest could reflect a restructuring of the cortical network connectivity in response to UMN degeneration. This observation suggests that PLS affects a sensorimotor brain network extending beyond the primary motor cortex. Correlations showed that higher CMC in specific brain regions was also observed in more-impaired PLS participants compared with those with less severe impairments. This may suggest these differences are compensatory/adaptive in nature, though these differences could arise from both the direct and indirect effects of UMN degeneration. The correlations with clinical UMN scores demonstrate the potential for CMC measurements to be used as a tool to identify dysfunction in specific cortical networks during motor tasks and prompt further development of quantitative neurophysiology-based biomarker candidates in PLS.

Acknowledgments

We thank the Wellcome-HRB Clinical Research Facility at St. James's Hospital in providing a dedicated environment for the conduct of high-quality clinical research. We would like to thank the participants of the study and their family.

Authors' contributions

Saroj Bista (Data curation, Formal analysis, Investigation, Methodology, Writing—review & editing), Amina Coffey (Investigation, Writing—original draft), Antonio Fasano (Investigation, Resources, Writing—review & editing), Teresa Buxo (Software, Investigation), Stefan Dukic (Investigation, Resources), Matthew Mitchell (Investigation, Resources), Eileen Giglia (Investigation, Resources), Mark Heverin (Project administration), Muthuraman Muthuraman (Conceptualization), Richard G. Carson (Validation, Writing—review & editing), Madeleine Lowery (Validation, Writing—review & editing), Orla Hardiman (Funding acquisition, Resources, Supervision, Validation, Writing—review & editing), Lara McManus (Methodology, Validation, Writing—review & editing), and Bahman Nasseroleslami (Conceptualization, Funding acquisition, Methodology, Supervision, Writing—review & editing)

Supplementary material

Supplementary material is available at Cerebral Cortex online.

Funding

This work was supported by Irish Research Council (GOIPD/2015/213, GOIPG/2019/748, and EPSPD/2020/108); the Health Research Board of Ireland (MRCG-2018-02); Science Foundation Ireland (16/ERCD/3854); Research Motor Neurone (MRCG-2018-02); Royal Society-Science Foundation Ireland (URF\R1\221917); Motor Neurone Disease Association (McManus/Apr22/888-791); and ALS Association (20-IIA-546).

Conflict of interest statement: Prof. Hardiman's work is funded by the Science Foundation Ireland (Grants 20/SP/8953, 16/RC/3948, and 16/ERCD/3854), Health Research Board, and Thierry Latran Foundation. She has served on advisory boards for the following companies: Cytokinetics, Wave Pharmaceuticals, Orion, Novartis, Biogen Denali, Neurosense, Pfizer, Sanofi, and Lilly. She is a member of the DSMC for Accelsior. She is a principal investigator on the PRECISION ALS Project and the Academic/Industry Collaboration funded by Science Foundation Ireland. Her industry partners include Biogen, Takeda, Cytokinetics, Novartis IQVIA, and Accenture. Her research group has collaborated with Biogen, Ionis, and Cytokinetics in delivering the IMPACT ALS Survey and with Cytokinetics in delivering the REVEALS study of respiratory decline in ALS. She is the editor in chief of the Journal ALS and the Frontotemporal Degenerations and is a member of the editorial board of the Journal of Neurology, Neurosurgery and Psychiatry. Prof. Richard Carson is a Senior Editor of the Journal of Physiology and an Associate Editor of Human Movement Science. Other authors declare no conflict of interest.

Data availability

The data that support the findings of this study are available from the corresponding author upon reasonable request and subject to the approvals by Data Protection Officer and Technology Transfer Office in Trinity College Dublin.

References

Abrahams S, Newton J, Niven E, Foley J, Bak TH. Screening for cognition and behaviour changes in ALS. *Amyotroph Lateral Scler Frontotemporal Degener*. 2014;15:9–14.

Agarwal S, Highton-Williamson E, Caga J, Matamala JM, Dharmadasa T, Howells J, Zoing MC, Shibuya K, Geevasinga N, Vucic S. Primary lateral sclerosis and the amyotrophic lateral sclerosis–frontotemporal dementia spectrum. *J Neurol*. 2018:265:1819–1828.

Agosta F, Canu E, Inuggi A, Chiò A, Riva N, Silani V, Calvo A, Messina S, Falini A, Comi G. Resting state functional connectivity alterations in primary lateral sclerosis. *Neurobiol Aging*. 2014:35:916–925.

Aikio R, Laaksonen K, Sairanen V, Parkkonen E, Abou Elseoud A, Kujala J, Forss N. CMC is more than a measure of corticospinal tract integrity in acute stroke patients. *NeuroImage Clin*. 2021:32:102818.

Ajemian R, D'Ausilio A, Moorman H, Bizzi E. A theory for how sensorimotor skills are learned and retained in noisy and nonstationary neural circuits. *Proc Natl Acad Sci*. 2013:110:E5078–E5087.

Amjad AM, Halliday DM, Rosenberg JR, Conway BA. An extended difference of coherence test for comparing and combining several independent coherence estimates: theory and application to the study of motor units and physiological tremor. *J Neurosci Methods*. 1997:73:69–79.

Bede P, Bogdahn U, Lope J, Chang KM, Xirou S, Christidi F. Degenerative and regenerative processes in amyotrophic lateral sclerosis: motor reserve, adaptation and putative compensatory changes. *Neural Regen Res*. 2021:16:1208–1209.

Benjamini Y, Krieger AM, Yekutieli D. Adaptive linear step-up procedures that control the false discovery rate. *Biometrika*. 2006:93:491–507.

Blain-Moraes S, Mashour GA, Lee H, Huggins JE, Lee U. Altered cortical communication in amyotrophic lateral sclerosis. *Neurosci Lett*. 2013:543:172–176.

Bradshaw LA, Wikswo JP. Spatial filter approach for evaluation of the surface Laplacian of the electroencephalogram and magnetoencephalogram. *Ann Biomed Eng*. 2001:29:202–213.

Brancaccio A, Tabarelli D, Belardinelli P. A new framework to interpret individual inter-hemispheric compensatory communication after stroke. *J Pers Med*. 2022:12:59.

Brown P, Salenius S, Rothwell JC, Hari R. Cortical Correlate of the Piper Rhythm in Humans. *Journal of Neurophysiology*, 1998:80:2911–2917. https://doi.org/10.1152/jn.1998.80.6.2911.

Brooks BR, Miller RG, Swash M, Munsat TL. El Escorial revisited: revised criteria for the diagnosis of amyotrophic lateral sclerosis. *Amyotroph Lateral Scler Other Motor Neuron Disord*. 2000:1:293–299.

Brovelli A, Ding M, Ledberg A, Chen Y, Nakamura R, Bressler SL. Beta oscillations in a large-scale sensorimotor cortical network: directional influences revealed by Granger causality. *Proc Natl Acad Sci*. 2004:101:9849–9854.

Calvert GH, Carson RG. Neural mechanisms mediating cross education: with additional considerations for the ageing brain. *Neurosci Biobehav Rev*. 2022:132:260–288.

Chen R, Gerloff C, Hallett M, Cohen LG. Involvement of the ipsilateral motor cortex in finger movements of different complexities. *Ann Neurol*. 1997:41:247–254.

Coffey A, Bista S, Fasano A, Buxo T, Mitchell M, Giglia ER, Dukic S, Fenech M, Barry M, Wade A, et al. Altered supraspinal motor networks in survivors of poliomyelitis: a cortico-muscular coherence study. *Clin Neurophysiol*. 2020:132:106–113.

Compston A. Aids to the investigation of peripheral nerve injuries. Medical Research Council: Nerve Injuries Research Committee. His Majesty's Stationery Office: 1942; pp. 48 (iii) and 74 figures and 7 diagrams; with aids to the examination of the peripheral nervous system. By Michael O'Brien for the Guarantors of Brain. Saunders Elsevier: 2010; pp. [8] 64 and 94 figures. *Brain*. 2010:133:2838–2844.

Conway BA, Halliday DM, Farmer SF, Shahani U, Maas P, Weir AI, Rosenberg JR. Synchronization between motor cortex and spinal motoneuronal pool during the performance of a maintained motor task in man. *J Physiol*. 1995:489:917–924.

D'Amico E, Pasmantier M, Lee Y-W, Weimer L, Mitsumoto H. Clinical evolution of pure upper motor neuron disease/dysfunction (PUMMD). *Muscle Nerve*. 2013:47:28–32.

Danna-Dos Santos A, Poston B, Jesunathadas M, Bobich LR, Hamm TM, Santello M. Influence of fatigue on hand muscle coordination and EMG-EMG coherence during three-digit grasping. *J Neurophysiol*. 2010:104:3576–3587.

de Carvalho M, Scotto M, Lopes A, Swash M. Clinical and neurophysiological evaluation of progression in amyotrophic lateral sclerosis. *Muscle Nerve*. 2003:28:630–633.

Dukic S, McMackin R, Buxo T, Fasano A, Chipika R, Pinto-Grau M, Costello E, Schuster C, Hammond M, Heverin M, et al. Patterned functional network disruption in amyotrophic lateral sclerosis. *Hum Brain Mapp*. 2019:40:4827–4842.

Dukic S, McMackin R, Costello E, Metzger M, Buxo T, Fasano A, Chipika R, Pinto-Grau M, Schuster C, Hammond M, et al. Resting-state EEG reveals four subphenotypes of amyotrophic lateral sclerosis. *Brain*. 2021:145:621–631.

Fang Y, Daly JJ, Sun J, Hvorat K, Fredrickson E, Pundik S, Sahgal V, Yue GH. Functional corticomuscular connection during reaching is weakened following stroke. *Clin Neurophysiol*. 2009:120:994–1002.

Finegan E, Chipika RH, Shing SLH, Hardiman O, Bede P. Primary lateral sclerosis: A distinct entity or part of the ALS spectrum? *Amyotroph Lateral Scler Frontotemporal Degener*. 2019:20:133–145.

Galea MP, Darian-Smith I. Multiple corticospinal neuron populations in the macaque monkey are specified by their unique cortical origins, spinal terminations, and connections. *Cereb Cortex*. 1994:4:166–194.

Gwin JT, Ferris DP. Beta- and gamma-range human lower limb corticomuscular coherence. *Front Hum Neurosci*. 2012:6:258–258.

Halliday DM, Rosenberg JR. Time and frequency domain analysis of spike train and time series data. In: Windhorst U, Johansson H, editors. editors*Modern techniques in neuroscience research*. Berlin, Heidelberg: Springer; 1999. pp. 503–543.

Halliday DM, Conway BA, Farmer SF, Rosenberg JR. Using electroencephalography to study functional coupling between cortical activity and electromyograms during voluntary contractions in humans. *Neurosci Lett*. 1998:241:5–8.

Hermens HJ, Freriks B, Disselhorst-Klug C, Rau G. Development of recommendations for SEMG sensors and sensor placement procedures. *J Electromyogr Kinesiol*. 2000:10:361–374.

Inuggi A, Riva N, González-Rosa JJ, Amadio S, Amato N, Fazio R, Del Carro U, Comi G, Leocani L. Compensatory movement-related recruitment in amyotrophic lateral sclerosis patients with dominant upper motor neuron signs: an EEG source analysis study. *Brain Res*. 2011:1425:37–46.

Issa NP, Frank S, Roos RP, Soliven B, Towle VL, Rezania K. Intermuscular coherence in amyotrophic lateral sclerosis: a preliminary assessment. *Muscle Nerve*. 2017:55:862–868.

Jeromin A, Bowser R. Biomarkers in neurodegenerative diseases. In: Beart P, Robinson M, Rattray M, Maragakis NJ, editors. editors*Neurodegenerative diseases: pathology, mechanisms, and potential therapeutic targets*. Cham: Springer International Publishing; 2017. pp. 491–528.

Kent-Braun JA, Walker CH, Weiner MW, Miller RG. Functional significance of upper and lower motor neuron impairment in amyotrophic lateral sclerosis. *Muscle Nerve*. 1998:21:762–768.

Lenzi D, Conte A, Mainero C, Frasca V, Fubelli F, Totaro P, Caramia F, Inghilleri M, Pozzilli C, Pantano P. Effect of corpus callosum damage on ipsilateral motor activation in patients with multiple sclerosis: a functional and anatomical study. *Hum Brain Mapp*. 2007:28:636–644.

MacKinnon CD. Chapter 1—sensorimotor anatomy of gait, balance, and falls. In: Day BL, Lord SR, editors. editors *Handbook of clinical neurology*. Elsevier; 2018. pp. 3–26. https://doi.org/10.1016/B978-0-444-63916-5.00001-X.

Maier MA, Armand J, Kirkwood PA, Yang HW, Davis JN, Lemon RN. Differences in the corticospinal projection from primary motor cortex and supplementary motor area to macaque upper limb motoneurons: an anatomical and electrophysiological study. *Cereb Cortex*. 2002:12:281–296.

Massey FJ. The Kolmogorov-Smirnov test for goodness of fit. *J Am Stat Assoc*. 1951:46:68–78.

McFarland DJ, McCane LM, David SV, Wolpaw JR. Spatial filter selection for EEG-based communication. *Electroencephalogr Clin Neurophysiol*. 1997:103:386–394.

McMackin R, Muthuraman M, Groppa S, Babiloni C, Taylor J-P, Kiernan MC, Nasseroleslami B, Hardiman O. Measuring network disruption in neurodegenerative diseases: new approaches using signal analysis. *J Neurol Neurosurg Psychiatry*. 2019:90:1011–1020.

McMackin R, Dukic S, Costello E, Pinto-Grau M, Fasano A, Buxo T, Heverin M, Reilly R, Muthuraman M, Pender N, et al. Localization of brain networks engaged by the sustained attention to response task provides quantitative markers of executive impairment in amyotrophic lateral sclerosis. *Cereb Cortex*. 2020:30:4834–4846.

Meoded A, Morrissette AE, Katipally R, Schanz O, Gotts SJ, Floeter MK. Cerebro-cerebellar connectivity is increased in primary lateral sclerosis. *NeuroImage Clin*. 2015:7:288–296.

Menon P, Kiernan MC, Yiannikas C, Stroud J, Vucic S. Split-hand index for the diagnosis of amyotrophic lateral sclerosis. *Clinical Neurophysiology*. 2013:124:410–416. https://doi.org/10.1016/j.clinph.2012.07.025.

Murray EA, Coulter JD. Organization of corticospinal neurons in the monkey. *J Comp Neurol*. 1981:195:339–365.

Nasseroleslami B, Lakany H, Conway BA. EEG signatures of arm isometric exertions in preparation, planning and execution. *NeuroImage*. 2014:90:1–14.

Nasseroleslami B, Dukic S, Broderick M, Mohr K, Schuster C, Gavin B, McLaughlin R, Heverin M, Vajda A, Iyer PM, et al. Characteristic increases in EEG connectivity correlate with changes of structural MRI in amyotrophic lateral sclerosis. *Cereb Cortex*. 2017:29:27–41.

Nasseroleslami B, Dukic S, Buxo T, Coffey A, McMackin R, Muthuraman M, Hardiman O, Lowery MM, Lalor EC. Non-parametric rank statistics for spectral power and coherence. *bioRxiv*. 2019:818906. https://doi.org/10.1101/818906.

Neilson PD, Neilson MD. An overview of adaptive model theory: solving the problems of redundancy, resources, and nonlinear interactions in human movement control. *J Neural Eng*. 2005:2:S279–S312.

Niinimaa A, Oja H. Multivariate median. In: *Encyclopedia of statistical sciences. Wiley StatsRef: statistics reference online*. Wiley Online Library: Wiley, 2014.

Nordhausen K, Oja H. Multivariate L_1 Methods: The Package MNM. *Journal of Statistical Software*, 2011:43. https://doi.org/10.18637/jss.v043.i05.

Oja H. Multivariate signs and ranks. *Lecture Notes in Statistics*, 2010: 29–46. https://doi.org/10.1007/978-1-4419-0468-3_4.

Oja H, Randles RH. Multivariate Nonparametric Tests. *Statistical Science*. 2004:19:598–605.

Oldfield RC. The assessment and analysis of handedness: the Edinburgh inventory. *Neuropsychologia*. 1971:9:97–113.

Omlor W, Patino L, Hepp-Reymond MC, Kristeva R. Gamma-range corticomuscular coherence during dynamic force output. *NeuroImage*. 2007:34:1191–1198.

Oostenveld R, Fries P, Maris E, Schoffelen J-M. FieldTrip: open source software for advanced analysis of MEG, EEG, and invasive electrophysiological data. *Comput Intell Neurosci*. 2011:2011:156869.

Perrin F, Pernier J, Bertrand O, Echallier JF. Spherical splines for scalp potential and current density mapping. *Electroencephalogr Clin Neurophysiol*. 1989:72:184–187.

Pinto-Grau M, Burke T, Lonergan K, McHugh C, Mays I, Madden C, Vajda A, Heverin M, Elamin M, Hardiman O, et al. Screening for cognitive dysfunction in ALS: validation of the Edinburgh Cognitive and Behavioural ALS Screen (ECAS) using age and education adjusted normative data. *Amyotroph Lateral Scler Frontotemporal Degener*. 2017:18:99–106.

Prak RF, Marsman J-BC, Renken R, Tepper M, Thomas CK, Zijdewind I. Increased ipsilateral M1 activation after incomplete spinal cord injury facilitates motor performance. *J Neurotrauma*. 2021:38:2988–2998.

Proudfoot M, van Ede F, Quinn A, Colclough GL, Wuu J, Talbot K, Benatar M, Woolrich MW, Nobre AC, Turner MR. Impaired corticomuscular and interhemispheric cortical beta oscillation coupling in amyotrophic lateral sclerosis. *Clin Neurophysiol*. 2018:129:1479–1489.

Sanei S, Chambers JA. Introduction to EEG. In: *EEG signal processing*. Wiley Online Library: Wiley, 2007. pp. 1–34.

Soteropoulos DS, Edgley SA, Baker SN. Lack of evidence for direct corticospinal contributions to control of the ipsilateral forelimb in monkey. *J Neurosci*. 2011:31:11208–11219.

Stouffer SA, Suchman EA, Devinney LC, Star SA, Williams RM Jr. *The American soldier: adjustment during army life. (Studies in social psychology in World War II), Vol. 1*. Oxford, England: Princeton Univ. Press; 1949.

Turner MR, Barohn RJ, Corcia P, Fink JK, Harms MB, Kiernan MC, Ravits J, Silani V, Simmons Z, Statland J, et al. Primary lateral sclerosis: consensus diagnostic criteria. *J Neurol Neurosurg Psychiatry*. 2020:91:373–377.

Ward N, Brown M, Thompson A, Frackowiak R. Neural correlates of outcome after stroke: a cross-sectional fMRI study. *Brain*. 2003:126:1430–1448.

Weiszfeld E. Sur le point pour lequel la somme des distances de n points donnés est minimum. *Tohoku Math J*. 1937:43:355–386.

Westfall PH. Combining P-values. In: *Wiley StatsRef: statistics reference online*. Wiley Online Library: Wiley, 2014

Westphal KP, Heinemann HA, Grözinger B, Kotchoubey BJ, Diekmann V, Becker W, Kornhuber HH. Bereitschaftspotential in amyotrophic lateral sclerosis (ALS): lower amplitudes in patients with hyperreflexia (spasticity). *Acta Neurol Scand*. 1998:98:15–21.

Witham CL, Riddle CN, Baker MR, Baker SN. Contributions of descending and ascending pathways to corticomuscular coherence in humans. *J Physiol*. 2011:589:3789–3800.

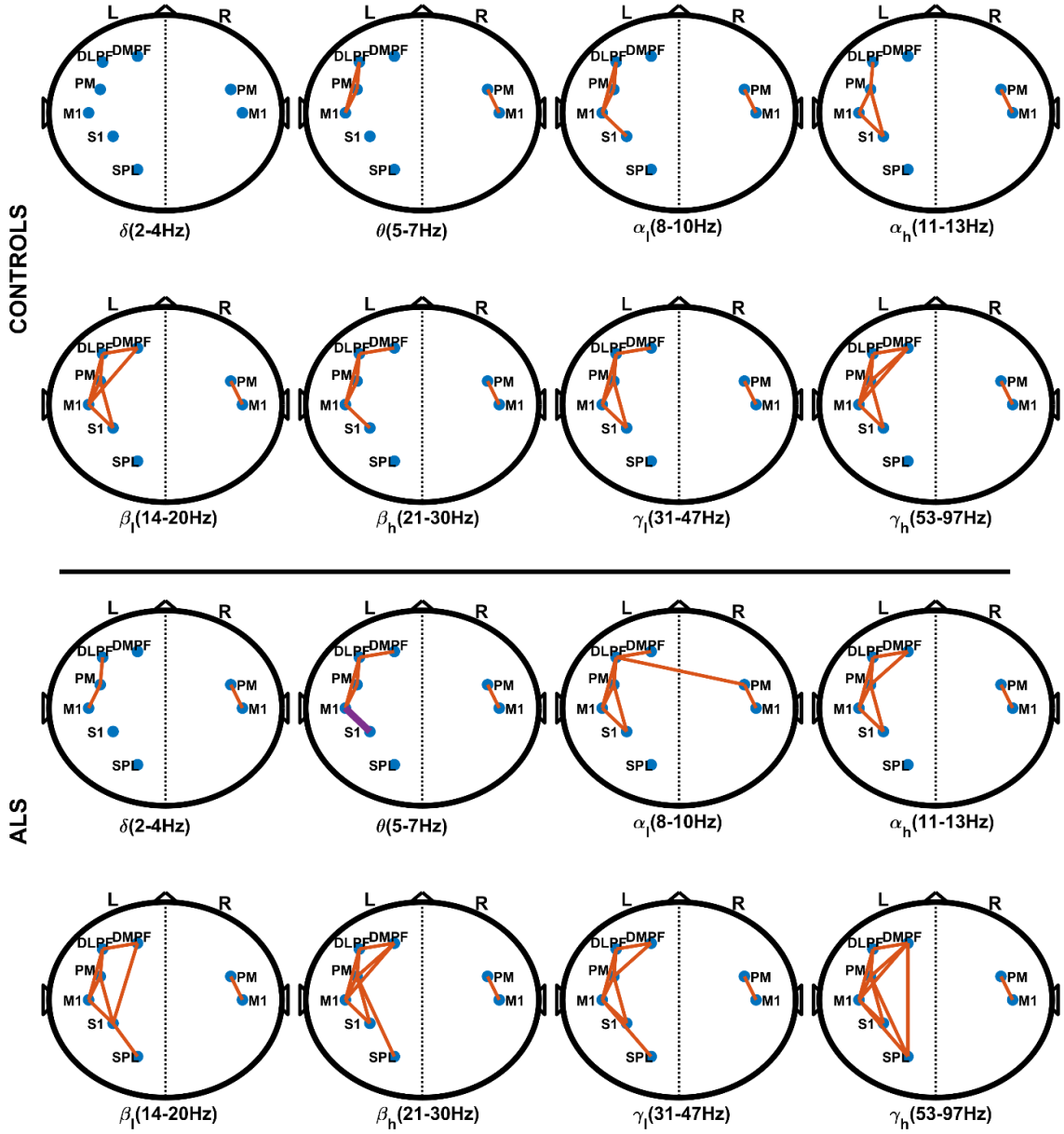

Appendix 6.1 Resting state functional connectivity networks in healthy controls and ALS patients at all 8 frequency bands.

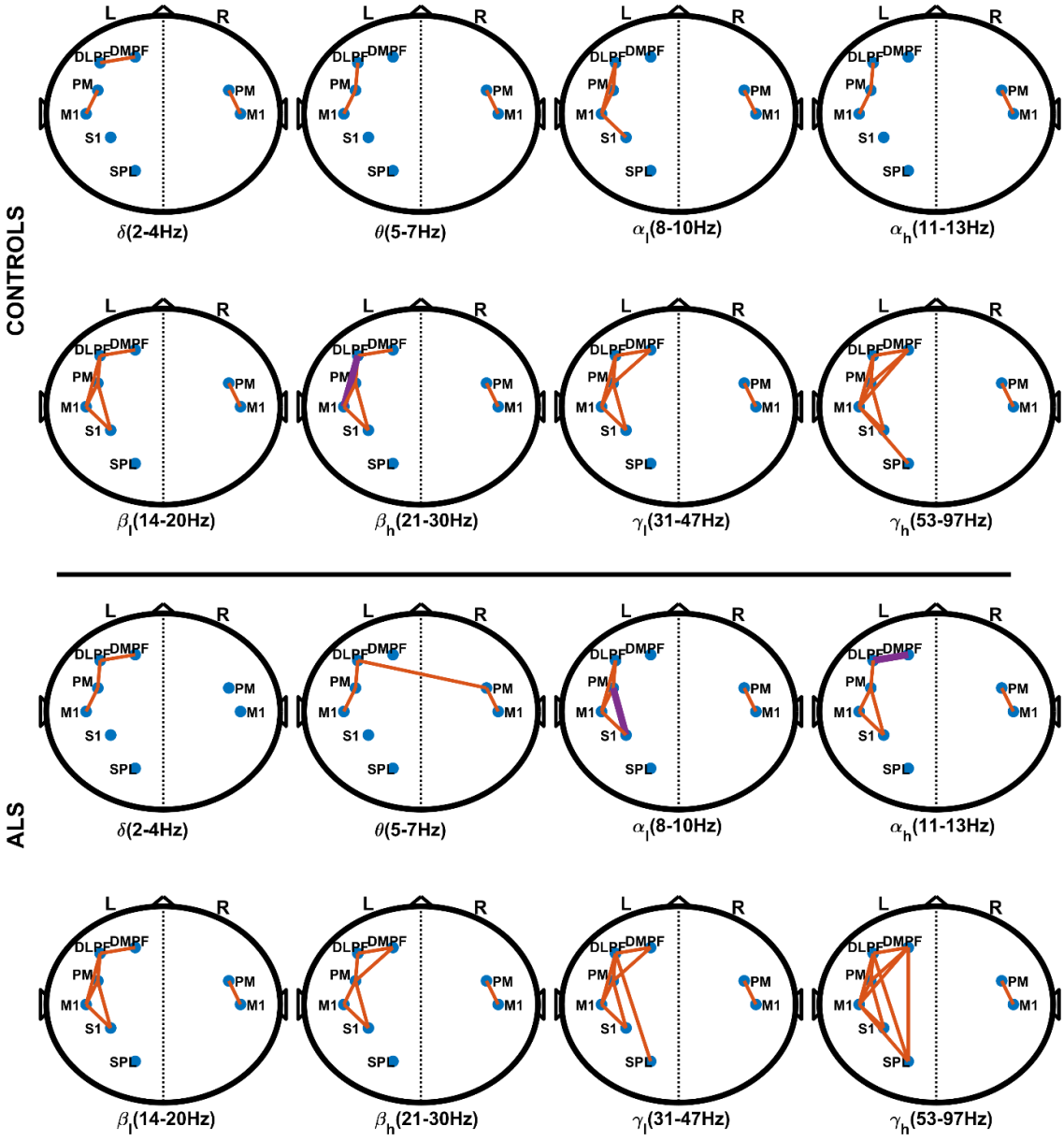

Appendix 6.2 Pre-motor stage functional connectivity networks in healthy controls and ALS patients at all 8 frequency bands.

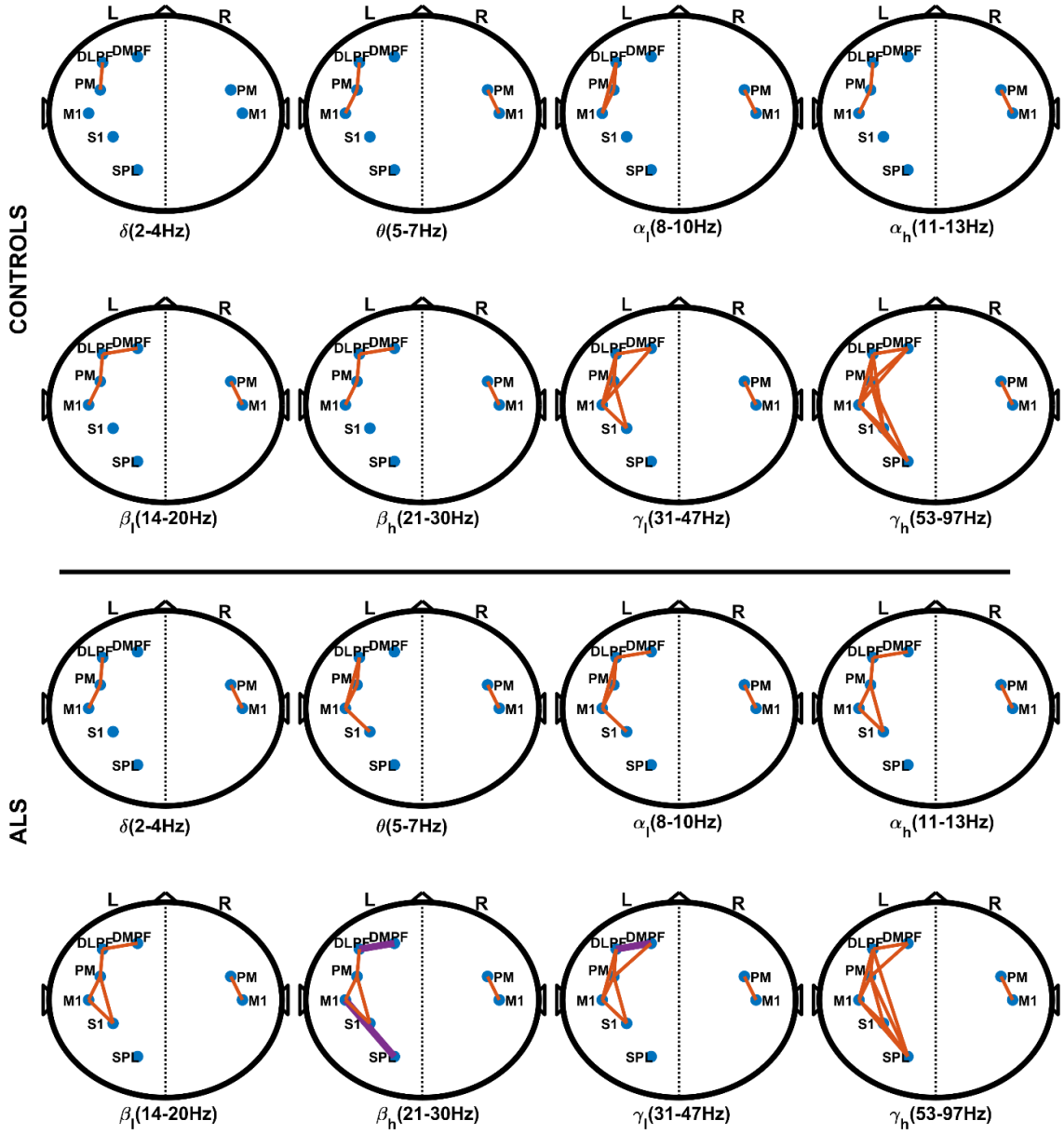

Appendix 6.3 Motor execution functional connectivity networks in healthy controls and ALS patients at all 8 frequency bands.

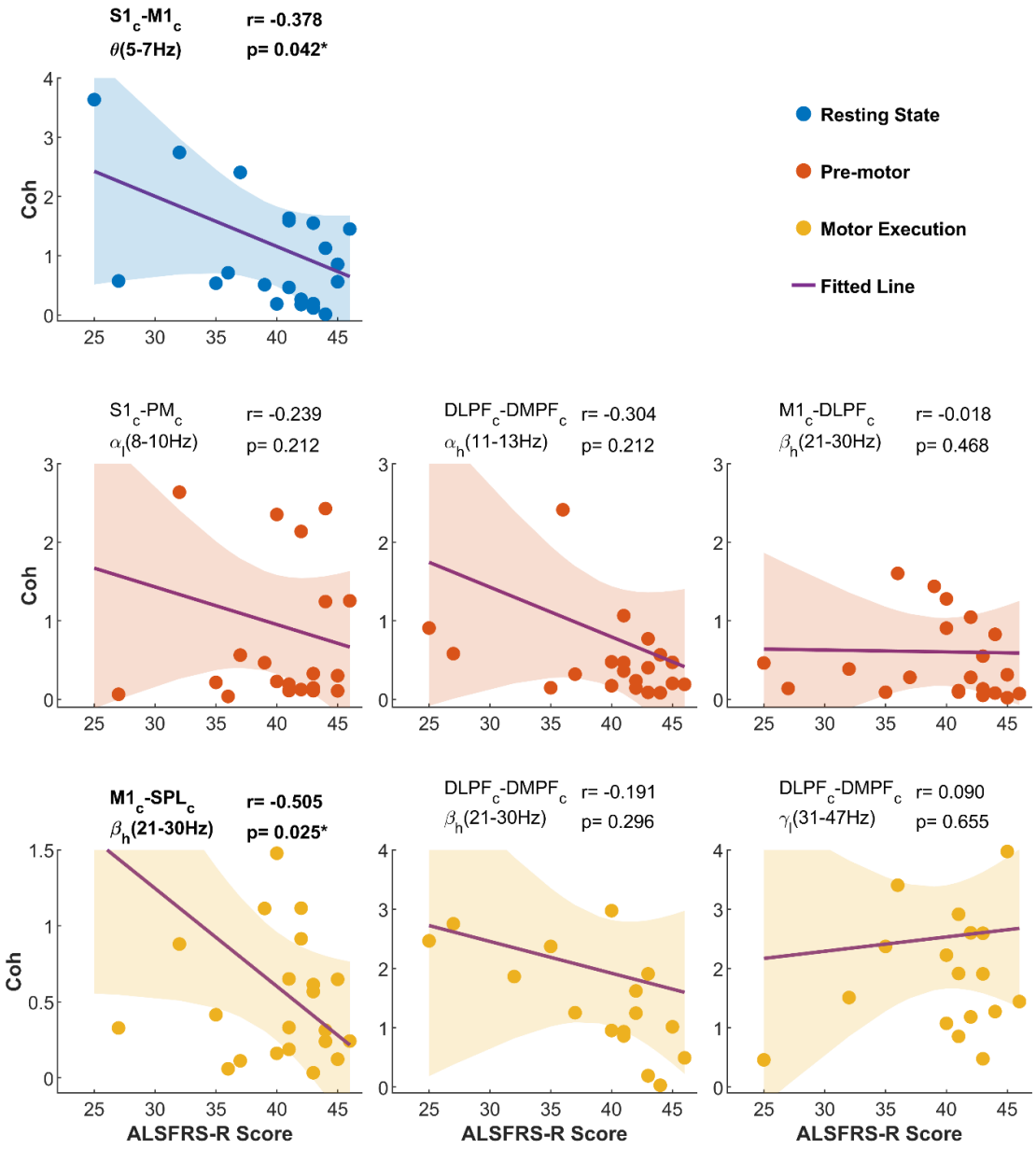

Appendix 6.4 Correlation of abnormal functional connectivity observed in ALS patients with ALSFRS-R scores during resting state (top row), pre-motor (middle row), and motor execution (bottom row). *r is Pearson's linear correlation coefficient and p is level of significance adjusted for false discovery rate at q = 0.05. Linear least-squares fitting was used to fit the line.*

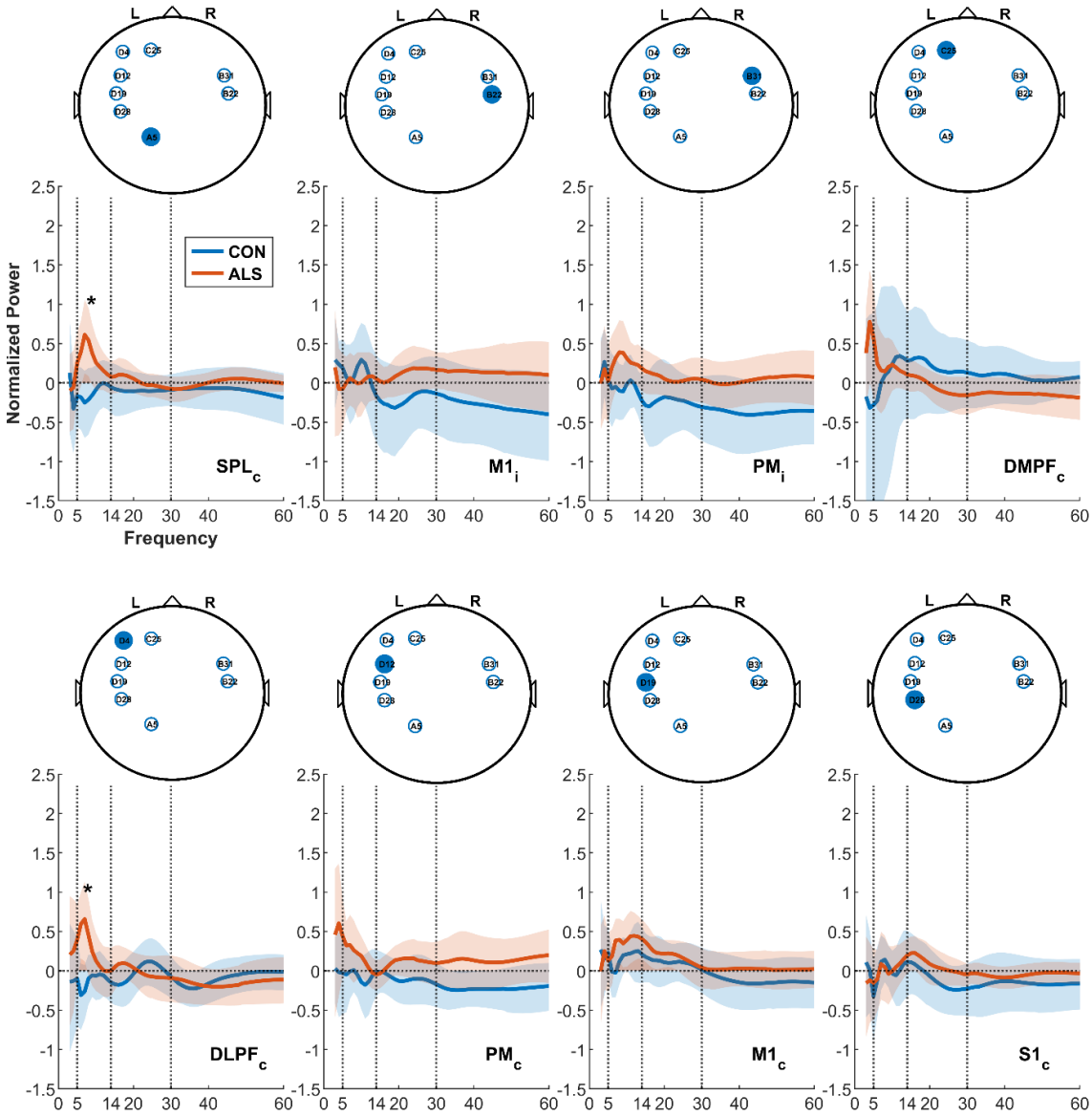

Appendix 6.5 Pre-motor stage non-phase locked normalised power (db) for ALS patients and healthy controls at cortical regions of interest.

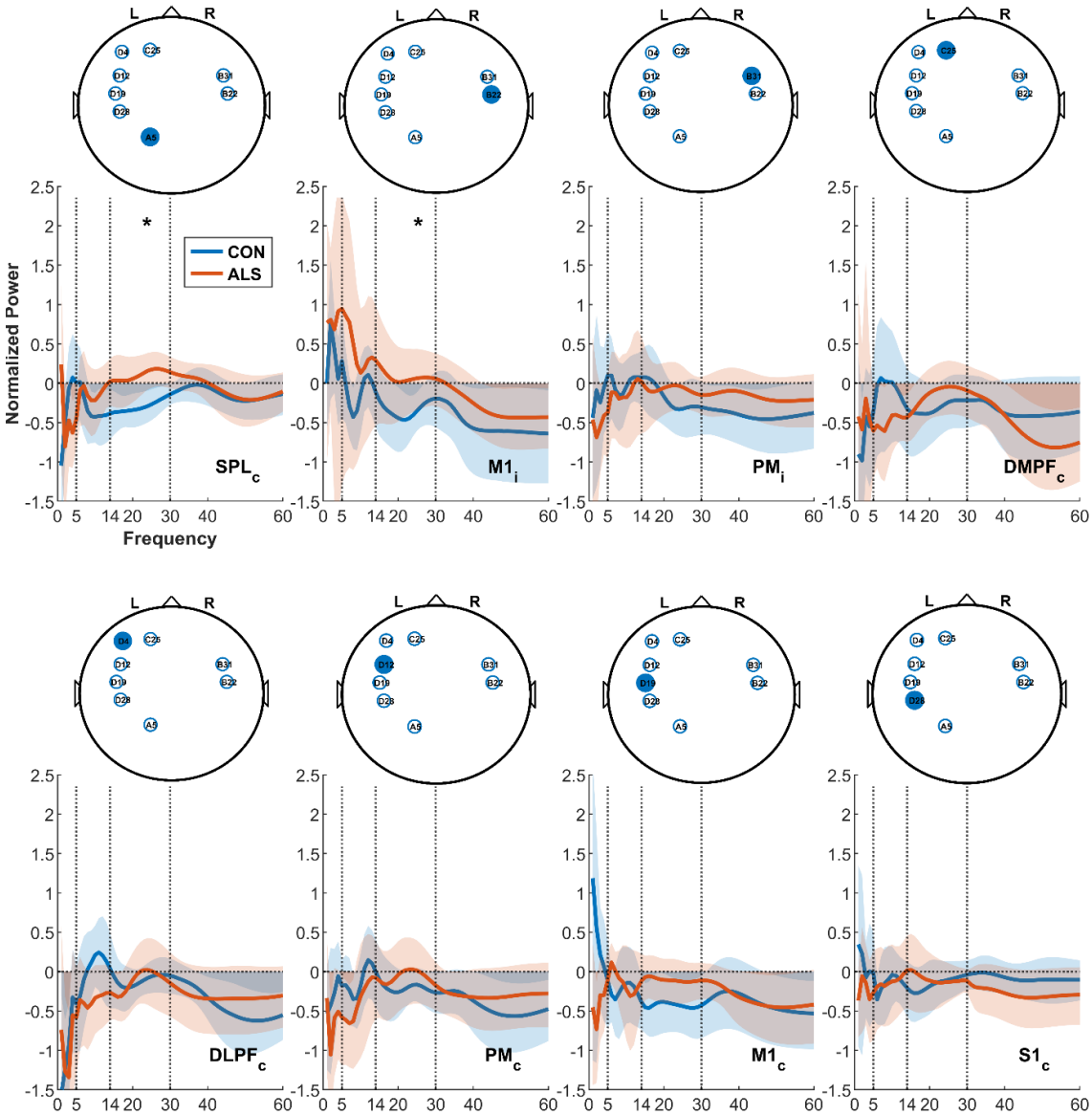

Appendix 6.6 Motor execution non-phase locked normalised power (db) for ALS patients and healthy controls at cortical regions of interest.